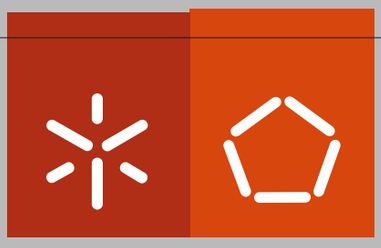

Universidade do Minho
Escola de Engenharia

Daniela Matilde Marques Correia

Systems analysis of metabolism in *Helicobacter pylori*

maio de 2014

Universidade do Minho
Escola de Engenharia

Daniela Matilde Marques Correia

Systems analysis of metabolism in *Helicobacter pylori*

Tese de Doutoramento em Engenharia Química e Biológica

Trabalho efetuado sob a orientação da
Doutora Isabel Cristina de Almeida Pereira da Rocha
da
Doutora Maria João Lopes da Costa Vieira
e do
Doutor Nuno Filipe Ribeiro Pinto de Oliveira Azevedo

maio de 2014

Autor: Daniela Matilde Marques Correia

E-mail: daniela.matilde@gmail.com

Título da tese:

Systems analysis of metabolism in Helicobacter pylori

Orientadores:

Doutora Isabel Cristina de Almeida Pereira da Rocha

Doutora Maria João Lopes da Costa Vieira

Doutor Nuno Filipe Ribeiro Pinto de Oliveira Azevedo

Ano de conclusão: 2014

Doutoramento em Engenharia Química e Biológica

Universidade do Minho, 23 de maio de 2014

Acknowledgments/Agradecimentos

Ao terminar esta longa jornada não poderia deixar de mostrar a minha gratidão a todos os que de alguma forma contribuíram para que este dia chegasse.

Em primeiro lugar queria agradecer aos meus orientadores Doutora Isabel Rocha, Doutor Nuno Azevedo e Doutora Maria João Vieira, por me terem dado a oportunidade de desenvolver este trabalho, pelo apoio, incentivo e orientação científica. Um agradecimento muito especial à Doutora Isabel Rocha por todo o empenho e dedicação, especialmente na fase final deste trabalho.

À instituição de acolhimento, Centro de Engenharia Biológica da Universidade do Minho.

Às pessoas que contribuíram diretamente para este trabalho: Tiago Resende, Rafael Carreira, Sophia Santos, Ana Guimarães e Lucinda Bessa.

Aos colegas do LMA, por todo o apoio a nível laboratorial e pessoal, em especial aqueles de quem me tornei mais próxima. Laura, Carina e Sónia, muito obrigada pela vossa amizade, incentivo e boa disposição que tornaram os dias "menos bons" no laboratório mais fáceis de suportar.

Aos meus colegas do grupo de Biologia de Sistemas e Bioinformática pelo bom ambiente proporcionado e partilha de ideias, com especial atenção às pessoas com quem partilhei o espaço de trabalho, e tive o prazer de almoçar nestes últimos anos (não menciono nomes para não me esquecer de ninguém, mas vocês sabem quem são). Rui e Sónia, obrigada pelo apoio e discussões científicas.

Aos colegas e amigos que descobri nos últimos dias de escrita e que muito me apoiaram. Sophia, Tiago, Ana, André, Filipe e Pedro, o vosso apoio foi muito importante! Uma nota

especial para o Tiago, por todo o seu empenho. E claro, para a Sophia, que se tem mostrado uma grande amiga e que foi incansável na fase final deste trabalho. Foi muito bom cruzar-me com pessoas como vocês!

Aos meus amigos por todo o apoio demonstrado.
À minha família por todo o amor e apoio incondicional que sempre me dedicaram.
Ao Paulo, pelo seu amor e dedicação, mas em especial pela sua paciência.
Sem vocês jamais teria sido possível!

The work presented in this thesis was only possible thanks to the finantial support from the research grant SFRH/BD/47596/2008 financed by FCT (Fundação para a Ciência e a Tecnologia).

This work was supported in part by the ERDF—European Regional Development Fund through the COMPETE Programme (operational programme for competitiveness), and National Funds through the FCT within the project FCOMP-01-0124-FEDER-009707 (HeliSysBio—molecular Systems Biology in Helicobacter pylori).

Abstract

Helicobacter pylori is associated with gastric diseases, such as gastritis, peptic and duodenal ulcers, mucosa associated lymphoid tissue lymphoma and gastric adenocarcinomas. Despite more than half of the global population being infected with this bacterium, not all individuals will develop clinical symptoms. Nevertheless, its association with gastric cancer, the high infection rate, as well as the failures on eradication efforts and vaccine development lead to an important health concern. In order to better understand the mechanisms leading to disease and also to develop effective ways to fight *H. pylori* infection, it is important to understand its physiological and metabolic behavior.

H. pylori is a microaerophilic, gram negative, fastidious organism, for which no effective defined medium has been developed. Furthermore, current cultivation procedures use media that, even when semi-defined, have a variety of nutrients that can be used as carbon and energy sources. Under those conditions, the metabolic and physiological characterization of *H. pylori* is very difficult.

The aim of this work was thus to study the physiology and metabolism of *H. pylori* to allow a better understanding of the behavior and pathogenicity of this organism. For that aim, a systems biology approach was used where Gas Chromatography-Mass Spectrometry (GC-MS) based metabolomics and genomics data were used to characterize the nutritional requirements and the preferred carbon sources and to build a reliable metabolic model.

Data on *H. pylori*'s exometabolome was for the first time collected from experiments performed with semi-defined media and allowed to establish the essentiality of several amino acids: L-histidine, L-leucine, L-methionine, L-valine, L-isoleucine and L-phenylalanine. Moreover, this analysis indicated that L-aspartate, L-glutamate, L-proline and L-alanine could be potential carbon sources for *H. pylori.* Thus, a comparative analysis of different amino and organic acids as carbon sources was performed and glutamine / glutamate emerged as the most effective compounds. However, since glutamine is

unstable under the conditions used, glutamate was selected the most adequate carbon source for growing *H. pylori*.

Then, a simplified medium containing only the essential amino acids and L-glutamate, besides vitamins and salts, as well as 5% of fetal bovine serum (FBS) was used to perform physiological studies. Under those conditions, the specific growth rate was determined to be 0.126 h^{-1}, while the use of uniformly labeled ^{13}C L-glutamate together with GC-MS measurements of proteinogenic amino acids allowed to confirm the essential amino acids and raise some clues about L-proline and L-alanine which, given their presence in FBS, had still unclear roles. L-proline, although not labeled, is probably not essential and could be obtained from arginine, while L-alanine showed very low labeling patterns and is hypothesized to originate from pyruvate. Finally, labeling experiments allowed to confirm the presence of a complete tricarboxylic acid cycle.

These collected data, together with genomics and other information available, were used to build and validate the first genome-scale metabolic model of *H. pylori* that is able to make quantitative predictions, covering roughly 23% of the genome. This model can be used, in the future, to investigate novel drug targets and elucidate the metabolic basis of infection.

Furthermore, a comparative study was performed that analyzed different methods for assessing growth, viability, culturability and morphology, as these are important physiological parameters.

Resumo

A caracterização fenotípica é de extrema importância para entender o metabolismo celular, especialmente em organismos patogénicos, para os quais, na sua maioria, a informação disponível é limitada. Compreender o metabolismo de um organismo patogénico é fundamental para desvendar os mecanismos de interação patogénio-hospedeiro, com vista à identificação de alvos para desenvolvimento de fármacos.

Neste trabalho estudou-se o metabolismo da bactéria *Helicobacter pylori*, um micro-organismo patogénico associado a doenças gástricas, usando uma estratégia de Biologia de Sistemas.

As experiências realizadas usando um meio liquido semi-definido para crescer *H. pylori* provaram a existência de um fator de *stress* associado a uma paragem do seu crescimento, acompanhada de uma mudança de morfologia. Sendo conhecido o caracter pleiomórfico da *H. pylori* quando sujeita a determinadas condições de *stress*, e dado que os requisitos nutricionais não se encontravam completamente definidos, foi levantada a hipótese deste fator de *stress* estar associado à falta de um nutriente essencial. Assim, foi efetuada uma análise de exometaboloma com vista a determinar os seus requisitos nutricionais e preferências. Verificou-se a existência de aminoácidos essenciais ao crescimento, e comprovou-se a preferência dos aminoácidos como fonte de carbono (glutamato, prolina, alanina e aspartato). No entanto, algumas dúvidas persistiram relativamente à essencialidade de prolina e alanina.

Para identificar a fonte de carbono preferencial foram testados diversos aminoácidos. Identificou-se que o aminoácido L-glutamato é o mais indicado ao crescimento de *H. pylori,* tendo-se efetuado a caracterização do seu crescimento com o referido aminoácido como fonte de carbono.

Como forma de comprovar a efetiva utilização de L-glutamato como fonte de carbono, foram efetuadas experiências com ^{13}C L-glutamato, tendo-se utilizado cromatografia gasosa com espectroscopia de massas para a análise das amostras. A

análise dos aminoácidos do hidrolisado de biomassa de *H. pylori* permitiu comprovar a utilização de L-glutamato como fonte de carbono. Comprovou-se ainda a essencialidade dos aminoácidos isoleucina, histidina, leucina, metionina, fenilalanina e valina. Foi possível também identificar algumas vias metabólicas ativas para as quais residiam dúvidas, como o caso da existência do ciclo de Krebs completo. As experiências realizadas permitiram ainda levantar hipóteses acerca da biossíntese de L-prolina e L-alanina em *H. pylori* a partir de L-arginina e piruvato, respetivamente.

Com a informação recolhida, associada à anotação do genoma recentemente efetuada foi possível reconstruir um modelo metabólico à escala genómica para *H. pylori* 26695. As previsões obtidas com o referido modelo estão de acordo com os dados experimentais. Este modelo contém informação biológica relevante para este organismo, com possível aplicação na identificação de potenciais alvos metabólicos, para a obtenção de fármacos mais efetivos na erradicação de *H. pylori*.

Table of Contents

1 Introduction 1

1.1 Thesis motivation and objectives 3

1.2 Structure of the thesis 4

1.3 References 6

2 State of the art 7

2.1 *Helicobacter pylori* – General Aspects 9

2.1.1 Taxonomy 9

2.1.2 Microbiological characteristics 10

2.2 Epidemiology of *Helicobacter pylori* infection 11

2.2.1 Prevalence of infection 11

2.2.2 Pathologies associated with *H. pylori* infection 12

2.3 In vitro growth of *Helicobacter pylori* 13

2.3.1 *In vitro* growth media 13

2.3.2 Environmental conditions 30

2.4 *Helicobacter pylori*'s Metabolism 31

2.4.1 Carbohydrates utilization 31

2.4.2 Central carbon metabolism 32

2.4.2.1 Glycolysis and gluconeogenesis 32

2.4.2.2 Entner-Doudoroff and Pentose Phosphate pathways 33

2.4.2.3 Pyruvate metabolism 33

2.4.2.4 Tricarboxylic acid cycle 35

2.5 Systems Biology 37

2.5.1 "Omics" Technologies 38

2.5.1.1 Metabolomics 39

2.5.1.2 *H. pylori* "Omics" data 44

2.5.2 Genome-scale metabolic models (GSMM) 58

2.5.2.1 Reconstruction process 58
2.5.2.2 *H. pylori* 26695 GSMMs 63
2.6 References 65

3. Growth and morphology assessment methods for *Helicobacter pylori* in liquid medium 89
3.1. Abstract 91
3.2. Introduction 93
3.3. Methods 95
3.3.1. Culture conditions 95
3.3.2. Cell-to-cell disaggregation 95
3.3.3. Growth assessment 96
3.3.4. Colony forming unit assay 96
3.3.5. Staining methods 96
3.4. Results and Discussion 98
3.4.1. Cell-to-cell disaggregation 98
3.4.2. Growth assessment and cell counts 100
3.4.3. Cellular Viability 103
3.4.4. Cellular Morphology 106
3.5. Conclusions 107
3.6. References 109
3.7. Supplementary material 115

4. Exometabolome analysis in *H. pylori* for the elucidation of nutritional requirements and preferences: reconciliation of *in silico* and *in vitro* metabolic capabilities 121
4.1. Abstract 123
4.2. Introduction 124
4.3. Methods 126
4.3.1. Culture conditions 126

4.3.2. Growth assessment 126
4.3.3. Extracellular metabolite analysis 127
4.4. Results 131
4.4.1. Exometabolome analysis 131
4.5. Discussion 139
4.5.1. Exometabolome analysis 139
4.5.2. Metabolic model simulations 149
4.6. Conclusions 151
4.7. References 152
4.8. Supplementary material 156

5. Evaluation of different carbon sources for the growth of *H. pylori* 26695 in liquid medium 163
5.1. Abstract 165
5.2. Introduction 166
5.3. Methods 168
5.3.1. Culture conditions 168
5.3.2. Media and Carbon Sources 169
5.3.3. Growth assessment and carbon source consumption 170
5.4. Results and discussion 170
5.4.1. *H. pylori* growth with different carbon sources 170
5.4.1. Metabolites analysis 176
5.5. Conclusions 180
5.6. References 182
5.7. Supplementary material 187

6. Characterization of the growth of *H. pylori* using glutamate as the main carbon source... 193
6.1. Abstract 195
6.2. Introduction 196
6.3. Methods 197
6.3.1. Culture conditions 197
6.3.2. Culture medium 198
6.3.3. Growth assessment 198
6.3.4. Metabolites analysis 199
6.3.5. ^{13}C labeling experiments 199
6.3.6. Data analysis 200
6.4. Results and Discussion 201
6.4.1. Growth of *H. pylori* with glutamate 201
6.4.2. Extracellular metabolites analysis 203
6.4.3. ^{13}C labeling analysis 205
6.5. Conclusions 211
6.6. References 212
6.7. Supplementary material 215

7 Reconstruction and validation of a genome–scale metabolic model for *Helicobacter pylori* 26695 221
7.1 Abstract 223
7.2 Introduction 224
7.3 Methods 225
7.3.1 Metabolic network assembly 226
7.3.2 Reactions compartmentation 226
7.3.3 Assignment of reversibility to reactions 226
7.3.4 Reactions stoichiometry 227
7.3.5 Gene-protein-reaction associations 227
7.3.6 Biomass formation 228

7.3.7 Growth medium requirements 229
7.3.8 Model curation 229
7.3.9 Simulation and model optimization 230
7.3.10 Model validation 230
7.4 Results and Discussion 231
7.4.1 Genome re-annotation and network assembly 231
7.4.2 Biomass formation 232
7.4.2.1 Protein entity 232
7.4.2.2 Nucleotide content 233
7.4.2.3 Peptidoglycans and Lipopolysaccharides 234
7.4.2.4 Lipids 234
7.4.2.5 Cofactors 235
7.4.2.6 Energy requirements 236
7.4.3 Model curation 237
7.4.4 Model Evaluation 237
7.4.4.1 Model characterization 237
7.4.4.2 Gene essentiality 239
7.4.4.3 Prediction of physiological data 240
7.4.5 Flux distribution analysis 245
7.5 Conclusions 248

8. Concluding Remarks 255

List of Figures

Figure 2.1. Worldwide prevalence of *H. pylori*. 12
Figure 2.2. TCA cycle in *H. pylori* with possible enzymes involved in each reaction. 36
Figure 2.3 "Omes" and respective "omics" technologies. 38
Figure 2.4. Workflow in a metabolomics approach 40
Figure 2.5. Genome-scale metabolic model reconstruction overview. 58

Figure 3.1. Growth of *H. pylori* 26695.....99
Figure 3.2. Epifluorescence microscope images of *H. pylori* 26695 in liquid culture after cell disaggregation... 102
Figure 3.3. Measurements of optical density (600 nm), culturable cells, and total cell counts with DAPI stain and PNA FISH probe counts..... 103
Figure 3.4. Percentage of viable cells and total cell counts (Live/Dead kit) and culturable cell counts along time in an *H. pylori* 26695 culture in liquid medium 104
Figure 3.5. Epifluorescence microscope images of a *H. pylori* 26695 culture stained with Syto9/Propidium iodide (Live/Dead kit)..... 105
Figure 3.6. Cell morphology of *H. pylori* 26695 along culture time. 107
Figure 3.7. OD600 and CFU/mL in disaggregation assays.....116

Figure 4.1. Evolution of organic acids (lactate, pyruvate, citrate, succinate) percentage along time in the extracellular medium and Optical Density measured at 600 nm.. 131
Figure 4.2. Analysis of the amino acids profiles obtained from the *H. pylori* culture. 134
Figure 4.3. Evolution of glucose and acetate concentrations 136
Figure 4.4. Schematic diagram of *H. pylori*'s metabolic map, and metabolites evolution analyzed in the extracellular medium during the culture..... 148
Figure 5.1. Growth (OD_{600}) of *H. pylori* 26695 using different carbon sources..... 172
Figure 5.2. Factor increase in optical density (OD600 nm) after 48 hours of culture and specific growth rate (exponential phase) for each carbon source tested. 172

Figure 5.3. Catabolic pathways predicted to be utilized by *H. pylori* 26695 for the utilization of the carbon sources tested..... 176
Figure 5.4. Carbon source consumption after 48 hours of culture..... 177

Figure 6.1. Flowchart applied for extracellular metabolites and biomass hydrolysates analysis by GC-MS. 200
Figure 6.2. Biomass concentration represented by Cell Dry Weight (CDW) and L-glutamate in the culture medium along time as a percentage of the initial concentration.. 202
Figure 6.3. Heat map obtained with MeV representing the compounds identified in the supernatant of the *H. pylori* culture along the fermentation 204
Figure 6.4. Fractional labeling (with and without unlabeled biomass correction) calculated for each amino acid present in the protein of biomass hydrolysates..... 206
Figure 6.5. Schematic representation of *H. pylori*'s metabolic pathways active under the conditions of the described experiments..... 210
Figure 6.6. Biomass calibration curve. 215

Figure 7.1. Genome-scale metabolic model reconstruction workflow. 225
Figure 7.2. *H. pylori* 26695 re-annotation results and statistics..... 231
Figure 7.3. Metabolites and flux distribution in the central carbon pathways when simulating *i*TR370 in minimal medium. 247

List of Tables

Table 2.1. Complex solid media described for *H. pylori* growth. 16
Table 2.2. Complex liquid media described for *H. pylori* growth. 21
Table 2.3. Semi-defined liquid media (defined media supplemented with undefined components) described for *H. pylori* growth..... 27
Table 2.4. Defined media described for *H. pylori* growth. 28
Table 2.5 Terms and respective definitions applied in metabolomic analysis.. 40
Table 2.6. *H. pylori* genomic features, obtained from the average of 54 fully-sequenced strains 45
Table 2.7. Transcriptomics studies with *H. pylori*.. 47
Table 2.8. Proteomics studies with *H. pylori*. 51
Table 2.9. Model curation steps 61
Table 2.10. Steps to be performed to evaluate the reconstructed metabolic model..... 63
Table 2.11. *In silico H. pylori* 26695 metabolic networks characterization..... 64

Table 3.1. Composition of the hybridization solution. 115
Table 3.2. Composition of the washing solution. 115
Table 3.3. Mean values of cell counts for each method performed for three biological replicates..... 117
Table 3.4. Total and viable cell counts using the Live/dead kit performed for three biological replicates.. 118
Table 3.5. Mean percentage of spiral cell counts for each method performed for three biological replicates. 119
Table 3.6. Mean percentage of intermediate and coccoid cell counts for each method performed for three biological replicates. 120

Table 4.1. Results of the simulations performed with the *I*T 341 GSM/GPR model, using Flux Balance Analysis in Optflux, showing the environmental conditions tested and the biomass predicted for each simulation. 138
Table 4.2. Comparison of amino acids essentiality (*in vitro* and *in silico*), or consumption reported in the published studies for *H. pylori* and results of the present study. 142
Table 4.3. Composition of the Ham's F-12 medium..... 156
Table 4.4. Compounds used to prepare the standards for GC-MS analysis. 158
Table 4.5. Mass to charge ratios for the molecular ions, major fragments and retention times for each compound in the in-house library. 160
Table 4.6. Percentage of compounds detected in the extracellular culture medium along time 161

Table 5.1. Composition of the media tested. 169
Table 5.2. Composition of the Ham's F-12 medium and characteristics of the compounds used to prepare the mixture. 187
Table 5.3. Compounds identified in the fetal bovine serum by GC-MS, mean of two technical replicates and the corresponding concentration in the final broth. 189
Table 5.4. Essential amino acids identified in the culture medium by GC/MS at 48 h of *H. pylori* culture in percentage. 190
Table 5.5. Compounds identified in the culture medium by GC/MS at 48 h of culture in percentage compared to the concentration at 0 h of culture.. 191

Table 6.1. Culture medium composition. 198
Table 6.2. Growth parameters for *H. pylori* 26695 growing in liquid medium with L-glutamate. 202
Table 6.3. Evolution of the compounds identified in the culture medium as a percentage of the initial concentrations obtained by GC/MS. 216
Table 6.4. Mass fractions calculated for mass isotopomers of each derivatized amino acid in biomass hydrolysates. 217
Table 6.5. Fractional labeling determined for the fragments used for each amino acid.. 220

Table 7.1. Macromolecular composition of the biomass of *H. pylori* and respective contribution to the overall biomass. 232
Table 7.2 Total amount of amino acids in biomass composition 233
Table 7.3. Total amount of dNTPs in the biomass composition. 233
Table 7.4. Total amount of NTPs in the biomass composition. 234
Table 7.5. Total amount of cell wall metabolites in the biomass composition. 234
Table 7.6. Total amount of different lipids in the biomass composition. 235
Table 7.7. Different cofactors in the biomass composition with the respective coefficient 236
Table 7.8. Metabolic model characteristics. 238
Table 7.9. Comparison between the *i*T341 GSM/GPR model and the metabolic model developed in this work (*i*TR370). 239
Table 7.10. Comparison between essential genes verified experimentally and retrieved from the OGEE database and model predictions. 240
Table 7.11. Metabolic model simulations performed using experimental data on uptake rates as environmental conditions and varying the flux of the ATP Maintenance reaction in the model 242

Abbreviations

$\Delta_f G$ – free Gibbs energy

ΔG - Gibbs energy

ala - alanine

AMDIS - automated mass spectral deconvolution and identification system

ADP - adenosine diphosphate

ANOVA - analysis of variance

Arg – arginine

Asn – asparagine

Asp – aspartic acid

ATP - adenosine triphosphate

BLAST – basic local alignment search tool

CBA - Columbia base agar

CDS – coding sequences

CDW - cell dry weight

CE-MS - capillary electrophoresis–mass spectrometry

CFU - colony-forming units

CTP - cytosine triphosphate

Cys - cysteine

DAPI - 4',6-diamidino-2-phenylindole

DNA - deoxyribonucleic acid

dATP – deoxyadenine triphosphate

dCTP - deoxycytosine triphosphate

dGTP - deoxyguanine triphosphate

dNTP – deoxyribonucleotide triphosphate

dTTP - deoxythymine triphosphate

DW – dry weight

EC - enzyme commission

ED - Entner-Doudoroff

EI - electron ionization

ELISA - enzyme-linked immunosorbent assay

FBA - flux balance analysis

FBS - fetal bovine serum

FMOC - 9-fluorenylmethyl chloroformate

FTIR - fourier transform infrared spectroscopy

gDW – grams dry weight

GC - gas chromatography

GC-MS - gas chromatography–mass spectrometry

GEO - gene expression omnibus

GPR - gene-protein-reaction

GSM – genome scale model

GSMM - genome scale metabolic model

GTP - guanine triphosphate

HCL - hierarchical clustering

His - histidine

HMMs – hiden Markov models

HPLC – high pressure liquid chromatography

Ile - isoleucine

KEGG - kyoto encyclopedia of genes and genomes

KMC - K-Means clustering

LC - liquid chromatography

LC-MS - liquid chromatography-mass spectrometry

Leu – leucine

LPS – lipopolysaccharides

Lys - lysine

MALDI - matrix-assisted laser desorption/ionization

MALT - mucosa associated lymphoid tissue

MCF - methyl chloroformate

merlin – metabolic models reconstruction using genome-scale information

Met – methionine

MS - mass spectrometry

m/z – mass to charge ratio

NADP - nicotinamide adenine dinucleotide phosphate

NADPH - nicotinamide adenine dinucleotide phosphate-oxidase

NCBI - National Center for Biotechnology Information

NGS - next-generation sequencing

NIST - National Institute of Standards and Technology

NMR - nuclear magnetic resonance

NTPs – nucleosides triphosphate

OD - optical density

OGEE – online gene essentiality database

OMP - outer membrane proteins

OPA - o-phthalaldehyde

ORF - open reading frames

PBS - phosphate saline buffer

Phe - phenylalanine

PNA FISH - peptic nucleic acid fluorescence in situ hybridization

PP - pentose phosphate

Pro - proline

RNA - ribonucleic acid

rRNA - ribosomal ribonucleic acid

RSD - relative standard deviation

SBML - systems biology markup language

SD – standard deviation

Ser – serine

TCA - tricarboxylic acid

Thr – threonine

tRNA – transfer ribonucleic acid

Trp - tryptophan

TSA - tryptic soy agar

Tyr - tyrosine

UHPLC - ultra high performance liquid chromatography

UV – ultra violet

UTP – uracil triphosphate

v/v – volume by volume

Val - valine

VBNC - viable but non culturable

w/o – without

w/v – weight by volume

Chapter 1

Introduction

1.1 *Thesis motivation and objectives*

Helicobacter pylori is one of the most thriving human pathogens, being disseminated all over the world[1]. Unless treated, *H. pylori* can persist in the human stomach for life, although not all individuals will develop disease. The disease outcome can vary from gastritis, peptic ulcer, gastric cancer to mucosal-associated lymphoid tissue lymphoma.

To fully understand the mechanisms associated with host colonization and host-pathogen interaction, it is indispensable to understand the pathogen's metabolism inside the host, where it must extract nutrients to fulfill its metabolic requirements[2]. In the particular case of *H. pylori*, its metabolism and physiology are not well studied, owing, in part, to the difficulties found until now in growing this pathogen *in vitro* under defined conditions.

Using Systems Biology approaches, different tools can be applied to understand the system as a whole. The use of "omics" data has made possible the reconstruction of genome-scale metabolic models for a large number of organisms. This type of *in silico* models allows to predict cellular behavior, bridging the gap between genotypes and phenotypes, aiding efforts to diverse areas, including drug discovery[3,4]. The availability of the genome sequence of *H. pylori* 26695 and its annotation have allowed the construction of metabolic models for this organism[5,6]. However, the accuracy of model predictions is associated with the data used to build and validate the model, which is limited for *H. pylori*.

This work aimed at studying *H. pylori*'s metabolism using a Systems Biology approach. The specific goals included:

- Contribute to understand the nutritional requirements and preferences of *H. pylori*;
- Collect physiological and metabolomics data that can help to understand more of *H. pylori*'s metabolism;

- Reconstruct a new genome-scale metabolic model based on novel results on genome (re-)annotation;
- Use the physiological data collected to validate the genome-scale metabolic model.

1.2 *Structure of the thesis*

This thesis is composed of eight chapters. Chapter 2 is a general introduction to the topics, and can be divided into two main subjects: *H. pylori* and Systems Biology. The part devoted to *H. pylori* addresses mainly topics related with *H. pylori*'s microbiological characteristics, growth, physiology and metabolism. In the Systems Biology part, emphasis on "omics" technologies is given, with an overview on omics studies reported for *H. pylori*. The Metabolomics approach, which is the "omics" technology used in this thesis, is further explored. Finally, the process of genome-scale metabolic model reconstruction is described.

Considering the well-known *H. pylori*'s pleiomorphic nature, in Chapter 3 a study of growth and morphology assessment methods for *H. pylori* growing in liquid medium is presented. This study allowed concluding about the suitable methods to monitor *H. pylori*'s growth.

Chapter 4 presents a reconciliation of *H. pylori*'s nutritional requirements, gathering experimental results and *in silico* predictions. A metabolic footprinting approach was applied to understand which are the components being used when *H. pylori* was growing using a "complete" liquid medium (containing all 20 amino acids) and thus, infer about amino acids requirements.

Chapter 5 and 6 are devoted to the study of *H. pylori*'s preferred carbon sources. In Chapter 5, different compounds (mainly amino acids) were tested and compared as carbon sources for *H. pylori*'s growth. Based on the results obtained in Chapter 5, glutamate was selected as the preferred carbon source, and the growth using this

substrate was further characterized in Chapter 6. A strategy of using an isotopically labelled substrate (^{13}C glutamate) was performed in order to determine the labelling profile in several biomass constituents.

The reconstruction of an updated genome-scale metabolic model for *H. pylori* 26695 is presented in Chapter 7. This chapter includes several steps: genome re-annotation, reconstruction using a semi-automated method, manual curation, definition of biomass composition (determined experimentally) and model validation with the experimental data obtained in previous chapters.

To conclude, in Chapter 8 the main conclusions and considerations about future work are presented.

1.3 *References*

1. Azevedo, N. F., Guimarães, N., Figueiredo, C., Keevil, C. W. & Vieira, M. J. A new model for the transmission of *Helicobacter pylori*: Role of environmental reservoirs as gene pools to increase strain diversity. *Crit. Rev. Microbiol.* **33,** 157–169 (2007).

2. Rohmer, L., Hocquet, D. & Miller, S. I. Are pathogenic bacteria just looking for food? Metabolism and microbial pathogenesis. *Trends Microbiol.* **19,** 341–348 (2011).

3. Yeh, I., Hanekamp, T., Tsoka, S., Karp, P. D. & Altman, R. B. Computational analysis of *Plasmodium falciparum* metabolism: Organizing genomic information to facilitate drug discovery. *Genome Res.* **14,** 917–924 (2004).

4. Chavali, A. K., Whittemore, J. D., Eddy, J. A, Williams, K. T. & Papin, J. A. Systems analysis of metabolism in the pathogenic trypanosomatid *Leishmania major*. *Mol. Syst. Biol.* **4,** 1–19 (2008).

5. Schilling, C. H. *et al.* Genome-scale metabolic model of *Helicobacter pylori* 26695. *J. Bacteriol.* **184,** 4582–4593 (2002).

6. Thiele, I., Vo, T. D., Price, N. D. & Palsson, B. Ø. Expanded metabolic reconstruction of *Helicobacter pylori* (*i*T341 GSM/GPR): an *in silico* genome-scale characterization of single- and double-deletion mutants. *J. Bacteriol.* **187,** 5818–5830 (2005).

Chapter 2

State of the art

2.1 *Helicobacter pylori* – General Aspects

In 1982, Barry J. Marshall and J. Robin Warren identified a bacillary organism in the gastric epithelium[1], and, at that time, they could not imagine that their discovery would result in the awarding of the Nobel Prize in Physiology and Medicine in 2005[2]. With their discovery, they changed the assumption that peptic ulcer was caused by stress and lifestyle[1,2]. In fact, the association of *Helicobacter pylori* with gastritis and peptic ulcer disease was proved later through studies with human volunteers[1–4].

Due to its relation with gastric diseases, in the last 20 years intense research has been performed around *H. pylori*, proved by the number of publications that increased from around 500 in 1992 to around 1500 in 2012, totalizing more than 32 000 publications in international peer-reviewed journals (searched with "*Helicobacter pylori*" terms in the PUBMED database)[5].

2.1.1 Taxonomy

H. pylori is a member of the Proteobacteria phylum, belonging to the class Epsilonproteobacteria, Campylobacterales order, Helicobacteraceae family[6]. Despite the differences found in flagella, in 1984 *H. pylori* was included in the *Campylobacter* genus and was named *Campylobacter pyloridis* [7]. In 1987, the nomenclature was revised and the species name was corrected to *Campylobacter pylori* [8]. In the following years, several studies revealed significant differences between this organism and *Campylobacter* species, being more closely related with *Wolinella succinogenes* [9,10]. In 1989, *C. pylori* was included in a new genus - *Helicobacter*. The name refers to its helical morphology, and this species was designated *Helicobacter pylori* [11]. In the *Helicobacter* genus there are more than 20 species, including human and animal pathogens, with new *Helicobacter* species being regularly discovered[6,12–14]. The features that can be used to differentiate *Helicobacter* species are: host, location, morphological characteristics (cell size, flagella), growth conditions, antibiotics susceptibility, biochemical characteristics (such as catalase, oxidase and urease activity, nitrate reduction, among others), or G+C content[6,13,14]. There are two

major groups of *Helicobacter* species: the gastric *Helicobacter* species (such as *H. felis*, *H. mustelae*, *H. acinonychis*, *H. pylori*, among others) and non-gastric (enterohepatic) *Helicobacter* species (such as *H. hepaticus, H. pullorum, H. cinaedi, H. canis*, among others)[13–15]. These groups present a high level of specificity relatively to the organ they colonize[15].

2.1.2 Microbiological characteristics

H. pylori is a gram-negative bacterium, measuring 2.0-5.0 μm in length and 0.5-1.0 μm in width[15–17]. Although it usually exhibits a spiral or curved rod shape[15,16], coccoid shapes can appear when the organism is subjected to certain adverse conditions, such as prolonged *in vitro* culture, increased temperature, alkaline pH, increased oxygen tension, or antibiotic treatment[18]. There is some controversy about the nature of these coccoidal forms, with some authors reporting that they represent a morphological manifestation of cell death[19], and others a viable but non culturable state (VBNC)[20,21]. It is thought that these forms cannot be cultured *in vitro*, although they are metabolically active. Despite evidences that these forms can induce infection, this is another controversial topic. The recovery of coccoid to spiral forms in *H. pylori* was reported, and notwithstanding this fact was proven in other species such as *E. coli* or *S. tiphymurum*, this result is still not universally accepted by the scientific community, since other authors were not able to prove these findings in *H. pylori*. During the conversion of *H. pylori* spiral to coccoid forms, intermediate U forms can also be observed[22].

H. pylori is motile, with 2-6 sheathed unipolar flagella of approximately 3 μm long and 2.5 nm thick. Each flagellum frequently carries a distinctive terminal bulb, which is an expansion of the flagellar sheath[16,23–25]. The sheath is an extension of the outer membrane and its role can be to protect the flagellar structure from the acidic environment of the stomach[16,17,24]. The flagella, in association with the spiral shape, are essential for host colonization, allowing the movement in viscous solutions such as the mucus layer of the gastric epithelium[25–27]. When cultured in plates with solid medium, *H. pylori* colonies appear

translucent, not clearly haemolytic and with 1-2 mm in diameter[23]. *H. pylori* is a microaerophilic and non-sporulating organism[28].

2.2 *Epidemiology of Helicobacter pylori infection*

2.2.1 Prevalence of infection

H. pylori is the agent of one of the most disseminated infections in the world[29]. There are many studies reporting the prevalence of *H. pylori* infection in different countries along time, with review articles being published every year within the last years[30–35]. The prevalence of *H. pylori* infection varies with geographical areas, age, race and socioeconomic status[30]. The global prevalence of *H. pylori* is depicted in Figure 2.1.

In general, more than 50% of the global population is infected with *H. pylori* [29], ranging from 25-50% of infection in developed countries to 70-90% in developing countries[12]. The infection rate observed in developing countries might be related with factors such as unsanitary conditions and contaminated water[12]. It is important to highlight that a high *H. pylori* prevalence does not mean a high rate of disease. For instance, in developed countries there is a low infection rate and a relatively high prevalence of gastric cancer and the opposite is also true for some countries[36].

H. pylori is mostly acquired in childhood, probably from close family members[12,15] and, if not treated, may become a lifelong infection[15,29]. It is clear that the infection rates have been decreasing in the last years, with emphasis in developed and developing countries[35], although this fact is more noticeable in developed countries and can be linked to improvements in hygiene practices[30] and with the decrease of family sizes[37].

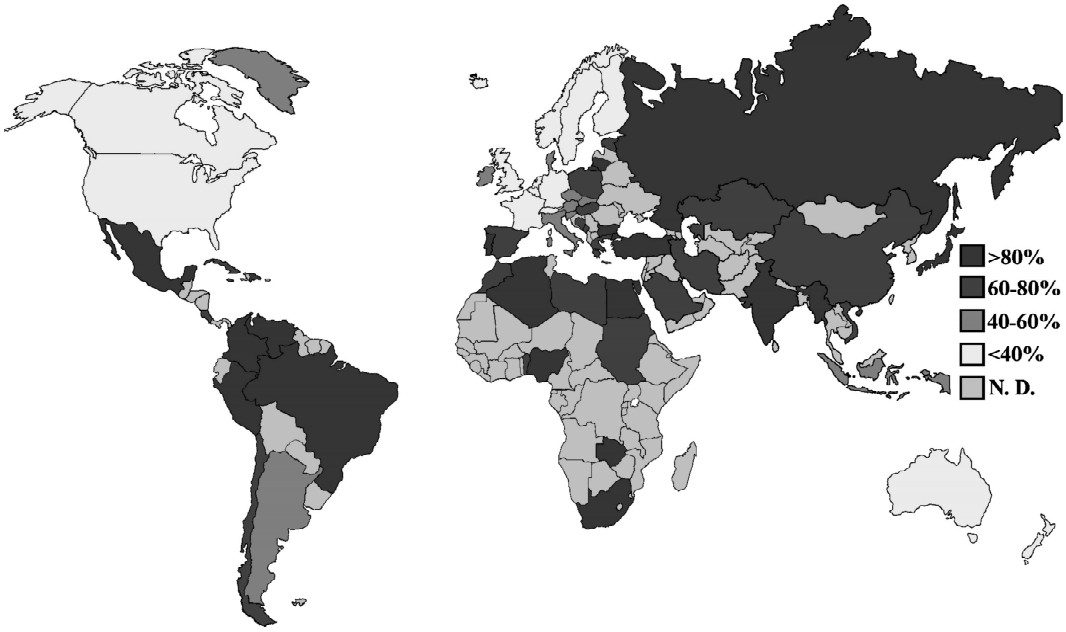

Figure 2.1. Worldwide prevalence of *H. pylori*. N.D. means that no consistent data were found. Adapted from Azevedo *et al.* (2007)[38].

2.2.2 Pathologies associated with *H. pylori* infection

Despite the fact that more than half of the global population is infected with *H. pylori*, the infection is frequently asymptomatic and only a small proportion of the individuals will develop clinical signs of its colonization[15,39].

H. pylori's association with gastric diseases is well known, and includes conditions such as gastritis, peptic ulcer, adenocarcinome and mucosa associated lymphoid tissue (MALT) lymphoma[12]. Gastric cancer is the second most prevalent cancer in the world[39]. In the last years, aspects related with *H. pylori* associated diseases have been systematically updated in the "Helicobacter" Journal. Those reviews are divided in non-malignant diseases[40–46] and gastric malignancies (cancer and lymphoma)[47–53]

It is estimated that patients who carry *H. pylori* have a 10-20% risk of developing a ulcer disease in their lifetime and a 1-2% risk of developing distal gastric cancer[15]. The particular risk of developing a disease in the presence of *H. pylori* infection has been associated with bacterial, host and environmental factors[15].

The possible association of *H. pylori* infection with other diseases, besides gastric diseases, has now been intensively investigated. Studied conditions include cardiovascular,

respiratory and ear, nose and throat diseases, hematologic, ophthalmology, oral mucosa and skin diseases, hepatobiliary diseases, diabetes mellitus and metabolic disorders, immunologic diseases, and neurological disorders. For some disorders, for instance Idiopathic Thrombocytopenic Purpura (ITP) there are strong evidences that there is a link between the disease and *H. pylori* infection[54,55], whilst for other diseases more studies are needed in order to prove *H. pylori* association. The studies published on extra gastric manifestations of *H. pylori* infection have been systematically reviewed in the last years in the "Helicobacter" Journal[54–63].

2.3 *In vitro growth of Helicobacter pylori*

2.3.1 *In vitro* growth media

Since its first culture in 1984, a considerable number of studies describing media have been published, either to transport, isolate, preserve or cultivate *H. pylori in vitro*. The use of both solid and liquid media has been reported, although the best results were obtained using solid media, frequently supplemented with sheep or horse blood (Table 2.1).

Growth in liquid media is not straightforward to achieve, as *H. pylori* grows very slowly even in rich media, and contamination with other organisms is a concern. Thus, antibiotics (vancomycin, polymyxin, trimethoprim, amphotericin, polymyxin, among others) are often added. Complex liquid media are mostly used (Table 2.2), although a few semi-defined media have also been developed, where defined medium are used but supplemented with undefined components (Table 2.3). The use of some defined supplements (cyclodextrins or cholesterol) has also been described as an adequate replacement for the complex supplements (Table 2.4). However, the cell densities obtained are quite low and the supplementation with undefined components drastically improves growth. The use of undefined components such as fetal bovine serum (FBS), horse serum (HS) or bovine serum albumin (BSA) is a setback when cultures with defined

media are required, such as in proteomics or metabolomics studies. The exact function of the supplements added to the culture medium is unknown, and it is not yet clear whether supplements have a nutritional function. Animal serum, for example, is a very rich mixture of components, considered undefined and variable, although some compounds have been identified such as protein components, hormones, fatty acids, vitamins and growth factors, among others[64]. It is hypothesized that serum may act as a growth-stimulating factor[65,66], but it can also be speculated that it acts as an attachment and/or detoxifying factor by binding to and inactivating toxic compounds, like in cell culture media[64].

Cyclodextrin, another frequently used supplement, was described to increase medium viscosity and osmolarity[67] and/or to act by chelating toxic molecules present in the culture medium or produced by microbial metabolism[65,67,68]. Cholesterol is considered a growth-enhancing compound[67,69], and it is present in serum and blood. It was found that *H. pylori* can incorporate cholesterol and it comprises around 25% of the lipid membrane content of *H. pylori* [70–73], although it seems that *H. pylori* cannot synthesize it, neither it is an absolute requirement for growth[67].

In fact, the use of defined liquid media for *H. pylori* was reported[74–76]. All of the described media have similar basis, with differences, in some cases, only in one amino acid[74]. Inorganic salts and vitamins are also present, although some media have only thiamine[75]. Other components are present, such as glucose[74–76], pyruvate[67], lipoic acid[67,77] among others. Ham's F-12 is the most complete medium in terms of compounds, but with lower concentrations of amino acids. In addition, it was described to support robust growth, even using small inocula[67,78].

However, in none of the reported studies has *H. pylori* survived in the defined medium without adaptation. This adaptation to completely defined media, without supplements, was achieved by either replacing complex by defined medium in continuous cultures[75] or by diluting semi-defined medium with fresh medium without supplements with subsequent passages to defined medium[79]. In other cases, *H. pylori* only survives in defined media if it is directly inoculated from plates for each liquid experiment.

Table 2.1. Complex solid media described for *H. pylori* growth.

Different media described for *H. pylori* growth. When the medium is a derivation from another medium this is indicated in the components column. When the purpose of the medium was other than cultivation, it is indicated in the notes column. Supplements: w/o – without; YE – yeast extract; Serum-based – with one of the following serum-based supplements, horse serum, fetal calf serum, calf serum, iron-supplemented calf serum, heat-treated fetal bovine serum; heat-treated adult bovine serum; Blood-based – with one of the following blood-based supplements, human blood, rabbit blood, horse blood, heated horse blood; lysed horse blood, defibrinated horse blood, sheep blood, defibrinated sheep blood; HM – hemin; EYE – egg yolk emulsion, CL – cholesterol; BSA – bovine serum albumin or lipid-rich bovine serum albumin; CD – β-cyclodextrin or 2,6-di-O-methyl-β-cyclodextrin; ST – starch or cornstarch; CC – charcoal or activated charcoal. TTC - Triphenyl tetrazolium chloride; IsoVitaleX – enrichment with glucose, amino acids, vitamins, nucleotides and iron.

Medium	Components added	Supplements											Notes	Reference
		w/o	YE	Serum-based	Blood-based	HM	EYE	CL	BSA	CD	ST	CC		
Belo Horizonte Medium	BHIA TTC				✓								-	Queiroz *et al.* (1987)[80]
Blood Agar Base	-				✓								Isolation and subcultivation	Ansorg *et al.* (1991)[81]
	-				✓								-	Hutton *et al.* (2012)[82]
	-			✓									-	
	-									✓			–	
	-								✓				-	
Brain Heart Infusion Agar (BHIA)	-	✓											-	Kehler *et al.* (1994)[83]
	IsoVitaleX Antibiotics				✓								-	Goodwin *et al.* (1985)[84]
	-				✓								Isolation	Hachem *et al.* (1995)[85]
	IsoVitaleX						✓						-	Westblom *et al.* (1991)[86]

Table 2.1. Complex solid media described for *H. pylori* growth. (Continued).

Medium	Components added	Supplements											Notes	Reference
		w/o	YE	Serum-based	Blood-based	HM	EYE	CL	BSA	CD	ST	CC		
Brain Heart Infusion Agar (BHIA)	-									✓			-	Ohno and Murano (2007)[87]
	-			✓									-	Shibayama *et al.* (2006)[88]
Brucella Agar (BA)	-			✓									-	Buck and Smith (1987)[89]
	-										✓		-	
	-											✓	-	
Brussels *Campylobacter* Charcoal Agar	TTC Antibiotics		✓	✓								✓	Isolation and subcultivation	Ansorg *et al.* (1991)[81]
Brugmann agar (Horse blood based)	Agar TTC Antibiotics				✓								Selective medium for isolation from biopsies	Deyi *et al.* (2010)[90]
Campylobacter pylori selective (CPS)	CBA Skirrow's medium with modifications				✓								Selective medium for isolation	Dent and McNulty (1988)[91]
Columbia base agar (CBA)	-				✓								-	Secker *et al.* (1991)[92]
	IsoVitaleX Urea Phenol red Granulated agar					✓							Detection of urease activity	Cellini, *et al.* (1992)[93]
	-									✓			-	Olivieri *et al.* (1993)[94]
	IsoVitaleX				✓								-	Albertson *et al.*(1998)[69]
	-				✓								-	Stevenson *et al.* (2000)[95]

Table 2.1. Complex solid media described for *H. pylori* growth. (Continued).

Medium base	Components added	Supplements											Notes	Reference
		w/o	YE	Serum-based	Blood-based	HM	EYE	CL	BSA	CD	ST	CC		
Chocolate agar (CBA based)	CBA	✓												Buck and Smith (1987)[89]
											✓		-	
												✓	-	
	CBA				✓								Transport medium	Xia *et al.*(1993)[96]
Egg Yolk Enulsion (EYE) Agar	CBA based IsoVitaleX TTC						✓						-	Westblom *et al.* (1991)[86]
GAB-CAMP medium modified	GC agar base IsoVitaleX Antibiotics				✓								-	Soltesz *et al.* (1992)[97]
	GC agar base			✓								✓	-	Taneera *et al.* (2002)[98]
Gonococci (GC) Agar Base	-	✓											-	Buck and Smith (1987)[89]
	-										✓		-	
	-											✓	-	
	-										✓	✓	-	
GCHI chocolate agar	Antibiotics	✓											-	Morgan *et al.* (1987)[99]
H. pylori special peptone agar (HPSPA)	Special peptone Yeast extract Beef extract Sodium chloride Pyruvic acid Sodium Salt Granulated agar	✓											Selective medium for isolation from cattle and beef samples	Stevenson *et al.* (2000)[95]
					✓								-	

Table 2.1. Complex solid media described for *H. pylori* growth. (Continued).

Medium base	Components added	Supplements											Notes	Reference
		w/o	YE	Serum-based	Blood-based	HM	EYE	CL	BSA	CD	ST	CC		
HP agar (HPSPA based)	Yeast extract Beef extract Special peptone Sodium chloride Hydrochloric acid Urea Phenol red Antibiotics			✓									Selective medium for water samples	Degnam *et al.* (2003)[100]
Iso-sensitest agar (Oxoid)	-				✓								Antimicrobial susceptibility test	Hartzen *et al.* (1997)[101]
Johnson Murano Agar	-				✓								-	Stevenson *et al.* (2000)[95]
Modified Glupczynski medium	BHIB Based Legionella CYE agar TTC Antibiotics		✓									✓	Selective medium	Tee *et al.* (1991)[102]
	BHIB Based Legionella CYE agar			✓									-	Stevenson *et al.* (2000)[95]
Mueller-Hinton Agar (MHA)	-	✓											-	Buck and Smith (1987)[89]
	-									✓			-	Olivieri *et al.* (1993)[94]

Table 2.1. Complex solid media described for *H. pylori* growth. (Continued).

Medium base	Components added	Supplements											Notes	Reference
		w/o	YE	Serum-based	Blood-based	HM	EYE	CL	BSA	CD	ST	CC		
Mueller-Hinton Agar (MHA)	-				✓								-	Walsh and Moran (1997)[103] Stevenson *et al.* (2000)[95] Vega *et al.*(2003)[104]
Skirrow Agar	Antibiotics	✓											Isolation from biopsies	Krajden *et al.* (1987)[105]
	Antibiotics				✓								Isolation from biopsies	Coudron and Kirby (1989)[106]
				✓	✓									
				✓	✓			✓						
Tryptic Soy Agar (TSA)	-				✓								Isolation from biopsies	Coudron and Kirby (1989)[106] Hachem *et al.* (1995)[85] Walsh and Moran (1997)[103]
	-			✓	✓								Isolation from biopsies	Coudron and Kirby (1989)[106]
Vestfold Charcoal (Charcoal agar based)	IsoVitaleX TTC			✓									-	Henriksen *et al.* (2000)[107]

Table 2.2. Complex liquid media described for *H. pylori* growth.

Different media described for *H. pylori* growth. When the objective of the medium was other than cultivation, this is indicated in the notes column. w/o – without; YE – yeast extract; Serum-based – with one of the following serum-based supplements, horse serum, fetal calf serum, new-born calf serum, iron-supplemented calf serum, heat-inactivated horse serum, heat-treated fetal bovine serum, heat-treated adult bovine serum, human serum; Blood-based – with one of the following blood-based supplements, human blood serum, human blood lysed, human erythrocyte lysate, lamb blood; PGM – porcine gastric mucin; BSA – bovine serum albumin or lipid-rich bovine serum albumin; HM – hemin; CL – cholesterol; CD – α-cyclodextrin, β-cyclodextrin or 2,6-di-O-methyl-β-cyclodextrin; CE – cyanobacterial extract; ST – starch or cornstarch; MC – methyl cellulose; AC – activated charcoal; IsoVitaleX – enrichment with glucose, amino acids, vitamins, nucleotides and iron; Vitox - enrichment with glucose, amino acids, vitamins, nucleotides and iron.

Medium base	Components added	Supplements													Notes	Reference
		w/o	YE	Serum-based	Blood-based	PGM	BSA	HM	CL	CD	CE	ST	MC	AC		
Brain Heart Infusion Broth (BHIB)	-	✓													-	Shahamat *et al.* (1991)[108] Kehler *et al.* (1994)[83]
	-		✓												-	Shahamat *et al.* (1991)[108]
	-			✓											Cultivation from biopsies	Shahamat *et al.* (1991)[108] Xia *et al.*(1993)[96] Jiang and Doyle (2000)[109] Sainsus *et al.* (2008)[78]
	-		✓	✓											Transport medium	Shahamat *et al.* (1991)[108] Xia *et al.*(1993)[96]
	-			✓											-	Stevenson *et al.* (2000)[95]

Table 2.2. Complex liquid media described for *H. pylori* growth. (Continued).

Medium base	Components added	Supplements													Notes	Reference
		w/o	YE	Serum-based	Blood-based	PGM	BSA	HM	CL	CD	CE	ST	MC	AC		
Brain Heart Infusion Broth (BHIB)	Antibiotics			✓											-	Jiang and Doyle (2000)[109]
	-			✓											Enzyme expression	Hutton *et al.* (2012)[82] Lin *et al.* (1996)[110]
	Ferrous sulphate Sodium pyruvate With or without antibiotics			✓		✓									-	Jiang and Doyle (2000)[109]
	-			✓											-	Shibayama *et al.* (2006)[88]
	-									✓					-	Ohno and Murano (2007)[87] Hutton *et al.* (2012)[82]
	Blood agarose Vitox Antibiotics (DENT)				✓										-	Duque-Jamaica *et al.* (2010)[111]
	-								✓						-	Hutton *et al.* (2012)[82]
	-						✓								-	
Brucella Broth (BB)	-			✓											Cultivation from biopsies	Buck and Smith (1987)[89] Shahamat *et al.* (1991)[108] Sainsus *et al.* (2008)[78]
	-		✓	✓											-	Shahamat *et al.* (1991)[108]

Table 2.2. Complex liquid media described for *H. pylori* growth. (Continued).

Medium base	Components added	Supplements													Notes	Reference
		w/o	YE	Serum-based	Blood-based	PGM	BSA	HM	CL	CD	CE	ST	MC	AC		
Brucella Broth (BB)	-			✓											-	Morgan *et al.* (1987)[99] Secker *et al.* (1991)[92] Olivieri *et al.* (1993)[94] Albertson *et al.* (1998)[69] Douraghi *et al.* (2010)[65]
	-					✓									-	Buck and Smith (1987)[89]
	-											✓			-	
	-												✓		-	
	-									✓					–	Olivieri *et al.* (1993)[94] Albertson *et al.*(1998)[69]
	Sodium polyanetholsulfonate	✓													-	Kehler *et al.* (1994)[83]
	Antibiotics									✓					-	Marchini *et al.* (1995)[68]
	IsoVitaleX			✓											–	Westblom *et al.* (1991)[86]
	IsoVitaleX							✓							-	Kitsos and Stadtlander (1998)[112]
	Glucose			✓											-	Sato *et al.* (2003)[113]
	-									✓					-	Douraghi *et al.* (2010)[65]
	-			✓											-	Park *et al.* (2011)[114]
	Hepes Trace metals Sodium pyruvate			✓	✓										Regrowth medium	Richards *et al.* (2011)[115]

Table 2.2. Complex liquid media described for *H. pylori* growth. (Continued).

Medium base	Components added	Supplements													Notes	Reference
		w/o	YE	Serum-based	Blood-based	PGM	BSA	HM	CL	CD	CE	ST	MC	AC		
Buffered yeast extract-α-ketoglutarate (BYEα)	-			✓											-	Shahamat *et al.* (1991)[108]
	-		✓	✓											-	
Customized	Tryptone Yeast extract Trace metals Tris Magnesium chloride			✓	✓										-	Andersen *et al.* (1997)[116]
Columbia Broth (CB)	-		✓												-	Shahamat *et al.* (1991)[108]
	-			✓											-	
	-		✓	✓											-	
Gonoccocal broth (GB)	-													✓	-	Taneera *et al.* (2002)[98]
H. pylori special peptone broth (HPSPB)	Special peptone Yeast extract Beef extract Sodium chloride Pyruvic acid Sodium salt			✓											-	Stevenson *et al.* (2000)[95]
Modified Brucella Broth	Tryptone Peptamine Glucose Yeast extract Sodium chloride			✓											-	Lin *et al.* (1996)[110]

Table 2.2. Complex liquid media described for *H. pylori* growth. (Continued).

Medium base	Components added	Supplements													Notes	Reference
		w/o	YE	Serum-based	Blood-based	PGM	BSA	HM	CL	CD	CE	ST	MC	AC		
Mueller-Hinton Broth (MHB)	-	✓													-	Shahamat *et al.* (1991)[108]
	-		✓												-	
	-			✓											Cultivation from biopsies	Shahamat *et al.* (1991)[108] Sainsus *et al.* (2008)[78]
	-		✓	✓											-	Shahamat *et al.* (1991)[108] Walsh and Moran (1997)[103]
	Cation-adjusted											✓			-	Coudron and Stratton (1995)[117]
	Cation-adjusted			✓											-	
	Proteose peptone n°3			✓											-	Walsh and Moran (1997)[103]
	-			✓											-	Stevenson *et al.* (2000)[95] Vega *et al.* (2003)[104]
	-										✓				-	Vega *et al.*(2003)[104]
	0.3% agar										✓				Transport medium	
Porcine stomach mucin (10% in water)	-	✓													Preservation medium	Ansorg *et al.* (1991)[81]
Stuart transport medium	-	✓													Transport medium	Soltesz *et al.* (1992)[97]
Supplemented peptone	-	✓													-	Kehler *et al.* (1994)[83]

Table 2.2. Complex liquid media described for *H. pylori* growth. (Continued).

Medium base	Components added	Supplements													Notes	Reference
		w/o	YE	Serum-based	Blood-based	PGM	BSA	HM	CL	CD	CE	ST	MC	AC		
Tryptic Soy Broth (TSB)	-	✓													-	Shahamat *et al.* (1991)[108]
	-		✓												-	
	-			✓											Cultivation from biopsies	Shahamat *et al.* (1991)[108] Sainsus *et al.* (2008)[78]
	-		✓	✓											-	Shahamat *et al.* (1991)[108] Walsh and Moran (1997)[103]
	Proteose peptone n°3			✓											-	Walsh and Moran (1997)[103]

Table 2.3. Semi-defined liquid media (defined media supplemented with undefined components) described for *H. pylori* growth.
Different media used for *H. pylori* growth. When the objective of the medium was other than cultivation, this is indicated in the notes column. w/o – without; YE – yeast extract; Serum-based – with horse serum or fetal calf; HG – haemoglobin; BSA – bovine serum albumin or lipid-rich bovine serum albumin; CD –2,6-di-O-methyl-β-cyclodextrin.

Medium base	Components added	Supplements					Notes	Reference
		YE	Serum-based	HG	BSA	CD		
Customized	Salts Trace metals (iron sulphate) Glucose Phenol red Adenine Lipoid acid Vitamins Amino acids (all 20, except tyr)				✓		-	Reynolds and Penn (1994)[77]
Customized	Reynolds and Penn medium		✓				-	Albertson *et al.* (1998)[69]
	Glucose				✓		-	Albertson *et al.* (1998)[69]
Customized	Agarose			✓			-	Vartanova *et al.* (2005)[118]
Culture Indication medium (CIM) – Modified Ham's F-12	-		✓				-	Sainsus *et al.* (2008)[78]
Dubelcco's Modified Eagle Medium (DMEM)		✓	✓				Thin-layer liquid culture technique	Joo *et al.* (2010)[119]
Ham's F-12	-				✓		Growth, storage and recovery BSA (98% purity)	Testerman *et al.* (2001)[67]
	-		✓				Growth, storage and recovery	Testerman *et al.* (2001)[67]
	-		✓				Cultivation from biopsies	Sainsus *et al.* (2008)[78]

Table 2.3. Semi-defined liquid media (defined media supplemented with undefined components) described for *H. pylori* growth. (Continued).

Medium base	Components added	Supplements					Notes	Reference
		YE	Serum-based	HG	BSA	CD		
Modified Isosensitest broth	Amino acids (all, except his and trp, with ornithine)				✓		Without saccharides, hydrolyzed casein and peptones	Mendz and Hazell (1995)[120]
Roswell Park Memorial Institute (RPMI).1640	-	✓	✓				Thin-layer liquid culture technique	Joo *et al.* (2010)[119]
	-	✓				✓	Thin-layer liquid culture technique	Joo *et al.* (2010)[119]

Table 2.4. Defined media described for *H. pylori* growth.

Different defined media described for *H. pylori* growth. When the objective of the medium was other than cultivation, this is indicated in notes column. w/o – without; CL – cholesterol; BCD - β-cyclodextrin; 2,6DMBCD - 2,6-di-O-methyl-β-cyclodextrin.

Medium base	Components added	Supplements				Notes	Reference
		w/o	CL	BCD	2,6DMBCD		
Customized	ACES buffer Salts Trace metals Thiamine Hypoxanthine Amino acids (all 20, except asn, cys, gln, gly, lys and thr)	✓				-	Nedenskov (1994)[74]

Table 2.4. Defined media described for *H. pylori* growth. (Continued).

Medium base	Components added	Supplements				Notes	Reference
		w/o	CL	BCD	2,6DMBCD		
Customized	Salts Trace metals Thiamine Hypoxanthine Nytropyrin Adenine Uracil Guanine Xanthine Glucose Amino acids (all 20, with cystine)			✓		Continuous culture	Stark *et al.* (1997)[121]
Customized by Reynolds and Penn	Glucose		✓		✓	-	Albertson *et al.* (1998)[69]
Ham's F-12	-	✓				Growth, storage and recovery	Testerman *et al.* (2001)[67]
	-		✓	✓			
F-12m: Ham's F-12 based	Salts Trace metals Phenol red Thiamine Hypoxanthine Sodium pyruvate Amino acids (all 20, except gly and lys)	✓				-	Testerman *et al.* (2001)[67]
Ham's F-12 based	Salts Trace metals Phenol red Thiamine Hypoxanthine Sodium pyruvate Amino acids (ala, arg, cys, his, leu, met, phe, val)	✓				-	Testerman *et al.* (2006)[79]

2.3.2 Environmental conditions

H. pylori has been considered a microaerophilic bacterium, growing at low percentages of oxygen. However, in the last years, some studies proved that percentages of oxygen between 5 and 21% are tolerated by *H. pylori*. In fact, *H. pylori* can grow in aerobic conditions at high cell concentrations, although at low cell densities *H. pylori* behaves more like an oxygen-sensitive microarophile[114,122]. An absolute requirement of carbon dioxide in the growth atmosphere has been reported, showing that *H. pylori* is a capnophilic organism[114,122]. Whereas some anaerobic features were identified in *H. pylori*'s metabolism, its growth under strictly anaerobic conditions has not been successfully reported[122–124], being oxygen an absolute requirement for growth. In fact, several experiments have been performed under the absence of oxygen with evidence for some metabolic activity such as substrates consumption and by-products formation and those will be mentioned along this text. Nevertheless, none of those authors has reported any growth in the absence of oxygen.

Despite the fact that *H. pylori* can grow *in vitro* under aerobic conditions, microaerobiosis seems to mimic better the physiology of the organisms grown in their natural habitat[122,125]. Thus, usually *H. pylori* is grown *in vitro* using an atmosphere with a mixture of 5% O_2, 10% CO_2 and 85% N_2, generated by microaerophilic gas-generating systems in jars, or in incubators where the gas mixture is continuously flushed, under high humidity content and at 37°C.

Usually, the pH is not adjusted during *H. pylori* cultures *in vitro*, and the media used are frequently buffered. Some studies in fermenters with pH control were also performed[121,126]. It is assumed that the optimal pH for *H. pylori* growth is around 7, although *H. pylori* can support a wide range of pH values (2-8.6)[127]. *H. pylori* has mechanisms to survive under acidic conditions, such as the urease enzyme, which decompose urea, generating bicarbonate and ammonia, thus, increasing pH. The adjustment of the pH by *H. pylori* during cultures was reported by Andersen *et al.* (1997), concluding that optimal growth occurs until the pH reaches 8.5[128].

Cultures with and without shaking have been described, although agitation is used the majority of times, since generally higher cell densities are obtained, unless small volumes of liquid and high interface areas are used[95].

A few studies[111,129] attempted to improve liquid cultivation based rational optimization strategies like statistical experimental design of culture conditions (atmosphere, pH, shaking speed, inoculum concentration, volume of culture).

2.4 *Helicobacter pylori's Metabolism*

H. pylori is very well adapted to its specific niche and able to persist in the human stomach lifelong. This ability is conferred by unique metabolic and physiological features[130]. However, the knowledge acquired about the metabolism of *H. pylori* is still very limited, needing further exploration. In this section, the current information on the most important metabolic pathways of this bacterium is summarized.

2.4.1 Carbohydrates utilization

The capability of *H. pylori* to acquire and metabolize carbohydrates is very limited. The capacity of consuming glucose was initially denied but the first genome sequencing[131] disproved this assumption, corroborating experimental data obtained by Mendz *et al.* (1993)[132]. Further enzymatic experiments proved that, notwithstanding glucose is minimally utilized by *H. pylori*, this organism presents a complex glucose metabolism[133].

A D-glucose sodium-dependent transport system was experimentally identified for *H. pylori* [134] and was also verified by genome analysis with the identification of a glucose/galactose transporter (gluP, HP1174)[131,135]. Psakis *et al.* (2009) showed that D-mannose can also be transported by the HP1174 transporter[136]. Further genome analyses indicate that this gene is possibly the only gene encoding a transport protein for sugars in *H. pylori* [136,137]. Glucose phosphorylation was proved to be associated with a glucokinase activity, that was both detected *in vitro* [138] and identified in the genomic sequence

(HP1103)[131]. Glucose catabolism via the pentose phosphate pathway was proved by Mendz *et al.* (1991)[139], who also suggested there is another pathway involved in glucose metabolism[140], with the main metabolic product detected from glucose being lactate. In contrast, Chalk *et al.* (1994) reported glucose oxidation via the Entner-Doudoroff (ED) pathway with mainly acetate as a product (aerobically). Sorbitol and gluconate were also identified as glucose products when dense cell suspensions were incubated with ^{13}C labeled glucose under anaerobic conditions[141]. In spite of the existing enzymatic capabilities for the utilization of glucose as the main source of carbon and energy, there are evidences that amino or organic acids are effectively the preferred carbon and energy sources for *H. pylori* growth[120]. This topic will be further explored in the next chapters.

2.4.2 Central carbon metabolism

2.4.2.1 Glycolysis and gluconeogenesis

In the glycolysis pathway, glucose is converted into pyruvate with ATP generation, providing part of the energy utilized by most organisms. Gluconeogenesis, the formation of glucose from non-carbohydrate sources, such as pyruvate, shares the enzymes with glycolysis with the exception of irreversible reactions that are only glycolytic or gluconeogenic. The presence of glycolysis in *H. pylori* is doubtful. Hoffman *et al.* (1996) reported enzymatic activities for all glycolytic enzymes, as well as gluconeogenic enzymatic activities. However, he found less enzymatic activity in exclusive glycolytic enzymes when compared with exclusive gluconegenic enzymes[133]. In contrast, Mendz *et al.* (1994) and Chalk *et al.* (1994) were not able to detect the presence of the glycolytic pathway[141,142]. Homologues to enzymes involved in glycolysis and gluconeogenesis are present in *H. pylori* with the exception of the glycolytic enzymes catalyzing irreversible reactions, the phosphofructose kinase and pyruvate kinase, which were not identified in the genome[130,131,135]. The absence of these two enzymes, and the presence of the irreversible gluconeogenic enzymes (fructose-1,6-biphosphatase and pyruvate dikinase) indicates that the gluconeogenesis pathway is active, but glycolysis is not [130,135].

2.4.2.2 Entner-Doudoroff and Pentose Phosphate pathways

In alternative to glycolysis, glucose can be catabolized by the Entner-Doudoroff (ED) or the Pentose Phosphate (PP) pathways. In agreement with the genomic sequence[131], there is experimental evidence for the presence of the ED pathway in *H. pylori*, proved with NMR[141,143], and enzymatic experiments[133]. Although the ED pathway can be viewed as an option for *H. pylori* to utilize glucose as an energy source, experiments with *H. pylori* in mice proved that this metabolic pathway is not essential for colonization of the mouse gastric mucosa[144], being a non-inducible pathway. It has been suggested that this pathway can also be used to consume gluconate or other aldonic acids, but without experimental evidence[144].

Evidences for the existence of the PP pathway (both oxidative and reductive branches) have been reported for *H. pylori* [133,139]. The PP pathway can provide NADPH for reductive biosynthesis and ribose-5-phosphate for nucleotides synthesis[139]. Chalk *et al.* (1994), in their experiments using ^{13}C NMR spectroscopy were not able to detect glucose oxidation by the PP pathway, suggesting that in *H. pylori* it may be mainly a biosynthetic route[141]. Regarding sequence similarity, all encoding enzymes of the PP pathway were identified in the genome, with the exception of the 6-phosphogluconate dehydrogenase, which is responsible for the oxidative decarboxylation of 6-phosphogluconate to ribulose-5-phosphate, leading to conclude that *H. pylori* may have another protein with a similar function[135] or that indeed only the reductive branch is active in this organism.

2.4.2.3 Pyruvate metabolism

Pyruvate is a key metabolite, being an important intermediary in *H. pylori*'s metabolism both for anabolic pathways or an intermediary for cofactors oxidation. The main sources for pyruvate in *H. pylori* were found to be lactate, L-alanine, L-serine and D-amino acids[130,142].

It has been described that *H. pylori* converts pyruvate to acetyl coenzyme A only by pyruvate:flavodoxin oxidoreductase (PFOR)[145,146]. The presence of this enzyme contributes to *H. pylori*'s microaerophilic phenotype, since PFOR is oxygen labile[146]. St

Maurice *et al.* (2007) identified activity of NADPH flavodoxin and quinone reductase (FqrB) (HP1164). FqrB is coupled by flavodoxin to the PFOR system and catalyzes a pyruvate-dependent production of NADPH[147]. The reverse reaction produces pyruvate via CO_2 fixation, which is consistent with *H. pylori*'s capnophilic nature[147].

According to experimental results, pyruvate is not a principal nutrient but it is quickly metabolized by cells, often with production of acetate, formate, lactate, succinate and alanine microaerobically[120,142]. However, homologues for pyruvate formate-lyase and pyruvate oxidase were not detected in *H. pylori*'s genome[130], and thus the enzyme associated with formate production is not known. In acetate formation from pyruvate, pyruvate is first converted to acetyl-CoA by PFOR, then to acetyl-phosphate by a phosphotransacetylase, (HP905) and finally to acetate by acetate kinase (HP903). Also, acetyl-CoA synthetase, that converts acetyl-CoA to acetate in a single step was identified (acoE, HP1045)[130]. D-Lactate dehydrogenase, responsible for D-lactate production was also identified by sequence homology (dld, HP1222)[148]. As shown experimentally, *H. pylori* exhibit some metabolic features characteristic of anaerobic organisms, such as the production of acetate and formate in mixed-acid fermentation. The presence of mixed-acid fermentation can be interpreted as a metabolic adaptation of its specific niche, as stressed by Mendz *et al.* (1995)[142]. The formation of succinate suggests that part of the TCA cycle is active and operating in the reductive direction, also characteristic of anaerobiosis[142]. Although, as referred previously, *H. pylori* fails to grow under strict anaerobic conditions in the laboratory, the mentioned anaerobic features may be important *in vivo* for survival under determined conditions, and may play an important role in transmission.

2.4.2.4 Tricarboxylic acid cycle

The existence of a complete oxidative tricarboxylic acid (TCA) cycle has been a controversial point about *H. pylori*'s metabolism. Genomic evidences had previously indicated that *H. pylori* does not have a complete TCA cycle, lacking genes codifying enzymes for three usual TCA cycle enzymes (alpha-ketoglutarate dehydrogenase, succinyl-CoA synthetase and malate dehydrogenase)[131,135]. The presence of the TCA cycle in *H. pylori*

was studied by Pitson *et al.* (1999) by enzyme activities measurements, proposing that *H. pylori* has a branched TCA cycle, typical of anaerobic metabolism[149]. According to this point of view, the operation of the cycle in *H. pylori* occurs in the oxidative direction from oxaloacetate to alpha-ketoglutarate and in the reductive direction from oxaloacetate to succinate, with an alpha-ketoglutarate oxidase linking the branches[149]. However, alternative enzymes for the missing TCA cycle steps were discovered, completing the TCA cycle[146,150].

The consensus enzymes and discrepancies detected in the TCA cycle are shown in Figure 2.2. There is a consensus about the presence of the following enzymes: citrate synthase, aconitase, isocitrate dehydrogenase, fumarate reductase and fumarase[149]. For the conversion of alpha-ketoglutarate to succinate, an alpha-ketoglutarate oxidase activity was detected[149]. The absence of the alpha-ketoglutarate dehydrogenase was proved by Corthezy-Theulaz *et al.* (1997)[151]. Hughes *et al.* (1995) and Hughes *et al.* (1998) also identified the presence of an alpha-ketoglutarate:ferredoxin oxidoreductase (also called alpha-ketoglutarate oxidoreductase - KOR), an oxygen sensitive enzyme that contributes to *H. pylori*'s microaerophilic requirements[145,146]. In addition, KOR was proved to be essential for the energy metabolism of *H. pylori*'s coccoid forms, and when this enzyme was inactivated there was no spiral to coccoid morphological conversion[152]. The conversion from succinyl-CoA to succinate was proved to be associated with succinyl-CoA: acetoacetate CoA-transferase, that catalyzes the transference of CoA from succinyl-coA to acetoacetate with formation of acetoacetyl-coA[151]. The existence of a succinate conversion to fumarate is not unanimous, with authors agreeing with the presence of a fumarate reductase activity, but disagreeing in the possible opposite succinate dehydrogenase activity. Pitson *et al.* (1999)[149] did not detect it, in contrast with Kather *et al.* (2000)[150] that reported this activity. Evidences of the presence of both fumarate reductase and fumarase were obtained by Mendz *et al.* (1993) by the detection of malate and succinate from fumarate[153]. Fumarate transport has also been characterized[154]. The fumarate reductase properties in *H. pylori* were studied, supporting the existence of an anaerobic metabolism, fumarate acting as a terminal acceptor in anaerobic respiration[155–157]. However, *H. pylori* is not able to grow under anaerobic conditions, being thought that anaerobic respiration and fermentation are not sufficient to support *H. pylori* growth[122]. In addition, several studies have arisen in order

to investigate fumarate reductase as a potential therapeutic target[156–158]. The role of fumarate reductase in host colonization was studied by Ge *et al.* (2000), concluding that, although it is not essential for *H. pylori*'s survival *in vitro*, it is very important for survival in gastric mice mucosa[158].

For the conversion of malate to oxaloacetate, the activity of a malate dehydrogenase was detected[149,159], whereas Kather *et al.* (2000) proved the presence of a malate:quinone oxidoreductase for the same conversion, without evidence of the reversibility of this step (reduction of oxaloacetate), showing that, in some situations, the TCA cycle of *H. pylori* can operate in the oxidizing direction[150]. In the genome, however, the gene codifying for malate dehydrogenase was not identified[131], but a malate:quinone oxidoreductase was identified (HP0086)[150]. The activity of the anaplerotic enzymes pyruvate carboxylase, phosphoenolpyruvate carboxylase and phosphoenolpyruvate carboxykinase was not detected[146] or was very low[159]. Anaplerotic reactions would nevertheless be very important to replenish oxaloacetate[159]. Additionally, the glyoxylate bypass was not identified, being only detected the activity of malate synthase and missing isocitrate lyase to complete the pathway[149]. The presence of malate synthase can be viewed as a direct entry for glyoxylate into the TCA cycle or into a glyoxylate oxidizing cycle[149]. However, malate synthase was not identified in the genomic sequence[131].

The gamma-aminobutyrate shunt, an alternative to convert alpha-ketoglutarate to succinate, was not detected in *H. pylori* [149] although it was detected in *H. bizzozeronii*, a canine-adapted organism cultivated from human gastric biopsies[160].

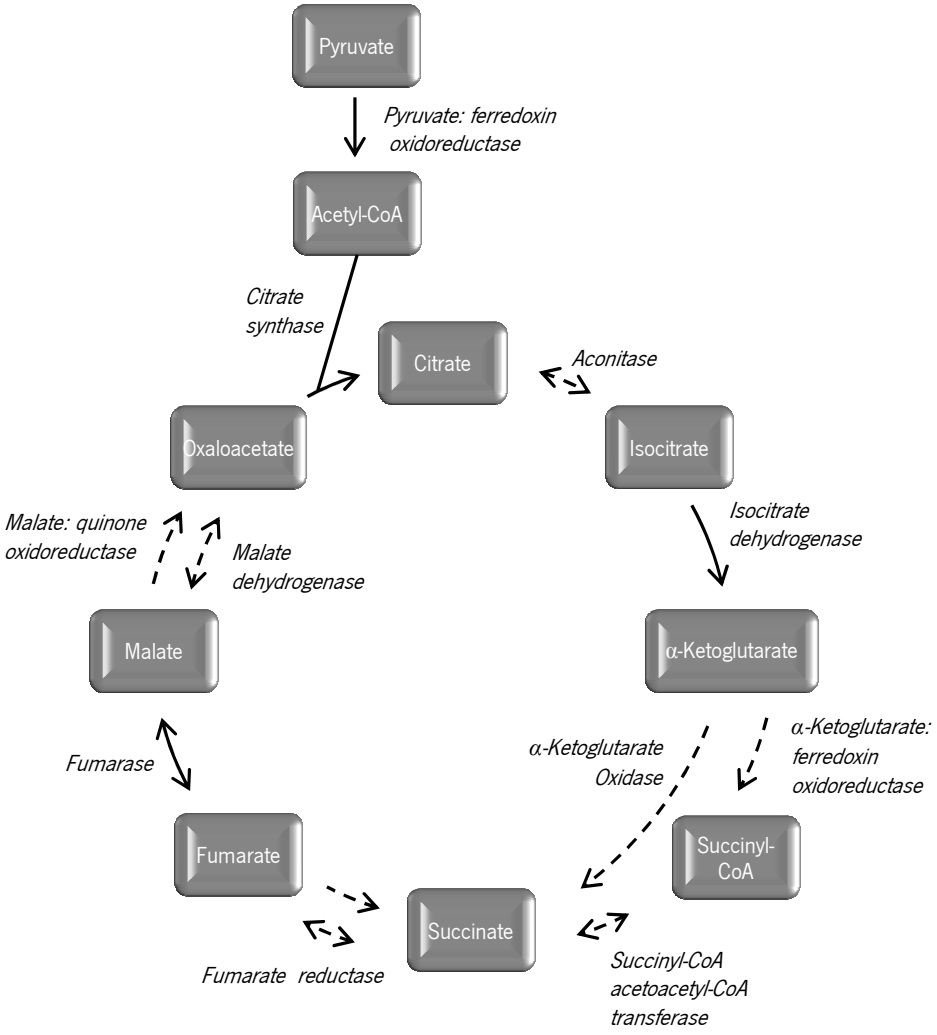

Figure 2.2. TCA cycle in *H. pylori* with possible enzymes involved in each reaction. When more than one possibility was described in the literature, both options are showed with dashed arrows. (Adapted from Pitson *et al.* (1999)[149] and Kather *et al.* (2000)[150]).

2.5 *Systems Biology*

The Systems Biology approach has been replacing the reductionist view of classical biology, which relies on the study of individual cellular components and their functions, and dominated research in the last decades[161]. Systems biology integrates different levels of information in order to understand biological systems (such as cells or organisms)[162–164]. By studying biological systems as a whole, systems biology bridges the

gap between molecules and physiology[165]. In the last years, with the advances in molecular biosciences, genome-sequencing and the development of high-throughput molecular methods that allow to characterize cellular components at a given time, the notion of cellular networks has arisen and turned into the research focus[161,165].

The systems biology approach is only possible by the integration of experimental and computational knowledge with the use of a range of analytical techniques, measurement technologies, experimental methods and software tools[162,163]. It is accepted that Systems Biology is inter-disciplinary, applying the knowledge of disciplines such as biology, physics, chemistry, engineering and computer science[166].

Depending on the goal to achieve, there are two different systems biology approaches that can be applied. One approach starts from the bottom (constitutive parts) and applies detailed knowledge about the system to construct mathematical models that can be used to simulate the system's behavior (bottom-up systems biology). In the other approach, biological information is extracted from "omics" data with the goal to disclose and characterize molecular mechanisms (top-down systems biology)[165,167–169].

2.5.1 "Omics" Technologies

The "omics" era started with the use of the word "genomics" by Thomas H. Roderick in 1986, to name a journal, which included sequencing data, discovery of new genes, gene mapping and new genetic technologies[170]. Nowadays, the term "omics" is largely applied to refer the study of a variety of "omes", encompassing the study of a complete set of a given type of system components. As such, genomics, transcriptomics, proteomics and metabolomics refer to the analysis of the genome (complete set of genes); transcriptome (complete set of transcripts), proteome (complete set of proteins) and metabolome (complete set of metabolites), respectively. The evolution in analytical methods and technologies and the introduction of high-throughput methods has supported the "omics" concept, allowing the analysis of cellular functions. The "omics" technologies rely on the generation of large-scale datasets, being a systems biology challenge to deal with all of these data, to extract the biological meaning and to integrate the different levels

of information with the final goal of understanding the system as a whole and characterize phenotypes.

In Figure 2.3 the various "omics" technologies are outlined, targeting different levels of cellular information, with indication of the most applied technologies in each "omic".

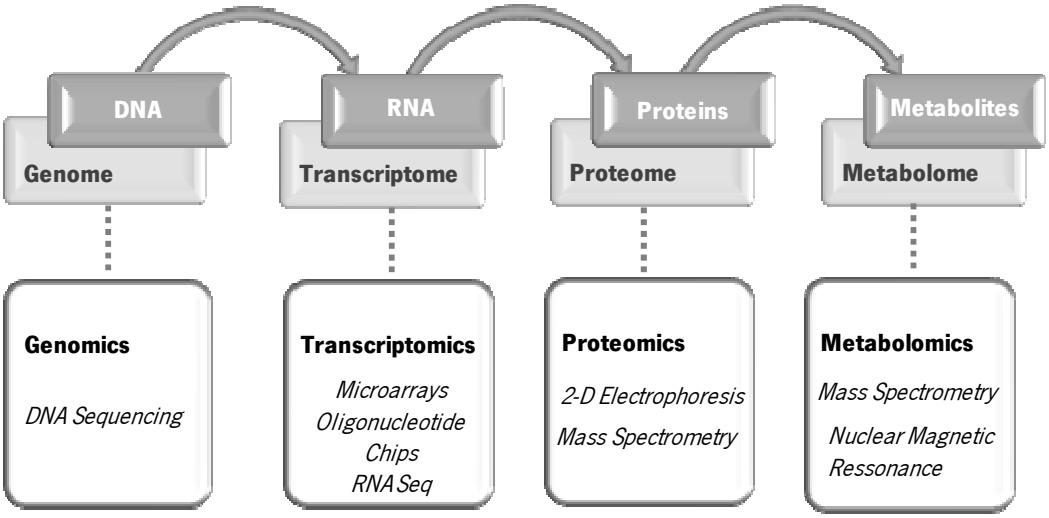

Figure 2.3 "Omes" and respective "omics" technologies. Examples of methods that allow their analysis.

According to the work developed under this dissertation, metabolomics is further explored in the next few pages.

2.5.1.1 Metabolomics

Metabolomics is the "omics" technology that aims to identify and quantify the complete set of small molecules (metabolites or metabolic intermediates) associated with an organism, tissue, cell or biological sample. In the last years, this approach has been largely applied to understand biological systems, having some definitions emerged in this field (Table 2.5).

The level and type of metabolites can be associated with the physiological, pathological or developmental status of a biological system, representing the closest indicator of a cell's phenotype[171].

In metabolism, an assortment of metabolite classes is included, such as amino acids, organic acids, sugars, lipids and coenzymes. Moreover, the number of metabolites that constitutes the metabolome is variable among different organisms, varying from hundreds in bacteria to thousands in plants[172]. As such, metabolomics has to deal with a large number of chemical entities with a huge chemical diversity in composition and structure[171,172]. Thereby, the main limitation in metabolomics is technical, being impossible with the current technologies to analyze the whole metabolome at a time. Besides that, the complexity and difficulties in metabolomics analysis is exacerbated by the dynamic nature of metabolites in the cell, which have a rapid turnover, varying their concentration and composition quickly in response to environmental stimuli[171,172].

Table 2.5 Terms and respective definitions applied in metabolomic analysis. (Adapted from Fiehn (2002)[173] Nielsen and Oliver (2005)[174], and Nielsen (2007)[175]).

Term	Definition
Metabolomics	Approaches use to analyze the metabolome or a fraction of it.
Metabolome	Complete set of metabolites synthesized by a cell associated with its metabolism.
Endometabolome	Total of intracellular metabolites
Exometabolome	Total of extracellular metabolites (excreted)
Metabolic profiling	Analysis of a specific group of compounds (for instance, lipids, carbohydrates). Frequently semi quantitative.
Metabolic footprinting	Exometabolome analysis. Applied to the analysis of specific metabolites or to spectra without information of particular metabolites.
Metabolic fingerprinting	Fingerprint of the metabolites that are produced by the cell. Usually, does not provide information about specific metabolites. Can be used to classify samples.
Metabolic target analysis	Analysis of metabolites that participate in a specific part of the metabolism. Quantitative. Mainly used for screening purposes.

The application of a metabolomics approach involves several steps from sampling to interpretation of biological meaning (Figure 2.4) that are briefly described below.

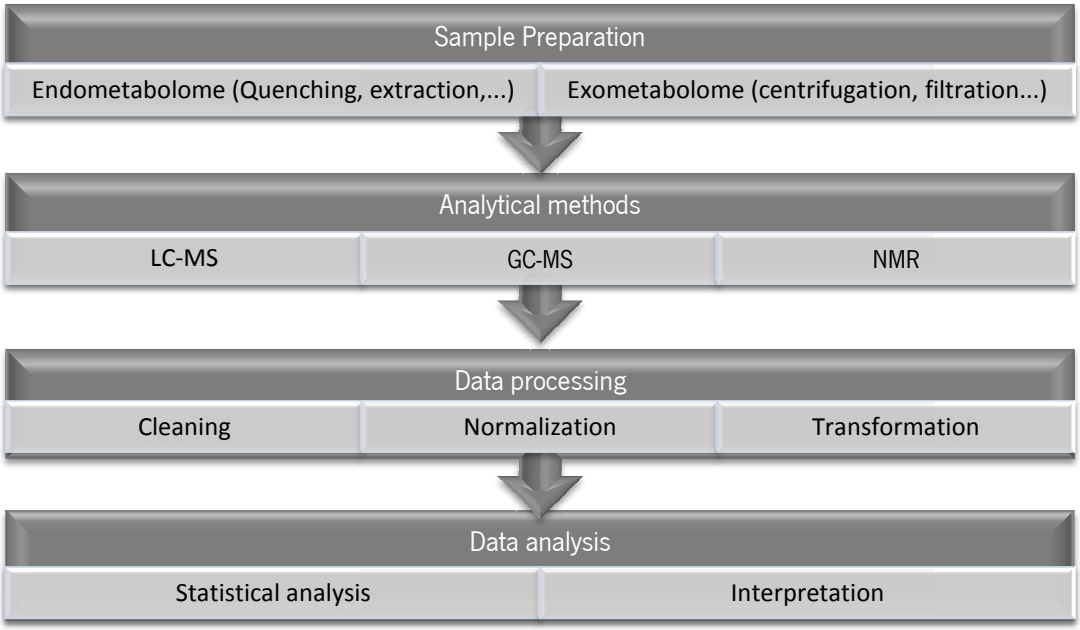

Figure 2.4. Workflow in a metabolomics approach with examples in each step.

i. *Sample preparation*

The chosen sample preparation procedure is associated with the specific objective. In microbial metabolome analysis, different sample preparation methods have to be considered, depending on whether a target class of metabolites or an untargeted analysis is sought, as well as the "localization" of the metabolites in the cell. These objectives determine the necessity of a specific extraction and quenching protocol. While for extracellular microbial metabolites sample preparation is not critical, with few steps performed, in intracellular metabolite analysis the sample preparation protocols have to be carefully chosen in order to obtain an accurate analysis[176]. The first step on microbial exometabolome analysis is the separation of the extracellular medium from the cells, usually performed by centrifugation or filtration[176,177]. The extracellular metabolites are directly analyzed from the culture supernatant. The preparation of samples for extracellular and intracellular analysis can be performed together or separately. Since intracellular metabolites have a high turnover rate, the metabolic enzymatic activity should be rapidly

stopped (quenching) after cells harvesting for intracellular metabolite analysis[178]. The quenching and extraction steps can be done simultaneously with solvents or separately[178]. The quenching/extraction protocols applied are variable and can include for instance rapid changes of temperature (low : < -40°C or high : > 80°C), pH (high alcali: KOH or NaOH or high acid: perchloric or trichloroacetic acid), the use of cold methanol, cold glycerol-saline solution, liquid nitrogen or fast filtration[176,177,179]. For further details, the methods applied for sample preparation have been thoroughly revised[175,180]. It should however be emphasized that different quenching/extraction protocols are being developed and applied for several organisms, for instance *E. coli* [181–183], *C. glutamicum* [182], *B. subtilis* [184], *L. bulgaricus* [185], *S. aureus* [186], or *S. cerevisiae* [182,187–189].

In terms of statistical analysis, it is important that a sufficient number of replicates is performed. Smart *et al.* (2010) recommend five technical replicates from three biological replicates for intracellular analysis and three technical replicates from each biological replicate for extracellular metabolite analysis[177].

Since the level of extracellular metabolites sometimes is very low and intracellular metabolites are often diluted during extraction procedures, a step of sample concentration is frequently needed, which can be achieved by freeze-drying at low temperatures to avoid metabolite degradation[177].

ii. *Analytical Methods*

There are various analytical platforms suitable to be applied to metabolomics analysis, such as Nuclear Magnetic Resonance (NMR) spectroscopy, several separation methods coupled with Mass Spectrometry (MS) or Fourier Transform Infrared Spectroscopy (FTIR). Nevertheless, NMR spectroscopy and MS are the mostly used analytical platforms in metabolomics. Both techniques exhibit advantages and limitations, and the choice depends on the sample characteristics and the purposes of the study [190].

NMR detects the specific resonance of absorption profiles of metabolites in a magnetic field. The most important advantages of NMR spectroscopy are that, besides the simple and easy sample preparation, it is a non-destructive technique that does not need further sample separation, and has high reproducibility[190,191]. The low sensitivity of this

platform compared with MS, and the requirement of large sample volumes are its major limitations[190,191].

Gas Chromatography (GC) or Liquid Chromatography (LC), where the compounds are separated, coupled with MS, which is based on ion molecular mass-to-charge ratio (m/z) determination is often used[179]. In the last years, a new evolution of LC, Ultra High Performance Liquid Chromatography (UHPLC), has been applied, increasing the sensitivity in comparison with LC[190]. UHPLC-MS has some advantages compared to the other platforms used, such as short separation time, analysis of a larger range of metabolites than GC-MS, high mass accuracy and resolution, and simple sample preparation[190,191]. However, unlike GC-MS, it presents a low reproducibility of retention times between different systems[190]. The high reproducibility of retention times and fragmentation patterns, allowing the construction of libraries and enabling compound identification without standards, makes the GC-MS the most popular platform in metabolomics studies. The consistent mass spectrum obtained for each compound in GC-MS is achieved by the use of electron ionization (EI), which is the most frequently used ionization method[191]. A very complete collection of studies published using GC-MS as the analytical platform in metabolomics was published by Koek *et al.* (2011)[192].

Besides the presented advantages, GC-MS exhibits some limitations related with the requirement for volatile samples, increasing the steps and difficulty on sample preparation due to the derivatization procedure, which can also lead to the introduction of additional sample to sample variation. The derivatization is a chemical modification of molecules that yields compounds with a similar chemical structure (derivative) but with specific characteristics, which in the case of GC-MS are volatility, less-polarity and thermal stability. In chemical derivatization, active hydrogens in functional groups, such as –COOH, –OH, –NH, and –SH are replaced by other chemical groups. The most applied derivatization method for analysis by GC-MS is using silylation reagents (reviewed by Koek *et al.* (2011).[192]). Alternative reagents, such as chloroformates are also used[193]. For instance, a propylchloroformate derivatization was applied in short-chain fatty acids and branched-chain amino acids analysis[194,195], an ethylclhoroformate derivatization was applied for analysis of amino and organic acids, fatty acids, phenolic compounds and amines[196,197],

and a methylchloroformate derivatization was applied in amino, organic and fatty acids analysis[198–200].

iii. *Data Processing and Analysis*

After performing the analyses in MS or NMR, in order to prepare the data for statistical analysis, a data processing step is needed. This stage can encompass some steps such as data cleaning, normalization and transformation. In MS data, an overlapping of the signal compounds is frequently observed. The deconvolution is thus a frequent treatment of data used to extract the individual metabolite signals from the raw signal[201]. The Automated Mass Spectral Deconvolution and Identification System (AMDIS)[202] from the National Institute of Standards and Technology (NIST) is one of most used software packages to perform the deconvolution and to match unknown spectra with libraries to identify detected compounds[203]. The next steps that could be necessary to perform are the baseline correction, normalization and sculling (data transformation included) (detailed in Liland, (2011)[204]).

The data analysis is the subsequent step, where statistical methods are applied with the final goal of extracting the biological meaning of the generated data. Here, supervised or unsupervised methods are applied.

2.5.1.2 *H. pylori* "Omics" data

H. pylori 26695 was one of the first bacteria to have its genome completely sequenced in 1997[131]. Since then, "omics" high-throughput methods have been applied to study the genome, proteome and transcriptome of *H. pylori*. The advances in omics technologies have allowed to make progress in targeting *H. pylori* and its association with disease, giving important clues about its inactivation, although it is not yet possible to uncover all mechanisms involved in *H. pylori* pathogenesis and host-pathogen interaction[205].

Recent advances in **genomics** made accessible next-generation sequencing (NGS) methods, which enabled the sequencing of a large variety of *H. pylori* strains, with

54 *H. pylori* strains fully sequenced and 329 strains with ongoing sequencing projects (Genebank database in March 2014)[206]. Due to the extensive list of sequenced genomes and the data availability on the NCBI genome online database (http://www.ncbi.nlm.nih.gov/genome) the referred data are not presented or analyzed here in detail. The sequenced genomes include strains isolated from patients with different pathologies (gastritis, duodenal ulcer, gastric cancer, MALT-lymphoma) and/or from different parts of the world (North and South America, Far East Asia, Europe, Malaysia, Africa, India and Australia), contributing to discover new disease-specific biomarkers and uncover new virulence mechanisms[207]. *H. pylori*'s genomic features are presented in Table 2.6. It is important to highlight that *H. pylori* has a high genomic plasticity that allows for host adaptation[208,209]. The comparison of genomic sequences of two *H. pylori* strains (26695 and J99), isolated from patients with different pathologies, showed that 6-7% of the genes are strain-specific[210]. Analysis by whole genome DNA microarray of 15 clinical isolates from different geographical origins, showed that a minimal *H. pylori* genome consists of 1281 genes, encoding mainly metabolic and cellular processes[211]. The genetic variability, high mutation and homologous recombination rates, led to a high diversity of *H. pylori* strains[208,212,213].

Table 2.6. *H. pylori* genomic features, obtained from the average of 54 fully-sequenced strains (data available in the NCBI genome database in March, 2014)[206].

Genomic features	
Genome size (Mb)	1.63 (1.51 – 1.71)
GC content (%)	38.9 (38.4 - 39.3)
Predicted genes	1601 (1429 - 1749)
Proteins	1540 (1382 - 1707)

Transcriptomics are applied in order to understand what are the genes actively expressed at a given time under a defined condition, typically involving measuring the complete set of RNA transcripts by the use of microarrays technology or by RNA sequencing. Gene expression omnibus (GEO)[214] (available online at

http://www.ncbi.nlm.nih.gov/geo/) is a public repository for functional genomics data that gathers high-throughput gene expression data for a large variety of organisms. The studies present in this database on *H. pylori* are gathered in Table 2.7. Owing to the scope of the present work, transcriptomics studies were filtered to "genome expression profiling", being excluded other types of studies such as "genome variation profiling by array" The published transcriptomics studies address topics such as gene expression under different conditions and stimuli in order to uncover regulatory mechanisms.

Table 2.7. Transcriptomics studies with *H. pylori.* (Extracted and adapted from GEO[214] (available online at http://www.ncbi.nlm.nih.gov/geo/).

Objectives	Technology used (Manufacturer)	*H. pylori* Strains	Experimental conditions	Experimental design	Reference
Study of the *modH* gene, a phase-variable DNA methytransferase of *H. pylori*	*in situ* oligonucleotide (Custom, Agilent)	P12	Culture on brain heart infusion broth, supplemented with 10% (v/v) fetal bovine serum, vitamin mix and vancomycin	Comparison of wild type and mutant strains (Wild Type P12 and P12 Δ modH5) (3 replicates each)	Srikhanta *et al.* (2000)[215]
Study of the effect of hpyAVIBM (a C5 cytosine methyltransferase) deletion on *H. pylori*'s transcriptome	*in situ* oligonucleotide (Custom, Agilent)	26695 AM5 SS1	Cells grown to 0.6 of optical density	Wild Type strains (26695, AM5 and SS1) *vs.* Mutant strains (26695 Δ hpyAVIBM, AM5 Δ hpyAVIBM, SS1 Δ hpyAVIBM) (2 replicates each)	Without publication[1]
Study of the biological cost of rifampicin resistance in *H. pylori*.	Spotted DNA/cDNA (Postgenome Lab (RIPCM))	26695	Culture on Brain heart infusion broth (3.7% brain heart infusion with 10% inactivated fetal bovine serum and 5% yeast extract).	Wild Type strain *vs.* 26695 Mutant 1 (phenotype: Rifampicin resistant; rpob mutation 1: G1588A; rpob mutation 2: D530N) *vs.* 26695 Mutant 2 (phenotype: Rifampicin resistant; rpob mutation 1: C1618T; rpob mutation 2: H540Y) (4 replicates each)	Momynaliev, 2009 (Publication in Russian[2])
Elucidation of factors required to sustain the transcription response to DNA damage.	Spotted DNA/cDNA (Stanford Functional Genomics Facility, Stanford School of Medicine)	Isogenic mutants of NSH57	Culture on Brucella broth with 10% fetal bovine serum. For antibiotic resistance marker selection, media were supplemented with antibiotics.	Wild Type ciprofloxacin-treated *vs* Wild Type untreated comB4 merodiploid (MSD89) *vs* Wild type addA *vs* Wilde Type; comB10 addA *vs* Wild Type recA untreated *vs* recA ciprofloxacin treated comB4 merodiploid recA *vs* Wild Type Wilde Type untreated *vs* gentamycin-treated recR - mutant (MSD49) *vs* Wild Type (3-4 replicates each)	Dorer *et al.* (2010)[216]

[1] Ritesh Kumar (Indian Institute of Science), 2011; [2] Kuvat Momynaliev (Research Institute for Phys-Chim Medicine, Russia), 2010.

Table 2.7. Transcriptomics studies with *H. pylori.* (Continued).

Objectives	Technology used (Manufacturer)	*H. pylori* Strains	Experimental conditions	Experimental design	Reference
Identification of the HP0244 regulon at different pH conditions	Spotted DNA/cDNA (TeleCom International, Inc. ArrayIt Division)	26695	Culture on agar plates. For exposure to experimental low-pH conditions, the brain heart infusion (BHI) medium was used	Wild-type *vs* HP0244-KO-pH7.4 Wild-type *vs* HP0244-KO-pH4.5 Wild-type *vs* HP0244-KO-pH2.5 (3 replicates each)	Wen *et al.* (2009)[217]
Characterization of *H. pylori* adaptations to the transition from chronic atrophic gastritis (ChAG) to gastric adenocarcinome and impact of these adaptations on gastric epithelial stem cells	*In situ* oligonucleotide (Custom, Affymetrix)	Clinical isolates Kx1 and Kx2	Culture on Brucella broth medium and addition to mouse gastric epithelial progenitor (mGEPs) cells in RPMI 1640 medium supplemented with 10% FBS at 37°C or just RPMI 1640 medium supplemented with 10% FBS (without mGEP cells)	*H.pylori* isolates associated with chronic atrophic gastritis (chAG) (Kx1) *H.pylori* isolates associated with gastric adenocarcinoma (Kx2) Kx1 infecting mGEP Kx2 infecting mGEP (2-3 replicates each)	Giannakis *et al.* (2008)[218]
Characterization of *H. pylori* adaptations to chronic atrophic gastritis (ChAG). Response of gastric epithelial progenitors (GEPs) to *H. pylori* isolates from Swedish patients with chronic atrophic gastritis (ChAG)	*in situ* oligonucleotide (Custom, Affymetrix)	HPAG1 Clinical isolates	Liquid culture on Brucella or Brain Heart Infusion (BHI) broth supplemented with 10% fetal calf serum and 1% IsoVitaleX. (enrichment)	Wild-type ChAG associated Wild-type HoZ-KO 488_Kx1 (ChAG associated) 488_Kx2 (gastric cancer associated) HPAG (ChAG associated) 1hr in rich media, pH7 HPAG (HopZ) 0hr in rich media, pH 7 HPAG (HopZ) 1hr in rich media, pH 7 HPAG (HopZ) 1hr in rich media, pH 5	Giannakis *et al.* (2009)[219]
Characterization of ArsRS regulon, associated with acid adaptation	Spotted DNA/cDNA (Max-Planck-Institute for Infection Biology – MPIIB)	G27 26695 G27 mutants	Brain heart infusion (BHI) broth with fetal calf serum and antibiotics	Global transcriptional profiling of an ArsS-deficient *H. pylori* mutant grown at pH 5.0 (ArsRS Regulon) (4 replicates)	Pflock *et al.* (2006)[220]

Table 2.7. Transcriptomics studies with *H. pylori.* (Continued).

Objectives	Technology used (Manufacturer)	*H. pylori* Strains	Experimental conditions	Experimental design	Reference
Characterization of the HP1021-dependent regulon	Spotted DNA/cDNA (Max-Planck-Institute for Infection Biology – MPIIB)	26695	Brain heart infusion (BHI) broth with fetal calf serum and antibiotics	Determination of differentially expressed genes in the HP1021-deficient mutant 26695/HP1021::km *vs* 26695 wild-type (4 replicates)	Pflock *et al.* (2007)[221]
Study of *H. pylori* G27 HP0518 mutant motility	Spotted DNA/cDNA (Max-Planck-Institute for Infection Biology – MPIIB)	G27 G27 mutant	RPMI1640 with fetal bovine serum	G27 wild-type *vs H. pylori* G27 HP0518 mutant	Asakura et al. (2010)[222]

Proteomics, the large-scale analysis of cellular proteins, with the use of two-dimensional gel electrophoresis for protein separation and identification by mass spectrometry, is the most applied technology in "omics" studies of *H. pylori*. The published studies in this field were mainly driven by the aim of discovering new proteins that can be used as vaccine candidates, or to investigate proteins differentially expressed under different conditions (mutant strains, environmental and / or stress conditions, among others). There are many different types of proteomic approaches that are being applied; notwithstanding, according to the aims of the present work, which include the reconstruction of a genome-scale metabolic model, the collection of proteomics data was focused on expression proteomics (Table 2.8).

Regarding **metabolomics** or **fluxomics**, to our knowledge, there are no *H. pylori* data published. The studies that covered topics related with metabolite analysis only analyzed specific internal or external metabolites.

Table 2.8. Proteomics studies with *H. pylori*.

Technologies: 1-DE – one-dimensional gel electrophoresis; 2-DE – two-dimensional gel electrophoresis; DIGE - Difference gel electrophoresis; MALDI – Matrix-assisted laser desorption/ionization; TOF – time of flight; MS – mass spectrometry; LC Nano-ESI QTOF MS - Liquid chromatography nano electrospray ionization- quadrupole time-of-flight mass spectrometry; IMAC - Immobilized-metal affinity chromatography; SELDI-TOF MS - Surface-enhanced laser desorption/ionisation time of flight mass spectrometry.

Objectives	Methodology (technology used)	*H. pylori* Strains	Results/Conclusions	Reference
Analysis of the proteins secreted by *H. pylori*, with optimization of culture conditions for minimal autolysis and efficient recovery method for extracellular proteins	2-DE MALDI MS	26695	Identification of 26 protein species (redox-active enzymes, components of flagellar apparatus, fragments of VacA, serine protease chaperone HtrA and uncharacterized proteins).	Bumann *et al.* (2002)[223]
Detect candidate antigens of *H. pylori* for diagnosis, therapy and vaccine development and to investigate potential associations between specific immune responses and manifestations of disease	2-DE MALDI MS Immunoblotting	26695	310 antigenic protein species were recognized by *H. pylori* positive sera (9 new antigens).	Haas *et al.* (2002)[224]
Establish a dynamic two-dimensional electrophoresis-polyacrylamide gel electrophoresis (2-DE-PAGE) database with multiple subproteomes of *H. pylori* (http://www.mpiib-berlin.mpg.de/2DPAGE) Elucidate protein composition of *H. pylori* soluble and structure-bound fractions (including membrane proteins).	Subcellular fractionation 2-DE MALDI MS	26695 P12 B128	Structure-bound fraction: 800 protein spots; Soluble protein fraction: 1000 protein spots. Generation of a subcellular reference map with a large number of structure-bound and soluble proteins identified in *H. pylori*.	Backert *et al.* (2005)[225]
Proteome characterization and comparative immunoproteomic analysis to identify antigenic patterns of *H. pylori* strains, by probing them against sera from patients affected by diverse gastrointestinal pathologies	2-DE Western blotting MALDI-TOF-MS Edman degradation analysis	Clinical isolates: 328 (Chronic gastritis) G39 (Duodenal ulcer) 10K (Gastric adenocarcinome)	Identification of 30 antigens (including 9 new antigens). Heterogeneous antigenic patterns, consequence of strain and a host-specificity.	Mini *et al.* (2006)[226]

Table 2.8. Proteomics studies with *H. pylori*. (Continued)

Objectives	Methodology (technology used)	*H. pylori* Strains	Results/Conclusions	Reference
Comparison of protein compositions of rod shaped *H. pylori* cells and coccoid cells.	2-DE MALDI-TOF MS	26695	1500 protein species were detected under both culture conditions. Identification of all 16 rod-shape-specific proteins and 11 of the 14 coccoid-specific proteins.	Bumann *et al.* (2004)[227]
Comparison of protein composition of three different strains, growth at different pH and identification of antigens.	2-DE MALDI-TOF MS	26695 J99 SS1 (mouse-adapted, "Sidney Strain")	Strain 26695: 1863 spots detected; Strain J99: 1622 spots identified; Strain SS1: 1448 spots identified. Identification of 10 protein spots common in strains 26695 and J99. 152 protein spots of strain 26695 identified in MALDI-MS. In pH dependent protein composition, 5 spots were identified as different at different pH for strain 26695.	Jungblut *et al.* (2000)[228]
Comparison of protein expression profiles of *H. pylori* grown under normal and high-salt conditions.	2-DE MALDI-TOF MS	Clinical isolates: HC28 (Human gastric cancer) HD30 (Human duodenal ulcer)	More than 40 spots identified in each gel. 190 proteins changed their expression levels after growth at high salt concentrations. Proteins with large differences in expression identified by peptide-mass fingerprinting (10 proteins: 9 upregulated and 1 downregulated).	Liao *et al.* (2013)[229]
Identification of proteins associated with *H. pylori* colonization in mice by comparing proteomic analysis of the wild-type *H. pylori* 26695 and the motile, mouse-passaged variant 88-3887.	2-DE MALDI-TOF/TOF MS	26695 Mouse-passaged homolog 88-3887 (isolated after 3 passages through the stomach of a C57BL/6 mouse)	Membrane proteins: 213 spots (strain 26695) and 215 spots (strain 88-3887). Cellular-protein fractions: 1532 spots (strain 26695) and 1546 spots (strain 88-3887). 29 proteins were differentially expressed between 2 strains (16 membrane-associated proteins and soluble-cellular-protein fragments).	Zhang *et al.* (2009)[230]

Table 2.8. Proteomics studies with *H. pylori*. (Continued)

Objectives	Methodology (technology used)	*H. pylori* Strains	Results/Conclusions	Reference
Identification of outer membrane proteins using the sarcosine-insoluble outer membrane fraction.	2-DE MALDI-TOF MS	26695	A total of more than 80 protein spots were detected. Identification of 62 protein spots, representing 35 genes, including 16 kinds of OMP.	Baik *et al.*(2004)[231]
Identification of proteins released by mechanisms other than specific lysis.	2-DE MS	11637 (ATCC 43504)	More than 160 spots were identified in pellets. Mass spectrometry analysis of proteins increased in radioactivity in the supernatant (18 proteins).	Kim *et al.* (2002)[232]
Proteome analysis of *H. pylori* NCTC 11637	2-DE MALDI-TOF MS	NCTC 11637	Consistent 318 protein spots were identified. Analysis by MALDI-TOF MS of 93 proteins. Identification of potential post-translational protein modifications.	Lock *et al.* (2001)[233]
Improve proteomic knowledge on coccoid cells formation by protein analysis of *H. pylori* coccoid cells under oxidative stress.	2-DE MALDI-TOF MS	Clinical isolate: HD13 (duodenal ulcer)	Protein spots detected: 635 for bacillary forms, 614 for coccoid forms. Analysis by MALDI-TOF/MS of 10 protein spots with most significant difference between forms. Proteins related to coccoid forms: 10 protein spots were overexpressed under different conditions (7 protein spots were identified, being 5 protein spots highly expressed and 2 protein spots lowly expressed in coccoid forms, compared to bacillary forms).	Zeng *et al.* (2008)[234]
Study the influence of oxidative stress. Proteomic approach to characterize and compare protein expression profile of *H. pylori* under aerobic stress (20% O_2) and microaerophilic (5% O_2) conditions.	2-DE MALDI-TOF MS	Clinical isolates: HC28 (Human gastric cancer) HD30 (Human duodenal ulcer)	More than 50 protein spots identified in 2-DE gels of *H. pylori* grown under microaerophilic and hiperoxia conditions. In total 11 protein were differentially expressed under aerobic and microaerophilic conditions (2 protein spot areas with apparently reduced expression) (analyzed by MALDI-TOF/MS).	Chuang *et al.* (2005)[235]

Table 2.8. Proteomics studies with *H. pylori*. (Continued)

Objectives	Methodology (technology used)	*H. pylori* Strains	Results/Conclusions	Reference
Define the adaptive response of *H. pylori* to nitrosamine stress. Simulation of antimicrobial process of NO in *H. pylori in vitro*, with sodium nitroprusside (SNP) as NO donor.	2-DE MALDI-TOF/TOF-tandem MS	26695	Based on 2-DE gels, and comparison of protein lysates of treated and untreated cells, 38 protein spots, which showed differential expression in response to nitric oxide, were digested and analyzed by MALDI-TOF/TOF-tandem mass spectrometer.	Zhou *et al.* (2009)[236]
Identification of outer membrane proteins (OMP) of *H. pylori* that contribute to antibiotic resistance using a comparative proteomics strategy of clarithromycin-resistant and susceptible strains.	1-DE MALDI-TOF/TOF-tandem MS	ATCC 43504 (clarithromycin susceptible) ATCC 700684 (clarithromycin resistant)	12 major proteins identified by 1-DE in sarcosine-insoluble fraction. Different level of protein expression for OMPs was found between resistant and sensitive strains. The 7 proteins that showed the most significant difference in protein expression were digested and analysed by MALDI-TOF/TOF MS.	Smiley *et al.* (2013)[237]
Understand the growth phase-dependent global regulation of proteins in *H. pylori*.	2-DE MALDI-TOF MS	26695	Approximately 1200 protein spots identified at 12 hours of culture. A total of 366 spots detected in all gels and selected for cluster analysis. The intensity of 151 protein spots significantly changed at any time point. 57 protein spots were identified (46 with increased intensity and 11 with decreased intensity during culture) by MALDI-TOF MS analysis. Protein levels were compared with mRNA transcript of each gene.	Choi *et al.* (2008)[238]
Explore the functions of SpoT, a global regulator for defending against oxidative stress *in vitro*, by comparison of protein expression profiles of a *spoT* deficient (*ΔspoT*) strain with wild-type after exposure to ambient atmosphere.	2-DE MALDI-TOF/TOF MS	26695 26695 *spoT* deficient (*ΔspoT*)	In total, 51 protein spots were differentially transcribed in strain *ΔspoT* and analysed by MALDI-TOF MS. Results confirmed in mRNA levels by RT-PCR, proved the downregulation in *ΔspoT* strain.	Sun *et al.* (2012)[239]

Table 2.8. Proteomics studies with *H. pylori*. (Continued)

Objectives	Methodology (technology used)	*H. pylori* Strains	Results/Conclusions	Reference
Identify changes in the proteome of *H. pylori* in response to low pH using a proteomics approach to study protein expression under neutral (pH 7) and acidic (pH 5) conditions.	2-DE LC-nanoESI-MS/MS	Clinical isolate HD30 (duodenal ulcer)	More than 412 protein spots were detected in 2-DE profiles of *H. pylori* grown under neutral or acidic conditions. About 10 proteins were differentially expressed under acidic conditions (increased amounts in 8 proteins and decreased amounts in 2 proteins), analysed by nano-LC-MS/MS.	Huang *et al.* (2010)[240]
Identify additional members of the ArsRs regulon and investigate the regulatory role of the ArsRs system by the analysis of protein expression in wild-type and arsS null mutant strains.	DIGE MALDI-TOF/TOF MS	J99 wild-type Mutant strain J99: J99A (*arsS::kan*) Mutant strain J99: J99B (*arsS::kan*)	Experiment 1: 639 protein spots in all gels. At pH 5.0, 25 differentially expressed proteins were identified by MS, in wild-type compared to the isogenic *arsS* mutant strain (also differentially expressed at pH 7.0). Experiment 2: similar results to experiment 1. 15 proteins identified as differentially expressed in wild-type and mutant strains in both proteomic experiments.	Loh *et al.* (2010)[241]
Investigate bismuth action against *H. pylori* by comparative proteomic analysis of *H. pylori* cells before and after treatment with colloidal bismuth subcitrate.	2-DE MALDI MS IMAC	11637	800 protein spots detected in 2-DE gels. Proteins differentially expressed (at least 2-fold) digested and analysed by MALDI-MS, 8 proteins identified. 7 bismuth-binding proteins were identified from cell extracts using IMAC.	Ge *et al.* (2007)[242]
Identify acid-related proteins (other than the urease system) by comparison of proteome profiles of *H. pylori* exposed to different levels of external pH, in absence of urea.	2-DE MALDI-TOF/TOF MS	26695	Differentially expressed protein spots analysed by MALDI-TOF/TOF MS; identification of 36 proteins with altered expression (more than two-fold) in response to acid (26 proteins induced and 10 proteins repressed).	Shao *et al.* (2008)[243]
Compare proteome maps of *H. pylori* clinical isolates.	2-DE MALDI-TOF MS	Clinical isolates from patients with duodenal ulcers and chronic gastritis:	500 protein spots analyzed by MALDI-TOF MS. 12 proteins identified with differences in proteome maps of clinical isolates.	Govorun *et al.* (2003)[244]

Table 2.8. Proteomics studies with *H. pylori*. (Continued)

Objectives	Methodology (technology used)	*H. pylori* Strains	Results/Conclusions	Reference
Identify extracellular proteins from *H. pylori*.	LC-nanoESI- MS/MS	26695 ATCC 43504 (nonsequenced strain)	172 different proteins identified in the cell-associated samples and 130 proteins from extracellular samples identified in at least two biological replicates. 45 of the extracellular proteins enriched in the extracellular fraction (11 previously identified).	Smith *et al.* (2007)[245]
Investigation of global gene regulation by Fur in response to iron in *H. pylori* by the comparison of protein expression profiles of wild-type and *fur* mutant grown under iron-rich and iron-depletion conditions.	2-DE MALDI-TOF MS	26695 Isogenic *fur* mutant strain of 26695	93 protein spots were found to be up or down-regulated by more than 2-fold by either a *fur* mutation or iron-depletion. 39 spots identified (MALDI-TOF MS) to be 29 different proteins. Expression of 6 proteins was higher in *fur* mutant than in wild-type.11 proteins activated by Fur (5 responded to iron). 12 proteins not Fur-regulated but responded to iron.	Lee *et al.* (2004)[246]
Establish the use of ProteinChip technology to compare outer membrane proteins profiles between fresh clinical isolates and strains that have been passaged *in vitro*.	ProteinChip array (WCX-2) SELDI-TOF MS	Clinical isolates: strain 119/95, strain 32, strain 33 (Sweden) CCUG 17874 CCUG 17875	Six proteins identified to be common in *the* strains studied. Clinical isolates strain 119/95 and strain 33 showed a similar profile.	Hynes *et al.* (2003)[247]
Establish the correlation of *H. pylori* clinical isolates with the prevalence of *H. pylori*-associated iron deficiency anaemia by the comparison of proteomic profiles of *H. pylori* strains from *H. pylori*-positive patients with or without iron deficiency anaemia.	2-DE MALDI-TOF MS	Clinical isolates from 10-18 years-old Korean adolescents: 8 strains from patients with gastritis; 7 strains from patients with iron deficiency anaemia 26695	Protein expression profiles displayed, in total, 1746 protein spots. Expression patterns of 189 protein spots were used to construct a phylogenetic tree. 18 spots expressed in iron deficiency anaemia strains identified by MALDI-TOF.	Park *et al.* (2006)[248]

Table 2.8. Proteomics studies with *H. pylori*. (Continued)

Objectives	Methodology (technology used)	*H. pylori* Strains	Results/Conclusions	Reference
Proteomics and genomics approaches for identification of genetic and phenotypic changes in *H. pylori* obtained from different locations of the stomach from patients with early gastric cancer or chronic gastritis.	2-DE 2D DIGE MALDI-TOF/TOF MS	Clinical isolates from fundus, corpus and antrum of the stomach o two patients (6 samples).	32 differentially expressed proteins detected related to early gastric cancer and 14 differentially expressed proteins related to chronic gastritis. In total, 28 variable proteins in all the *H. pylori* isolates were identified.	Momynaliev *et al*. (2010)[249]
Characterization of *H. pylori*'s phosphoproteome.	Affinity chromatography LC-MS/MS	26695	67 phosphoproteins were identified. An interaction network with 28 phosphoproteins was constructed with a total of 163 proteins.	Ge *et al*. (2011)[250]
Analysis of cellular and antigen proteins. Comparison of automatic and manual procedures of data generation and Identification.	2-DE MALDI MS	26695	384 protein spots analysed by MALDI MS. 24 new protein identified.	Krah *et al*. (2003)[251]
Investigate the changes in protein expression of *H. pylori* under oxidative stress, induced by hydrogen peroxide.	2-DE LC Nano-ESI QTOF MS	Clinical isolates: HC28 (Human gastric cancer) HD30 (Human duodenal ulcer) HS65 (Human gastritis)	Around 390 spots identified in each gel. Most overexpressed proteins were identified under oxidative stress (9 proteins).	Huang and Chiou (2011)[240]
Analysis of urea-solubilized proteins, proteins insoluble in urea but solubilized by SDS, proteins precipitating in the Sephadex layer at the application side of IEF and proteins precipitating close to the application side within the IEF gel.	2-DE 1-DE-LC/MS	26695	567 proteins identified (36.6% proteome coverage) Data stored at http://www.mpiib-berlin.mpg.de/2D-PAGE/	Jungblut *et al*. (2010)[252]

2.5.2 Genome-scale metabolic models (GSMM)

The ultimate aim of systems biology is to develop mathematical models so that the response of biological complex systems to any kind of perturbation can be predicted *in silico*, even under conditions that are not easily accessible with experiments, and iteratively producing polished models and insight into the system[253]. Each biological process can be described using different mathematical models, depending on the problem, and the purposes of the investigation[253].

In the last years, several mathematical models for many organisms have been developed. In particular, the development of mathematical models of metabolism and more specifically genome-scale metabolic models is now considered a fundamental part of the study of the cell[168].

Among several types of metabolic networks, the stoichiometric models are the most broadly used, encompassing a set of stoichiometric equations representing the metabolic pathways of the system. Mass balance constrains on the metabolites, in a steady state assumption, are then used to determine intracellular fluxes through all the biochemical reactions occurring in the cell[254,255]. Due to the lack of information on cellular processes such as regulatory events, this type of models does not account for information on kinetics, regulatory or other cellular processes [256].

Since the first genome-scale metabolic model reconstruction in 1999[257] by Edwards and Palsson, an increasing number of metabolic model reconstructions are being published with over 100 reconstructed models for more than 60 different organisms available[258].

2.5.2.1 Reconstruction process

The reconstruction of a genome-scale metabolic model is an iterative process that begins with the collection of information about genome annotation and organism-specific metabolic knowledge from various sources of information. After several intermediate steps, the metabolic model is constructed and simulations are performed to compare *in silico* obtained results with experimental data. The model is revised until the *in silico* predictions

reasonably agree with experimental data,[259] (Figure **2.5**). The process of reconstructing a metabolic network is a very laborious task, requiring manual evaluation on several steps to achieve a high-quality reconstruction[259]. To settle this problem, in the last years a series of software tools and platforms has been developed, and a recent review was published, addressing the use of software platforms that facilitate metabolic model reconstruction in several steps[260]. In the last years, a few reviews with guidelines to develop genome-scale metabolic models have been published [259,261–263].

According to the protocol published by Thiele and Palsson, the generation of a metabolic network includes more than 90 steps, and encompasses four main stages which are briefly discussed in the next pages[262].

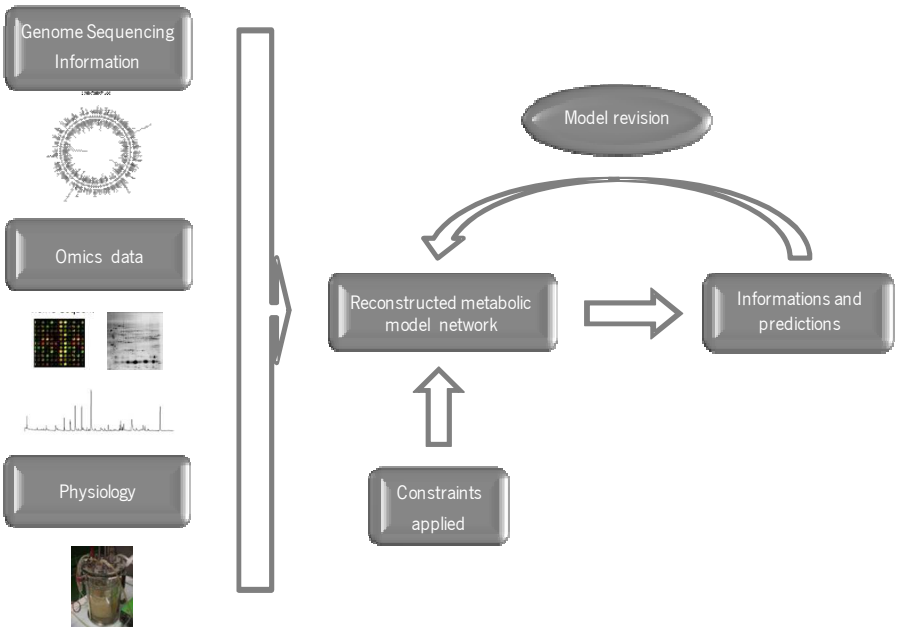

Figure 2.5. Genome-scale metabolic model reconstruction overview.

i. *Draft model creation*

This first step can be a manual or an automatic (or semi-automatic) process, with several software tools available to generate the draft reconstruction such as Pathway tools[264], The Seed[265], merlin[266], or RAVEN[267], among others[262].

As each model is organism specific, the draft model creation is based on genome annotation and specific biochemical information available for the target organism[261]. When available, it is important to use the latest genome annotation for the creation of the draft reconstruction, since the annotation is the backbone of the draft model, thus contributing to the quality of the reconstructed model[262]. Nowadays, several databases with genome annotations for a variety of organisms are available. Some of them are organism-specific such as the PyloriGene[268] (*H. pylori*), SGD[269] (*S. cerevisiae*), or Ecocyc[264] (*E. coli*), while others contain annotations for a large spectrum of organisms, such as EntrezGene[270] or IMG[271] (Integrated Microbial genome) (for a review see Thiele and Palsson (2010)[262]). From these databases, data about genes, open reading frames (ORF), cellular function, sequence similarities, and Enzyme commission (EC) number for the enzyme coding genes can be retrieved. Only genes encoding enzymes and membrane transporters are included in the reconstruction[259]. In the identification of candidate metabolic functions, other databases that contain information about pathways and biochemical reactions can also be used[259,262], such as KEGG[272], Brenda[273], MetaCyc[274], or Transport DB[275]. At this point, a list of possible metabolic functions, possibly incomplete or with functions that are not considered in metabolic model reconstructions (such as proteins involved in DNA methylation) is obtained[262]. Subsequently, the draft reconstruction is assembled.

ii. *Curation and refinement*

At this stage, manual curation of the draft model has to be done by inspecting all gene-protein-reactions to identify wrong information, gaps in network, and inconsistencies. It is a very important step, since the databases used are not always organism-specific, and sometimes wrong information is included[262,263]. In order to curate and refine the model, there are several steps to be performed (Table 2.9), according to Rocha *et al.* (2007)[259] and Thiele and Palsson (2010)[262].

Table 2.9. Model curation steps[259,262].

Steps of model curation	Sources of information/Comments
Metabolic function verification	Experimental data and literature; Information about phylogenetically close organisms (for less-characterized organisms).
Substrates and cofactors	Literature and databases search for organism-specific biochemical studies.
Charged formula for metabolites	Predict with software packages
Reaction stoichiometry	Based on online databases (if an EC number has been assigned) and literature data.
Reaction directionality	Estimation of standard Gibbs free energy can be used; No information available: the reaction is set reversible.
Gene and reaction localization	Online databases and literature Algorithms to predict cellular localization (such as PSORT[276])
Gene-protein-reaction association	Important to determine the existence of enzyme complexes or isoenzymes
Extracellular and periplasmic transport reactions	Extracellular reactions can occur with interconversions.
Exchange reactions	Considered system inputs and outputs.
Intracellular transport reactions	Applicable to multi-compartment networks.
Biomass compositions	Experimental determination from cells growing in log phase of all known biomass constituents and fractional contributions to the overall biomass; A generic biomass equation can be used but taking into account that biomass composition can change depending on physiological conditions.
Growth associated ATP and maintenance ATP	Included in biomass equation and in a reaction converting ATP to ADP; ATP molecules needed per gram of biomass formed and needed for maintenance processes; Experimentally determined from chemostat growth experiments; Biomass ATP can be estimated by determining the energy required for macromolecular synthesis.
Growth medium requirements	Experimentally determined or retrieved from literature.

iii. *Generation of a stoichiometric steady-state metabolic model*

At this stage, the reconstructed metabolic network is converted to a mathematical format, that is the basis of the genome-scale model[261]. This conversion can be performed automatically[262]. A stoichiometry matrix (S) of the reaction list is generated, in which rows represent network metabolites and columns the network reactions. For each reaction, substrate and product coefficients are entered in the corresponding cell of the matrix[255,262]. It was defined that substrates in reactions have a negative coefficient and products a positive coefficient[262]. After that, the system boundaries need to be defined. For that, for all metabolites that are produced or consumed to or from the external medium, an exchange reaction needs to be added to the model. In mass balances, the mass conservation is

applied. Thus, the steady-state can be described by S.v = 0, where v is a vector of reaction fluxes[262,277]. The definition of constraints for the exchange reactions, indicating for example availability of medium components, completes the mathematical formulation of the model.

The definition of an objective function is important to perform simulations, as the previous model by itself represents a variety of solutions. Usually, the objective function is defined to be the maximization of the generation of biomass[261]. This requires a previous inclusion of an additional biomass formation reaction that represents the macromolecular cell composition, including building blocks, and requirements of energy needed to generate biomass[261,278]. The use of objective functions within stoichiometric models requires the formulation of a Linear Programming problem, within the so-called flux balance analysis (FBA) approach. FBA was developed with the aim of characterizing the capabilities and properties of a biochemical network[277]. The maximization of the biomass objective function is usually applied, using FBA to identify the flux distribution through the metabolic network, considering the constraints imposed by the mass balance equations and reaction bounds, thus predicting the organism growth rate[277].

Standards for model representation were developed, and one extensively used is the Systems Biology Markup Language (SBML), which is XML-based and is used to represent and exchange models between simulation tools[279,280].

iv. *Model evaluation*

At this stage, the reconstructed model, predicting biomass formation, is evaluated and validated by several tests and additional experimental data[262,263]. Phenotypes of gene-deletion strains provide very useful data to test the network, but are not always available. Physiological parameters (such as growth rates, yields, substrate utilization and product formation rates), preferentially from chemostat experiments, represent additional data that are very useful for model validation[263]. The model should agree with the measured fluxes or predict some of the fluxes[263]. The steps to be done are summarized in Table 2.10.

Table 2.10. Steps to be performed to evaluate the reconstructed metabolic model[262].

Model debugging	Procedure/Comments
Metabolic dead-ends verification and gap analysis	Gap analysis (search for missing reactions and functions) in order to identify dead-end metabolites (not connected to the metabolic network); Literature search to find information to fill the gaps.
Biomass precursor production	Test if the model is able to produce all biomass precursors.
Test other growth media for biomass precursor production	The model should produce biomass in a variety of different media.
Blocked reactions verification	Verify if there is a reaction that cannot carry any flux in any situation (blocked reactions).
Simulate single gene deletion phenotypes	If there is information available about deletions, should be compared with model predictions.
Check known incapacities of the organism	Such as auxotrophies, etc.
Evaluate growth rate	Compare experimental with *in silico* predicted growth rates; If the *in silico* growth rate is very low, a component in the growth medium may be growth limiting; If the growth rate is very high, one possible explanation is that the objective function was not correctly set.

Once the model reaches a satisfactory agreement with experimental data, it can be used for a variety of applications.

2.5.2.2 *H. pylori* 26695 GSMMs

H. pylori 26695 is a highly pathogenic strain that was originally isolated from a patient with gastritis in the United Kingdom. Its complete genome was sequenced by whole-genome random sequencing and published in 1997[131]. This pathogenic organism presents a small genome with 1.67 Mbp, with an average G+C content of 39% and approximately 1590 predicted coding regions[131].

H. pylori strain 26695 is motile, catalase, urease and oxidase positive. Regarding virulence, it possess a cytotoxin-associated gene A (cagA gene) and expresses the vacuolating cytotoxin (VacA) encoded by the vacA gene, contributing to this strain's pathogenicity[281].

In 2002, the first genome-scale metabolic model of *H. pylori* 26695 was published[282]. This reconstruction was based on the first genome annotation provided by the TIGR Microbial Database and Genebank[282]. A genome re-annotation of *H. pylori* 26695 was published in 2003, generating a specific database – Pylorigene[268] (publically available at

http://genolist.pasteur.fr/PyloriGene/). In 2005, a GSMM reconstruction (*i*T341 GSM/GPR) was published for the same strain, where the genome information was updated for the revised annotation of the *H. pylori* 26695 genome and also accounted for the new experimental data made available[283]. The metabolic network characterization for both published models is showed in Table 2.11. This new reconstruction accounts for 50 new gene loci, 88 new reactions, and 82 more metabolites than the first model created by Schilling *et al*. (2002) (Table 2.11). Also, some pathways were more accurately described and gene-protein-reaction associations were introduced[283].

Table 2.11. *In silico H. pylori* 26695 metabolic networks characterization.

***In silico* metabolic networks**	***i*CS291 (2002)**[282]	***i*T341 GSM/GPR (2005)**[283]
No. genes included	291	341
No. of reactions	388	476
No. of metabolites (internal/external)	339/64	411/74
S matrix	649 x 403	554 x 485

Note: The "*i*" in the model name refers to an *in silico* model, the following initials correspond to the person who developed the model and then the number of genes are presented. "GSM" indicates "Genome Scale Model" and "GPR" refers to "Gene-Protein-Reaction" association.

2.6 *References*

1. Marshall, B. J. & Warren, J. R. Unidentified curved Bacilli in the stomach of patients with gastritis and peptic ulceration. *Lancet* **1,** 1311–1315 (1984).
2. "Press Release: The 2005 Nobel Prize in Physiology or Medicine." *Nobelprize.org*
3. Goodwin, C. S., Strong, J. A. & Marshall, B. J. Review article *Campylobacter pyloridis*, gastritis, and peptic ulceration. *J. Clin. Pathol.* **39,** 353–365 (1986).
4. Marshall, B. J., Armstrong, J. A., McGechie, D. B. & Glancy, R. J. Attempt to fulfil Koch's postulates for pyloric *Campylobacter*. *Med. J. Aust.* **142,** 436–439 (1985).
5. Sayers, E. W. *et al.* Database resources of the National Center for Biotechnology Information. *Nucleic Acids Res.* **37,** D5–15 (2009).
6. Garrity, G. M., Bell, J. A. & Lilburn, T. *Family II. Helicobacteraceae fam. nov. in Bergey's Manual of Systematic Bacteriology Volume Two The Proteobacteria*. 1168–1194 (Spinger, 2005).
7. Marshall, B. J. *et al.* Original isolation of *Campylobacter pyloridis* from human gastric mucosa. *Microbios Lett.* **25,** 83–88 (1984).
8. Marshall, B. J. & Goodwin, C. S. Notes: Revised nomenclature of *Campylobacter pyloridis*. *Int. J. Syst. Bacteriol.* **37,** 68 (1987).
9. Romaniuk, P. J. *et al. Campylobacter pylori*, the spiral bacterium associated with human gastritis, is not a true *Campylobacter* sp. *J. Bacteriol.* **169,** 2137–2141 (1987).
10. Thompson, L. M., Smibert, R. M., Johnson, J. L. & Krieg, N. R. Phylogenetic study of the genus *Campylobacter*. *Int. J. Sist. Bacteriol.* **38,** 190–200 (1988).
11. Goodwin, C. S. *et al.* Transfer of *Campylobacter pylori* and *Campylobacter mustelae* to *Helicobacter* gen. nov. as *Helicobacter pylori* comb. nov. and *Helicobacter mustelae* comb.nov., respectively. *Int. J. Sist. Bacteriol.* **39,** 397–405 (1989).
12. Marshall, B. *Helicobacter pylori*: 20 years on. *Clin. Med. (Northfield. Il).* **2,** 147–152 (2002).

13. Hua, J.-S., Zheng, P.-Y. & Ho, B. Species differentiation and identification in the genus of *Helicobacter*. *World J. Gastroenterol.* **5,** 7–9 (1999).

14. Solnick, J. V & Schauer, D. B. Emergence of diverse *Helicobacter* species in the pathogenesis of gastric and enterohepatic diseases. *Clin. Microbiol. Rev.* **14,** 59–97 (2001).

15. Kusters, J. G., van Vliet, A. H. M. & Kuipers, E. J. Pathogenesis of *Helicobacter pylori* infection. *Clin. Microbiol. Rev.* **19,** 449–490 (2006).

16. Goodwin, C. S., McCulloch, R. K., Armstrong, J. A. & Wee, S. H. Unusual celular fatty acids and distinctive ultrastructure in a new spiral bacterium (*Campylobacter pyloridis*) from the human gastric mucosa. *J. Med. Microbiol.* **19,** 257–267 (1985).

17. Jones, D. M., Curry, A. & Fox, A. J. An ultrastructural study of the gastric Campylobacter-like organism "*Campylobacter pyloridis*." *J. Gen. Microbiol.* **131,** 2335–2341 (1985).

18. Bode, G., Mauch, F. & Malfertheiner, P. The coccoid forms of *Helicobacter pylori*. Criteria for their viability. *Epidemiol. Infect.* **111,** 483–490 (1993).

19. Kusters, J. G., Gerrits, M. M., Van Strijp, J. A. G. & Vandenbroucke-Grauls, C. M. J. E. Coccoid forms of *Helicobacter pylori* are the morphologic manifestation of cell death. *Infect. Immun.* **65,** 3672–3679 (1997).

20. Azevedo, N. F. *et al.* Coccoid form of *Helicobacter pylori* as a morphological manifestation of cell adaptation to the environment. *Appl. Environ. Microbiol.* **73,** 3423–3427 (2007).

21. Saito, N. *et al.* Plural transformation-processes from spiral to coccoid *Helicobacter pylori* and its viability. *J. Infect.* **46,** 49–55 (2003).

22. Nilsson, H., Blom, J., Al-soud, W. A., Andersen, L. P. & Wadström, T. Effect of cold starvation, acid stress, and nutrients on metabolic activity of *Helicobacter pylori*. *Appl. Environ. Microbiol.* **68,** 11–19 (2002).

23. Goodwin, C. S. & Armstrong, J. A. Microbiological Aspects of *Helicobacter pylori* (*Campylobacter pyloridis*). *Eur. J. Clin. Microbiol. Infect. Dis.* **9,** 1–13 (1990).

24. Geis, G., Suerbaum, S., Forsthoff, B., Leying, H. & Opferkuch, W. Ultrastructure and biochemical studies of the flagellar sheath of *Helicobacter pylori*. *J. Med. Microbiol.* **38,** 371–7 (1993).

25. O'Toole, P. W., Lane, M. C. & Porwollik, S. *Helicobacter pylori* motility. *Microbes Infect.* **2,** 1207–1214 (2000).

26. Suerbaum, S. The complex flagella of gastric *Helicobacter* species. *Trends Microbiol.* **3,** 168–70; discussion 170–1 (1995).

27. Fox, J. G., Wang, T. C. & Parsonnet, J. *Infections Causing Human Cancer - Chapter 10 -* Helicobacter*, Chronic Inflammation and Cancer*. (WILEY-VCH, 2006).

28. Hill, M. The microbiology of *Helicobacter pylori*. *Biomed & Pharmacother* **51,** 161–163 (1991).

29. Beswick, E. J., Suarez, G. & Reyes, V. E. *H. pylori* and host interactions that influence pathogenesis. *World J. Gastroenterol.* **12,** 5599–565 (2006).

30. Brown, L. M. *Helicobacter pylori*: Epidemiology and routes of transmission. *Epidemiol. Rev.* **22,** 283–297 (2000).

31. Bruce, M. G. & Maaroos, H. I. Epidemiology of *Helicobacter pylori* infection. *Helicobacter* **13 Suppl.,** 1–6 (2008).

32. Azevedo, N. F., Huntington, J. & Goodman, K. J. The epidemiology of *Helicobacter pylori* and public health implications. *Helicobacter* **14 Supp.1,** 1–7 (2009).

33. Ford, A. C. & Axon, A. T. R. Epidemiology of *Helicobacter pylori* infection and public health implications. *Helicobacter* **15 Suppl.,** 1–6 (2010).

34. Goh, K.-L., Chan, W.-K., Shiota, S. & Yamaoka, Y. Epidemiology of *Helicobacter pylori* infection and public health implications. *Helicobacter* **16 Suppl.1,** 1–9 (2011).

35. Tonkic, A., Tonkic, M., Lehours, P. & Mégraud, F. Epidemiology and diagnosis of *Helicobacter pylori* infection. *Helicobacter* **17 Suppl.1,** 1–8 (2012).

36. Tanih, N. F., Ndip, L. M., Clarke, A. M. & Ndip, R. N. An overview of pathogenesis and epidemiology of *Helicobacter pylori* infection. *African J. Microbiol. Res.* **4,** 426–436 (2010).

37. Mourad-Baars, P., Hussey, S. & Jones, N. L. *Helicobacter pylori* infection and childhood. *Helicobacter* **15 Suppl 1,** 53–59 (2010).

38. Azevedo, N. F., Guimarães, N., Figueiredo, C., Keevil, C. W. & Vieira, M. J. A new model for the transmission of *Helicobacter pylori*: Role of environmental reservoirs as gene pools to increase strain diversity. *Crit. Rev. Microbiol.* **33,** 157–169 (2007).

39. Dunn, B. E., Cohen, H. & Blaser, M. J. *Helicobacter pylori*. *Clin. Microbiol. Rev.* **10,** 720–741 (1997).

40. Isakov, V. & Malfertheiner, P. *Helicobacter pylori* and nonmalignant diseases. *Helicobacter* **8 Suppl.1,** 36–43 (2003).

41. Kuipers, E. J. & Malfertheiner, P. *Helicobacter pylori* and nonmalignant diseases. *Helicobacter* **9 Suppl.1,** 29–34 (2004).

42. Kupcinskas, L. & Malfertheiner, P. *Helicobacter pylori* and non-malignant diseases. *Helicobacter* **10 Suppl.1,** 26–33 (2005).

43. Shirin, H., Leja, M. & Niv, Y. *Helicobacter pylori* and non-malignant diseases. *Helicobacter* **13 Suppl.1,** 29–27 (2008).

44. Furuta, T. & Delchier, J.-C. *Helicobacter pylori* and non-malignant diseases. *Helicobacter* **14 Suppl.1,** 29–35 (2009).

45. Alakkari, A., Zullo, A. & O'Connor, J. H. *Helicobacter pylori* and nonmalignant diseases. *Helicobacter* **16 Suppl.1,** 33–37 (2011).

46. Shmuely, H., Katicic, M., Filipec Kanizaj, T. & Niv, Y. *Helicobacter pylori* and nonmalignant diseases. *Helicobacter* **17 Suppl.1,** 22–25 (2012).

47. Sepulveda, A. R. & Coelho, L. G. V. *Helicobacter pylori* and gastric malignancies. *Helicobacter* **7 Suppl.1,** 37–42 (2002).

48. Nardone, G. & Morgner, A. *Helicobacter pylori* and gastric malignancies. *Helicobacter* **8 Suppl.1,** 44–52 (2003).

49. Asaka, M. & Dragosics, B. A. *Helicobacter pylori* and gastric malignancies. *Helicobacter* **9 Suppl.1,** 35–41 (2004).

50. Fischbach, W., Chan, A. O. & Wong, B. C. *Helicobacter pylori* and gastric malignancy. *Helicobacter* **10 Suppl.1,** 34–39 (2005).

51. Starzyñska, T. & Malfertheiner, P. *Helicobacter* and digestive malignancies. *Helicobacter* **11 Suppl.1,** 32–35 (2006).

52. Moss, S. F. & Malfertheiner, P. *Helicobacter* and gastric malignancies. *Helicobacter* **12 Suppl.1,** 23–30 (2007).

53. Ferreira, A. C. *et al. Helicobacter* and gastric malignancies. *Helicobacter* **13 Suppl.1,** 28–34 (2008).

54. Suzuki, H., Franceschi, F., Nishizawa, T. & Gasbarrini, A. Extragastric manifestations of *Helicobacter pylori* infection. *Helicobacter* **16 Supp.1,** 65–69 (2011).

55. Figura, N. *et al.* Extragastric manifestations of *Helicobacter pylori* infection. *Helicobacter* **15 Suppl.1,** 60–68 (2010).

56. Banić, M., Franceschi, F., Babić, Z. & Gasbarrini, A. Extragastric manifestations of *Helicobacter pylori* infection. *Helicobacter* **17 Suppl. ,** 49–55 (2012).

57. Solnick, J. V, Franceschi, F., Roccarina, D. & Gasbarrini, A. Extragastric manifestations of *Helicobacter pylori* infection-other *Helicobacter* species. *Helicobacter* **11 Suppl.,** 46–51 (2006).

58. Bohr, U. R. M., Annibale, B., Franceschi, F., Roccarina, D. & Gasbarrini, A. Extragastric manifestations of *Helicobacter pylori* infection – other Helicobacters. *Helicobacter* **12 Suppl.1,** 45–53 (2007).

59. Moyaert, H. *et al.* Extragastric manifestations of *Helicobacter pylori* infection : Other Helicobacters. *Helicobacter* **13 Suppl.1,** 47–57 (2008).

60. Gasbarrini, A., Carloni, E., Gasbarrini, G. & Chisholm, S. A. *Helicobacter pylori* and extragastric diseases - other Helicobacters. *Helicobacter* **9 Suppl.1,** 57–66 (2004).

61. Gasbarrini, A., Carloni, E., Gasbarrini, G. & Ménard, A. *Helicobacter pylori* and extragastric diseases - other Helicobacters. *Helicobacter* **8 Suppl.1,** 68–76 (2003).

62. Nilsson, H. *et al. Helicobacter pylori* and extragastric diseases - other Helicobacters. **10 Suppl.1,** 54–65 (2005).

63. Pellicano, R. *et al.* Helicobacters and extragastric diseases. *Helicobacter* **14 Suppl 1,** 58–68 (2009).

64. Brunner, D. *et al.* Serum-free cell culture: the serum-free media interactive online database. *ALTEX* **27,** 53–62 (2010).

65. Douraghi, M. *et al.* Comparative evaluation of three supplements for *Helicobacter pylori* growth in liquid culture. *Curr. Microbiol.* **60,** 254–262 (2010).

66. Cover, T. L. Perspectives on methodology for *in vitro* culture of *Helicobacter pylori*. *Methods Mol. Biol.* **921,** 2012–2015 (2012).

67. Testerman, T. L., Gee, D. J. M. C. & Mobley, H. L. T. *Helicobacter pylori* growth and urease detection in the chemically defined medium Ham's F-12 nutrient mixture. *J. Clin. Microbiol.* **39,** 3842–3850 (2001).

68. Marchini, A. *et al.* Cyclodextrins for growth of *Helicobacter pylori* and production of vacuolating cytotoxin. *Arch. Microbiol.* **164,** 290–293 (1995).

69. Albertson, N., Wenngren, I. & Sjöström, J. E. Growth and survival of *Helicobacter pylori* in defined medium and susceptibility to Brij 78. *J. Clin. Microbiol.* **36,** 1232–1235 (1998).

70. Haque, M., Yokota, K., Hirai, Y. & Oguma, K. Lipid profiles of *Helicobacter pylori* and *Helicobacter mustelae* grown in serum-supplemented and serum-free media. *Acta Med. Okayama* **49,** 205–211 (1995).

71. Hirai, Y. *et al.* Unique cholesteryl glucosides in *Helicobacter pylori*: composition and structural analysis. *Microbiology* **177,** 5327–5333 (1995).

72. Trampenau, C. & Müller, K.-D. Affinity of *Helicobacter pylori* to cholesterol and other steroids. *Microbes Infect.* **5,** 13–17 (2003).

73. McGee, D. J. *et al.* Cholesterol enhances *Helicobacter pylori* resistance to antibiotics and LL-37. *Antimicrob. Agents Chemother.* **55,** 2897–2904 (2011).

74. Nedenskov, P. Nutritional requirements for growth of *Helicobacter pylori*. *Appl. Environ. Microbiol.* **60,** 3450–3453 (1994).

75. Stark, R. M., Suleiman, M. S., Hassan, I. J., Greenman, J. & Millar, M. R. Amino acid utilisation and deamination of glutamine and asparagine by *Helicobacter pylori*. *J. Med. Microbiol.* **46,** 793–800 (1997).

76. Testerman, T. L., Gee, D. J. M. C. & Mobley, H. L. T. *Helicobacter pylori* growth and urease detection in the chemically defined medium Ham's F-12 nutrient mixture. *J. Clin. Microbiol.* **39,** 3842–3850 (2001).

77. Reynolds, D. J. & Penn, C. W. Characteristics of *Helicobacter pylori* growth in a defined medium and determination of its amino acid requirements. *Microbiology* **140,** 2649–2956 (1994).

78. Sainsus, N., Cattori, V., Lepadatu, C. & Hofmann-Lehmann, R. Liquid culture medium for the rapid cultivation of *Helicobacter pylori* from biopsy specimens. *Eur. J. Clin. Microbiol. Infect. Dis.* **27,** 1209–1217 (2008).

79. Testerman, T. L., Conn, P. B., Mobley, H. L. T. & McGee, D. J. Nutritional requirements and antibiotic resistance patterns of *Helicobacter* species in chemically defined media. *J. Clin. Microbiol.* **44,** 1650–1658 (2006).

80. Queiroz, D. M., Mendes, E. N. & Rocha, G. a. Indicator medium for isolation of *Campylobacter pylori*. *J. Clin. Microbiol.* **25,** 2378–2379 (1987).

81. Ansorg, R., Von Recklinghausen, G., Pomarius, R. & Schmid, E. N. Evaluation of techniques for isolation, subcultivation, and preservation of *Helicobacter pylori*. *J. Clin. Microbiol.* **29,** 51–53 (1991).

82. Hutton, M. L., Kaparakis-Liaskos, M. & Ferrero, R. L. The use of AlbuMAX II(®) as a blood or serum alternative for the culture of *Helicobacter pylori*. *Helicobacter* **17,** 68–76 (2012).

83. Kehler, E. G., Midkiff, B. R. & Westblom, T. U. Evaluation of three commercially available blood culture systems for cultivation of *Helicobacter pylori*. *J. Clin. Microbiol.* **32,** 1597–1598 (1994).

84. Goodwin, C. S., Mcculloch, R. K., Armstrong, J. A. & Wee, S. H. Unusual fatty acids and distinctive ultrastructure in a new spiral bacterium (*Campylobacter pyloridis*) from the human gastric mucosa. *J. Med. Microbiol.* **19,** 257–267 (1985).

85. Hachem, C. Y., Clarridge, J. E., Evans, D. G. & Graham, D. Y. Comparison of agar based media for primary isolation of *Helicobacter pylori*. *J. Clin. Pathol.* **48,** 714–716 (1995).

86. Westblom, T. U., Madan, E. & Midkiff, B. R. Egg yolk emulsion agar, a new medium for the cultivation of *Helicobacter pylori*. *J. Clin. Microbiol.* **29,** 819–821 (1991).

87. Ohno, H. & Murano, A. Serum-free culture of *H. pylori* intensifies cytotoxicity. *World J. Gastroenterol.* **13,** 532–537 (2007).

88. Shibayama, K. *et al.* Usefulness of adult bovine serum for *Helicobacter pylori* culture media. *J. Clin. Microbiol.* **44,** 4255–4257 (2006).

89. Buck, G. E. & Smith, J. S. Medium supplementation for gowth of *Campylobacter pyloridis*. *J. Clin. Microbiol.* **25,** 597–599 (1987).

90. Miendje Deyi, V. Y., Van den Borre, C. & Fontaine, V. Comparative evaluation of 3 selective media for primary isolation of *Helicobacter pylori* from gastric biopsies under routine conditions. *Diagn. Microbiol. Infect. Dis.* **68,** 474–476 (2010).

91. Dent, J. & McNulty, C. A. Evaluation of a new selective medium for *Campylobacter pylori*. *Eur. J. Clin. Microbiol. Infect. Dis.* **7,** 555–558 (1988).

92. Secker, D. a, Tompkins, D. S. & Alderson, G. Gas-permeable lifecell tissue culture flasks give improved growth of *Helicobacter pylori* in a liquid medium. *J. Clin. Microbiol.* **29,** 1060–1061 (1991).

93. Cellini, L. *et al.* New plate medium for growth and detection of urease activity of *Helicobacter pylori*. *Notes* **30,** 1351–1353 (1992).

94. Olivieri, R. *et al.* Growth of *Helicobacter pylori* containing cyclodextrins. *J. Clin. Microbiol.* **31,** 160–162 (1993).

95. Stevenson, T. H., Castillo, A., Lucia, L. M. & Acuff, G. R. Growth of *Helicobacter pylori* in various liquid and plating media. *Lett. Appl. Microbiol.* **30,** 192–196 (2000).

96. Xia, H. X., Keane, C. T. & O'Morain, C. A. Determination of the optimal transport system for *Helicobacter pylori* cultures. *J. Med. Microbiol.* **39,** 334–337 (1993).

97. Soltesz, V., Zeeberg, B. & Wadstrom, T. Optimal survival of *Helicobacter pylori* under various transport conditions. *Helicobacter* **30,** 1453–1456 (1992).

98. Taneera, J. *et al.* Influence of activated charcoal, porcine gastric mucin and beta-cyclodextrin on the morphology and growth of intestinal and gastric *Helicobacter* spp. *Microbiology* **148,** 677–684 (2002).

99. Morgan, D. R., Freedman, R., Depew, C. E. & Kraft, W. G. Growth of *Campylobacter pylori* in liquid media. *J. Clin. Microbiol.* **25,** 2123–2135 (1987).

100. Degnan, A. J., Sonzogni, W. C. & Standridge, J. H. Development of a plating medium for selection of *Helicobacter pylori* from water samples. *Appl. Environ. Microbiol.* **69,** 2914–2918 (2003).

101. Hartzen, S. H. *et al.* Antimicrobial susceptibility testing of 230 *Helicobacter pylori* strains: importance of medium, inoculum, and incubation time. *Antimicrob. Agents Chemother.* **41,** 2634–2349 (1997).

102. Tee, W., Fairley, S., Smallwood, R. & Dwyer, B. Comparative evaluation of three selective media and a nonselective medium for the culture of *Helicobacter pylori* from gastric biopsies. *J. Clin. Microbiol.* **29,** 2587–2589 (1991).

103. Walsh, E. J. & Moran, a P. Influence of medium composition on the growth and antigen expression of *Helicobacter pylori*. *J. Appl. Microbiol.* **83,** 67–75 (1997).

104. Vega, A. E., Cortin, T. I., Mattana, C. M., Silva, H. J. & Centorbi, O. P. De. Growth of *Helicobacter pylori* in medium supplemented with cyanobacterial extract. *J. Clin. Microbiol.* **41,** 5384–5388 (2003).

105. Krajden, S. *et al.* Comparison of selective and nonselective media for recovery of *Campylobacter pylori* from antral biopsies. *J. Clin. Microbiol.* **25,** 1117–1118 (1987).

106. Coudron, P. E. & Kirby, D. F. Comparison of rapid urease tests, staining techniques, and growth on different solid media for detection of *Campylobacter pylori*. *J. Clin. Microbiol.* **27,** 1527–1530 (1989).

107. Henriksen, T. H., Brorson, O., Thoresen, T., Setegn, D. & Madebo, T. Rapid growth of *Helicobacter pylori*. *Rev. Infect. Dis.* **14,** 1008–1011 (1995).

108. Shahamat, M., Mai, U. E. H., Paszko-Kolva, C., Yamamoto, H. & Colwell, R. R. Evaluation of liquid media for growth of *Helicobacter pylori*. *J. Clin. Microbiol.* **29,** 2835–2837 (1991).

109. Jiang, X. & Doyle, M. P. Growth supplements for *Helicobacter pylori*. *J. Clin. Microbiol.* **38,** 1984–1987 (2000).

110. Lin, Y. L., Lee, N. & Chan, E. C. Determination of optimal liquid medium for enzyme expression by *Helicobacter pylori*. *J. Clin. Pathol.* **49,** 818–820 (1996).

111. Duque-Jamaica, R., Arévalo-Galvis, A., Poutou-Piñales, R. A. & Trespalacios, A. A. Sequential statistical improvement of the liquid cultivation of *Helicobacter pylori*. *Helicobacter* **15,** 303–312 (2010).

112. Kitsos, C. M. & Stadtländer, C. T. *Helicobacter pylori* in liquid culture: evaluation of growth rates and ultrastructure. *Curr. Microbiol.* **37,** 88–93 (1998).

113. Sato, F. *et al.* Ultrastructural observation of *Helicobacter pylori* in glucose-supplemented culture media. *J. Med. Microbiol.* **52,** 675–679 (2003).

114. Park, S. A., Ko, A. & Lee, N. G. Stimulation of growth of the human gastric pathogen *Helicobacter pylori* by atmospheric level of oxygen under high carbon dioxide tension. *BMC Microbiol.* **11,** 1–14 (2011).

115. Richards, C. L. *et al.* Optimizing the growth of stressed *Helicobacter pylori*. *J. Microbiol. Methods* **84,** 174–182 (2011).

116. Andersen, A. P. *et al.* Growth and morphological transformations of *Helicobacter pylori* in broth media. *J. Clin. Microbiol.* **35,** 2918–2922 (1997).

117. Coudron, P. E. & Stratton, C. W. Factors affecting growth and susceptibility testing of *Helicobacter pylori* in liquid media. *J. Clin. Microbiol.* **33,** 1028–1030 (1995).

118. Vartanova, N. O., Arzumanyan, V. G., Serdyuk, O. a & Temper, R. M. Creation of a new synthetic medium for culturing *Helicobacter pylori*. *Bull. Exp. Biol. Med.* **139,** 580–584 (2005).

119. Joo, J.-S. *et al.* A thin-layer liquid culture technique for the growth of *Helicobacter pylori*. *Helicobacter* **15,** 295–302 (2010).

120. Mendz, G. L. & Hazell, S. L. Aminoacid utilization by *Helicobacter pylori*. *Int. J. Biochem. Cell Biol.* **27,** 1085–1093 (1995).

121. Stark, R. M., Suleiman, M. S., Hassan, I. J., Greenman, J. & Millar, M. R. Amino acid utilisation and deamination of glutamine and asparagine by *Helicobacter pylori*. *J. Med. Microbiol.* **46,** 793–800 (1997).

122. Bury-Moné, S. *et al.* Is *Helicobacter pylori* a true microaerophile? *Helicobacter* **11,** 296–303 (2006).

123. Donelli, G. *et al.* The effect of oxygen on the growth and cell morphology of *Helicobacter pylori*. *FEMS Microbiol. Lett.* **168,** 9–15 (1998).

124. Shirai, M. *et al.* Accumulation of polyphosphate granules in *Helicobacter pylori* cells under anaerobic conditions. *J. Med. Microbiol.* **49,** 513–519 (2000).

125. Cottet, S., Corthésy, B. & Spertini, F. Microaerophilic conditions permit to mimic *in vitro* events occurring during *in vivo Helicobacter pylori* infection and to identify Rho/Ras-associated proteins in cellular signaling. *J. Biol. Chem.* **277,** 33978–33986 (2002).

126. Deshpande, M., Calenoff, E. & Daniels, L. Rapid large-scale growth of *Helicobacter pylori* in flasks and fermentors. *Appl. Environ. Microbiol.* **61,** 2431–2435 (1995).

127. Rektorschek, M., Weeks, D., Sachs, G. & Melchers, K. Influence of pH on metabolism and urease activity of. *Gastroenterology* **115,** 628–641 (1998).

128. Andersen, a P. *et al.* Growth and morphological transformations of *Helicobacter pylori* in broth media. *J. Clin. Microbiol.* **35,** 2918–2922 (1997).

129. Bessa, L. J., Correia, D. M., Cellini, L., Azevedo, N. F. & Rocha, I. Optimization of culture conditions to improve *Helicobacter pylori* growth in Ham's F-12 medium by response surface methodology. *Int. J. Immunopathol. Pharmacol.* **25,** 901–909 (2012).

130. Doig, P. *et al. Helicobacter pylori* physiology predicted from genomic comparison of two strains. *Microbiol. Mol. Biol. Rev.* **63,** 675–707 (1999).

131. Tomb, J. F. *et al.* The complete genome sequence of the gastric pathogen *Helicobacter pylori*. *Nature* **388,** 539–547 (1997).

132. Mendz, G. L., Hazell, S. L. & Burns, B. P. Glucose metabolism by *Helicobacter pylori*. *J. Gen. Microbiol.* **139,** 3023–3028 (1993).

133. Hoffman, P. S., Goodwin, A., Johnsen, J. O. N., Magee, K. & Veldhuyzen van Zanten, S. J. O. Metabolic activities of metronidazole-sensitive and -resistant strains of *Helicobacter pylori*: repression of pyruvate oxidoreductase and expression of isocitrate lyase activity correlate with resistance. *J. Bacteriol.* **178,** 4822–9 (1996).

134. Mendz, G. L., Burns, B. P. & Stuart, L. H. Characterization of glucose transport in *Helicobacter pylori*. *Biochim. Biophys. Acta* **1244,** 269–276 (1995).

135. Marais, A., Mendz, G. L., Hazell, S. L. & Mégraud, F. Metabolism and genetics of *Helicobacter pylori*: the genome era. *Microbiol. Mol. Biol. Rev.* **63,** 642–674 (1999).

136. Psakis, G. *et al.* The sodium-dependent D-glucose transport protein of *Helicobacter pylori*. *Mol. Microbiol.* **71,** 391–403 (2009).

137. Pawłowski, K., Zhang, B., Rychlewski, L. & Godzik, A. The *Helicobacter pylori* genome: from sequence analysis to structural and functional predictions. *Proteins Struct. Funct. Genet.* **36,** 20–30 (1999).

138. Mendz, G. L. & Hazell, S. L. Glucose phosphorylation in *Helicobacter pylori*. *Appl. Biochem. Biophys.* **300,** 522–525 (1993).

139. Mendz, G. L. & Hazell, S. L. Evidence for a pentose phosphate pathway in *Helicobacter pylori*. *FEMS Microbiol. Lett.* **84,** 331–336 (1991).

140. Mendz, G. L., Hazell, S. L. & Burns, B. P. Glucose utilization and lactate production by *Helicobacter pylori*. *J. Gen. Microbiol.* **139,** 3023–3028 (1993).

141. Chalk, P. A., Roberts, A. D. & Blows, W. M. Metabolism of pyruvate and glucose by intact cells of *Helicobacter pylori* studied by 13C NMR spectroscopy. *Microbiology* **140,** 2085–2092 (1994).

142. Mendz, G. L., Hazell, S. L. & van Gorkom, L. Pyruvate metabolism in *Helicobacter pylori*. *Arch. Microbiol.* **162,** 187–192 (1994).

143. Mendz, G. L., Hazell, S. L. & Burns, B. P. The Entner-Doudoroff pathway in *Helicobacter pylori*. *Arch. Biochem. Biophys.* **312,** 349–356 (1994).

144. Wanken, A. E., Conway, T. & Eaton, K. A. The Entner-Doudoroff pathway has little effect on *Helicobacter pylori* colonization of mice. *Infect. Immun.* **71,** 2920–2923 (2003).

145. Hughes, N. J., Chalk, P. a, Clayton, C. L. & Kelly, D. J. Identification of carboxylation enzymes and characterization of a novel four-subunit pyruvate:flavodoxin oxidoreductase from *Helicobacter pylori*. *J. Bacteriol.* **177,** 3953–3959 (1995).

146. Hughes, N. J., Clayton, C. L., Chalk, P. a & Kelly, D. J. *Helicobacter pylori* porCDAB and oorDABC genes encode distinct pyruvate:flavodoxin and 2-oxoglutarate:acceptor oxidoreductases which mediate electron transport to NADP. *J. Bacteriol.* **180,** 1119–1128 (1998).

147. St Maurice, M. *et al.* Flavodoxin:quinone reductase (FqrB): a redox partner of pyruvate:ferredoxin oxidoreductase that reversibly couples pyruvate oxidation to NADPH production in *Helicobacter pylori* and *Campylobacter jejuni*. *J. Bacteriol.* **189,** 4764–4673 (2007).

148. Tomb, J.-F. *et al.* The complete genome sequence of the gastric pathogen *Helicobacter pylori*. *Nature* **388,** 539–547 (1997).

149. Pitson, S. M., Mendz, G. L., Srinivasan, S. & Hazell, S. L. The tricarboxylic acid cycle of *Helicobacter pylori*. *Eur. J. Biochem.* **267,** 258–267 (1999).

150. Kather, B., Stingl, K., van der Rest, M. E., Altendorf, K. & Molenaar, D. Another unusual type of citric acid cycle enzyme in *Helicobacter pylori*: the malate:quinone oxidoreductase. *J. Bacteriol.* **182,** 3204–3209 (2000).

151. Corthésy-theulaz, I. E. *et al.* Cloning and characterization of *Helicobacter pylori Succinyl Prokaryotic* member of the CoA-transferase family. *J. Biol. Chem.* **272,** 25659–25667 (1997).

152. Tsugawa, H. *et al.* Alpha-ketoglutarate oxidoreductase, an essential salvage enzyme of energy metabolism, in coccoid form of *Helicobacter pylori*. *Biochem. Biophys. Res. Commun.* **376,** 46–51 (2008).

153. Mendz, G. L. & Hazell, S. L. Fumarate catabolism in *Helicobacter pylori*. *Biochem. Mol. Biol. Int.* **31,** 325–332 (1993).

154. Mendz, G. L., Meek, D. J. & Hazell, S. L. Characterization of fumarate transport in *Helicobacter pylori*. *J. Membr. Biol.* **76,** 65–76 (1998).

155. Birkholz, S., Knipp, U., Lemma, E., Kroger, A. & Opferkuch, W. Fumarate reductase of *Helicobacter pylori*-an immunogenic protein. *J. Med. Microbiol.* **41,** 56–62 (1994).

156. Mendz, G. L., Hazell, S. L. & Srinivasan, S. Fumarate reductase: a target for therapeutic intervention against *Helicobacter pylori*. *Arch. Biochem. Biophys.* **321,** 153–159 (1995).

157. Ge, Z., Jiang, Q., Kalisiak, M. S. & Taylor, D. E. Cloning and functional characterization of *Helicobacter pylori* fumarate reductase operon comprising three structural genes coding for subunits C, A and B. *Gene* **204,** 227–234 (1997).

158. Ge, Z. *et al.* Fumarate reductase is essential for *Helicobacter pylori* colonization of the mouse stomach. *Microb. Pathog.* **29,** 279–287 (2000).

159. Hoffman, P. S., Goodwin, A., Johnsen, J., Magee, K. & Veldhuyzen van Zanten, S. J. O. Metabolic activities of metronidazole-sensitive and -resistant strains of *Helicobacter pylori*: repression of pyruvate oxidoreductase and expression of isocitrate lyase activity correlate with resistance. *J. Bacteriol.* **178,** 4822–4829 (1996).

160. Schott, T., Kondadi, P. K., Hänninen, M.-L. & Rossi, M. Comparative genomics of *Helicobacter pylori* and the human-derived Helicobacter bizzozeronii CIII-1 strain reveal the molecular basis of the zoonotic nature of non-pylori gastric *Helicobacter* infections in humans. *BMC Genomics* **12,** 1–21 (2011).

161. Barabási, A.-L. & Oltvai, Z. N. Network biology: understanding the cell's functional organization. *Nat. Rev. Genet.* **5,** 101–113 (2004).

162. Kitano, H. Perspectives on Systems Biology. *New Gener. Comput.* **18,** 199–216 (2000).

163. Kitano, H. Computational Systems Biology. *Nature* **420,** 206–210 (2002).

164. Kitano, H. Systems biology: a brief overview. *Science* **295,** 1662–4 (2002).

165. Bruggeman, F. J. & Westerhoff, H. V. The nature of systems biology. *Trends Microbiol.* **15,** 45–50 (2007).

166. Medina, M. Á. Systems biology for molecular life sciences and its impact in biomedicine. *Cell. Mol. Life Sci.* **70,** 1035–1053 (2013).

167. Oltvai, Z. N. & Barabási, A. Life's complexity pyramid. *Science (80-.).* **298,** 763–765 (2002).

168. Nielsen, J. & Vidal, M. Systems biology of microorganisms. *Curr. Opin. Microbiol.* **13,** 335–336 (2010).

169. Nielsen, J. & Lee, S. Y. Systems biology: the "new biotechnology". *Curr. Opin. Biotechnol.* **23,** 583–584 (2012).

170. Kuska, B. Beer, Bethesda, and biology: how "genomics" came into being. *J. Natl. Cancer Inst.* **90,** 93 (1998).

171. Milne, S. B., Mathews, T. P., Myers, D. S., Ivanova, P. T. & Brown, H. A. Sum of the parts: mass spectrometry-based metabolomics. *Biochemistry* **52,** 3829–3840 (2013).

172. Tang, Y. J. *et al.* Advances in analysis of microbial metabolic fluxes via 13C isotopic labeling. *Mass Spectrom. Rev.* **28,** 362–375 (2009).

173. Fiehn, O. Metabolomics–the link between genotypes and phenotypes. *Plant Mol. Biol.* **48,** 155–71 (2002).

174. Nielsen, J. & Oliver, S. The next wave in metabolome analysis. *Trends Biotechnol.* **23,** 544–6 (2005).

175. Nielsen, J. in *Metabolome Anal. - An Introd.* (Villas-Bôas, S. G., Roessner, U., Hansen, M. A. E., Smedsgaard, J. & Nielsen, J.) 310 (John Wiley & Sons, Inc, 2007).

176. Bolten, C. J., Kiefer, P., Letisse, F., Portais, J.-C. & Wittmann, C. Sampling for metabolome analysis of microorganisms. *Anal. Chem.* **79,** 3843–3849 (2007).

177. Smart, K. F., Aggio, R. B. M., Van Houtte, J. R. & Villas-Bôas, S. G. Analytical platform for metabolome analysis of microbial cells using methyl chloroformate derivatization followed by gas chromatography-mass spectrometry. *Nat. Protoc.* **5,** 1709–1729 (2010).

178. Toya, Y. & Shimizu, H. Flux analysis and metabolomics for systematic metabolic engineering of microorganisms. *Biotechnol. Adv.* **31,** 818–826 (2013).

179. Mashego, M. R. *et al.* Microbial metabolomics: past, present and future methodologies. *Biotechnol. Lett.* **29,** 1–16 (2007).

180. Álvarez-Sánchez, B., Priego-Capote, F. & Castro, M. D. L. de. Metabolomics analysis II. Preparation of biological samples prior to detection. *Trends Anal. Chem.* **29,** 120–127 (2010).

181. Winder, C. L. *et al.* Global metabolic profiling of *Escherichia coli* cultures: an evaluation of methods for quenching and extraction of intracellular metabolites. *Anal. Chem.* **80,** 2939–2948 (2008).

182. Spura, J. *et al.* A method for enzyme quenching in microbial metabolome analysis successfully applied to gram-positive and gram-negative bacteria and yeast. *Anal. Biochem.* **394,** 192–201 (2009).

183. Taymaz-Nikerel, H. *et al.* Development and application of a differential method for reliable metabolome analysis in *Escherichia coli*. *Anal. Biochem.* **386,** 9–19 (2009).

184. Meyer, H., Weidmann, H. & Lalk, M. Methodological approaches to help unravel the intracellular metabolome of *Bacillus subtilis*. *Microb. Cell Fact.* **12,** 1–13 (2013).

185. Chen, M. *et al.* Optimization of the quenching method for metabolomics analysis of *Lactobacillus bulgaricus*. *J. Zhejiang Univ. Sci. B* **15,** 333–342 (2014).

186. Meyer, H., Liebeke, M. & Lalk, M. A protocol for the investigation of the intracellular *Staphylococcus aureus* metabolome. *Anal. Biochem.* **401,** 250–259 (2010).

187. Villas-Bôas, S. G., Højer-Pedersen, J., Akesson, M., Smedsgaard, J. & Nielsen, J. Global metabolite analysis of yeast: evaluation of sample preparation methods. *Yeast* **22,** 1155–69 (2005).

188. Canelas, A. B. *et al.* Leakage-free rapid quenching technique for yeast metabolomics. *Metabolomics* **4,** 226–239 (2008).

189. Ewald, J. C., Heux, S. & Zamboni, N. High-throughput quantitative metabolomics: workflow for cultivation, quenching, and analysis of yeast in a multiwell format. *Anal. Chem.* **81,** 3623–3629 (2009).

190. Johnson, C. H. & Gonzalez, F. J. Challenges and opportunities of metabolomics. *J. Cell. Physiol.* **227,** 2975–2981 (2012).

191. Putri, S. P., Yamamoto, S., Tsugawa, H. & Fukusaki, E. Current metabolomics: technological advances. *J. Biosci. Bioeng.* **116,** 9–16 (2013).

192. Koek, M. M., Jellema, R. H., van der Greef, J., Tas, A. C. & Hankemeier, T. Quantitative metabolomics based on gas chromatography mass spectrometry: status and perspectives. *Metabolomics* **7,** 307–328 (2011).

193. Husek, P. Chloroformates in gas chromatography as general purpose derivatizing agents. *J. Chromatogr. B. Biomed. Sci. Appl.* **717,** 57–91 (1998).

194. Kaspar, H., Dettmer, K., Gronwald, W. & Oefner, P. J. Automated GC-MS analysis of free amino acids in biological fluids. *J. Chromatogr. B,* **870,** 222–232 (2008).

195. Zheng, X. *et al.* A targeted metabolomic protocol for short-chain fatty acids and branched-chain amino acids. *Metabolomics* **9,** 818–827 (2013).

196. Qiu, Y. *et al.* Application of ethyl chloroformate derivatization for gas chromatography-mass spectrometry based metabonomic profiling. *Anal. Chim. Acta* **583,** 277–283 (2007).

197. Gao, X. *et al.* Metabolite analysis of human fecal water by gas chromatography/mass spectrometry with ethyl chloroformate derivatization. *Anal. Biochem.* **393,** 163–75 (2009).

198. Villas-Bôas, S. G., Delicado, D. G., Akesson, M. & Nielsen, J. Simultaneous analysis of amino and nonamino organic acids as methyl chloroformate derivatives using gas chromatography-mass spectrometry. *Anal. Biochem.* **322,** 134–8 (2003).

199. Kvitvang, H. F. N., Andreassen, T., Adam, T., Villas-Bôas, S. G. & Bruheim, P. Highly sensitive GC/MS/MS method for quantitation of amino and nonamino organic acids. *Anal. Chem.* **83,** 2705–2711 (2011).

200. Azizan, K. A., Baharum, S. N. & Noor, N. M. Metabolic profiling of *Lactococcus lactis* under different culture conditions. *Molecules* **17,** 8022–8036 (2012).

201. Hendriks, M. M. W. B. *et al.* Data-processing strategies for metabolomics studies. *Trends Anal. Chem.* **30,** 1685–1698 (2011).

202. Stein, S. E. Chemical substructure identification by mass spectral library searching. *J. Am. Soc. Mass Spectrom.* **6,** 644–655 (1995).

203. Lu, H., Liang, Y., Dunn, W. B., Shen, H. & Kell, D. B. Comparative evaluation of software for deconvolution of metabolomics data based on GC-TOF-MS. *TrAC Trends Anal. Chem.* **27,** 215–227 (2008).

204. Liland, K. H. Multivariate methods in metabolomics – from pre-processing to dimension reduction and statistical analysis. *Trends Anal. Chem.* **30,** 827–841 (2011).

205. Loughlin, M. F. Using "omic" technology to target *Helicobacter pylori*. *Expert Opin. Drug Discov.* **2,** 1041–1051 (2007).

206. Benson, D. a *et al.* GenBank. *Nucleic Acids Res.* **41,** D36–D42 (2013).

207. Ahmed, N., Loke, M. F., Kumar, N. & Vadivelu, J. *Helicobacter pylori* in 2013: multiplying genomes, emerging insights. *Helicobacter* **18 Suppl 1,** 1–4 (2013).

208. De Reuse, H. & Bereswill, S. Ten years after the first *Helicobacter pylori* genome : comparative and functional genomics provide new insights in the variability and adaptability of a persistent pathogen. *FEMS Immunol. Med. Microbiol.* **50,** 165–176 (2007).

209. Linz, B. & Schuster, S. C. Genomic diversity in *Helicobacter* and related organisms. *Res. Microbiol.* **158,** 737–744 (2007).

210. Alm, R. A. *et al.* Genomic-sequence comparison of two unrelated isolates of the human gastric pathogen *Helicobacter pylori*. *Nature* **397,** 176–180 (1999).

211. Salama, N. *et al.* A whole-genome microarray reveals genetic diversity among *Helicobacter pylori* strains. *Proc. Natl. Acad. Sci. U. S. A.* **97,** 14668–14673 (2000).

212. Suerbaum, S. & Achtman, M. *Helicobacter pylori*: recombination, population structure and human migrations. *Int. J. Med. Microbiol.* **294,** 133–139 (2004).

213. Kraft, C. & Suerbaum, S. Mutation and recombination in *Helicobacter pylori*: mechanisms and role in generating strain diversity. *Int. J. Med. Microbiol.* **295,** 299–305 (2005).

214. Edgar, R., Domrachev, M. & Lash, A. E. Gene expression omnibus: NCBI gene expression and hybridization array data repository. *Nucleic Acids Res.* **30,** 207–210 (2002).

215. Srikhanta, Y. N. *et al.* Phasevarion mediated epigenetic gene regulation in *Helicobacter pylori*. *PLoS One* **6,** e27569 (2011).

216. Dorer, M. S., Fero, J. & Salama, N. R. DNA damage triggers genetic exchange in *Helicobacter pylori*. *PLoS Pathog.* **6,** e1001026 (2010).

217. Wen, Y., Feng, J., Scott, D. R., Marcus, E. a & Sachs, G. The pH-responsive regulon of HP0244 (FlgS), the cytoplasmic histidine kinase of *Helicobacter pylori*. *J. Bacteriol.* **191,** 449–460 (2009).

218. Giannakis, M., Chen, S. L., Karam, S. M., Engstrand, L. & Gordon, J. I. *Helicobacter pylori* evolution during progression from chronic atrophic gastritis to gastric cancer and its impact on gastric stem cells. *Proc. Natl. Acad. Sci. U. S. A.* **105,** 4358–4363 (2008).

219. Giannakis, M. *et al.* Response of gastric epithelial progenitors to *Helicobacter pylori* isolates obtained from Swedish patients with chronic atrophic gastritis. *J. Biol. Chem.* **284,** 30383–30394 (2009).

220. Pflock, M. *et al.* Characterization of the ArsRS regulon of *Helicobacter pylori*, involved in acid adaptation. *J. Bacteriol.* **188,** 3449–3462 (2006).

221. Pflock, M. *et al.* The orphan response regulator HP1021 of *Helicobacter pylori* regulates transcription of a gene cluster presumably involved in acetone metabolism. *J. Bacteriol.* **189,** 2339–49 (2007).

222. Asakura, H. *et al. Helicobacter pylori* HP0518 affects flagellin glycosylation to alter bacterial motility. *Mol. Microbiol.* **78,** 1130–1144 (2010).

223. Bumann, D. *et al.* Proteome analysis of secreted proteins of the gastric pathogen *Helicobacter pylori*. *Infect. Immun.* **70,** 3396–3403 (2002).

224. Haas, G. *et al.* Immunoproteomics of *Helicobacter pylori* infection. *Proteomics* **2,** 313–324 (2002).

225. Backert, S. *et al.* Subproteomes of soluble and structure-bound *Helicobacter pylori* proteins analyzed by two-dimensional gel electrophoresis and mass spectrometry. *Proteomics* **5,** 1331–1345 (2005).

226. Mini, R. *et al.* Comparative proteomics and immunoproteomics of *Helicobacter pylori* related to different gastric pathologies. *J. Chromatogr. B. Analyt. Technol. Biomed. Life Sci.* **833,** 63–79 (2006).

227. Bumann, D. *et al.* Lack of stage-specific proteins in coccoid *Helicobacter pylori* cells. *Society* **72,** 6738–6742 (2004).

228. Jungblut, P. R. *et al.* Comparative proteome analysis of *Helicobacter pylori*. *Mol. Microbiol.* **36,** 710–25 (2000).

229. Liao, J.-H. *et al.* Up-regulation of neutrophil activating protein in *Helicobacter pylori* under high-salt stress: structural and phylogenetic comparison with bacterial iron-binding ferritins. *Biochimie* **95,** 1136–45 (2013).

230. Zhang, M.-J. *et al.* Comparative proteomic analysis of passaged *Helicobacter pylori*. *J. Basic Microbiol.* **49,** 482–90 (2009).

231. Baik, S. *et al.* Proteomic analysis of the sarcosine-insoluble outer membrane fraction of *Helicobacter pylori* strain 26695. *Society* **186,** 949–955 (2004).

232. Kim, N. *et al.* Proteins released by *Helicobacter pylori In Vitro*. *Society* **184,** 6155–6162 (2002).

233. Lock, R. a, Cordwell, S. J., Coombs, G. W., Walsh, B. J. & Forbes, G. M. Proteome analysis of *Helicobacter pylori*: major proteins of type strain NCTC 11637. *Pathology* **33,** 365–374 (2001).

234. Zeng, H., Guo, G., Mao, X. H., Tong, W. De & Zou, Q. M. Proteomic insights into *Helicobacter pylori* coccoid forms under oxidative stress. *Curr. Microbiol.* **57,** 281–286 (2008).

235. Chuang, M.-H., Wu, M.-S., Lin, J.-T. & Chiou, S.-H. Proteomic analysis of proteins expressed by *Helicobacter pylori* under oxidative stress. *Proteomics* **5,** 3895–3901 (2005).

236. Qu, W. *et al. Helicobacter pylori* proteins response to nitric oxide stress. *J. Microbiol.* **47,** 486–493 (2009).

237. Smiley, R., Bailey, J., Sethuraman, M., Posecion, N. & Showkat Ali, M. Comparative proteomics analysis of sarcosine insoluble outer membrane proteins from

clarithromycin resistant and sensitive strains of *Helicobacter pylori*. *J. Microbiol.* **51,** 612–618 (2013).

238. Choi, Y. W., Park, S. A., Lee, H. W., Kim, D. S. & Lee, N. G. Analysis of growth phase-dependent proteome profiles reveals differential regulation of mRNA and protein in *Helicobacter pylori*. *Proteomics* **8,** 2665–2675 (2008).
239. Sun, Y. *et al.* Proteomic analysis of the function of spot in *Helicobacter pylori* anti-oxidative stress *in vitro* and colonization *in vivo*. *J. Cell. Biochem.* **113,** 3393–3402 (2012).
240. Huang, C.-H. & Chiou, S.-H. Proteomic analysis of upregulated proteins in *Helicobacter pylori* under oxidative stress induced by hydrogen peroxide. *Kaohsiung J. Med. Sci.* **27,** 544–553 (2011).
241. Loh, J. T., Gupta, S. S., Friedman, D. B., Krezel, A. M. & Cover, T. L. Analysis of protein expression regulated by the *Helicobacter pylori* ArsRS two-component signal transduction system. *J. Bacteriol.* **192,** 2034–43 (2010).
242. Ge, R. *et al.* A proteomic approach for the identification of bismuth-binding proteins in *Helicobacter pylori*. *J. Biol. Inorg. Chem.* **12,** 831–842 (2007).
243. Shao, C. *et al.* The changes of proteomes components of *Helicobacter pylori* in response to acid stress without urea. *J. Microbiol.* **46,** 331–7 (2008).
244. Govorun, V. M. *et al.* Comparative analysis of proteome maps of *Helicobacter pylori* clinical isolates. *Biochem. Biokhimiia* **68,** 42–49 (2003).
245. Smith, T. G., Lim, J.-M., Weinberg, M. V, Wells, L. & Hoover, T. R. Direct analysis of the extracellular proteome from two strains of *Helicobacter pylori*. *Proteomics* **7,** 2240–2245 (2007).
246. Lee, H. W., Choe, Y. H., Kim, D. K., Jung, S. Y. & Lee, N. G. Proteomic analysis of a ferric uptake regulator mutant of *Helicobacter pylori*: regulation of *Helicobacter pylori* gene expression by ferric uptake regulator and iron. *Proteomics* **4,** 2014–2027 (2004).
247. Hynes, S. O., Mcguire, J., Falt, T. & Wadström, T. The rapid detection of low molecular mass proteins differentially expressed under biological stress for four *Helicobacter spp.* using ProteinChip. *Proteins* 273–278 (2003).

248. Park, J.-W. *et al.* Quantitative analysis of representative proteome components and clustering of *Helicobacter pylori* clinical strains. *Helicobacter* **11,** 533–543 (2006).

249. Momynaliev, K. T. *et al.* Functional divergence of *Helicobacter pylori* related to early gastric cancer research articles. *J. Proteome Res.* **9,** 254–267 (2010).

250. Ge, R. *et al.* Phosphoproteome analysis of the pathogenic bacterium *Helicobacter pylori* reveals over-representation of tyrosine phosphorylation and multiply phosphorylated proteins. *Proteomics* **11,** 1449–1461 (2011).

251. Krah, A. *et al.* Analysis of automatically generated peptide mass fingerprints of cellular proteins and antigens from *Helicobacter pylori* 26695 separated by two-dimensional electrophoresis. *Mol. Cell. Proteomics* **2,** 1271–1283 (2003).

252. Jungblut, P. R. *et al. Helicobacter pylori* proteomics by 2-DE/MS, 1-DE-LC/MS and functional data mining. *Proteomics* **10,** 182–193 (2010).

253. Stelling, J. Mathematical models in microbial systems biology. *Curr. Opin. mMcrobiology* **7,** 513–518 (2004).

254. Patil, K. R., Akesson, M. & Nielsen, J. Use of genome-scale microbial models for metabolic engineering. *Curr. Opin. Biotechnol.* **15,** 64–69 (2004).

255. Palsson, B. Metabolic systems biology. *FEBS Lett.* **583,** 3900–3904 (2009).

256. Price, N. D., Papin, J. a, Schilling, C. H. & Palsson, B. O. Genome-scale microbial *in silico* models: the constraints-based approach. *Trends Biotechnol.* **21,** 162–169 (2003).

257. Edwards, J. S. & Palsson, B. O. Systems properties of the *Haemophilus influenzae Rd* Metabolic Genotype. *Cell Biol. Metab.* **274,** 17410–17416 (1999).

258. Feist, A. M., Herrgård, M. J., Thiele, I., Reed, J. L. & Palsson, B. Ø. Reconstruction of biochemical networks in microorganisms. *Nat. Rev. Microbiol.* **7,** 129–143 (2009).

259. Rocha, I., Förster, J. & Nielsen, J. in *Methods Mol. Biol. vol. 416 Gene Essentiality* (Gerdes, S. Y. & Osterman, A. L.) **416,** 409–433 (Humana Press Inc., 2007).

260. Hamilton, J. J. & Reed, J. L. Software platforms to facilitate reconstructing genome-scale metabolic networks. *Environ. Microbiol.* **16,** 49–59 (2014).

261. Feist, A. M., Herrgård, M. J., Thiele, I., Reed, J. L. & Palsson, B. Ø. Reconstruction of biochemical networks in microorganisms. *Nat. Rev. Microbiol.* **7,** 129–43 (2009).

262. Thiele, I. & Palsson, B. Ø. A Protocol for generating a high-quality genome-scale metabolic reconstruction. *Nat. Protoc.* **5,** 93–121 (2010).

263. Santos, F., Boele, J. & Teusink, B. in *Methods Enzymol. Vol. 500* (Jameson, D., Verma, M. & Westerhoff, H. V) **500,** 509–532 (Elsevier Inc., 2011).

264. Karp, P. D., Paley, S. & Romero, P. The Pathway Tools software. *Bioinformatics* **18 Suppl 1,** S225–S232 (2002).

265. Overbeek, R. *et al.* The subsystems approach to genome annotation and its use in the project to annotate 1000 genomes. *Nucleic Acids Res.* **33,** 5691–5702 (2005).

266. Dias, O., Rocha, M., Ferreira, E. C. & Rocha, I. Merlin: metabolic models reconstruction using genome-scale information. in *Proc. 11th Int. Symp. Comput. Appl. Biotechnol. (CAB 2010)* (Banga, J. R., Bagaerts, P., Impe, J. Van, Dochain, D. & Smets, I.) 120–125 (2010).

267. Agren, R. *et al.* The RAVEN toolbox and its use for generating a genome-scale metabolic model for *Penicillium chrysogenum*. *PLoS Comput. Biol.* **9,** e1002980 (2013).

268. Boneca, I. G., De Reuse, H., Epinat, J., Pupin, M. & Labigne, Agnès, Moszer, I. A revised annotation and comparative analysis of *Helicobacter pylori* genomes. *Nucleic Acids Res.* **31,** 1704–1714 (2003).

269. Cherry, J. M. *et al.* SGD : *Saccharomyces* Genome Database. *Nucleic Acids Res.* **26,** 73–79 (1998).

270. Maglott, D., Ostell, J., Pruitt, K. D. & Tatusova, T. Entrez Gene: gene-centered information at NCBI. *Nucleic Acids Res.* **33,** D54–D58 (2005).

271. Markowitz, V. M. *et al.* The integrated microbial genomes (IMG) system. *Nucleic Acids Res.* **34,** D344–D348 (2006).

272. Kanehisa, M. & Goto, S. KEGG: Kyoto Encyclopedia of Genes and Genomes. *Nucleic Acids Res.* **28,** 27–30 (2000).

273. Schomburg, I., Chang, A. & Schomburg, D. BRENDA, enzyme data and metabolic information. *Nucleic Acids Res.* **30,** 47–49 (2002).

274. Caspi, R. *et al.* The MetaCyc database of metabolic pathways and enzymes and the BioCyc collection of pathway/genome databases. *Nucleic Acids Res.* **40,** D742–D753 (2012).

275. Ren, Q., Chen, K. & Paulsen, I. T. TransportDB: a comprehensive database resource for cytoplasmic membrane transport systems and outer membrane channels. *Nucleic Acids Res.* **35,** D274–D279 (2007).

276. Nakai, K. & Horton, P. PSORT : a program for detecting sorting signals in proteins and predicting their subcellular localization. *Trends Biochem. Sci.* **24,** 34–35 (1999).

277. Orth, J. D., Thiele, I. & Palsson, B. Ø. What is flux balance analysis? *Nat. Biotechnol.* **28,** 245–248 (2011).

278. Feist, A. M. & Palsson, B. O. The biomass objective function. *Curr. Opin. Microbiol.* **13,** 344–349 (2010).

279. Hucka, M. *et al.* The systems biology markup language (SBML): a medium for representation and exchange of biochemical network models. *Bioinformatics* **19,** 524–531 (2003).

280. Ghosh, S., Matsuoka, Y., Asai, Y., Hsin, K.-Y. & Kitano, H. Software for systems biology: from tools to integrated platforms. *Nat. Rev. Genet.* **12,** 821–832 (2011).

281. Ge, Z. & Taylor, D. E. Contributions of genome sequencing to understanding the biology of *Helicobacter pylori*. *Annu. Rev. Microbiol.* **53,** 353–387 (1999).

282. Schilling, C. H. *et al.* Genome-scale metabolic model of *Helicobacter pylori* 26695. *J. Bacteriol.* **184,** 4582–4593 (2002).

283. Thiele, I., Vo, T. D., Price, N. D. & Palsson, B. Ø. Expanded metabolic reconstruction of *Helicobacter pylori* (*i*T341 GSM/GPR): an *in silico* genome-scale characterization of single- and double-deletion mutants. *J. Bacteriol.* **187,** 5818–5830 (2005).

Chapter 3

Growth and morphology assessment methods for *Helicobacter pylori* in liquid medium

Daniela M. Correia, Lucinda J. Bessa, Maria J. Vieira, Nuno F. Azevedo and Isabel Rocha

Growth and morphology assessment methods for *Helicobacter pylori* in liquid medium

(To be submitted)

3.1. *Abstract*

Helicobacter pylori is known to be associated with gastric diseases. The lack of physiological data has hampered the uncovering of mechanisms associated with infection and consequently, many aspects related with the appearance of diseases remain unclear.
It is well known that *H. pylori* can change cell morphology from spiral to coccoid forms when exposed to adverse conditions. Moreover, in those circumstances, *H. pylori* cells can aggregate in clusters when in liquid culture. Such phenomenon makes it difficult to assess growth using conventional methods. Also, some authors have reported the existence of a viable but nonculturable state of this bacterium. The development of robust methods to grow this bacterium and reliable methods for the assessment of growth are thus needed for a better characterization of its physiology.

The purpose of this work was thus to study *H. pylori*'s growth in a chemically semi-defined medium, to compare different methods to assess growth, and observe the changes in morphology. Cultures were grown at 37°C under controlled conditions in a Ham´s F-12 medium supplemented with fetal bovine serum. In order to evaluate total cell counts, viability and cell morphology, the following methods were used and compared, when appropriate: cultivable cell counts, total cell counts using DAPI staining, evaluation of viability with the Live/Dead viability kit and a PNA FISH probe which evaluates the presence of stable rRNA. Additionally, a method that allows efficient cell disaggregation was developed, since an increasing number and size of cell clusters were observed during cell growth, accompanied by cell morphology conversion.

Differences of cell counts between methods were observed. The Live/Dead viability kit was not suitable for analysis of *H. pylori*'s viability after the exponential cell phase, especially during morphological cell conversion. In comparison to total counts using DAPI, cultivable cell counts displayed, in general, lower counts, particularly after cells have reached the stationary phase, indicating the presence of nonculturable cells. Changes in morphology and viability were also observed, with viable and culturable coccoid cells identified, besides spiral cells. Moreover, after 60 hours of culture, cells were mainly coccoid and nonviable.

Keywords: *Helicobacter pylori*, morphology, cell-to-cell aggregation.

3.2. *Introduction*

H. pylori is a pathogenic, spiral-shaped bacterium, but it has been described that it can change cell morphology from spiral to coccoid when exposed to adverse conditions, such as aerobiosis[1,2], alkaline pH[3], low temperature[4], nutrient starvation[2,5], extended incubation[6], use of proton pump inhibitors[3] or treatment with antibiotics[7,8]. This pleomorphic nature of *H. pylori* has been intensively studied in order to understand its importance and implications in the transmission of infection. However, the nature of coccoid forms is a controversial topic, with some studies yielding opposite evidences. Essentially, different types of behavior for coccoid forms were reported with respect to viability and culturability. It is thought that this different behavior might be associated with different types of coccoid cells, which are associated with different processes of transformation[9,10]. Some authors concluded that the mentioned cell forms represent a degenerative nonviable bacterial form[11] or a "morphological manifestation of cell death"[12]. Culturable *H. pylori* coccoid cells were described[9,10,13], in opposition to the most commonly found viable but nonculturable (VBNC) form[7,9,10], also proved in other bacteria[14,15]. This last type of cells is the most plausible and accepted by the scientific community.

The aim of morphological change in *H. pylori* is a key question, being pointed out as a strategy of survival inside and outside of the human host[16,17], with some authors claiming that coccoid forms can revert to spiral when exposed to favorable conditions, as proved in experiments with mice[18,19].

Whether coccoid forms are capable of inducing disease remains another open question, with several authors proving that coccoid cells, like spiral cells, express virulence factors, emphasizing their potential pathogenicity[20–22]. Saito *et al.* (2012) showed in their experiments that, similarly to spiral cells, coccoid forms can infect human gastric epithelial cells[23].

The conversion from spiral to coccoid forms occurs through intermediary forms such as the U-shape[24], C-shape and doughnut shape. In the last years, several studies have been published, addressing topics related with bacterial cell shape and its modifications, with the peptidoglycan layer having a prominent role[25], including in *H. pylori*

[26–28]. Some genetic determinants involved in cell morphology and shape transition in *H. pylori* were also revealed[29–32].

If there is indeed a viable but nonculturable (VBNC) form of *H. pylori,* then the use of culturing techniques for growth assessment is not always adequate. Since the number of cells can be underestimated using culturable cell counts, the enumeration of total cells by direct count of stained cells in epifluorescent microscopy can be an alternative, also allowing to enumerate viable and nonviable cells.

In addition, *H. pylori* cell-to-cell aggregation in liquid culture (complex and defined media)[4,33–35], as well as in water[36], was described. It has been reported that this phenomenon is more noticeable for *H. pylori* in liquid culture when oxygen is scarce[34]. Cell-to-cell aggregation was reported in several other gram-negative species[37–39] and it is hypothesized that aggregation represents a strategy to survive and grow in unfavorable environments[34].

In previous experiments, we observed cell-to-cell aggregation on Ham's F-12 nutrient mixture, making it difficult to assess the growth of *H. pylori* using conventional methods such as cultivable cell counts and total cell counts using fluorochromes.

The development of robust methods to grow this bacterium and reliable methods for the assessment of growth and morphology are thus needed for a better characterization of its physiology and morphology.

The goals of this work were to study the growth of *H. pylori* in a semi-chemically defined liquid medium using optimal environmental conditions previously found by experimental design[40]. More specifically, we aimed at comparing different methods for growth assessment and morphology evaluation, in order to be able to observe changes in morphology during growth, giving special relevance to clusters formation. Furthermore, we aimed at developing a method that allows to disaggregate cell clusters in order to achieve a more reliable and accurate assessment of growth.

3.3. *Methods*

3.3.1. Culture conditions

Helicobacter pylori 26695 (strain NCTC 12455) was cultivated in Columbia Base Agar (CBA) (Liofilchem, Italy) supplemented with 5% (v/v) defibrinated horse blood (Probiologica, Portugal) at 37 °C under microaerophilic conditions (5% O_2, 10% CO_2, 85% N_2) in a Cell Culture Incubator (Incubator HERAcell 150, Kendro Laboratory, Germany) for 3 days.

An inoculum was prepared in Ham's F-12 nutrient mixture with glutamine (catalog no 21765-037, Invitrogen-Gibco, Spain) previously supplemented with 5% (v/v) FBS (catalog no 10500-064, origin: South America, Invitrogen-Gibco, Spain)[41], incubated at 37 °C under 120 rpm of shaking speed (Heidolph Unimax 1010 orbital shaker, Germany) in microaerophilic (5% O_2, 10% CO_2, 85% N_2) conditions for approximately 17 h, in order to reach the exponential phase.

The initial cell concentration of the culture was adjusted to an optical density at 600 nm (OD_{600}) of 0.1 (corresponding to approximately 10^7 CFU/mL) in 1000 mL Erlenmeyer flasks with the same medium as described for the inoculum by manipulating the amount of cells incubated from the inoculum. The pH was adjusted to 8.0 with 5M NaOH (Panreac). The culture was incubated at 37 °C under 130 rpm of shaking speed under microaerophilic conditions (6.5% O_2, 10% CO_2, 83.5% N_2). The experiment was carried out in triplicate and samples were collected at selected time points up to 72 hours of culture.

3.3.2. Cell-to-cell disaggregation

At each time point 1 mL of culture was vortexed (Press-to-Mix model 34524, Snidjers) at maximum speed during 5 minutes in a 2-mL tube with 8-10 glass beads (1 mm diameter, Sigma). Subsequently, growth and morphology were assessed using the methods described in the following subsections.

3.3.3. Growth assessment

At each time point, after the application of the disaggregation method, optical density (OD) at 600 nm was immediately assessed by using an ELISA microplate reader (Model Sunrise, Tecan, Switzerland)

3.3.4. Colony forming unit assay

The cultivable cell counts represented by Colonies Forming Units (CFU/mL) were assessed at each time point by the method of serial dilutions in phosphate saline buffer (PBS) (pH 7.2), after disaggregation. For each dilution, five spots of 10 µl were plated in CBA medium and the plates were incubated under microaerophilic conditions (5% O_2; 10% CO_2; 85% N_2) for 5 to 7 days at 37°C. Three to thirty colonies per spot were considered for the counting. To determine CFU/mL the dilution rate was taken into account.

Purity control was carried out at each time of sample collection by plating each sample in Trypticase Soy Agar (TSA) (Liofilchem, Italy).

3.3.5. Staining methods

3.3.5.1. Total Cell Counts

The total cell counts at each time point were determined using 4',6-diamidino-2-phenylindole (DAPI) (Sigma-Aldrich). Briefly, 10 µL of disaggregated bacterial culture were filtered under vacuum in a black Nucleopore® polycarbonate membrane (0.2 µm pore size, 25 mm diameter, Whatman). Subsequently, 40 µL of the DAPI solution (100 µg/mL dissolved in water) were added to the membrane that was then covered with a coverslip and kept for 10 minutes in the dark at room temperature. The membrane was washed with 10 mL of filtered water and air dried. Then, it was placed in a microscope slide and a drop of nonfluorescent immersion oil (Merck) was placed on the top of the membrane that was covered with a coverslip before microscopy observation.

3.3.5.2. Viability evaluation

A bacterial viability Live/Dead® BacLight™ (Molecular Probes, USA) kit was used to determine cellular viability at each time point. In short, 1 mL of bacterial culture was centrifuged at 10 000 rpm during 5 minutes, the supernatant was discarded and the pellet re-suspended in 1 mL of phosphate saline buffer (PBS) (pH 7.2) and 3 µL of a mixture of Syto9 and propidium iodide (1:1) (included in kit), and stained for 15 minutes in the dark. 5 µL of suspension were placed in a clean glass microscope slide and covered with a coverslip. All samples were observed within 15 minutes.

3.3.5.3. Evaluation of stable rRNA

The presence of stable rRNA was evaluated at each time point using a peptic nucleic acid fluorescence *in situ* hybridization (PNA FISH) probe (Hpy 769)[42]. The whole procedure was performed according to Guimarães *et al.*, 2007[42]. The composition of solutions (hybridization and washing) and chemicals used are described in supplementary material 1.

Ten microliters of *H. pylori* culture (after disaggregation) were placed in an 8-mm well slide and let to air dry. The samples were fixed at room temperature by covering the sample with 30 µL of 4% (w/v) paraformaldehyde (Sigma-Aldrich) for 10 minutes. Afterwards, 30 µL of 50% (v/v) ethanol (Fisher Chemical) were added to the wells with care to cover the entire well surface for another 10 minutes. Then, slides were allowed to air dry. The PNA FISH probe Hpy 769 (30 µL, 200 nM prepared in hybridization solution) was added to each well. A negative control was prepared by adding 30 µL of hybridization solution to another well slide. The wells were covered with coverslips and incubated in the dark, during 90 minutes at 57°C. After that, the slides (without coverslips) were placed in a coplin jar, immersed in prewarmed washing solution for 30 minutes at 57°C. After the washing step the slides were left to dry in the dark. A drop of nonfluorescent immersion oil (Merck) was placed on the wells and covered with a coverslip.

3.3.5.4. Microscopic visualization

Samples were observed in an epifluorescence microscope (BX51 Olympus, Hamburg, Germany) equipped with a camera (DP71; Olympus) with filters adapted to the fluorochromes used in each method at a magnification of x1000. Pictures of each sample were taken and a total of 10-20 random fields per sample were enumerated. The total cells per mL of sample, percentage of viable cells, as well as percentages of spiral, coccoid and intermediate forms (U-shape, C-shape and doughnut-shape) were determined at each time point in three biological replicates.

3.4. *Results and Discussion*

3.4.1. Cell-to-cell disaggregation

We observed the cell-to-cell aggregation phenomenon on Ham's F-12 nutrient mixture supplemented with FBS, making it difficult to assess the growth of *H. pylori* using the conventional methods such as cultivable cell counts and total cell counts using fluorochromes. Other authors also reported the presence of cell aggregates, particularly for coccoid cells, explained by the adhesive properties of these cells[43]. The described behavior was associated with an answer to adverse conditions[34]. In the present work, the increase of cell clumps was also observed with the time of culture; also, bigger coccoid cell clusters were found to be more difficult to disaggregate.

During the optimization of the cell-to-cell disaggregation method, different numbers of glass beads and different times of shaking in the vortex were tested in order to achieve the best cell-to-cell disaggregation, breaking the clumps of cells without cell lysis. The influence of the time of shaking using 8-10 glass beads in CFU/mL and OD_{600}, in a culture of *H. pylori*, at exponential phase, growing in Ham's F-12 liquid medium supplemented with 5% (v/v) FBS is displayed in supplementary material 2. The time of shaking was fixed in 5 minutes, with no significant difference in CFU/mL between the tested times of shaking ($p=0.57$, one-way ANOVA).

The application of the disaggregation method made possible to assess more accurately the cultivable cells (CFU/mL). In fact, an increase of the cultivable cells number was observed after applying the disaggregation method, being the difference between disaggregated samples and non-disaggregated samples more noticeable during the exponential and stationary phases (Figure 3.1 (B)). After 36 hours of culture, when cells start to change their morphology, there was no visible advantage in the application of the disaggregation method. There are some facts that can explain this result, namely: 1) when cells are undergoing a morphological transition they may be more susceptible to the process of disaggregation, the viability becoming compromised by this procedure; 2) when cells are in the coccoid form, the disaggregation of the cell clumps is more difficult to achieve (as observed in microscopic visualization) and 3) after 36 hours of culture, the culturable cells are declining, and the aggregated cells are proportionally less viable than non-aggregated cells.

The same increase was observed in optical density after cell-to-cell disaggregation, although in this case the increase is constant through the entire culture time, showing that cell-to-cell disaggregation is performed in both viable and non-viable cells and also in all cell forms (Figure 3.1(A)). By combining these two sets of results, hypothesis 2 mentioned above is less likely as it would originate a similar profile in the OD curve as the one observed for the CFU data.

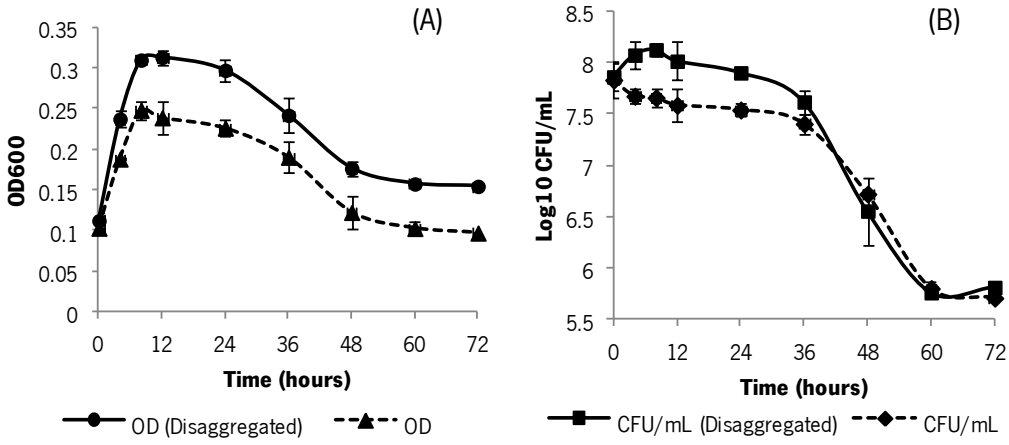

Figure 3.1. Growth of *H. pylori* 26695, Mean of three biological replicates with standard deviations. OD_{600} with and without cell-to-cell disaggregation (A); $\log_{10}$ CFU/mL with and without cell-to-cell disaggregation (B).

3.4.2. Growth assessment and cell counts

The growth was assessed by optical density at 600 nm and by microscopy using DAPI and PNA FISH. In order to estimate the total cell counts, DAPI, a fluorescent dye that binds strongly to DNA with a binding preference for A-T rich regions, was used. It passes through an intact cell membrane, stains both live and dead cells, being suitable to determine total cell counts[44]. PNA FISH has been largely applied to identify[45–49] and also to discriminate bacterial species[50,51]. A specific method based on a red fluorescent PNA FISH probe (Hpy769), developed by Guimarães *et al*. (2007) for the detection of *H. pylori* was applied in order to evaluate the stable rRNA (for a method review see Cerqueira *et al*.(2008) [52]). The cells are stained red due to the Alexa fluor 546 fluorochrome used in the *H. pylori* probe referred above[42].

Comparing the methods used in terms of fluorescence for cells in the exponential phase of growth, cells stained with PNA FISH showed a brighter and more stable signal than cells stained with DAPI. In Figure 3.2, epifluorescence microscope images of *H. pylori* 26695 growing in semi-defined liquid medium are shown. It is clearly visible that at 0 hours of culture the cells present a higher fluorescence signal intensity with more defined contours, with both methods (Figure 3.2 A and C). This high fluorescence intensity observed is due to the high rRNA content in cells and the presence of intact DNA in growing cells, for the Hpy probe and DAPI staining application, respectively. In general, a decrease in the fluorescent signal for both fluorochromes (DAPI and Alexa fluor 546) and an increase in cell clusters were observed with time. In fact, cells were impossible to count at 60 and 72 hours of culture due to large aggregates of coccoid cells even after performing the disaggregation procedure. The referred fluorescent signal reduction and the increase of cell clusters are noticeably visible in Figure 3.2 (B and D) for cells at 36 hours of culture, which start undergoing morphological conversion.

Figure 3.3 shows the results for cell counts using DAPI and PNA FISH (until 48 hours of culture) and culturable cells and optical density (up to 72 hours of culture). In general, the Hpy 769 probe yielded the lesser cell counts and the DAPI stain the higher cell counts, with significant differences in counts at 4 and 12 hours of culture ($p<0.05$; T-test, equal variances). In order to evaluate the differences between methods, ratios

between counts were calculated (presented in supplementary material 3). Comparing PNA FISH probe counts with DAPI stain counts, the PNA FISH counts ranged from 24 to 63% of the DAPI cell counts. This may indicate that some of the cells that were counted with DAPI did not have stable rRNA, therefore were not observed with the PNA FISH probe. Similarly, the culturable cell counts varied between 2 and 86 % of the DAPI counts, with the biggest difference at 48 hours of culture (2% of DAPI counts), showing the decrease in culturability, with significant differences in all times of sampling ($p<0.05$; T-test, equal variances), with exception of 0 and 8 hours of culture. At the start of the experiment, 86% of the cells appear to be culturable. Regarding PNA FISH probe counts and CFUs, large differences were observed, with 28 to 93% of culturable cells counted with the PNA FISH probe until 8 hours of culture, and a higher number of cells counted with PNA FISH after that time. The observed differences are significant in all times of sampling ($p<0.05$; T-test, equal variances), with the exception of 4, 8 and 12 hours of culture. After 36 hours, a considerable decrease in culturable cell counts accompanied by an OD decrease was observed, although not observed in the DAPI and PNA FISH counts (Figure 3.3.). In fact, at this time of culture, cells start becoming very aggregated, which may impact OD measurements and CFU/mL counts, but that does not impair cell counts using fluorochromes.

In general, all methods used make predictions that follow the same trend, except for the OD and CFUs. Since they are affected, as stated above, by aggregation phenomena, the OD data are less reliable than fluorescence for total cell counts, while the results for culturability should also be questioned after 36 hours.

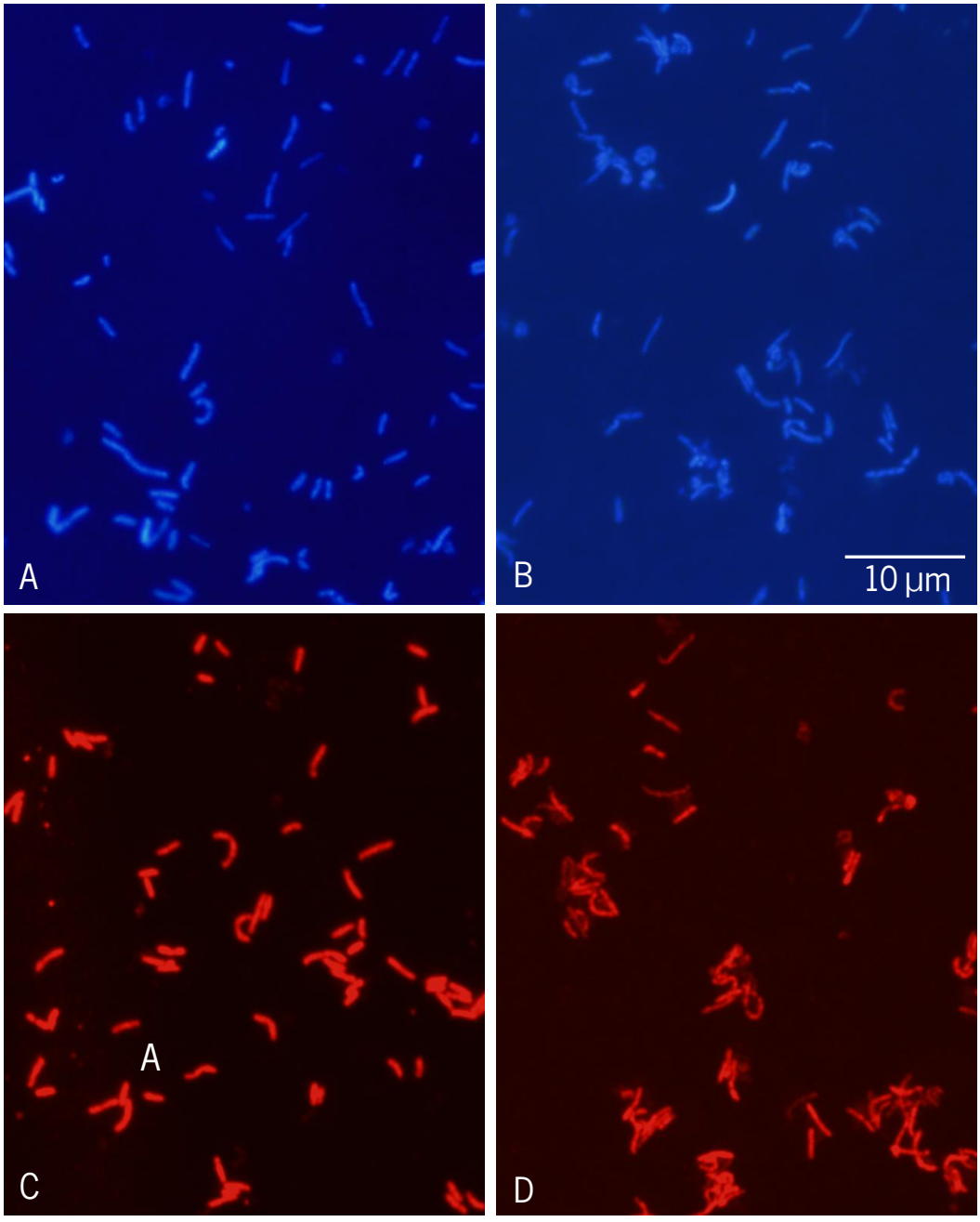

Figure 3.2. Epifluorescence microscope images of *H. pylori* 26695 in liquid culture after cell disaggregation. DAPI staining, 0 hours of culture (A); DAPI staining, 36 hours of culture (B); PNA FISH probe (Hpy469), 0 hours of culture (C); PNA FISH probe, 36 hours of culture (D). Magnification: 1000x.

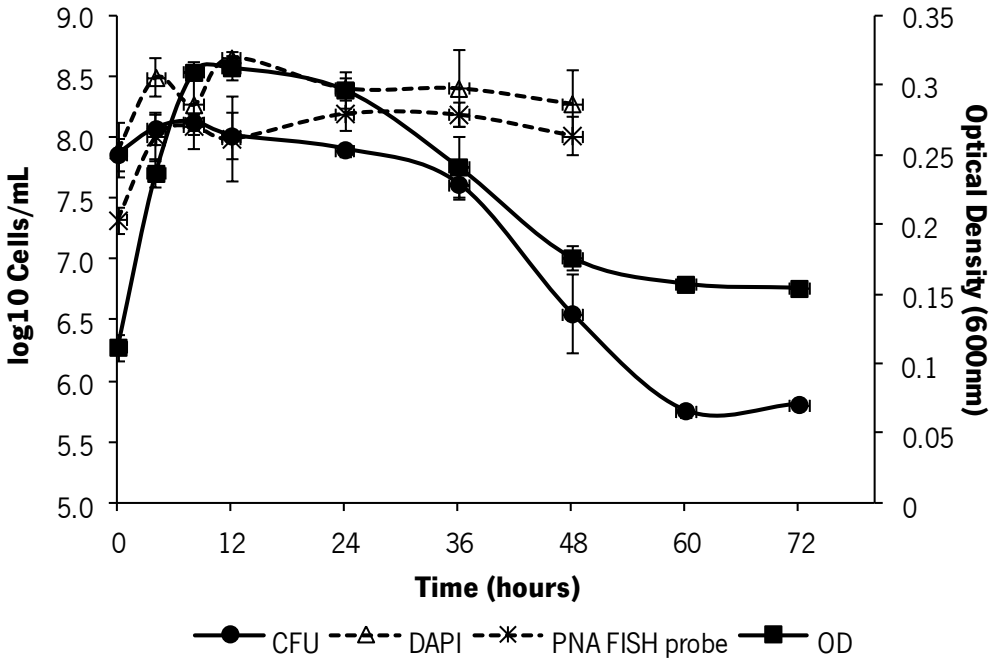

Figure 3.3. Measurements of optical density (600 nm), culturable cells, and total cell counts with DAPI stain and PNA FISH probe counts. Mean of three biological replicates. Error bars represents standard deviation.

3.4.3. Cellular Viability

Cellular viability was evaluated using a Live/Dead Baclight Viability Kit which is based on cell's membrane integrity by the staining of nucleic acids with Syto 9 and propidium iodide fluorochromes. If a cell has an intact membrane it will stain green with Syto 9 and is considered to be viable, whereas if a cell has a damaged or compromised membrane it will stain red with propidium iodide and is considered to be nonviable[53]. In the last years, this commercial kit has been extensively applied in viability evaluation of bacterial species[54–56] including *H. pylori*[17,36,57,58].

Figure 3.4 depicts the percentage of viable and total cell counts obtained with the Live Dead kit by epifluorescence microscope visualization, and culturable cell counts represented by CFU/mL in the same samples of an *H. pylori* 26695 liquid culture in optimized environmental conditions.

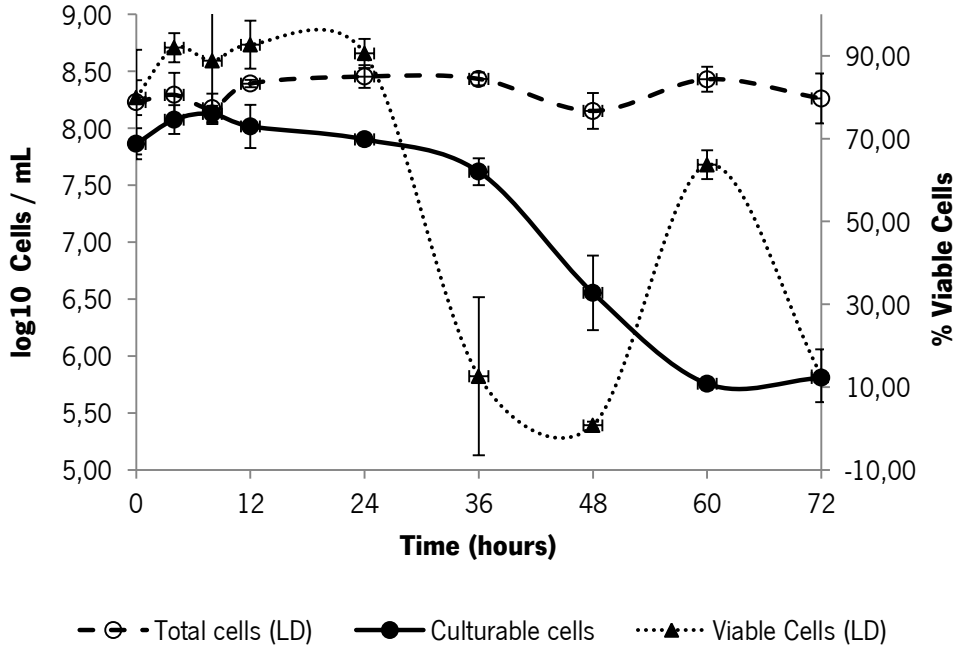

Figure 3.4. Percentage of viable cells and total cell counts (Live/Dead kit) and culturable cell counts along time in an *H. pylori* 26695 culture in liquid medium. Mean of three biological replicates. Error bars represent standard deviation.

The difference between measurements of viable and culturable cells is not significant during the exponential and stationary phases (4-12 hours) ($p>0.05$; T-test: equal variances). The total cells (viable and nonviable) counted with the Live/Dead kit at the exponential phase (4-10 hours) is higher than the culturable cells, although without significant differences ($p>0.05$; T-test: equal variances). At those time points (0-24 hours), the percentage of viable cells varies between 80% and 93% (Figure 3.4.). In addition, the percentage of spiral cells is around 87% (0-24 hours of culture), proving that some cells with other morphologies besides spiral cells are present (intermediate forms and cocci).

The application of the Live/Dead kit is only consistent and coherent for cells growing at the exponential phase. In fact, there is a low number of viable cells observed at 36 and 48 hours of culture, when cells are changing their morphology (confirmed by morphological analysis). At this stage, there are significant changes occurring in the cytoplasmatic membrane of cells, probably allowing the entrance of propidium iodide and

thus, the appearance of nonviable cells in microscopy, explaining the discrepant results between culturable and viable cells at these time points (Figure 3.4. and detailed results in supplementary material 4). Berney *et al.* (2007) also reported that a specific gram-negative bacteria phenomenon can occur in stationary-phase cells, which is related with the presence of the outer membrane, being to some degree a barrier to the Syto9 stain[55].

After the conversion phase (60 hours of culture), from spirals to coccoids, the viable cells become significantly higher than culturable cells, showing the viable but non culturable (VBNC) state of the coccoid cells[17,57]. This result also proves that culturability and viability are two independent features. Moreover, the presence of a higher number of cells with stable rRNA identified in PNA FISH probe compared with CFUs at 36 and 48 hours (results detailed in supplementary material 3) can also be associated to the VBNC state, allowing to conclude that several methods have to be applied to obtain a detailed characterization of viability[59].

Figure 3.5 shows epifluorescence microscope images for 0, 36 and 72 hours of culture, where it is possible to observe the increase of intermediate and coccoid cells and the decrease of viable cells (stained green) with culture time.

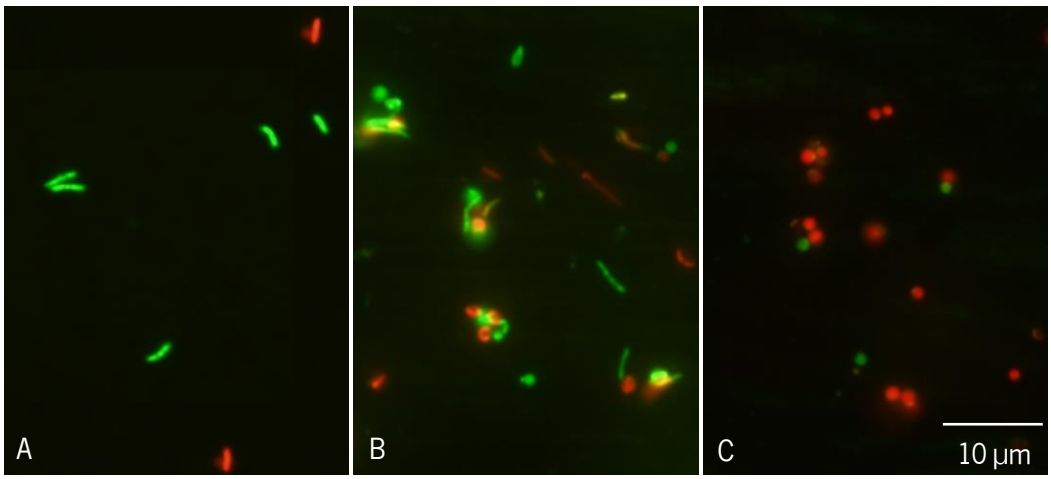

Figure 3.5. Epifluorescence microscope images of a *H. pylori* 26695 culture stained with Syto9/Propidium iodide (Live/Dead kit). 0 hours of culture (A); 36 hours of culture (B); 72 hours of culture (C). Magnification: 1000x.

3.4.4. Cellular Morphology

Cell morphology can be observed using different fluorochromes, such as Syto9/Propidium iodide[36,57], Acridine orange or DAPI[44]. In agreement with Guimarães *et al.* (2007) the Hpy769 probe was able to detect not only spiral cells but also cells with intermediate shapes (U, C and doughnut) and coccoid morphology, which have a low number of rRNA copies per cell[42]. In the present study, cell morphology was evaluated using DAPI, Syto 9/Propidium iodide and the Hpy 769 probe (PNA FISH probe) (Figure 3.6). The standard deviation among the methods applied is presented in supplementary material 5 (Table 3.5 and Table 3.6) with the higher standard deviation at 48 hours of culture, due to large differences observed between the Live/Dead kit and the other methods applied. Even after applying the cell-to-cell disaggregation method, DAPI and PNA FISH were not suitable to analyze cell morphology after cell conversion to the coccoid shape, due to the formation of cell clusters, which were higher in number and size (Figure 3.6). Curiously, the application of Syto 9/Propidium iodide dyes allowed observing and counting cells with different morphologies during the entire experiment, including coccoid shape samples, which had smaller cell clusters with these stains.

As shown in Figure 3.6, the percentage of spiral cells decreases during the time of experiment, with cells remaining mainly in the spiral shape until 48 hours of culture (although showing a decrease, especially after the exponential phase - 24 hours). Until 24 hours of culture, no significant difference in the percentage of spiral cells was observed ($p=0.66$; one-way ANOVA test). However, there was a significant difference between the methods performed to estimate the percentage of spiral cells ($p<0.05$; one-way ANOVA test) (detailed results in supplementary material 5, Table 3.5). In general, the percentage of spiral cells observed with the Hpy 759 probe until 24 hours is higher than the percentage of spiral cells counted with the other methods (supplementary material 5, Table 3.6). As discussed above, after 48 hours of culture, it was only possible to observe cell morphology using Syto 9/Propidium iodide stains and a huge decrease in the number of spiral cells was observed with around 7% of spiral cells at 72 hours of culture.

In general, a slight decrease in the coccoid cells was observed in the exponential phase (until 12 hours), and a subsequent increase was observed, with mostly coccoid cells

observed at 60 hours of culture. (around 80%, evaluated with Syto9/Propidium iodide dyes) (Figure 3.6). The presence of coccoid cells using Ham's F-12 nutrient mixture, analyzed by Live/Dead kit, was also observed by Azevedo and co-workers, with 100% of coccoid cells at 48 hours of cells in F-12 medium and in contact with a copper surface[17]. Mean percentage of intermediate cells, in general, is increasing with time (results detailed in supplementary material 5, Table 3.6.).

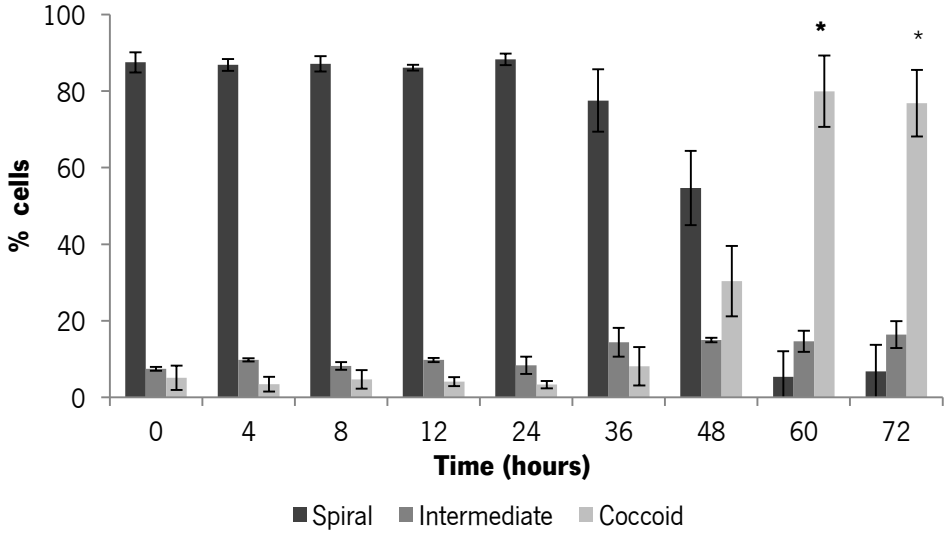

Figure 3.6. Cell morphology of *H. pylori* 26695 along culture time. For each time the mean of cells in different morphologies counted using the DAPI stain, PNA FISH probe and Live/Dead kit are shown for three biological culture replicates. Error bars represents standard deviation of values for three biological replicates. * - values obtained only with Live/Dead staining.

3.5. *Conclusions*

Although the application of staining methods to enumerate cells and evaluate cell morphology, as well as the use of the Live/Dead kit to evaluate viability have been largely applied, the comparison of the results obtained between methods in *H. pylori* has, to our knowledge, never been reported. Another important comparison, performed in this work, was of the mentioned methods with a PNA FISH probe, specific to *H. pylori*. In addition, a

cell-to-cell disaggregation method was applied, allowing improvements in the counting of cells using "conventional" methods.

In general, differences between methods used to enumerate cells were observed, with DAPI yielding the higher number of total cell counts when compared with the PNA FISH probe applied. Culturable cell counts were in general less than total cell counts performed with DAPI, especially after the exponential phase, showing the presence of nonculturable cells. The viable but non-culturable state was observed after 60 hours of culture. The number of culturable cells was, in general, similar to the viable cells during the exponential phase. The evaluation of cell viability using Syto9/propidium iodide was not effective to analyze cell morphological changes, giving exaggerated numbers of nonviable cells, explained by the entrance of propidium iodide through the permeable cytoplasmatic membrane. Under the referred conditions, another method to estimate cell viability must be used, such as measurement of membrane potential[59]. The culturable cell counts at 60 and 72 hours of culture were higher compared with the spiral cells observed at these time points, thus, proving the presence of culturable coccoid cells, previously shown by other authors[9,10,57], however under controversy. After 60 hours of culture, mainly coccoid cells were observed. Taking into account that coccoid forms represent a cell adaptation to less favorable conditions[17], the present results suggests that some stressing factor is present that causes morphological changes, probably the unavailability of an essential nutrient. The presence of an increasing number and size of cell clusters also support this hypothesis.

3.6. *References*

1. Catrenich, C. & Makin, K. Characterization of the morphologic conversion of *Helicobacter pylori* from bacillary to coccoid forms . *Scand. J. Gastroenterol.* **181,** 58–64 (1991).

2. Mizoguchi, H. *et al.* Diversity in protein synthesis and viability of *Helicobacter pylori* coccoid forms in response to various stimuli. *Infect. Immun.* **66,** 5555–5560 (1998).

3. Cellini, L., Allocati, N., Emanuela, D. C. & Dainelli, B. *Helicobacter pylori*: a fickle germ. *Microb. Immunol.* **38,** 25–30 (1994).

4. Shahamat, M., Mai, U., Paszko-Kolva, C., Kessel, M. & Colwell, R. R. *Helicobacter pylori* in water. Use of autoradiography to assess viability of *Helicobacter pylori* in water. *Appl. Environ. Microbiol.* **59,** 1231–1235 (1993).

5. West, A. P., Millar, M. R. & Tompkins, D. S. Effect of physical environment on survival of *Helicobacter pylori*. *J. Clin. Pathol.* **45,** 228–31 (1992).

6. Sorberg, M., Nilsson, M., Handerger, H. & Nilsson, L. Morphologic conversion of *Helicobacter pylori* from bacillary to coccoid form. *Eur. J. Clin. Microbiol. Infect. Dis.* **15,** 216–219 (1996).

7. Bode, G., Mauch, F. & Malfertheiner, P. The coccoid forms of *Helicobacter pylori*. Criteria for their viability. *Epidemiol. Infect.* **111,** 483–490 (1993).

8. Berry, V., Jennings, K. & Woodnutt, G. Bactericidal and morphological effects of amoxicillin on *Helicobacter pylori*. *Antimicrob. Agents Chemother.* **39,** 1859–1861 (1995).

9. Saito, N. *et al.* Plural transformation-processes from spiral to coccoid *Helicobacter pylori* and its viability. *J. Infect.* **46,** 49–55 (2003).

10. Sato, F. *et al.* Ultrastructural observation of *Helicobacter pylori* in glucose-supplemented culture media. *J. Med. Microbiol.* **52,** 675–679 (2003).

11. Eaton, K. A., Catrenich, C. E., Makin, K. M. & Krakowka, S. Virulence of coccoid and bacillary forms of *Helicobacter pylori* in gnotobiotic piglets. *J. Infect. Dis.* **171,** 459–462 (1995).

12. Kusters, J. G., Gerrits, M. M., Van Strijp, J. A. G. & Vandenbroucke-Grauls, C. M. J. E. Coccoid forms of *Helicobacter pylori* are the morphologic manifestation of cell death. *Infect. Immun.* **65,** 3672–3679 (1997).

13. Brenciaglia, M. I., Fornara, A. M., Scaltrito, M. M. & Dubini, F. *Helicobacter pylori*: cultivability and antibiotic susceptibility of coccoid forms. *Int. J. Antimicrob. Agents* **13,** 237–241 (2000).

14. Oliver, J. D. The viable but nonculturable state in bacteria. *J. Microbiol.* **43,** 93–100 (2005).

15. Oliver, J. D. Recent findings on the viable but nonculturable state in pathogenic bacteria. *FEMS Microbiol. Rev.* **34,** 415–425 (2010).

16. Nilsson, H., Blom, J., Al-soud, W. A., Andersen, L. P. & Wadström, T. Effect of cold starvation, acid stress, and nutrients on metabolic activity of *Helicobacter pylori*. *Appl. Environ. Microbiol.* **68,** 11–19 (2002).

17. Azevedo, N. F. *et al.* Coccoid form of *Helicobacter pylori* as a morphological manifestation of cell adaptation to the environment. *Appl. Environ. Microbiol.* **73,** 3423–3427 (2007).

18. Cellini, L. *et al.* Coccoid *Helicobacter pylori* not culturable *in vitro* reverts in mice. *Microb. Immunol.* **38,** 843–850 (1994).

19. She, F.-F., Lin, J.-Y., Liu, J.-Y., Huang, C. & Su, D.-H. Virulence of water-induced coccoid *Helicobacter pylori* and its experimental infection in mice. *World J. Gastroenterol.* **9,** 516–520 (2003).

20. Sisto, F., Brenciaglia, M. I., Scaltrito, M. M. & Dubini, F. *Helicobacter pylori*: ureA, cagA and vacA expression during conversion to the coccoid form. *Int. J. Antimicrob. Agents* **15,** 277–82 (2000).

21. Can, F. *et al.* Urease activity and urea gene sequencing of coccoid forms of *H. pylori* induced by different factors. *Curr. Microbiol.* **56,** 150–155 (2008).

22. Poursina, F. *et al.* Assessment of cagE and babA mRNA expression during morphological conversion of *Helicobacter pylori* from spiral to coccoid. *Curr. Microbiol.* **66,** 406–13 (2013).

23. Saito, N. *et al.* Coccoid *Helicobacter pylori* can directly adhere and invade in agminated formation to human gastric epithelial cells. *Adv. Microbiol.* **2,** 112–116 (2012).

24. Benaissa, M. *et al.* Changes in *Helicobacter pylori* ultrastructure and antigens during conversion from the bacillary to the coccoid form. *Infect. Immun.* **64,** 2331–23355 (1996).

25. Cabeen, M. T. & Jacobs-Wagner, C. Bacterial cell shape. *Nat. Rev. Microbiol.* **3,** 601–610 (2005).

26. Sycuro, L. K. *et al.* Relaxation of peptidoglycan cross-linking promotes *Helicobacter pylori*'s helical shape and stomach colonization. *Cell* **141,** 822–833 (2010).

27. Sycuro, L. K. *et al.* Multiple peptidoglycan modification networks modulate *Helicobacter pylori*'s cell shape, motility, and colonization potential. *PLoS Pathog.* **8,** e1002603 (2012).

28. Costa, K. *et al.* The morphological transition of *Helicobacter pylori* cells from spiral to coccoid is preceded by a substantial modification of the cell wall. *J. Bacteriol.* **181,** 3710–3715 (1999).

29. Takeuchi, H., Shirai, M., Akada, J. K., Tsuda, M. & Nakazawa, T. Nucleotide sequence and characterization of cdrA, a cell division-related gene of *Helicobacter pylori* . *J. Bacteriol.* **180,** 5263–5268 (1998).

30. Chaput, C. *et al.* Role of AmiA in the morphological transition of *Helicobacter pylori* and in immune escape. *PLoS Pathog.* **2,** e97 (2006).

31. Waidner, B. *et al.* A novel system of cytoskeletal elements in the human pathogen *Helicobacter pylori*. *PLoS Pathog.* **5,** e1000669 (2009).

32. Chiou, P.-Y., Luo, C.-H., Chang, K.-C. & Lin, N.-T. Maintenance of the cell morphology by MinC in *Helicobacter pylori*. *PLoS One* **8,** e71208 (2013).

33. Cellini, L. *et al.* Recovery of *Helicobacter pylori* ATCC43504 from a viable but not culturable state: regrowth or resuscitation? *APMIS* **106,** 571–579 (1998).

34. Donelli, G. *et al.* The effect of oxygen on the growth and cell morphology of *Helicobacter pylori*. *FEMS Microbiol. Lett.* **168,** 9–15 (1998).

35. Williams, J. C., McInnis, K. a & Testerman, T. L. Adherence of *Helicobacter pylori* to abiotic surfaces is influenced by serum. *Appl. Environ. Microbiol.* **74,** 1255–1258 (2008).

36. Azevedo, N. F., Pacheco, a P., Keevil, C. W. & Vieira, M. J. Adhesion of water *Helicobacter pylori* to abiotic surfaces. *J. Appl. Microbiol.* **101,** 718–724 (2006).

37. Monier, J. & Lindow, S. E. Frequency, size, and localization of bacterial aggregates on bean leaf surfaces. *Appl. Environ. Microbiol.* **70,** 346–355 (2004).

38. Klebensberger, J., Lautenschlager, K., Bressler, D., Wingender, J. & Philipp, B. Detergent-induced cell aggregation in subpopulations of *Pseudomonas aeruginosa* as a preadaptive survival strategy. *Environ. Microbiol.* **9,** 2247–2259 (2007).

39. Maisonneuve, E., Fraysse, L., Moinier, D. & Dukan, S. Existence of abnormal protein aggregates in healthy *Escherichia coli* cells. *J. Bacteriol.* **190,** 887–893 (2008).

40. Bessa, L. J., Correia, D. M., Cellini, L., Azevedo, N. F. & Rocha, I. Optimization of culture conditions to improve *Helicobacter pylori* growth in Ham's F-12 medium by response surface methodology. *Int. J. Immunopathol. Pharmacol.* **25,** 901–909 (2012).

41. Testerman, T. L., Gee, D. J. M. C. & Mobley, H. L. T. *Helicobacter pylori* growth and urease detection in the chemically defined medium Ham's F-12 nutrient mixture. *J. Clin. Microbiol.* **39,** 3842–3850 (2001).

42. Guimarães, N., Azevedo, N. F., Figueiredo, C., Keevil, C. W. & Vieira, M. J. Development and application of a novel peptide nucleic acid probe for the specific detection of

Helicobacter pylori in gastric biopsy specimens. *J. Clin. Microbiol.* **45,** 3089–3094 (2007).

43. Cole, S. P., Cirillo, D., Kagnoff, M. F. & Guiney, D. G. Coccoid and spiral *Helicobacter pylori* differ in their abilities to adhere to gastric epithelial cells and induce interleukin-8 secretion. *Microbiology* **65,** 843–846 (1997).

44. Kepner, R. L. & Pratt, J. R. Use of fluorochromes for direct enumeration of total bacteria in environmental samples: Past and present. *Microbiol. Mol. Biol. Rev.* **58,** 603–615 (1994).

45. Almeida, C. *et al.* Development and application of a novel peptide nucleic acid probe for the specific detection of *Cronobacter* genomospecies (*Enterobacter sakazakii*) in powdered infant formula. *Appl. Environ. Microbiol.* **75,** 2925–2930 (2009).

46. Almeida, C., Azevedo, N. F., Fernandes, R. M., Keevil, C. W. & Vieira, M. J. Fluorescence *in situ* hybridization method using a peptide nucleic acid probe for identification of *Salmonella* spp. in a broad spectrum of samples. *Appl. Environ. Microbiol.* **76,** 4476–4485 (2010).

47. Almeida, C. *et al.* Rapid detection of urinary tract infections caused by *Proteus* spp. using PNA-FISH. *Eur. J. Clin. Microbiol. Infect. Dis.* **32,** 781–786 (2013).

48. Azevedo, N. F. *et al.* Application of flow cytometry for the identification of *Staphylococcus epidermidis* by peptide nucleic acid fluorescence in situ hybridization (PNA FISH) in blood samples. *Antonie Van Leeuwenhoek* **100,** 463–470 (2011).

49. Machado, A. *et al.* Fluorescence *in situ* hybridization method using a peptide nucleic acid probe for identification of *Lactobacillus* spp. in milk samples. *Int. J. Food Microbiol.* **162,** 64–70 (2013).

50. Almeida, C., Azevedo, N. F., Santos, S., Keevil, C. W. & Vieira, M. J. Discriminating multi-species populations in biofilms with peptide nucleic acid fluorescence *in situ* hybridization (PNA FISH). *PLoS One* **6,** e14786 (2011).

51. Machado, A. *et al.* Fluorescence in situ hybridization method using peptide nucleic acid probes for rapid detection of *Lactobacillus* and *Gardnerella* spp . *BMC Microbiol.* **13,** 1–12 (2013).

52. Cerqueira, L. *et al.* DNA mimics for the rapid identification of microorganisms by fluorescence *in situ* hybridization (FISH). *Int. J. Mol. Sci.* **9,** 1944–1960 (2008).

53. LIVE / DEAD ® BacLight ™ Bacterial Viability Kits Technical Sheet. *Mol. Probes , Invit. Detect. Technol.* **MP 07007,** (2004).

54. Alonso, J. L., Mascellaro, S., Moreno, Y., Ferru, M. A. & Hernández, J. Double-staining method for differentiation of morphological changes and membrane integrity of *Campylobacter coli* cells. *Appl. Environ. Microbiol.* **68,** 5151–5154 (2002).

55. Berney, M., Hammes, F., Bosshard, F., Weilenmann, H.-U. & Egli, T. Assessment and interpretation of bacterial viability by using the LIVE/DEAD BacLight Kit in combination with flow cytometry. *Appl. Environ. Microbiol.* **73,** 3283–3290 (2007).

56. Boulos, L., Prévost, M., Barbeau, B., Coallier, J. & Desjardins, R. Methods LIVE / DEAD ® Bac Light TM: application of a new rapid staining method for direct enumeration of viable and total bacteria in drinking water. *J. Microbiol. Methods* **37,** 77–86 (1999).

57. Adams, B. L., Bates, T. C. & Oliver, J. D. Survival of *Helicobacter pylori* in a Natural Freshwater Environment. *Appl. Environ. Microbiol.* **69,** 7462–7466 (2003).

58. Queralt, N. & Araujo, R. Analysis of the survival of *H. pylori* within a laboratory-based aquatic model system using molecular and classical techniques. *Microb. Ecol.* **54,** 771–777 (2007).

59. Keer, J. T. & Birch, L. Molecular methods for the assessment of bacterial viability. *J. Microbiol. Methods* **53,** 175–183 (2003).

3.7. *Supplementary material*

3.7.1. Supplementary material 1

Table 3.1 describes the composition and chemicals used to make the hybridization solution for the PNA-FISH experiments, according to Guimarães *et al.* (2007)[42]. The solution was prepared in distillate sterilized water and the pH was adjusted to7.5.

Table 3.1. Composition of the hybridization solution.

Compounds	Chemicals	Concentration
Dextran sulphate	Sigma-Aldrich	10% (w/v)
NaCl	Sigma-Aldrich	10 mM
Formamide	Sigma-Aldrich	30% (v/v)
Sodium pyrophosphate	Sigma-Aldrich	0.1% (w/V)
Polyvinylpyrrolidone	Sigma-Aldrich	0.2% (w/v)
FICOLL	Sigma-Aldrich	0.2% (w/v)
Disodium EDTA	Pronalab	5 mM
Triton X-100	Sigma-Aldrich	0.1% (v/v)
Tris-HCl	Sigma-Aldrich	50 mM

Table 3.2 describes the composition and chemicals used to prepare the washing solution, according to Guimarães *et al.* (2007)[42]. The solution was prepared in distilled water and the pH was adjusted to10. The solution was sterilized (121°C, 15 minutes) and kept at 4°C until use.

Table 3.2. Composition of the washing solution.

Compounds	Chemicals	Concentration
Tris Base	Sigma-Aldrich	5 mM
NaCl	Sigma-Aldrich	15 mM
Triton-X	Sigma-Aldrich	1% (v/v)

3.7.2. Supplementary material 2

Figure 3.7 depicts the results of disaggregation assays, showing the influence of the vortex shaking time (3, 5, 7, 10 and 15 minutes) in Optical Density (600 nm) and Colonies Forming Units (CFU/mL) using 8-10 glass beads. The assay was performed with cells in the exponential phase, growing in liquid medium (Ham's F-12) supplemented with 5% (v/v) FBS.

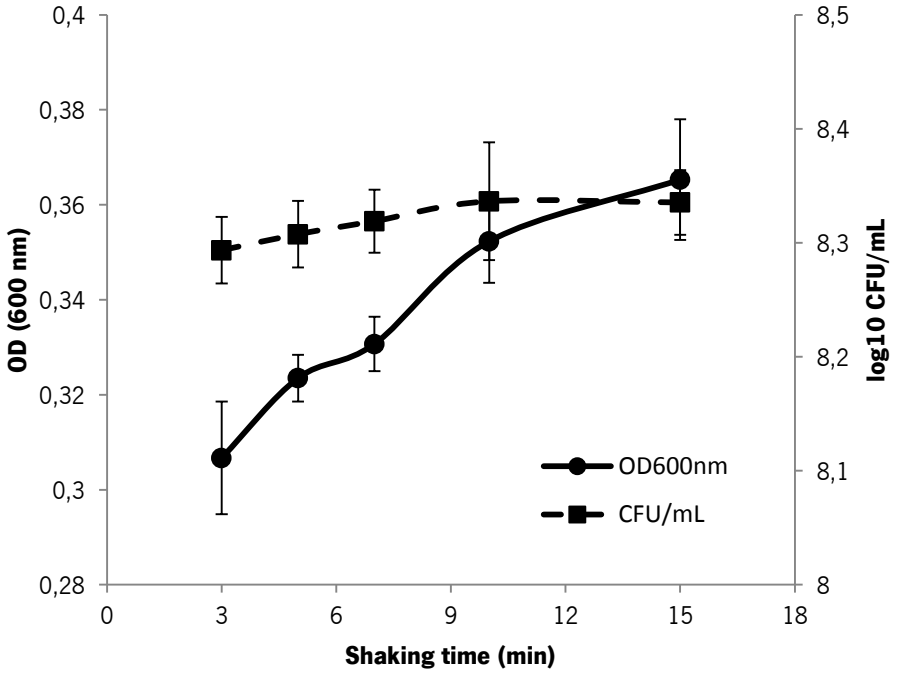

Figure 3.7. OD_{600} and CFU/mL in disaggregation assays using 8-10 glass beads and vortex shaking (3,5,7,10 and 15 minutes)

3.7.3. Supplementary material 3

Table 3.3 shows the mean values (± standard deviation) of cell counts for three biological replicates for each method applied. A ratio between methods is also presented, showing the differences between counts among methods.

Table 3.3. Mean values (±SD) of cell counts for each method performed for three biological replicates.

Time (hours)	log_{10} CFU/mL Mean ± SD	CFU/DAPI (%)	log_{10} cells/mL DAPI Mean ± SD	PNA/DAPI (%)	log_{10} cells/mL Hpy769 probe Mean ± SD	PNA/ CFU (%)
0	7.86±0.14	86.30	7.90±0.22	24.51	7.32±0.10	28.40
4	8.08±0.13	37.24	8.50±0.15	33.48	8.01±0.19	89.91
8	8.13±0.07	60.00	8.27±0.35	56.05	8.10±0.06	93.41
12	8.02±0.19	24.23	8.66±0.05	25.71	7.99±0.35	106.11
24	7.90±0.05	30.81	8.41±0.09	63.44	8.20±0.15	205.90
36	7.62±0.12	13.85	8.41±0.32	51.71	8.19±0.11	373.46
48	6.55±0.33	1.92	8.28±0.28	49.91	8.02±0.16	2601.54
60	5.76±0.05	-	-	-	-	-
72	5.81±0.01		-	-	-	-

3.7.4. Supplementary material 4

Table 3.4 depicts the percentage and $\log_{10}$ of viable cell counts obtained using Syto9/propidium iodide stains contained in the Live/Dead kit. The values presented are the mean of three biological replicates (± standard deviation).

Table 3.4. Total and viable cell counts using the Live/dead kit performed for three biological replicates. Mean ± Standard deviation.

Time (hours)	Total Cells	Viable Cells	
	$\log_{10}$ cells Mean ± SD	**$\log_{10}$cells Mean ± SD**	**% cells Mean ± SD**
0	8.23±0.46	8.13±0.46	79.89±4.18
4	8.29±0.19	8.26±0.19	91.95±3.49
8	8.18±0.13	8.12±0.20	88.79±15.25
12	8.39±0.03	8.36±0.02	92.66±5.81
24	8.45±0.10	8.41±0.09	90.57±3.50
36	8.43±0.06	7.05±0.85	12.61±19.06
48	8.15±0.16	4.16±3.61	0.77±0.86
60	8.43±0.11	8.23±0.13	63.68±3.48
72	8.26±0.22	7.33±0.42	12.76±6.38

3.7.5. Supplementary material 5

Table 3.5 shows the percentage of spiral cell counts for each method performed. Mean of three biological replicates for each method and mean values (± standard deviation) for all the methods performed.

Table 3.5. Mean percentage of spiral cell counts for each method performed for three biological replicates.

Time (hours)	% Spiral cells			Mean ± SD
	DAPI	Hpy 769 probe	Syto9/PI	
0	86.90	94.29	81.36	87.52±6.48
4	87.89	94.33	78.35	86.86±8.04
8	85.62	92.57	83.18	87.12±4.87
12	83.97	89.47	84.96	86.13±2.93
24	80.93	98.99	85.09	88.34±9.46
36	76.58	87.36	68.67	77.54±9.38
48	67.86	75.69	20.49	54.68±29.87
60	-	-	5.37	-
72	-	-	6.76	-

Table 3.6 shows the percentage of intermediate (U-shape, C-shape and doughnut shape) and coccoid cell counts for each method performed. Mean of three biological replicates for each method and mean values (± standard deviation) of the methods performed.

Table 3.6. Mean percentage of intermediate and coccoid cell counts for each method performed for three biological replicates.

Time (hours)	% Intermediate forms				% Coccoid cells			
	DAPI	**Hpy 769 probe**	**Syto9/PI**	**Mean ± SD**	**DAPI**	**Hpy 769 probe**	**Syto9/PI**	**Mean ± SD**
0	9.62	4.97	7.65	7.41±2.34	3.48	0.75	10.99	5.07±5.30
4	11.22	4.48	13.53	9.75±4.70	0.89	1.18	8.12	3.40±4.09
8	11.79	6.24	6.61	8.22±3.10	2.59	1.19	10.20	4.66±4.85
12	13.39	6.68	9.16	9.74±3.39	2.64	3.85	5.89	4.13±1.64
24	14.79	0.97	9.30	8.35±6.96	4.28	0.04	5.61	3.31±2.91
36	16.98	8.70	17.45	14.38±4.92	6.44	3.94	13.88	8.09±5.17
48	17.24	12.95	14.77	14.99±2.15	14.91	11.35	64.74	30.33±29.85
60	-	-	14.66	-	-	-	79.97	-
72	-		16.39	-	-	-	76.86	-

Chapter 4

Exometabolome analysis in *H. pylori* for the elucidation of nutritional requirements and preferences: reconciliation of *in silico* and *in vitro* metabolic capabilities

Daniela M. Correia, Ana Guimarães, Lucinda J. Bessa, Maria J. Vieira, Nuno F. Azevedo and Isabel Rocha. Exometabolome analysis in *H. pylori* for the elucidation of nutritional requirements and preferences: reconciliation of *in silico* and *in vitro* metabolic capabilities (To be submitted).

4.1. *Abstract*

Helicobacter pylori is a human pathogen associated with gastric diseases. Understanding the growth of pathogenic organisms inside the host is of major importance to develop new and efficient drugs that can be used to treat and eradicate these microbes. However, uncovering the mechanisms associated with *H. pylori*'s associated diseases has been hindered by the difficulties found in growing this organism under defined conditions.

The present study was conducted with the goal of clarifying *H. pylori*'s nutritional requirements, using a metabolic footprinting approach and bringing together *in vitro* and *in silico* data. For that purpose, *H. pylori* 26695 was grown under controlled conditions, without strain adaptation, in a defined medium supplemented with fetal bovine serum and samples were collected to analyze extracellular metabolites using GC-MS after a chemical derivatization.

Discrepancies among *in vitro* studies were found, as well as between *in vitro* and *in silico* predictions, revealing the importance of data reconciliation. Under the conditions used, some amino acids were identified as absolutely required for *H. pylori* 26695 growth: L-arginine, L- histidine, L-isoleucine, L-leucine, L-methionine, L-phenylalanine and L-valine. In addition, other amino acids were identified as possible preferential carbon sources, namely, aspartate, glutamate, alanine and proline, although some doubts persist regarding the need of proline and alanine in *H. pylori*. The clarification of *H. pylori* nutritional requirements will allow not only to adjust the culture medium components and perform experiments under more defined conditions, but especially to gain new insights about *H. pylori*'s physiology and metabolism.

Keywords: *Helicobacter pylori*, exometabolome, nutritional requirements, *in silico*, *in vitro*.

4.2. *Introduction*

H. pylori is a microaerophilic, gram negative, fastidious organism, requiring 3-4 days of growth in complex solid media. Over the last 20 years, scientists have pursued the development of defined liquid media for *in vitro* growth of *H. pylori* [1–4]; however, the cell densities obtained using these defined media are quite low, and the addition of supplements[5] (cyclodextrins, bovine serum albumin (BSA) or fetal bovine serum (FBS)) significantly improves growth, hence hampering the identification of nutritional requirements. Moreover, growth in defined media has required previous strain adaptation or has been mostly achieved with non-reference strains, as discussed in the state of the art section. Also, despite several studies that tried to identify the nutritional requirements of this pathogenic organism, there are discrepancies between published studies.

Additionally, relevant information is still missing in terms of metabolic capabilities, and different published studies lead to different conclusions. It has been described that *H. pylori* can metabolize glucose, although evidences suggest the operation of the pentose phosphate and Entner Doudoroff pathways[6,7] rather than glycolysis as the major routes for catabolism. Nevertheless, most of the glycolytic enzymes are present, which may fulfill the requirement for gluconeogenesis[8]. Mendz *et al.* (1995) proved that *H. pylori* can grow employing aminoacids as carbon and energy sources, and suggested that even though oxygen is essential for the growth of this organism, some aminoacids are utilized via fermentative pathways characteristic of anaerobiosis[9]. *H. pylori* also uses some amino acids, urea and ammonium as nitrogen sources. According to some authors, there are few absolute requirements for *H. pylori* growth: nine amino acids (arginine, histidine, leucine, methionine, phenylalanine, valine, alanine, cysteine and proline), sodium and potassium chloride, thiamine, iron, zinc, magnesium, hypoxanthine and pyruvate[3]. However, those experiments have been performed with more than one carbon source.

Uncovering the mechanisms associated with *H. pylori* infection has been hindered by the lack of physiological data and consequently, many aspects related with the appearance of diseases remain unclear.

Metabolites, the intermediates of biochemical reactions, have a key role in connecting the many different pathways that operate within a living cell[10]. The group of all metabolites synthesized or used by a biological system is called the metabolome[11,12]. In the metabolomics field, metabolic footprinting has been extensively used to understand cell physiology under diverse states or conditions on various biological systems[13,14], relying on the investigation of metabolites consumed from and secreted into the culture medium[15].

Genomic information, combined with biochemical knowledge made possible the development of metabolic models for several organisms[16,17], which can be used to predict the phenotypic behavior under different genetic and environmental conditions[16]. Nowadays, there are several software tools for using stoichiometric models of microbial metabolism for simulation and optimization[18]. The genome sequence of *H. pylori*, together with accumulated biochemical and physiological knowledge, allowed the construction of genome-scale metabolic models for this organism[19,20]. The first one was published in 2002 (*i*CS291)[19] and an updated version was published in 2005 (*i*T341 GSM/GPR)[20]. Nevertheless, the predictions obtained with these stoichiometric models are only as good as allowed by the data used to build the model. In the particular case of *H. pylori*, physiological data collected under defined conditions are scarce, hindering model validation, and consequently making the models unrealistic and inaccurate.

The present study was conducted with the main goal of elucidating *H. pylori*'s preferences and nutritional requirements, with special relevance for carbon and energy sources. One of the applications of this study is the design of a more rational *H. pylori* growth medium. For those purposes, *H. pylori* was grown in liquid medium and samples were collected to analyze the extracellular metabolites. Simulations were performed using the existing genome-scale metabolic model in order to link the *in vitro* obtained results with the predictions made by the model and gain new insights about the metabolism of this pathogenic organism. The development of robust methods to grow *H. pylori* would allow for a much faster and reproducible path to obtain biomass, and consequently lead to a significant development in studies on *H. pylori* physiology and metabolism, as well as protein characterization. Moreover, the identification of the nutritional requirements and

active metabolic pathways of this organism is of major importance to understand its growth in the host and to help to design alternative strategies for microbial inactivation.

4.3. *Methods*

4.3.1. Culture conditions

Helicobacter pylori 26695 (strain NCTC 12455) was cultivated in Columbia Blood Agar (CBA) at 37 °C under microaerophilic conditions (5% O_2, 10% CO_2, 85% N_2) in a Cell Culture Incubator (Incubator HERAcell 150, Kendro Laboratory, Germany) for 3 days.

An inoculum was prepared in 150 mL of Ham's F-12 nutrient mixture with glutamine (catalog no 21765-037, Invitrogen-Gibco, Spain) (composition detailed in supplementary material 1), previously supplemented with 5% of FBS (catalog no 10500-064, origin: South America, Invitrogen-Gibco, Spain)[21], incubated at 37 °C under 120 rpm of shaking speed (Heidolph Unimax 1010 orbital shaker, Germany) in microaerophilic conditions for approximately 17 h, in order to reach the exponential phase.

Cultivations were performed in 1000-mL Erlenmeyer flasks with the same medium as described for the inoculum at 37 °C under 130 rpm of shaking speed, under microaerophilic conditions (6.5% O_2, 10% CO_2, 83.5% N_2). The initial cell concentration was adjusted to an optical density at 600 nm (OD_{600}) of 0.1 (corresponding to approximately 10^7 CFU/mL). The experiment was carried out in triplicate during 72 hours. More details can be found on previously published work[22] in which the culture conditions were optimized by experimental design.

4.3.2. Growth assessment

In order to assess growth, for each experiment performed, samples were collected at defined time points (until 72 hours), and the optical density (OD) at 600 nm was read using a microplate reader (TECAN Sunrise, Switzerland) after performing the

disaggregation procedure described in the previous chapter. Cell dry weight (CDW) was determined by using a calibration curve (as described in Chapter 6). A conversion factor of 0.82 was achieved to convert OD (600nm) to CDW (g/L). Based on the growth curve, the specific growth rate (μ) was calculated. To ensure that all samples collected had not been contaminated, aliquots were plated both on Tryptic Soy Agar (TSA) and CBA plates, at each time point for all experiments.

4.3.3. Extracellular metabolite analysis

The extracellular metabolite analysis was performed according to the method described by Smart *et al.* (2010)[23], with minor modifications.

4.3.3.1. Chemicals

Amino and organic acids standards stock solutions were prepared at a concentration of 500 mM in ultra-pure water, with the exception of lactic acid and isocitric acid which were prepared at a concentration of 250 mM and 2-oxoadipic acid which was prepared at 100 mM. In working standard solutions, prepared at 10 mM, the pH was set to values above 12 with sodium hydroxide (1 M). A range of standard solutions between 0.0005 and 10 mM was prepared and a total of three replicates per standard concentration were analyzed. The standard solutions were treated the same way as the samples. All solutions were stored at -20 °C while not in use. Information about standard compounds used in this study is detailed in supplementary material 2.

4.3.3.2. Sample preparation

At each time point (0, 4, 8, 12, 24, 48 and 72 hours) samples were collected for exometabolome analysis by Gas Chromatography coupled with Mass Spectrometry (GC-MS). 1-mL samples at each time point (in triplicate) were filtered through a syringe cellulose acetate filter (0.2-μm pore size, 25 mm), to remove bacterial cells, and 20 μL of d_4- alanine (2,3,3,3-d_4-alanine) (internal standard) at 10 mM were added to each sample. 1-mL samples (3 in total) of noninoculated culture medium were prepared in the same

way, and were used as controls (blank samples). The samples were frozen at -80 °C and then lyophilized during 24 hours.

4.3.3.3. Sample derivatization

The samples for extracellular metabolites analysis were derivatized using the methyl chloroformate (MCF) method described by Smart *et al.* (2010)[23]. All solutions and standards used were prepared according to the same protocol. Together with the samples, one blank of derivatization (all derivatization reagents without sample) was prepared. After derivatization, the samples were analyzed in 24 hours, to avoid sample degradation.

4.3.3.4. GC-MS analysis

GC-MS analysis was performed with a Varian 4000 GC-MS (Varian, USA) with a gas chromatograph (Varian CP-3800) equipped with an autosampler (CP-8410), coupled to a mass spectrometer with an Ion Trap analyzer (Varian 4000), operating in electron impact (EI) ionization mode (70eV). The chromatographic column used was a ZB1701 – GC capillary column (30 m x 0.25 mm ID x 0.15 µm film thickness) with a 5-m guard column (Phenomenex, USA).

The 1-µL sample was injected using a splitless mode, and after 1 minute of injection the split ratio was 1:20. The GC oven temperature was initially held at 45 °C for 2 min. Thereafter the temperature was raised at 9°C/min until 180°C and held for 5 min. Then, the temperature was raised at 40°C/min until 220°C, and held for 5 min. After that the temperature was again raised at 40°C/min until 240°C and held for 11.5 min. Then, the temperature was raised at 40°C/min until 280°C and held for 2 min, totalizing 43 min of analysis time. Helium was used as the carrier gas, at a constant flow rate of 1.0 mL/min.

The injector temperature was set to 290 °C, and the interface temperature to 250 °C, while the trap temperature was set to 190 °C. The MS was operated in the full-scan acquisition mode (38-650 *m/z* – mass to charge ratios), after 5 minutes at 1.64 scan/s.

The GC-MS software used to control the system was the Varian MS Workstation System Control – version 6.6.

4.3.3.5. Data analysis

A standard library with retention times and mass spectra of derivatized standards was created. Retention times, molecular ions, and major fragment ions identified for all analyzed compounds are detailed in supplementary material 3. The metabolite identification was based on the matching of retention times and mass spectra against the created library. The peak intensity of MCF derivatives of standards (amino and nonamino organic acids) was used to quantify the metabolites in samples. The data normalization was achieved by the normalization of the peak intensities by the intensity of the internal standard (d_4 –alanine) in each sample.

Data processing and statistical analysis were performed with Excel and Multi Experiment Viewer (MeV)[24].

In order to evaluate if there were significant differences between the mean values of each compound identified in MS spectra of the biological replicates (three), an analysis of variance (ANOVA) was performed. An ANOVA analysis was also applied to examine if the consumption of each compound along time was significant.

To further examine the relation between the amino acids profile and to evaluate which amino acids had a similar profile along time, a hierarchical clustering (HCL) and K-Means analysis were applied on the GC-MS data acquired until 72 hours of culture. Thus, percentage values of biological replicates were averaged and the MeV[24] software was used to perform clustering analysis. Hierarchical clustering, based on Kendall's Tau metrics, was used to have a global view of the possible clusters. Additionally, in order to categorize the amino acids into clusters, a K-Means clustering analysis was performed using the same metrics as described for HCL, with the following parameters: number of clusters – 3; maximum iterations – 50.

4.3.3.6. Acetate and glucose analysis

For glucose and acetate analysis, 1-mL samples at each time point were filtered by a 0.2-µm syringe filter, to remove bacterial cells, and were immediately frozen at -20 °C until analysis. The analysis of acetate and glucose were performed using an acetic acid UV-method (Cat. No. 10 148 261 035, Boehringer Mannheim/R-Biopharm, Roche, Germany) and a D-glucose UV-method (Cat. No. 10 716 251 035, Boehringer Mannheim/R-Biopharm, Roche, Germany) kits, respectively. In order to stop enzymatic reactions, according to the kit's instructions, prior to analysis samples were heated in a water-bath at 80°C during 15 min, and then were centrifuged at 5000 rpm for 5 min. Afterwards, the experimental procedure was performed according to the manufacturer's instructions.

4.3.3.7. Metabolic model simulations

In order to compare the experimental data with the simulated data supplied by the existing genome-scale metabolic model, simulations using Flux Balance Analysis (FBA) were performed. The model used to predict the behavior of *H. pylori* under the conditions used *in vivo* was the *i*T341 GSM/GPR, published by Thiele *et al.* (2005)[20]. Optflux[18], an open source software, was the platform used to perform the simulations using the Systems Biology Markup Language (SBML) file of the aforementioned model. In the simulated environmental conditions the uptake rates for the metabolites present in the culture medium were set to 10 mmol/h/g (dry weight). Additionally, the uptake rates for sodium, sulphate, iron, ammonia, phosphate and protons were not constrained. The mentioned uptake rates were set based on the information contained in the model for the minimal medium[20].

4.4. *Results*

To shed light on preferences and nutritional requirements of *H. pylori*, experiments (in triplicate) in Erlenmeyer flasks were performed. From each experiment, samples were harvested at regular intervals, during 72 hours of culture. Under the conditions used, *H. pylori* was in the exponential phase from 2 to 6 hours (μ=0.163 h^{-1}) (consistent with results from a previous work by the authors[22]) (Figure 4.1).

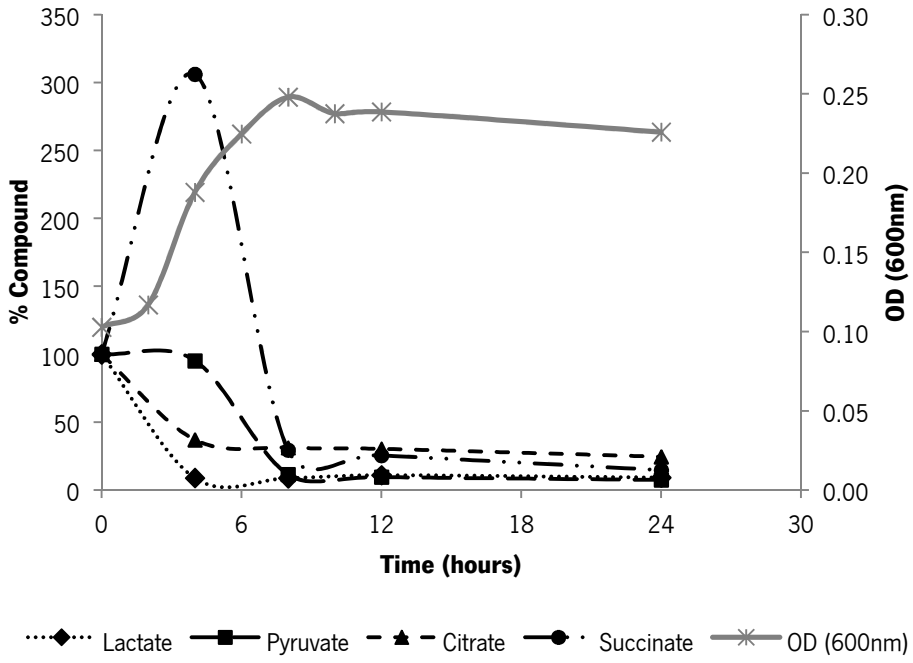

Figure 4.1. Evolution of organic acids (lactate, pyruvate, citrate, succinate) percentage along time in the extracellular medium and Optical Density measured at 600 nm. Mean values of biological replicates (n=3) with 3 technical replicates.

4.4.1. Exometabolome analysis

The extracellular medium was analyzed by GC/MS to evaluate the consumption and/or secretion of amino and nonamino organic acids by *H. pylori*. One hundred percent corresponded to the initial concentration of each acid detected in the supernatant. Each

value represents the mean of three biological replicates (replicates of the culture), each with three technical replicates (replicates of each time point of the same culture).

4.4.1.1. Organic acids

Pyruvate, citrate, lactate and succinate were identified in the supernatant of *H. pylori* cultures. In Figure 4.1, the evolution of organic acids in the extracellular medium is depicted until 24 hours of culture. Samples were collected until 72 hours but their percentages presented no significant changes after 24 hours ($p>0.05$, one-way ANOVA). Citrate, lactate and succinate were detected in the culture medium used (Ham's F-12+5 % FBS). Since they are not part of the composition of Ham's F-12, they should have been present in the FBS. All compounds detected in the liquid medium with the respective percentage and variations are detailed in supplementary material 4.

In general, at 4 hours of culture the concentration of all organic acids had decreased in the culture medium, with the exception of succinate, that had approximately tripled. Before 24 hours of culture, all organic acids had been consumed with a significant decrease in percentage in the extracellular medium ($p<0.05$, one-way ANOVA). Pyruvate, which was in culture medium with an initial concentration of about 1 mM, was almost completely exhausted, remaining only approximately 2% of the initial concentration at the end of the culture. Citrate, lactate and succinate, which were present in the culture medium with initial concentrations of about 0.08 mM, 1.21 mM and 0.02 mM, respectively, were not completely consumed.

4.4.1.2. Amino acids

Based on the hypothesis that metabolites that show similar time profiles are somehow related, the amino acids detected in the extracellular medium along time were classified into clusters by Hierarchical (HCL) and K-Means clustering (KMC), using a Kendall's Tau metrics (Figure 4.2). Although the culture medium contains 20 amino acids, not all were detected, owing to problems of suitability of the derivatization method used

(arginine), instability of the derivatized compounds (histidine), or low concentrations (glutamine, glycine and serine). As such, a total of 15 amino acids were detected.

From the HCL analysis (Figure 4.2a), three main clusters can be distinguished (clusters I-III), and it is possible to observe that clusters II and III are the closest ones. Furthermore, the examination of the clusters obtained with K-Means (Figure 4.4b), reveals that amino acids classified in the same cluster follow a similar profile along the culture. In these plots, each grey line represents one amino acid, while the centroid of each cluster profile is also shown (blue line).

Cluster I includes amino acids that were completely (alanine, aspartate, glutamate, methionine and proline), or partially consumed (isoleucine, leucine, and valine), with percentages of consumption higher than 50%. Performing a statistical test allowed to verify that all amino acids in this cluster were significantly consumed ($p<0.05$, one-way ANOVA).

Asparagine, tryptophan and cysteine were grouped in cluster II, with a decrease in percentage at 4 hours of culture, and a subsequent increase, remaining at a percentage higher than 50% in the supernatant at the end of the culture. The amino acids included in cluster II did not show further significant changes ($p>0.05$, one-way ANOVA).

Cluster III groups amino acids which were not consumed (lysine, phenylalanine, threonine and tyrosine), being some of them accumulated in the extracellular medium (lysine and tyrosine) at the end of the culture with a percentage about twofold higher than initially. However, a decrease in percentage was observed for all amino acids of cluster III at 4 hours of culture. Though these amino acids were not consumed, a significant change ($p<0.05$, one-way ANOVA) in their percentage on the extracellular medium until 72 hours of culture was observed. Phenylalanine was the exception, with no significant changes ($p=0.300$, one-way ANOVA) in its percentage in the supernatant.

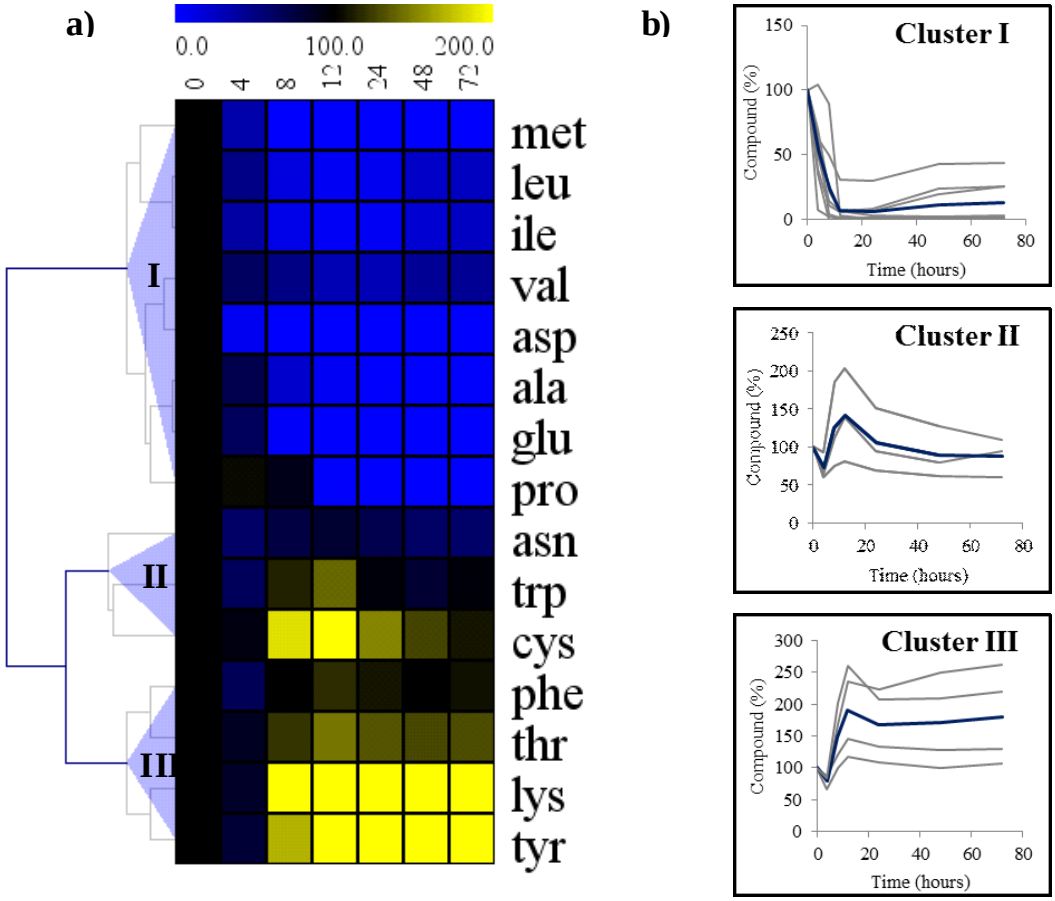

Figure 4.2. Analysis of the amino acids profiles obtained from the *H. pylori* culture. (a) Hierarchical clustering (HCL) representing in vertical the extracellular samples taken until 72 hours of growth (mean of replicates) and three amino acid clusters (horizontal clusters) that characterize the changes on the amino acid profiles in the extracellular medium, based on Kendall's Tau metrics. (b) K-Means clustering (KMC) giving the results of amino acid clusters (same groups as for HCL) based on the KMC input parameters; each individual line represents the profile of one amino acid and the blue line in the middle represents the centroid (average of all compounds) of the amino acids profile grouped in each cluster. Amino acid abbreviations: *ile* - isoleucine; *leu* - leucine; *met* - methionine; *glu* - glutamate; *ala* - alanine; *val* - valine; *asp* - aspartate; *pro* - proline; *asn* - asparagine; *trp* - tryptophan; *cys* - cysteine; *tyr* - tyrosine; *lys* - lysine; *thr* - threonine; *phe* - phenylalanine.

4.4.1.3. Results reproducibility

In order to evaluate the precision of the obtained results, the relative standard deviation expressed as a percentage (%RSD) was calculated for technical (n=3) and biological replicates (n=9) for each compound at each time point analyzed. This calculation was made after normalization of compound intensity by the internal standard intensity in each analysis.

The %RSDs observed for the detected compounds for technical replicates were in general lower than 40%. The low concentration levels for the metabolites detected can contribute for the high level of variation between technical replicates. In general, the %RSDs observed for the metabolites detected between biological replicates were in the order of 50%, with some exceptions. Taking together the %RSDs obtained for technical and biological replicates, there seems to be evidence that the variations observed in the amount of the metabolites analyzed were due to the method used rather than biological variability.

4.4.1.4. Glucose consumption and acetate formation

Glucose and acetate along time in the culture medium were analyzed using UV-kits. A significant consumption of glucose was observed during the experiments' time series ($p < 0.05$; one-way ANOVA). However, glucose was not completely consumed, remaining at almost 50% in the end culture (Figure 4.3). Formation of acetate was observed with a pronounced increase in the concentration, mainly after 12 hours of culture (Figure 4.3).

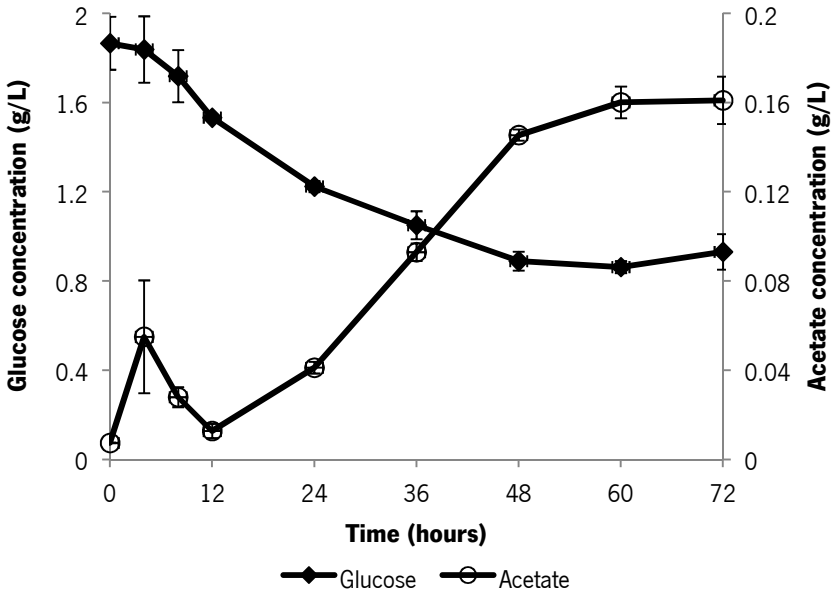

Figure 4.3. Evolution of glucose and acetate concentrations (g/L). Mean values of biological replicates (n=3), error bars represent the standard deviation.

4.4.1.5. Metabolic model simulations

With the purpose of reconciliating the *in silico* with the *in vitro H. pylori* metabolic capabilities and to collect relevant metabolic information, simulations using the *H. pylori* genome-scale metabolic model (*i*T341 GSM/GPR)[20], were performed. Flux Balance Analysis, a linear programming method, based on the steady-state assumption and the application of constraints, was applied to maximize biomass production in a wild type strain. This approach allows the analysis of the metabolic network and prediction of an organism's growth rate[25], even in absence of detailed kinetic information. The conditions tested *in silico* (environmental conditions) were based on the *in vitro* conditions used. Thus, simulations with all 20 amino acids, organic acids and glucose present in the *in vitro* medium were performed. In order to evaluate the effect of compounds individually or in group, simulations were also performed by removing one or more compounds, as well as by removing the compounds that were not consumed *in vitro*. The predicted biomass for each environmental condition tested is given in Table 4.1 and is represented as a specific

growth rate (h^{-1}) and as a percentage of the nominal value obtained with the minimum medium described[20]. It is clearly visible an increase of the predicted biomass when all the Ham's F12 ingredients are added. Moreover, in the presence of glucose, a noteworthy increase in the predicted biomass was observed. Individually, threonine and pyruvate seem to have important effects. On the other hand, other carbon sources (citrate, lactate and succinate) added to the *in silico* medium resulted in a low (lactate) or even null effect (citrate and succinate) in the predicted biomass. The *in silico* secreted metabolites were also assessed, being acetate, ammonia, carbon dioxide and succinate predicted to be secreted in all simulations. However, the secretion rates for the metabolites predicted to be excreted are not the same for all conditions tested. For instance, an increase on the ammonia flux was observed when organic acids and glucose were added to the *in silico* medium. Besides that, for the minimal medium described[20], formate and ornithine were also predicted to be excreted. The detailed flux distribution obtained for each simulation is given in supplementary material E1 (Electronic version).

Table 4.1. Results of the simulations performed with the *i*T 341 GSM/GPR model, using Flux Balance Analysis in Optflux, showing the environmental conditions tested and the biomass predicted for each simulation. Abbreviations: *cit* – citrate*; D-ala* – D-alanine; *glc* – D-glucose; *lac* – lactate; *L-ala* – L-alanine; *L-arg* – L-arginine; *L-cys* – L-cysteine; *L-his* – L-histidine; *L-ile* – L-isoleucine; *L-lys* – L-lysine; *L-met* – L-methionine; *L-phe* – L-phenylalanine; *L-thr* – L-threonine; *L-trp* – L-tryptophan; *L-tyr* – L-tyrosine; *L-val* – L-valine; *pyr* - pyruvate; *succ* – succinate.

in silico	**Components**		**Predicted biomass**	
Environmental conditions	**Amino acids**	**Other carbon sources**	**(h^{-1})**	**%**
1*	L-ala, D-ala, L-arg, L-his, L-ile, L-met, L-val	-	0.693	100
2	all 20	glc, pyr	1.568	226
3	all 20	glc, pyr, cit, lac, succ	1.593	230
4	all 20	glc, pyr, lac, succ	1.593	230
5	all 20	glc, pyr, cit, succ	1.568	226
6	all 20	glc, pyr, cit, lac	1.593	230
7	all 20	glc, cit, lac, succ	1.493	216
8	all 20	pyr, cit, lac, succ	1.299	187
9	all, except L-cys	glc, pyr, cit, lac, succ	1.593	230
10	all, except L-trp	glc, pyr, cit, lac, succ	1.588	229
11	all, except L-tyr	glc, pyr, cit, lac, succ	1.586	229
12	all, except L-phe	glc, pyr, cit, lac, succ	1.586	229
13	all, except L-thr	glc, pyr, cit, lac, succ	1.286	186
14	all, except L-lys	glc, pyr, cit, lac, succ	1.581	228
15	all, except L-cys, L-lys, L-thr, L-trp, L-tyr, L-phe	glc, pyr, cit, lac, succ	1.261	182
16	all, except L-cys, L-lys, L-thr, L-trp, L-tyr, L-phe	pyr, cit, lac, succ	0.963	139

* Simulation performed with the minimal medium described by Thiele *et al.* (2005)[20].

4.5. *Discussion*

4.5.1. Exometabolome analysis

The characterization of microbial phenotypes is of major importance in understanding cell's metabolism, and the analysis of the extracellular metabolome can help in that characterization, since the level and the variety of the secreted metabolites are associated with the metabolic state of the cell[26]. The metabolites detected in the extracellular medium can represent metabolites secreted/excreted by the cells or metabolites present in the culture medium that were not completely depleted. The detection and quantification of the compounds present in the extracellular medium can thus aid in the identification of nutritional requirements and contribute to rationally adjust the components of the culture medium.

4.5.1.1. Organic acids analysis

Some organic acids (citrate, lactate and succinate) that were detected in blank samples (without cells), had not been described as part of the composition of the defined culture medium used (Ham's F-12). Pyruvate was also detected, but it is present in Ham's F-12 medium. Since the culture medium was supplemented with Fetal Bovine Serum (FBS), the aforementioned acids might have been present in FBS. FBS is considered an undefined component and is almost uncharacterized, although some components have been identified, such as protein components, hormones, growth factors and cytokines, fatty acids and lipids, vitamins and trace elements, carbohydrates and non-protein nitrogens[27,28]. The presence of some organic acids, such as malate, fumarate and succinate in fetal bovine serum was also reported[29].

The evolution of pyruvate, citrate, lactate and succinate (Figure 4.1) shows that all organic acids were totally or partly consumed. After the end of the exponential phase (8h), pyruvate and lactate had been almost fully depleted, whilst the consumption of citrate and succinate was slower and only partial. A 3-fold increase in the succinate concentration at

4h of culture was observed (Figure 4.1) and it can be interpreted as this compound might be a metabolic by-product of amino acids and pyruvate catabolism[30,31]. The consumption of pyruvate, D-lactate and succinate by *H. pylori*, had also been reported; nevertheless, these compounds were reported as not being the preferred carbon sources[30], which could not be confirmed in the present study, at least for lactate and pyruvate. However, another experiment was performed with an increased concentration of organic acids in the culture medium, but that did not lead to a pronounced increase in growth (data not shown).

Regarding the consumption of pyruvate, published studies have reported that acetate is the main product when pyruvate is metabolized by *H. pylori* under aerobic conditions, whereas acetate, lactate and ethanol were detected when *H. pylori* cells where submitted to anaerobic conditions with labeled pyruvate[7,31]. Under microaerophilic conditions, Mendz *et al.* (1994) observed the formation of lactate, acetate, formate, succinate and alanine from pyruvate[32] Ethanol and formate were not detected in the present study (ethanol analyzed by liquid chromatography, data not shown).

4.5.1.2. Glucose consumption and acetate formation

In the present study, glucose was partially consumed, as previously reported by other authors[6] (Figure 4.3). Some studies stated that glucose can be utilized by *H. pylori*, since the penthose phosphate and the Entner-Doudoroff pathways have been identified[33,34]. In addition, a glucose transporter was identified in *H. pylori*[35,36] and further confirmed by the genomic sequence[37]. In the present study, glucose consumption occurs until 48 hours of growth, but with a more pronounced consumption after 12 hours of culture, matching with the depletion of some amino acids, such as alanine, proline, aspartate and glutamate. This result suggests that glucose is not the preferred carbon and energy source and is in agreement with the conclusions taken by other authors, that also reported that in the presence of amino acids, glucose was not consumed until the amino acids were exhausted[6,31] and therefore could be removed from the culture medium[9]. It is also worth mentioning that most of the glucose consumed (50%) did not contribute significantly for growth, as cells stopped growing at around 8 hours of cultivation, when glucose

consumption had only just started. The presence of acetate in the extracellular medium was observed, specially between 12 and 48 hours of growth, in agreement with the decrease of glucose in the culture medium, indicating that glucose might be contributing to acetate production, as described by other authors[7], although the amounts of acetate accumulated are quite low compared with the levels of glucose consumed.

4.5.1.3. Amino acids analysis

Amino acids have been described as potential sources of carbon, nitrogen and energy in *H. pylori*[1]. There are several studies describing the *in vitro* amino acid requirements for *H. pylori.* Some of published studies are based on essentiality analysis by the evaluation of growth when a given amino acid is present or not in the culture medium[1–3]. Other studies are based on consumption[4,9,38], measuring the concentration of a given amino acid by analytical methods. In addition, the *in silico* amino acids requirements were also described[19,20]. It is important to highlight that environmental cultivation conditions, culture media and the strains used in published studies are not standardized, and the essentiality of a compound could be related to the mentioned factors, hampering results comparison, and making difficult to conclude about the amino acid requirements for *H. pylori* growth. There is an extra difficulty in the evaluation and comparison of the results obtained in different studies, since the analytical procedures are not uniform and sometimes the results presented are not sufficiently clear to conclude about a specific compound consumption and/or essentiality. Table 4.2 summarizes the results obtained in the aforementioned studies, together with the results obtained in the present study. In order to facilitate the comparison and interpretation, an attempt of standardization was made. The term “essential” was used to refer amino acids that are required for *H. pylori* growth, with no growth in the absence of that specific compound. Additionally, the term “preferential” is applied when a given amino acid is not absolutely required for growth but, when present, it is preferable and firstly consumed. In studies where it was not possible to conclude about the essentiality or preferences, the amino acids were classified as “consumed”, “not consumed” or “accumulated”. The term “no consensus” was applied

when the published studies are contradictory, and it is not possible to conclude about essentiality or consumption.

Table 4.2. Comparison of amino acids essentiality (*in vitro* and *in silico*), or consumption reported in the published studies for *H. pylori* and results of the present study.

Amino acids	*in vitro* essentiality[a]	*in silico* essentiality[b]	*in vitro* consumption[c]	This study
Glycine	Not essential[1]	Not essential	No consensus	Not detected
L - Alanine	Essential[1]	Essential	Consumed	**Consumed, not essential**
L - Asparagine	Not essential	Not essential	Consumed	Consumed
L - Aspartate	Not essential[1]	Not essential	Consumed	Consumed
L - Arginine	Essential	Essential	Consumed	Not analyzed
L - Cysteine	No consensus	Not essential	Consumed	**Not consumed, not essential**
L - Glutamate	Not essential[1]	Not essential	Consumed	Consumed
L - Glutamine	Not essential	Not essential	Consumed	Not detected
L - Histidine	Essential	Essential	Consumed	Not analyzed
L - Isoleucine	No consensus	Essential	Consumed	**Consumed, essential**
L - Leucine	Essential	Essential	Consumed	Consumed
L - Lysine	Not essential[1]	Not essential	No consensus	**Accumulated, not essential**
L - Methionine	Essential	Essential	Consumed	Consumed
L - Phenylalanine	Essential	Not essential	Consumed[2]	**Not consumed,essential**
L – Proline	Essential[1]	Not essential	Consumed	Consumed
L – Serine	Not essential[1]	Not essential	Consumed	Not detected
L – Threonine	Not essential[1]	Not essential	No consensus	**Not consumed, Not essential**
L – Tryptophan	Not essential[1]	Not essential	No information	**Not consumed, not essential**
L – Tyrosine	Not essential[1]	Not essential	No consensus	**Accumulated, not essential**
L – Valine	Essential	Essential	Consumed	Consumed

[a]The essentiality was based on the growth results when amino acids were present or absent[1–3]. [b] Based on the existing genome-scale metabolic models[19,20]. [c]Based on measurement of amino acids consumption in *in vitro* studies[4,9,38]. [1]For most of the strains analyzed; [2]Very low percentage of consumption.

i. Essential Amino acids

There is a general consensus about some amino acids requirements: L-arginine, L- histidine, L-leucine, L-methionine and L-valine, results corroborated with the present study. In fact, for those reported amino acids there are no biosynthetic capabilities described in *H. pylori* [31,39].

ii. Non-essential Amino acids

Preferential

Asparagine, aspartate, glutamine and glutamate were consumed in the present study, results in accordance with other studies[4,9,38]. There is a general consensus about the non-essentiality of these amino acids, with no auxotrophies having been identified, and with biosynthetic capabilities being predicted from the genomic sequence[39]. In fact, aspartate and glutamate were completed consumed in this study, being aspartate the first amino acid to be completely depleted from the extracellular medium. Asparagine was not completely consumed, 60% of the initial amount remaining at the end of the culture. The deamination of asparagine and glutamine was reported[38], yielding ammonia and aspartate or glutamate, respectively. The incorporation of asparagine and glutamine was proved to be via indirect pathways, with the deamination reactions taking place in the periplasm[40]. These amino acids can serve as carbon sources and it has also been speculated that the role of this type of incorporation is not only for nutrient acquisition but could also be associated with *H. pylori*'s pathogenesis[40,41]. The production of ammonia and fumarate in the presence of aspartate, due to the aspartase activity was also described[9], although fumarate was not detected in the extracellular medium in this study.

Based on the hypothesis that amino acids which were completely consumed (L-alanine, L- aspartate, L-glutamate, L-methionine and L-proline) could be growth limiting, these amino acids were added to the medium (Ham's F-12) at a concentration tenfold higher, but such change did not increase *H. pylori*'s growth (data not shown). Interestingly, the same result was not obtained when all amino acids were increased tenfold, resulting in a threefold increment in growth. This result is contradictory with the one reported by

Testerman *et al.* (2006), that verified that a twofold increase in the amino acids concentration in Ham's F-12 had no effect in *H. pylori*'s growth[3].

Non-preferential

There is a general consensus between *in vitro* and *in silico* studies (Table 4.2) regarding dispensability of L-lysine, L-serine, L- threonine, L-tryptophan and L- tyrosine in the culture medium. This study corroborates that information, with the exception of L-serine, which was not detected. These results are in accordance with the predicted biosynthetic abilities based on the genome sequence information[39] and on the genome annotation[42]. However, some studies reported requirements or the consumption of lysine, threonine, tyrosine and tryptophan for some *H. pylori* strains[1,2,4,9]. Lysine and tyrosine, in the present study, were accumulated in the extracellular medium at the end of the culture, suggesting that these amino acids are not being used as carbon sources.

iii. Non-consensus Amino acids

Regarding the essentiality of proline, the *in vitro* and *in silico* information are contradictory, as this amino acid was deemed as essential in most *in vitro* studies whilst it was classified as not essential in *in silico* studies. However, according to published studies, this compound is not needed for the growth of some strains [1,2]. In the present study proline was completely depleted from the culture medium after 12 hours of culture, indicating that it is either essential or can be a preferential substrate for *H. pylori*'s growth. Looking at the metabolic pathways in which proline could be biosynthesized, there are two possibilities, the first one from glutamate (via L-glutamate 5-semialdehyde synthesis), and the second one from arginine (via urea cycle, with production of ornithine and subsequent production of L-glutamate 5-semialdehyde). While for the first alternative all the genes have been identified in *H. pylori* (HP0056 and HP1158), for the second case the gene associated with the conversion of L-ornithine to L-glutamate 5-semialdehyde, so far, was not proved as present in *H. pylori*, which indicates that proline synthesis might be achieved from glutamate.

Isoleucine is another amino acid for which there is no consensus about its requirement for *H. pylori* growth. Some studies referred the essentiality of isoleucine, but other studies reported that isoleucine is not essential, although the addition of this compound together with tryptophan enhances growth, without any effect when added alone[3]. In the present study, isoleucine was partially consumed. In order to evaluate its essentiality, isoleucine was removed from the culture medium and no growth was observed in the absence of this amino acid. Like leucine and valine, for which there are missing enzymes in the biosynthetic pathways, *H. pylori* is not able to synthesize isoleucine as well, owing to similar constraints[31,39].

Regarding the essentiality of cysteine, different studies lead to different conclusions. Some authors conclude that cysteine is required to grow *H. pylori* in specific conditions (serum absence)[3] or that it is needed for some strains[1], whilst other authors conclude that cysteine is not required at all[2]. Regarding *in silico* models[19,20], both studies concluded that cysteine is not essential for *H. pylori*'s growth if another source of sulfur is present. The sulfur source utilized by *H. pylori* can be methionine[20] or sulfide, as it is unable to use sulphate as a source of inorganic sulfur[39]. In the present study cysteine was not consumed, and since methionine was present in the culture medium, this might have enabled the network to synthesize other sulfur-containing compounds.

Based on the obtained results, the amino acids that were not consumed (L-cysteine, L-lysine, L- phenylalanine, L- treonine, L-tryptophan and L-tyrosine) were removed from the culture medium, one by one. However, *H. pylori* was not able to grow in media without L-phenylalanine, indicating that this amino acid is essential. Indeed, in the present study, phenylalanine is consumed in a very small amount, and consumption is masked by the method's precision (20% RSD in the case of phenylalanine). Other studies also reported the non-exhaustion of phenylalanine from de extracellular medium[9,38]. Analyzing the minimal *in silico* medium[20], phenylalanine was not deemed as essential. *In silico*, the biosynthesis of phenylalanine is made via the shikimate pathway with D-erythrose 4-phosphate as precursor, with sequential formation of prephenate from chorismate (genes identified in *H. pylori*). However, the enzymatic conversion of prephenate in phenylpyruvate (precursor of phenylalanine) is not proven, since the domain of prephenate dehydratase in

the PheA protein in *H. pylori* is missing[20,42]. Nevertheless, it is reported that prephenate can be converted spontaneously into phenylpyruvate[42]. The need of phenylalanine in some studies, according to some authors, can thus be due to experimental growth conditions, although these conditions have not been reported[20,42].

Although having been considered essential at least for some strains, L-alanine has been totally consumed, which is in accordance with data in the online[43]. An experiment was thus performed where alanine has been removed from the medium and growth was still verified. Thus, alanine essentiality was questioned and it has been removed from the set of essential amino acids in *H. pylori* in this work.

For some amino acids, which were not detected or not analyzed, it was not possible to conclude about their roles. These compounds include arginine, glutamine, glycine, histidine and serine. Nevertheless, arginine and histidine auxotrophies have been reported and are in agreement with the genomic sequence[31,39]. The dispensability of glycine, serine and glutamine was also proved, being glutamine and serine possible carbon sources for *H. pylori*'s growth.

In Figure 4.4, the main *H. pylori*'s metabolic pathways are outlined, giving an overview of the central metabolism together with profiles of the metabolites analyzed in the present work.

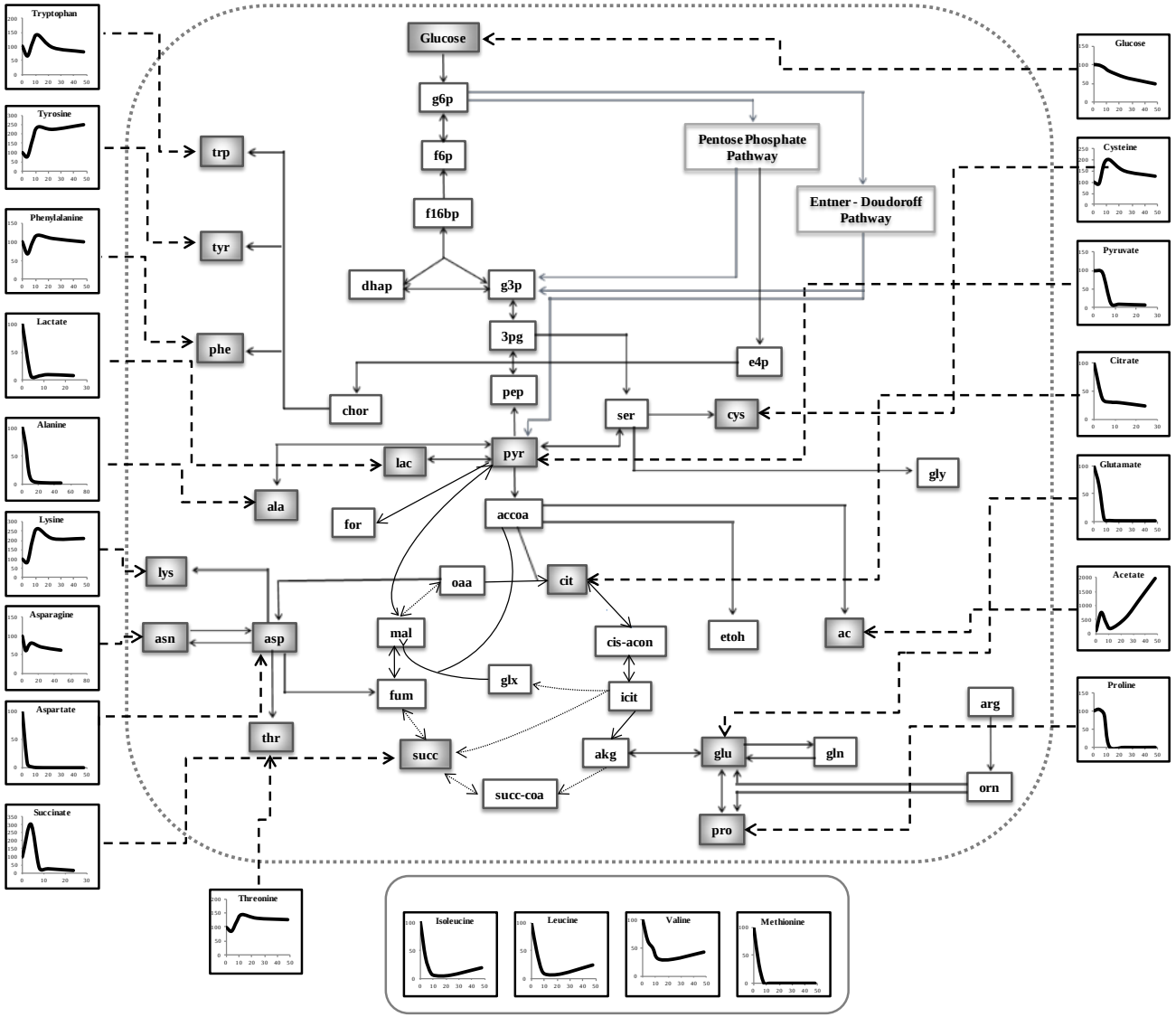
Tryptophan
Tyrosine
Phenylalanine
Lactate
Alanine
Lysine
Asparagine
Aspartate
Succinate
Threonine
Glucose
g6p
f6p
f16bp
dhap
g3p
3pg
pep
e4p
Pentose Phosphate Pathway
Entner - Doudoroff Pathway
trp
tyr
phe
chor
ser
cys
lac
pyr
gly
ala
for
accoa
lys
oaa
cit
asn
asp
mal
cis-acon
etoh
ac
glx
icit
fum
arg
thr
succ
akg
glu
gln
succ-coa
orn
pro
Isoleucine
Leucine
Valine
Methionine
Glucose
Cysteine
Pyruvate
Citrate
Glutamate
Acetate
Proline

Metabolite Abbreviations					
3pg	3-phosphoglycerate	etoh	ethanol	met	methionine
ac	acetate	f16bp	fructose-1,6-biphosphate	oaa	oxaloacetate
accoa	acetyl-coa	f6p	fructose-6-phosphate	orn	ornithine
akg	alpha-ketoglutarate	for	formate	pep	phosphoenolpyruvate
ala	alanine	fum	fumarate	phe	phenylalanine
arg	arginine	g3p	glyceraldehyde-3-phosphate	pro	proline
asn	asparagine	g6p	glyceraldehyde-6-phosphate	pyr	pyruvate
asp	aspartate	gln	glutamine	ser	serine
chor	chorismate	glu	glutamate	succ	succinate
cys	cysteine	gly	glycine	succ-coa	succinyl-coa
cit	citrate	icit	isocitrate	thr	threonine
cis-acon	cis-aconitate	ile	isoleucine	trp	tryptophan
dhap	dihydroxyacetone phosphate	lac	lactate	tyr	tyrosine
e4p	erythrose-4-phosphate	leu	leucine	val	valine

Figure 4.4. Schematic diagram of *H. pylori*'s metabolic map, and metabolites evolution analyzed in the extracellular medium during the culture. The metabolites highlighted in grey boxes were the ones analyzed in the present study, for which the profile is also displayed (connected with dashed lines). White boxes represent metabolites that were not detected in this study but which are known to be part of *H. pylori*'s metabolism. The profile of the metabolites that were analyzed for which no complete pathways are identified in *H. pylori*, such as methionine, isoleucine, leucine and valine, are shown in a separate box, disconnected from the map.

4.5.2. Metabolic model simulations

The simulations performed using the most updated genome scale metabolic model[20] were based on the environmental conditions used *in vitro*. The output of each simulation performed was the predicted biomass (h^{-1}) and the secreted metabolites (Table 4.1 and suplementary material E1 (electronic version)).Concerning the performed simulations, a twofold increment in the predicted biomass was observed when the Ham's F-12 medium used was simulated, comparing with the conditions provided by the model (*in silico* minimal medium) (Table 4.1 simulation 2). Even though the addition of some organic acids (citrate, lactate and succinate) (simulations 3-6) to the *in silico* simulations did not lead to an increase in the predicted biomass, the effect of organic acids was observed in the *in silico* excreted metabolites, increasing the excretion of acetate. When pyruvate was removed from the *in silico* environmental conditions, a slight decrease in biomass was observed (simulation 7), showing that pyruvate has an effect on *in silico H. pylori*'s growth and is being used as a carbon and energy source, as opposed to the other organic acids tested. The existence of a mixed-acid fermentation pathway in *H. pylori* was proved *in vitro*, with accumulation of acetate and formate as metabolic products from pyruvate[32]. The succinate formation from pyruvate was also reported *in vitro*, suggesting the incorporation of the carbon derived from pyruvate into the Krebs cycle[32]. An increase in acetate and succinate production was also predicted when pyruvate is present on *in silico* medium (simulation 7 compared with simulation 3).

Additionally, when glucose was removed from the *in silico* environmental conditions (simulation 8) a decrease in the biomass was observed. In fact, as previously discussed, glucose is not preferred or required for *H. pylori*'s growth, but in the metabolic model glucose is being used when present in culture medium. An increase of *in silico* acetate excretion was also observed in the presence of glucose. Additionally, lactate and glucose are contributing to the *in silico* succinate formation.

When the amino acids that were not *in vitro* consumed (cysteine, tryptophan, tyrosine, phenylalanine, threonine and lysine) were individually removed from environmental conditions (simulations 8-14), no difference in the predicted biomass was

observed, with the exception of threonine. When the aforementioned amino acids were removed from the *in vitro* medium, no effect on the growth was observed as well, with the exception of phenylalanine, which showed to be essential for *H. pylori* under the *in vitro* used conditions, as already discussed. Furthermore, when those amino acids were removed together from the environmental conditions (simulation 15), a remarkable decrease on the predicted biomass was observed, becoming more pronounced when glucose is also removed (simulation 16) from the *in silico* medium.

As outlined by other authors, amino acids are important sources of carbon and nitrogen for *H. pylori*. The main metabolic products reported from amino acids consumption are acetate, formate, succinate and lactate[31], although in the performed *in silico* simulations lactate was not secreted into the culture medium, and formate was only secreted with the minimal medium suggested by Thiele *et al.* (2006)[20]. In present study, formate was not detected in the extracellular medium, while lactate, although being detected, it is not possible to conclude if was or not secreted, since it was present in the culture medium. Acetate and succinate were detected, with a 3-fold increase of succinate in the extracellular medium observed at 4 hours of culture, which can be related to amino acids and pyruvate consumption and the incorporation of carbon into the Krebs cycle.

Taking together the *in vitro* and *in silico* results it can be inferred that amino acids are being used as the preferred carbon sources, while organic acids are being consumed but are not preferential.

In addition, when the *in silico* prediction for biomass maximization using Ham's F-12 medium (simulation 2) is compared with *in vitro* obtained results, the predicted biomass (μ=1.593 h^{-1}) is far from the biomass achieved *in vitro* (μ=0.163 h^{-1}). Thereby, an adjustment of the existing genomic scale metabolic model is needed to minimize the differences between the *in silico* predictions and *in vitro* results.

4.6. *Conclusions*

In the present study, the suggestion made by other authors concerning the non-preference of glucose as a carbon source by *H. pylori* was corroborated. According to the obtained results and previous studies, some aminoacids are absolutely required, namely, L-arginine, L- histidine, L-isoleucine, L-leucine, L-methionine L-phenylalanine and L-valine. Some aminoacids for which there was no consensus between *in vitro* or *in silico* data, such as phenylalanine and isoleucine, were proved to be essential for *H. pylori* 26695 growing under the conditions used. Regarding preferences and possible carbon sources, aspartate, glutamate, proline and alanine are potentially preferred by *H. pylori*, since they were completely consumed in the mentioned order. Organic acids were not the preferred carbon sources, and, among the identified compounds, pyruvate seems to be the preferred one.

The present work provides a review on the existing experimental data about amino acids requirements and makes a comparison with *in silico* data, revealing discrepancies between *in vitro* and *in silico* predicted metabolic capabilities. At the same time, as far as we know, this is the first metabolomics approach applied to *H. pylori* growing *in vitro* under optimized environmental culture conditions and with metabolite analysis along time, revealing the metabolic behavior along the different growth phases. It is also important to highlight that the present *in vitro* results were obtained without strain adaptation to the culture medium, with fetal bovine serum. Moreover, some of the identified discrepancies among *in vitro* results could be related with the strains used, culture conditions or even the experimental procedures used. The data presented here will be very useful to adjust and rationalize the culture medium in order to obtain a more defined medium, that could be used to validate a genome-scale metabolic model reconstruction.

4.7. *References*

1. Nedenskov, P. Nutritional requirements for growth of *Helicobacter pylori*. *Appl. Environ. Microbiol.* **60,** 3450–3453 (1994).
2. Reynolds, D. J. & Penn, C. W. Characteristics of *Helicobacter pylori* growth in a defined medium and determination of its amino acid requirements. *Microbiology* **140,** 2649–2956 (1994).
3. Testerman, T. L., Conn, P. B., Mobley, H. L. T. & McGee, D. J. Nutritional requirements and antibiotic resistance patterns of *Helicobacter* species in chemically defined media. *J. Clin. Microbiol.* **44,** 1650–1658 (2006).
4. Vartanova, N. O., Arzumanyan, V. G., Serdyuk, O. A. & Temper, R. M. Creation of a New Synthetic Medium for Culturing *Helicobacter Pylori*. *Bull. Exp. Biol. Med.* **139,** 580–584 (2005).
5. Douraghi, M. *et al.* Comparative evaluation of three supplements for *Helicobacter pylori* growth in liquid culture. *Curr. Microbiol.* **60,** 254–262 (2010).
6. Mendz, G. L., Hazell, S. L. & Burns, B. P. Glucose utilization and lactate production by *Helicobacter pylori*. *J. Gen. Microbiol.* **139,** 3023–3028 (1993).
7. Chalk, P. A., Roberts, A. D. & Blows, W. M. Metabolism of pyruvate and glucose by intact cells of *Helicobacter pylori* studied by 13C NMR spectroscopy. *Microbiology* **140,** 2085–2092 (1994).
8. Kelly, D. J. The physiology and metabolism of *Campylobacter jejuni* and *Helicobacter pylori*. *J. Appl. Microbiol. Symp. Suppl.* **90,** 16S–24S (2001).
9. Mendz, G. L. & Hazell, S. L. Aminoacid Utilization by *Helicobacter pylori*. *Int. J. Biochem. Cell Biol.* **27,** 1085–1093 (1995).
10. Nielsen, J. in *Metabolome Anal. - An Introd.* (Villas-Bôas, S. G., Roessner, U., Hansen, M. A. E., Smedsgaard, J. & Nielsen, J.) 310 (John Wiley & Sons, Inc, 2007).
11. Oliver, S. G., Winson, M. K., Kell, D. B. & Baganz, F. Systematic functional analysis of the yeast genome. *Trends Biotechnol.* **16,** 373–378 (1998).
12. Nielsen, J. & Oliver, S. The next wave in metabolome analysis. *Trends Biotechnol.* **23,** 544–6 (2005).

13. Carneiro, S., Villas-bôas, S. G., Rocha, I. & Ferreira, E. C. Applying a metabolic footprinting approach to characterize the impact of the recombinant protein production in *Escherichia coli*. *Adv. Bioinformatics* **AISC 74,** 193–200 (2010).

14. Mo, M. L., Palsson, B. O. & Herrgård, M. J. Connecting extracellular metabolomic measurements to intracellular flux states in yeast. *BMC Syst. Biol.* **3,** 1–17 (2009).

15. Kell, D. B. *et al.* Metabolic footprinting and Systems Biology: The medium is the message. *Nat. Rev. Microbiol.* 1–9 (2005). doi:10.1038/nrmicro1177

16. Rocha, I., Förster, J. & Nielsen, J. in *Methods Mol. Biol. vol. 416 Gene Essentiality* (Gerdes, S. Y. & Osterman, A. L.) **416,** 409–433 (Humana Press Inc., 2007).

17. Durot, M., Bourguignon, P.-Y. & Schachter, V. Genome-scale models of bacterial metabolism: reconstruction and applications. *FEMS Microbiol. Rev.* **33,** 164–190 (2009).

18. Rocha, I. *et al.* OptFlux: an open-source software platform for *in silico* metabolic engineering. *BMC Syst. Biol.* **4,** 1–12 (2010).

19. Schilling, C. H. *et al.* Genome-scale metabolic model of *Helicobacter pylori 26695*. *J. Bacteriol.* **184,** 4582–4593 (2002).

20. Thiele, I., Vo, T. D., Price, N. D. & Palsson, B. Ø. Expanded Metabolic Reconstruction of *Helicobacter pylori* (iIT341 GSM / GPR): an *In Silico* Genome-Scale Characterization of Single- and Double-Deletion Mutants. *J. Bacteriol.* **187,** 5818–5830 (2005).

21. Testerman, T. L., Gee, D. J. M. C. & Mobley, H. L. T. *Helicobacter pylori* growth and urease detection in the chemically defined medium Ham ' s F-12 nutrient mixture. *J. Clin. Microbiol.* **39,** 3842–3850 (2001).

22. Bessa, L. J., Correia, D. M., Cellini, L., Azevedo, N. F. & Rocha, I. Optimization of culture conditions to improve *Helicobacter pylori* growth in Ham's F-12 medium by response surface methodology. *Int. J. Immunopathol. Pharmacol.* **25,** 901–909 (2012).

23. Smart, K. F., Aggio, R. B. M., Van Houtte, J. R. & Villas-Bôas, S. G. Analytical platform for metabolome analysis of microbial cells using methyl chloroformate derivatization followed by gas chromatography-mass spectrometry. *Nat. Protoc.* **5,** 1709–1729 (2010).

24. Saeed, A. I. *et al.* TM4: a free, open-source system for microarray data management and analysis. *Biotechniques* **34,** 374–378 (2003).

25. Orth, J. D., Thiele, I. & Palsson, B. Ø. What is flux balance analysis? *Nat. Biotechnol.* **28,** 245–248 (2011).

26. Carneiro, S., Villas-Bôas, S. G., Ferreira, E. C. & Rocha, I. Metabolic footprint analysis of recombinant *Escherichia coli* strains during fed-batch fermentations. *Mol. Biosyst.* **7,** 899–910 (2011).

27. Baker, H., De Angelis, B. & Frank, O. Vitamins and other metabolites in various sera commonly used for cell culturing. *Experientia* **44,** 1007–1010 (1988).

28. Brunner, D. *et al.* Serum-free cell culture: the serum-free media interactive online database. *ALTEX* **27,** 53–62 (2010).

29. Koek, M. M. *et al.* Metabolic profiling of ultrasmall sample volumes with GC/MS: from microliter to nanoliter samples. *Anal. Chem.* **82,** 156–162 (2010).

30. Chang, H. T. *et al.* Kinetics of substrate oxidation by whole cells and cell membranes of *Helicobacter pylori*. *FEMS Microbiol. Lett.* **129,** 33–38 (1995).

31. Marais, A., Mendz, G. L., Hazell, S. L. & Mégraud, F. Metabolism and genetics of *Helicobacter pylori*: the genome era. *Microbiol. Mol. Biol. Rev.* **63,** 642–674 (1999).

32. Mendz, G. L., Hazell, S. L. & van Gorkom, L. Pyruvate metabolism in *Helicobacter pylori*. *Arch. Microbiol.* **162,** 187–192 (1994).

33. Mendz, G. L. & Hazell, S. L. Evidence for a pentose phosphate pathway in *Helicobacter pylori*. *FEMS Microbiol. Lett.* **84,** 331–336 (1991).

34. Mendz, G. L., Hazell, S. L. & Burns, B. P. The Entner-Doudoroff pathway in *Helicobacter pylori*. *Arch. Biochem. Biophys.* **312,** 349–356 (1994).

35. Mendz, G. L., Burns, B. P. & Hazell, S. L. Characterisation of glucose transport in *Helicobacter pylori*. *Biochim. Biophys. Acta* **1244,** 269–276 (1995).

36. Psakis, G. *et al.* The sodium-dependent D-glucose transport protein of *Helicobacter pylori*. *Mol. Microbiol.* **71,** 391–403 (2009).

37. Tomb, J.-F. *et al.* The complete genome sequence of the gastric pathogen *Helicobacter pylori*. *Nature* **388,** 539–547 (1997).

38. Stark, R. M., Suleiman, M. S., Hassan, I. J., Greenman, J. & Millar, M. R. Amino acid utilisation and deamination of glutamine and asparagine by *Helicobacter pylori*. *J. Med. Microbiol.* **46,** 793–800 (1997).

39. Doig, P. *et al. Helicobacter pylori* physiology predicted from genomic comparison of two strains. *Microbiol. Mol. Biol. Rev.* **63,** 675–707 (1999).

40. Leduc, D., Gallaud, J., Stingl, K. & Reuse, H. De. Coupled amino acid deamidase-transport systems essential for *Helicobacter pylori* colonization. *Infect. Imunity* **78,** 2782–2792 (2010).

41. Shibayama, K. *et al.* Metabolism of glutamine and glutathione via g-glutamyltranspeptidase and glutamate transport in *Helicobacter pylori*: possible significance in the pathophysiology of the organism. *Mol. Microbiol.* **64,** 396–406 (2007).

42. Boneca, I. G. A revised annotation and comparative analysis of *Helicobacter pylori* genomes. *Nucleic Acids Res.* **31,** 1704–1714 (2003).

43. Caspi, R. *et al.* The MetaCyc database of metabolic pathways and enzymes and the BioCyc collection of pathway/genome databases. *Nucleic Acids Res.* **40,** D742–D753 (2012).

4.8. *Supplementary material*

4.8.1. Supplementary material 1

Table 4.3. Composition of the Ham's F-12 medium

Compounds	Molecular weight (g/mol)	Concentration (mM)
Amino acids		
Glycine	75.07	0.10
L-alanine	89.09	0.10
L-arginine hydrochloride	211.00	1.0
L-asparagine	132.12	0.098
L-aspartate	133.10	0.10
L-cysteine hydrochloride	157.62	0.23
L-glutamate	147.13	0.10
L-glutamine	146.15	1.0
L-histidine hydrochloride	209.63	0.10
L-isoleucine	131.18	0.030
L-leucine	131.18	0.10
L-lysine hydrochloride	182.65	0.20
L-methionine	149.21	0.030
L-phenylalanine	165.19	0.030
L-proline	115.13	0.30
L-serine	105.09	0.10
L-threonine	119.12	0.10
L-tryptophan	204.23	0.010
L-tyrosine	181.19	0.030
L-valine	117.15	0.10

Table 4.3. Composition of the Ham's F-12 medium. (Continue)

Compounds	Molecular weight (g/mol)	Concentration (mM)
Vitamins		
Biotin	244.31	0.000030
Choline chloride	139.62	0.10
D- Calcium panthotenate	476.54	0.0010
Niacinamide	122.13	0.00030
Pyridoxine hydrochloride	205.64	0.00030
Riboflavin	376.37	0.000098
Thiamine hydrochloride	337.27	0.00089
Vitamin B12	1355.00	0.0010
i-inositol	180.16	0.10
Folic acid	441.41	0.0030
Inorganic Salts		
Calcium chloride ($CaCl_2.2H_2O$)	147.02	0.30
Cupric sulphate ($CuSO_4.5H_2O$)	249.69	0.000010
Iron sulphate ($FeSO_4.7H_2O$)	278.02	0.0030
Zinc sulphate ($ZnSO_4.7H_2O$)	287.54	0.0030
Potassium chloride (KCl)	74.56	2.98
Magnesium chloride ($MgCl_2.6H_2O$)	203.30	0.601
Sodium bicarbonate ($NaHCO_3$)	84.01	14
Sodium chloride (NaCl)	58.44	131
Sodium phosphate dibasic (Na_2HPO_4)	177.99	1.0
Other components		
Thymidine	194.00	0.0030
Putrescine	88.15	0.0010
Linoleic acid	280.00	0.00030
Lipoic acid	206.33	0.0010
Phenol red	354.38	0.0030
Hypoxanthine	136.11	0.029
Sodium pyruvate	110.04	1.0
D-glucose	180.00	10

4.8.2. Supplementary material 2

Table 4.4 lists the compounds used as standards for GC-MS analysis.

Table 4.4. Compounds used to prepare the standards for GC-MS analysis.

Compound	Chemical Formula	M.W. (g/mol)	Purity (%)	Company
Organic Acids				
α-Ketoglutaric acid	$C_5H_6O_5$	146.10	>99.0	Fluka
Adipic acid	$C_6H_{10}O_4$	146.14	>99.5	Fluka
Citraconic acid	$C_5H_6O_4$	130.10	>99.0	ACROS Organics
Citric acid	$C_6H_8O_7$	192.12	>99.5	Sigma-Aldrich
Fumaric acid	$C_4H_4O_4$	116.07	>99.0	ACROS Organics
Glyoxylic acid monohydrate	$C_2H_6O_3.H_2O$	92.05	>98.0	Aldrich
Itaconic acid	$C_5H_6O_4$	130.10	>99.0	ACROS Organics
D-Lactate sodium	$C_3H_5NaO_3$	112.06	>99.0	Aldrich
Oxaloacetic acid	$C_4H_4O_5$	132.07	>98.0	Sigma
2-oxodipic acid	$C_6H_8O_5$	160.12	>97.0	Sigma
Pyruvic acid	C3H4O3	88.06	98.0	ACROS Organics
Succinic acid	$C_4H_6O_4$	118.09	>99.0	Sigma-Aldrich
DL-Isocitric acid trisodium salt	$C_6H_5Na_3O_7$	258.07	17.9% H_2O; 98.0%	Sigma
DL-Malic acid	$C_4H_6O_5$	134.09	>98.0	Aldrich

Table 4.4. Compounds used to prepare the standards for GC-MS analysis. (Continue)

Compound	Chemical Formula	M.W. (g/mol)	Purity (%)	Company
Amino Acids				
Glycine	$C_2H_5NO_2$	75.07	>99.0%	Biochemika. Fluka
L-Aspartic acid	$C_4H_7NO_4$	133.10	>99.0%	Sigma-Ultra. Sigma
L-Glutamic acid	$C_5H_9NO_4$	147.13	>99.0%	Sigma
L-Alanine	$C_3H_7NO_2$	89.09	>99.5%	BioUltra. Fluka
L-Arginine	$C_6H_{14}N_4O_2$	174.20	>99.5%	Biochemika. Fluka
L-Asparagine anhydrous	$C_4H_8N_2O_3$	132.12	>99.5%	BioUltra. Sigma
L-Cysteine hydrochloride anhydrous	$C_3H_7NO_2.S.HCl$	157.62	>99.0%	Fluka Analytical
L-Phenylalanine	$C_9H_{14}NO_2$	165.19	>99.0%	Biochemika. Fluka
L-Glutamine	$C_5H_{10}N_2O_3$	146.15	>99.0%	Sigma
L-Histidine	$C_6H_9N_3O_2$	155.16	>99.5%	Biochemika. Fluka
L-Isoleucine	$C_6H_{13}NO_2$	131.18	>99.5%	Biochemika. Fluka
L-Leucine	$C_6H_{13}NO_2$	131.18	>99.0%	Aldrich
L-Lysine Monohydrochloride	$C_6H_{14}N_2O_2$	182.65	No information	Sigma
L-Methinonine	$C_5H_{11}NO_2S$	149.21	>99.5%	BioUltra. Sigma
L-Proline	$C_5H_9NO_2$	115.15	>99.0%	Aldrich
L-Serine	$C_3H_7NO_3$	105.09	>99.5%	Biochemika. Fluka
L-Tyrosine	$C_9H_{11}NO_3$	181.19	>99.0%	Sigma-Ultra. Sigma
L-Threonine	$C_4H_9NO_3$	119.12	>99.5%	Biochemika. Fluka
L-Tryptophan	$C_{11}H_{12}N_2O_2$	204.23	>98.0%	Sigma-Aldrich
L-Valine	$C_5H_{11}NO_2S$	117.15	>99.5%	Biochemika. Fluka
L-Alanine- 2,3,3,3-D4	$C_3H_3D_4NO_2$	93.13	98 atom % D	ISOTEC

4.8.3. Supplementary material 3

Table 4.5 depicts the mass to charge ratio (m/z) of the molecular ions and major fragments detected for each compound derivatized with methylchloroformate and analyzed by GC/MS.

Table 4.5. Mass to charge ratios for the molecular ions and major fragments and retention times for each compound in the in-house library.

Compound	RT (min.)	Molecular ion (m/z)	Major fragments ions (m/z)
Organic Acids			
2-oxoadipic acid	14.664	188	101,129,59
α-Ketoglutaric acid/2-oxoglutaric acid	13.213	174	115,55,87
Adipic acid	12.557	175	175,114,143
Citraconic acid	10.416	158	127,99
Citric acid	16.495	235	235,143,236
D-Lactate sodium	9.361	104	59,163,177
DL-Isocitric acid trisodium salt	21.361	234	129,157
DL-Malic acid	9.330	162	113,115,85
Fumaric acid	9.354	144	113,85
Glyoxylic acid monohydrate	11.328	106	75,106,62
Itaconic acid	10.329	159	127,126,69,99,159
Oxaloacetic acid	10.848	160	101,69
Pyruvic acid	7.507	102	89,117,57
Succinic acid	9.228	166	115,87,147
Amino Acids			
Glycine	11.628	148	148,44,88
L-Alanine	11.275	162	162,102,58
L-arginine	Not derivatized		
L-Asparagine	16.735	262	187,56,127
L-Aspartic acid	16.521	220	220,128, 160
L-Cysteine	21.145	192	117,192,176
L-Glutamic acid	18.431	234	234,114,174
L-Glutamine	25.200	276	84,219,114
L-Histidine	26.888	285	210,140,85
L-Isoleucine	14.349	204	204,144,205
L-Leucine	14.245	204	204,144,205,58
L-Lysine	26.817	277	142,277
L-Methionine	18.655	222	222,190,162
L-Phenylalanine	20.670	238	238,162,161
L-Proline	15.211	188	128,188,84
L-Serine	15.900	178	178,115,74,118
L-Threonine	15.814	192	192,115,174
L-Tryptophan	34.812	277	130,131
L-Tyrosine	29.410	253	121,236,161,192
L-Valine	13.045	190	190,130,191
L-Alanine – 2, 3, 3, 3 – D4 (Internal standard)	11.181	174	106,166,62

4.8.4. Supplementary material 4

Table 4.6 shows the compounds detected in the extracellular culture medium and the respective percentage relative to the initial amounts. Mean of three biological replicates, with three technical replicates (± Standard deviation).

Table 4.6. Percentage of compounds detected in the extracellular culture medium along time, with 0 hours representing the 100%.

Compounds	% Mean (± SD)					
	4h	8h	12h	24h	48h	72h
ala	73 (± 35)	12 (± 5)	3 (± 1)	0	0	0
asn	61 (± 34)	75 (± 16)	81 (± 12)	70 (± 16)	61 (± 12)	60 (± 25)
asp	7 (± 3)	0	0	0	0	0
cys	93 (± 56)	186 (± 115)	203 (± 138)	151 (± 76)	127 (± 78)	109 (± 77)
glu	65 (± 18)	4 (± 1)	0	0	0	0
ile	38 (± 7)	11 (± 5)	5 (± 2)	6 (± 3)	19 (± 7)	25 (± 5)
leu	49 (± 18)	14 (± 8)	6 (± 2)	8 (± 3)	24 (± 6)	26 (± 5)
lys	84 (± 1)	202 (± 1)	261 (± 2)	208 (± 1)	209 (± 1)	219 (± 1)
met	35 (± 21)	0	0	0	0	0
phe	66 (± 24)	99 (± 16)	118 (± 24)	109 (± 17)	100 (± 29)	107 (± 24)
pro	104 (± 33)	90 (± 20)	3 (± 2)	0	0	0
thr	87 (± 44)	121 (± 27)	146 (± 22)	133 (± 23)	128 (± 22)	130 (± 21)
trp	65 (± 27)	113 (± 45)	140 (± 45)	95 (± 37)	80 (± 33)	95 (± 22)
tyr	78 (± 25)	169 (± 40)	40 (± 56)	236 (± 48)	224 (± 62)	263 (± 66)
val	63 (± 24)	50 (± 14)	31 (± 5)	30 (± 4)	43 (± 10)	44 (± 15)
cit	37 (± 17)	31 (± 16)	30 (± 14)	24 (± 11)	32 (± 15)	33 (± 13)
lac	9 (± 24)	2 (± 24)	11 (± 24)	9 (± 24)	6 (± 24)	8 (± 24)
pyr	95 (± 82)	115 (± 6)	10 (± 5)	8 (± 4)	3 (± 2)	2 (± 1)
succ	306 (± 160)	29 (± 11)	26 (± 14)	15 (± 3)	16 (± 8)	18 (± 8)

4.9. *Supplementary material (Electronic version)*

Supplementary material E1 - Simulation_IT341.xlsx

Chapter 5

Evaluation of different carbon sources for the growth of *H. pylori* 26695 in liquid medium

Daniela M. Correia, Ana Guimarães, Maria João Vieira, Nuno F. Azevedo and Isabel Rocha.
Evaluation of different carbon sources for the growth of *H. pylori* 26695 in liquid medium.
(To be submitted).

5.1. *Abstract*

Helicobacter pylori is considered to be a fastidious pathogenic organism that colonizes the human stomach. Like other pathogenic organisms, *H. pylori* developed mechanisms and evolved to survive and inhabit in its host, specifically in the human gastric mucosa.

The gastric environment is a rich medium for *H. pylori*, with a large variety of carbon sources available, including amino acids. However, no previous experiments were conducted to identify the preferred carbon sources for *H. pylori* growth that could then be used for designing a minimal medium.

In the present study, *H. pylori* 26695 was grown using several amino and organic acids as the main substrates in order to determine which are the preferential carbon sources. A metabolic footprinting approach was also applied to conclude about substrate consumption and identify secreted metabolites. Under the conditions used, L-glutamine was identified as the preferred carbon source for *H. pylori* 26695 growth, evaluated by the highest biomass concentration achieved using this substrate and the highest growth rate obtained. However, L-glutamate allowed to achieve also high growth rates and biomass concentrations and presented a greater efficiency in terms of the biomass produced per substrate consumed. In addition, it is now clear that L-glutamine is a substrate for the production of L- glutamate in *H. pylori* in the periplasm, being L-glutamate then transported and catabolized. Therefore, we suggest L-glutamate as the most suitable carbon source for *H. pylori in vitro* growth.

Keywords: *Helicobacter pylori*, carbon sources, nutritional requirements.

5.2. *Introduction*

Animal tissues contain a variety of nutrients (sugars, amino acids and other nitrogen-containing compounds), being outstanding sources of nutrients for bacteria[1]. Additionally, in the human body, the nutrients needed for bacterial growth are replenished over time[2].

The compounds found in the host environment are used by pathogenic bacteria to extract the energy, carbon and nitrogen needed to grow and replicate[1]. Thus, pathogens have evolved specific mechanisms to access host nutrients and use them by various specific pathways and uptake systems[1,3].

Unfortunately, in host-pathogen interactions, the *in vivo* metabolism of bacterial pathogens is not well understood[3]. In fact, the preferred *in vivo* carbon sources of a variety of pathogens persist unidentified and the growth conditions in numerous sites of infections are poorly defined, hampering the nutritional modeling of infections[2].

H. pylori is a pathogenic organism that dwell in the mucous layer of the human stomach, causing gastric diseases[4]. *H. pylori* is known to be adhered to gastric epithelial cells, next to tight junctions[5,6]. That particular location gives some advantages to *H. pylori*, namely, wash-out prevention from the stomach, favorable pH near the gastric epithelium, and access to nutrients released by gastric epithelial cells[6]. The gastric environment is a rich medium, providing the nutritional requirements for *H. pylori* growth, with several possible carbon and nitrogen sources. It is known that *H. pylori* utilizes amino acids and uses them as preferred carbon sources[7,8]. Also, a chemotactic motility in response to amino acids was reported, with some acting as attractants[9,10]; however, if this mechanism contributes to virulence and transmission, beside nutritional acquisition, is still an open question[11].

Gastric juice, which results from the secretion of many gastric glands into the stomach[12], contains amino acids at relative high concentrations. Segawa and coworkers (1985) were able to identify 15 amino acids in human gastric juice of healthy subjects and in patients with gastric diseases (gastric ulcer, duodenal ulcer, gastroduodenal ulcers and gastric cancer)[13]. D and L-amino acids were also detected in gastric juices of subjects

infected with *H. pylori,* as well as in the gastric juice of uninfected subjects. Among the detected amino acids, proline, alanine, serine, aspartate and glutamate were detected at higher concentrations[4,12]. In addition, increased levels of aromatic amino acids (phenylalanine, tryptophan and tyrosine) were detected in the gastric juice of patients with malign gastric lesions when compared to benign gastric lesions[14,15]. The concentration of amino acids in the gastric mucous layer is unclear but it is likely that it is approximately the same as in the gastric juice[16]. The amino acids present in the gastric juice are derived in part from the blood plasma amino acid pool and by secretion from the cells of the gastric mucosa[17]. Proteolysis, to which proteins are subjected in the stomach by the action of pepsins, also contribute to the presence of amino acids in the gastric juice 15-17. Some organic acids were also detected in the gastric juice, such as lactate[18], pyruvate, or citrate[19].

Several strategies to grow *H. pylori in vitro* have been delineated, being the use of complex media supplemented with growth factors the most common one. Recently, some liquid media for *H. pylori* growth were compared, being the defined medium Ham's F-12 nutrient mixture supplemented with 5% of horse serum the best option, since it gives the most consistent growth even using a small inoculum size[20]. Several other chemically defined or semi-defined media were developed for *H. pylori* growth with focus on the determination of amino acids requirements[8,21–24]. However, in none of these studies the carbon sources were clearly identified, being various amino acids co-metabolized simultaneously, together with glucose or pyruvate. Furthermore, there is a lack of knowledge about the preferential substrate used by *H. pylori,* with some authors pointing alanine, arginine, aspartate, asparagine, glutamate, glutamine, proline and serine as the potential carbon sources[7,8]. The identification of the preferential *in vivo* carbon sources and their use as substrates for *H. pylori* growth *in vitro* would result in more reliable growth, leading to a significant breakthrough in its study by contributing to understand how this organism lives in the host and delineate new strategies to eradicate it. On the other hand, it would extend the knowledge about bacterial pathogenesis.

The main goal of the present work was thus to study *H. pylori's* potential carbon sources in order to determine the preferential ones and use the obtained information to

design a culture medium containing only one carbon source that could be used to *grow H. pylori* under more defined conditions and thus contribute to understand better the physiology and metabolism of that pathogenic organism. Also, a metabolic footprinting strategy was applied in order to determine the consumption and secretion of metabolites into the culture medium.

5.3. *Methods*

5.3.1. Culture conditions

Helicobacter pylori 26695 (strain NCTC 12455) was cultivated in Columbia Base Agar (CBA) (Liofilchem, Italy) supplemented with 5% (v/v) defibrinated horse blood (Probiologica, Portugal) at 37 °C under microaerophilic conditions (5% O_2, 10% CO_2, 85% N_2) in a Cell Culture Incubator (Incubator HERAcell 150, Kendro Laboratory, Germany) for 3 days.

An inoculum was prepared in Ham's F-12 nutrient mixture with glutamine (catalog no 21765-037, Invitrogen-Gibco, Spain) previously supplemented with 5% of fetal bovine serum (FBS) (vol/vol) (catalog no 10500-064, origin: South America, Invitrogen-Gibco, Spain), incubated at 37 °C under 130 rpm of shaking speed (Heidolph Unimax 1010 orbital shaker, Germany) in microaerophilic conditions for approximately 16 h, in order to reach the exponential phase. Afterwards, cells were harvested by centrifugation (5000 x *g*, 10 min.), washed twice in phosphate buffer saline solution (PBS) and ressuspended in culture medium. The initial Optical Density of the culture at 600 nm (OD_{600}) was adjusted to 0.03-0.06. Each experiment was performed in 100 mL Erlenmeyer flasks with 15 mL of media with different carbon sources. A single inoculum was used to inoculate all Erlenmeyer flasks. The initial pH was adjusted to 7.0. The culture was incubated at 37 °C under 130 rpm of shaking speed under microaerophilic conditions. The experiment was carried out during 48 hours.

5.3.2. Media and Carbon Sources

The culture medium used in the experiments was a modified version of the Ham's F-12 nutrient mixture, in which the amino acids that had not been consumed in the previous work (Chapter 4) were removed from the medium and only one carbon source was used in each experiment. The remaining compounds from Ham's F-12 were kept (inorganic salts, vitamins and other components) in the same concentrations (detailed in Supplementary Material 1). The carbon sources tested were based on screening growth experiments previously performed. The following carbon sources were tested: L-alanine, L-asparagine, L- aspartic acid, L-glutamine, L-glutamic acid, L-proline, L-serine, pyruvate and alpha-ketoglutarate. The concentration of each carbon source was the same in terms of moles of carbon (10 mM). All media were supplemented with 5% fetal bovine serum (FBS) (vol/vol). A control experiment without any carbon source and with only the essential components was performed. The composition of each medium tested is described in Table 5.1. All media were prepared in distilled water and filter-sterilized using a filtration unit Sartolab P20, 0.2 µm (Sartorius, Germany).

Table 5.1. Composition of the media tested.

Abbreviations of compounds: L-ala – L-alanine, L-asn - L-asparagine, L-asp – L-arginine, L-gln - L-glutamine, L-glu – L-glutamate; L-pro – L-proline; L-ser – L-serine; pyr – pyruvate; α- ket – alpha-ketoglutarate.

Compounds	**Media**									
	1	**2**	**3**	**4**	**5**	**6**	**7**	**8**	**9**	**10***
Carbon sources (mM)	L-ala (3.34)	L-asn (2.50)	L-asp (2.50)	L-gln (2.00)	L-glu (2.00)	L-pro (2.00)	L-ser (3.34)	pyr (3.34)	α-ket (2.00)	-
Essential Amino acids	L-arginine (10.00 mM), L-histidine (1.00 mM), L-isoleucine (0.30 mM), L-leucine (1.00 mM), L-methionine (0.30 mM), L-phenylalanine (0.30 mM) L-valine (1.00 mM).									
Inorganic salts	Calcium chloride (0.2993 mM), Cupric sulphate (0.00001 mM), Ferric sulphate (0.003 mM), Magnesium chloride (0.6010 mM), Potassium chloride (2.981 mM), Sodium bicarbonate (14 mM), Sodium chloride (131.017 mM), Sodium phosphate dibasic anhydrous (1 mM), Zinc sulphate (0.0030 mM).									
Vitamins	Biotin (0.00003 mM), Choline chloride (0.1 mM), D-calcium panthothenate (0.0010 mM), Folic acid(0.0029 mM), Niacinamide (0.0003 mM), Pyridoxine hydrochloride(0.0003 mM), Riboflavin(0.0001 mM), Thiamine hydrochloride (0.0009 mM), Vitamin B12 (0.0010 mM), *i*inositol (0.1 mM).									
Other components	Hypoxanthine (0.0294 mM), Linoleic acid (0.0003 mM), Lipoic acid (0.0010 mM), Phenol red (0.0032 mM) Putrescine (0.0010 mM), Thymidine (0.0029 mM).									

* Control experiment with only essential amino acids, without carbon source.

5.3.3. Growth assessment and carbon source consumption

During the cultures, samples were collected at different time points (0, 4, 6, 8, 10, 12, 24, 36 and 48 hours) to evaluate the Optical Density at 600 nm by using a microplate reader (TECAN Sunrise, Switzerland). To verify culture purity at each time point a sample of the bacterial culture was plated in Columbia base agar (CBA) (Liofilchem, Italy) supplemented with 5% (v/v) defibrinated horse blood and Tryptic Soy Agar (Liofilchem, Italy) media and then incubated at 37°C in microaerophilic and aerobic conditions, respectively, during 5-7 days.

At 0 and 48 hours of each experiment, samples of the supernatant were collected to analyze amino and non-amino organic acids by GC-MS in order to measure the consumption of the carbon source and other amino acids and detect possible by-products secreted by *H. pylori* (method detailed in Chapter 3).

Acetate and formate production were assayed by an enzymatic kit (Acetic acid UV-method - Cat. No. 10 148 261 035, Boehringer Mannheim/R-Biopharm, Roche, Germany and Formic acid UV method - Cat. No. 10 979 732 035, Boehringer Mannheim/R-Biopharm, Roche, Germany) (Experimental procedure according to kits' instructions).

The specific growth rates (h^{-1}) were determined by plotting the logarithm of the absorbance of the culture at 600 nm along time.

5.4. *Results and discussion*

5.4.1. *H. pylori* growth with different carbon sources

It has been described that amino acids can be used by *H. pylori* as carbon and energy sources. In our previous experiments, *H. pylori* 26695 was grown in the Ham's F-12 medium, which contains all 20 amino acids in concentrations between 0.03 and 1 mM (medium composition detailed in supplementary material 1). Additionally, some organic acids (citrate, lactate and succinate) were detected in the culture medium when supplemented with fetal bovine serum (FBS).

Two experiments using 10-fold higher concentrations of amino acids and organic acids (citrate, lactate, succinate, and pyruvate) were also performed. The obtained results showed that an increase in amino acids concentrations originated and increase in *H. pylori*'s growth, while the same increase was not observed for the experiment with higher concentration of organic acids. These results suggest that either essential amino acids are found in limiting conditions in the original medium formulation or that the remaining amino acids are the preferential carbon sources.

In addition, the analysis of extracellular metabolites, previously performed, enabled us to determine which amino and organic acids were consumed by *H. pylori* growing in Ham's F-12 (Chapter 3). Based on these results, some L-amino acids (alanine, asparagine, aspartate, glutamate, glutamine, proline and serine) and one organic acid (pyruvate) were chosen to be tested as possible carbon sources for *H. pylori* 26695 in liquid medium.

Additionally, alpha-ketoglutarate was also tested, since glutamine and glutamate are assimilated via alpha-ketoglutarate in the TCA cycle[25]. Although the transporter for that organic acid was identified in *H. pylori* 26695's genome[26,27], in our experiments, when using alpha-ketoglutarate as the sole carbon source, we observed no growth, indicating that possibly this transporter is not active under the conditions used. As such, the results of that experiment are not presented next.

It should be emphasized that, although an effort was made such that in each experiment only one compound was serving as the carbon source, this was not completely achieved given the presence of additional carbon sources in FBS (used in 5% v/v), such as organic acids. In fact, it was not possible to remove FBS from the culture medium, which suggests that some nutrients are still missing in the defined medium, or that FBS has another unknown function that is not supported by the medium without this complex supplement. FBS was also analyzed by GC-MS (results detailed in supplementary material 2) and it is clear that, although several of the carbon sources were found, those are in low concentrations in the final medium, and it is possible to separate their influence (as also shown in supplementary material 2).

To assess *H. pylori*'s growth using different carbon sources, the optical density at 600 nm (OD_{600}) was analyzed for each time point until 48 hours of culture. The growth along time using different carbon sources is showed in Figure 5.1. The OD_{600} increase and the respective specific growth rate (μ) for each carbon source tested are depicted in Figure 5.2. As expected, no growth was observed in the control experiment without any carbon source (results not shown).

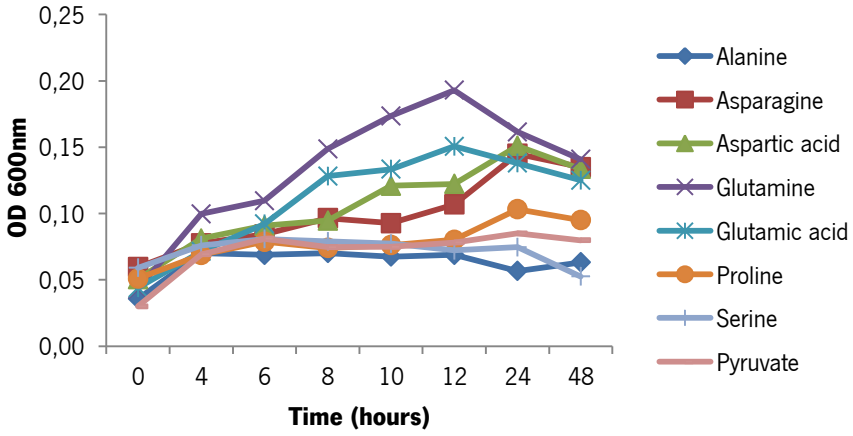

Figure 5.1. Growth (OD_{600}) of *H. pylori* 26695 using different carbon sources.

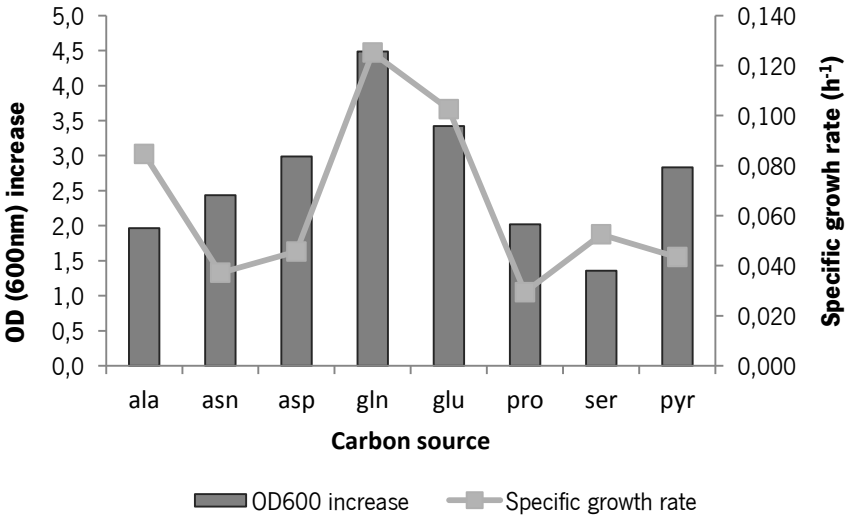

Figure 5.2. Factor increase in optical density (OD 600nm) after 48 hours of culture and specific growth rate (exponential phase) for each carbon source tested.

The tested carbon sources have different effects on growth, as shown by the specific growth rates obtained, which range from 0.125 h^{-1} with glutamine to 0.029 h^{-1} with proline (Figure 5.2).

The analysis of these results suggests that the amino acids that are catabolized by conversion to intermediates of the TCA cycle, such as aspartate and glutamate, are the preferred substrates. The maximum specific growth rates were achieved for glutamine and glutamate as carbon sources (0.125 h^{-1} and 0.103 h^{-1}, respectively). Moreover, glutamine allowed to achieve the higher optical density, indicating that it is the best among the carbon sources tested for *H. pylori* growth. These results can be justified by several facts, first and foremost the abundance of glutamine in the human body and its functions besides nutrition, being essential for the correct function of a variety of tissues and cells[28,29]. Concerning glutamate concentration in the gastric environment, it is present in the gastric juice of infected and uninfected subjects, although in lower amounts than other amino acids[4,12,13].

However, before entering the metabolism, glutamine must be converted to glutamate by gamma-glutamyltranspeptidase (GGT) in the periplasm with ammonium production, being then the resulting glutamate transported to the cytoplasm by the GltS transporter in a Na^+- dependent process[16,30]. GGT was detected in the extracellular medium and in the periplasm of growing *H. pylori* [30,31]. The referred transporter was also identified by homology in the last *H. pylori* 26695 genome reannotation as a sodium/glutamate symporter (HP1506)[27].

It is likely that these specific mechanisms that allow *H. pylori* to use glutamine and glutamate are not restrict to nutrient acquisition, contributing to *H. pylori*'s virulence by the depletion of amino acids that have a protective role of the gastric mucosa (such as glutamine, as referred above)[32] and the production of ammonia[16,30], which causes damage in gastric epithelial cells[32]. Moreover, it was suggested that GGT in *H. pylori* contribute to maintain a constant level of ammonia[16,33], which can be used by *H. pylori* as a nitrogen source, as well as a neutralizing agent against acidic gastric environment[34]. A recent review

about the role of GGT in *H. pylori*'s pathogenesis stresses the importance of ammonia production in gastric damage during *H. pylori* infection[34].

Thus, *H. pylori* does not possess a direct glutamine transporter, using glutamine as a source of glutamate[16], which in turn is converted to alpha-ketoglutarate by glutamate dehydrogenase (GdhA) and incorporated into the TCA cycle[16,25,35]. Moreover, the spontaneous hydrolysis of glutamine in aqueous buffer solutions at 37°C and pH of 7.4 has been described[8,36], thus limiting its use in *in vitro* liquid culture medium.

The use of aspartate and asparagine as sole carbon sources to grow *H. pylori* resulted in low specific growth rates, with the maximum biomass achieved at 24 hours of culture (Figure 5.1 and Figure 5.2). Like for glutamate and glutamine, a specific aspartate transporter (DcuA) was described[30] and predicted[27], and asparagine catabolism starts with its deamination in the periplasm by L-asparaginase (AnsB), resulting in ammonia and aspartate, which is assimilated via fumarate in the TCA cycle[30]. It is presumed that the fumarate used in the TCA cycle is formed preferentially from aspartate than from malate, in contrast with *C. jejuni*[37]. L-aspartate was detected in the gastric juice of patients with cancer and without cancer, but a controversy exists regarding its correlation with the existence of cancer [12,134]. Concerning virulence, the transport of aspartate was proved to be essential in the colonization of the gastric mucosa in mice[30].

When proline was used as the sole carbon source, the specific growth rate (μ=0.029 h^{-1}) was the lowest obtained, being the maximum optical density obtained at 24 hours of growth (Figure 5.1 and Figure 5.2). This result suggests that proline was not being efficiently used by *H. pylori*. L-proline can also be transported by a Na^{+}-dependent transporter (PutP)[27,38]. The use of L-proline as a carbon source was also reported by other authors[7,8] as well as its high concentration in the human gastric juice[4,12]. An evidence on the usage of proline in the catabolism comes from the identification of the gene (putA), encoding for proline dehydrogenase, in *H. pylori*'s 26695 genome[26,27], which is also associated with the respiratory chain[4].

It is thought that proline is not an essential amino acid for *H. pylori* growth, but the specific precursor for its formation is unknown, as mentioned in the previous chapter: L-glutamate[39] or L-arginine[6] are two possible precursors for proline biosynthesis.

Alanine and serine as carbon sources resulted in a low OD increase when compared with glutamine or glutamate, with the maximum biomass achieved at 8 and 6 hours of culture, respectively, but with low specific growth rates (Figure 5.1 and Figure 5.2). L-alanine and L-serine have been described to be essential amino acids for some strains[21], but results from this work presented in the previous chapter indicated that under the conditions used, alanine and serine are not essential for *H. pylori*. Regarding the composition of the gastric juice, alanine and serine are both present at high amounts[4,12]. L-serine uptake is accomplished by the SdaC transporter, a specific serine transporter[27,37], while, although a transporter for D-alanine was predicted on *H. pylori*'s 26695 genome (dagA, HP0942)[27,39,40], a specific L-alanine transporter has not been identified. For promoting L-alanine transport only a non-specific amino acid ABC (ATP binding cassette) transporter was predicted[27,40,41]. Regarding the catabolic pathways, L-serine and L-alanine can be both incorporated into the metabolism via pyruvate by a one-step conversion to pyruvate and ammonia, by serine deaminase (sdaA)[6,26,39] and alanine dehydrogenase (ald)[26,39], respectively. However, OD_{600} achieves higher values when pyruvate is used as the carbon source in comparison with L-alanine and L-serine, showing that these carbon sources have different effects, being pyruvate more efficiently used.

Pyruvate metabolism in *H. pylori* was studied by several authors[42,43]. Pyruvate can be used as a sole carbon source and is catabolized by the conversion to Acetyl-CoA and subsequent incorporation into the TCA cycle. Evidence of the reductive part of TCA cycle was obtained by Mendz *et al.* (1994) by detecting succinate when cells were incubated with pyruvate[42]. Mendz *et al.* (1994) also detected the formation of alanine and lactate, in addition to acetate and formate as by-products when pyruvate was used as carbon source, proving the existence of the mixed-acid fermentation pathway in *H. pylori*[42]. In contrast, Chalk *et al.* (1994) only detected acetate as a by-product of pyruvate under aerobic conditions[43].

In summary, the observed discrepancies in consumption of different compounds used as carbon sources confirm their differential use and different effectiveness, and suggest that some amino acids also have other functions related with host colonization and virulence. A connection between carbon source availability and bacterial virulence

based on a mechanism identical to the one that controls carbon catabolite repression was established in Proteobacteria[44].

H. pylori 26695's catabolic pathways for the studied carbon sources are summarized in Figure 5.3. The specific transporters, when identified, are also indicated.

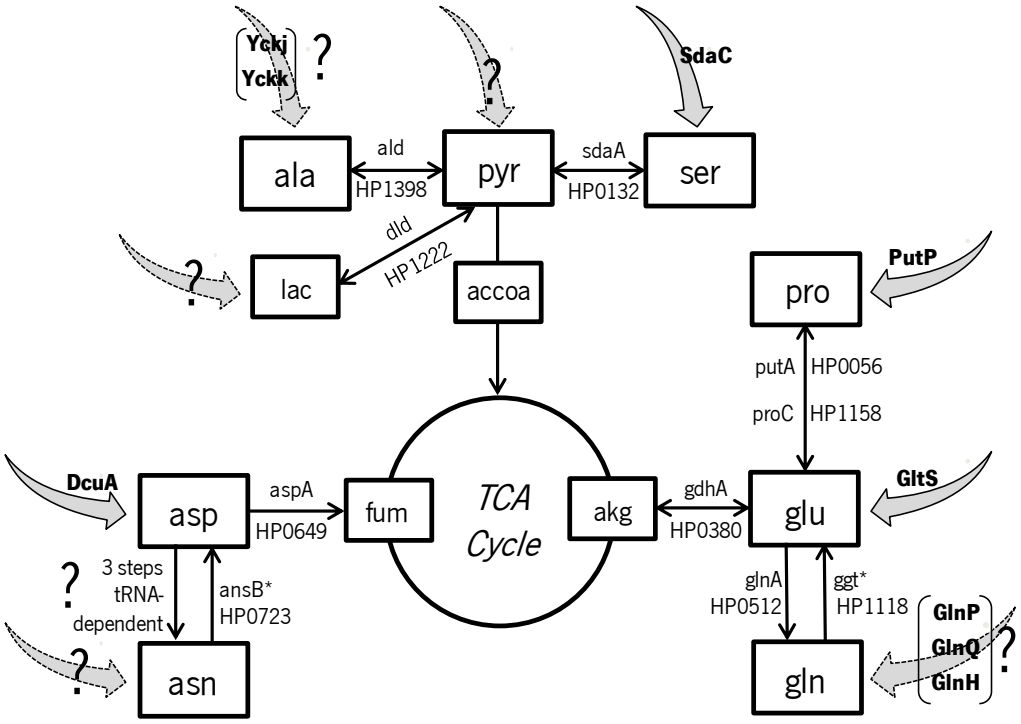

Figure 5.3. Catabolic pathways predicted to be utilized by *H. pylori* 26695 for the utilization of the carbon sources tested. The rectangles indicate metabolites; black arrows indicate a reaction catalyzed by an enzyme, codified by the referred gene; grey arrows indicate a transporter; a question mark indicates that the transporter for that specific compound is unknown. * Reactions occuring in the periplasm.

Abreviattions of compounds: accoa – acetyl-coA, akg – alpha-ketoglutarate, ala- L-alanine, asn – L-asparagine, asp – L- aspartate, fum – fumarate, glu- L-glutamate, gln – L-glutamine, lac – lactate, pro – proline, pyr – pyruvate, ser – L:serine.

5.4.1. Metabolites analysis

Metabolites detected in the samples represent metabolites that were present or were secreted/excreted into the medium. Extracellular metabolite analysis was performed in order to evaluate if the carbon sources and essential amino acids were being consumed from the culture medium and identify by-products excreted by *H. pylori* when different

carbon sources are used. The percentage of carbon source consumption in each experiment at 48 hours of culture, analyzed by GC-MS is displayed in Figure 5.4.

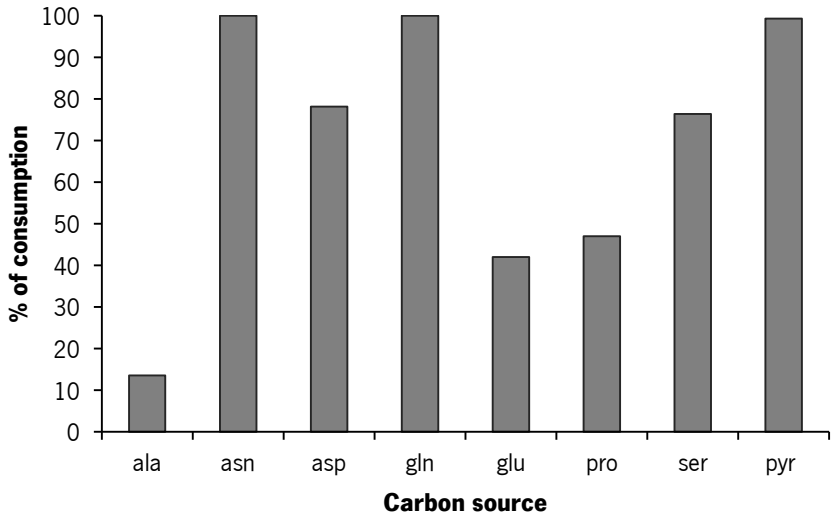

Figure 5.4. Carbon source consumption after 48 hours of culture (Mean of three technical replicates).

The analysis of the culture medium after 48 hours revealed that glutamine, asparagine and pyruvate were completely consumed by *H. pylori* when those were used as the main carbon sources (Figure 5.4). Aspartate, glutamate, proline and serine were not completely consumed, with percentages of consumption between 40% and 80%. A very low percentage (around 14%) of alanine was consumed in the experiment in which it was used as carbon source. Looking at the obtained results, it is clear that in these cases growth was not arrested by the lack of the carbon source.

Associating the intake of the carbon source with the biomass formed (Figure 5.1) it is noticeable that glutamate and alanine have the highest yields, while pyruvate and serine have the lowest yields.

The GC-MS analysis of the FBS indicates that some of the carbon sources tested (alanine, aspartate, glutamate and proline) and other potential carbon sources (lactate, citrate and succinate) are present in this component. It is thus important to analyze their

evolution in each experiment in order to inspect if they were also being used by the organism.

As such, the exometabolome analysis performed allowed to detect the compounds consumed from the culture medium, besides the main compounds used as carbon sources (results detailed in supplementary materials 3). Analyzing the results, it can be seen that alanine, aspartate, glutamate, proline, citrate, lactate and succinate were identified in all experiments initially (0 h) in the culture medium. At 48 hours of culture, alanine and lactate were completely consumed. Lactate transport, by lactate permeases, was predicted from the genome (lctp1, HP0140; lctp2, HP01421)[26,27]. A D-lactate dehydrogenase was also identified by homology in the genome (dld, Hp1222) which is responsible for the conversion of D-lactate into pyruvate [26,27]. Furthermore, Takahashi *et al.* (2007) proved that the L-lactic acid secreted by gastric mucosal cells has a stimulatory effect on *H. pylori* growth in microaerobic conditions, and since L-lactate dehydrogenase is not predicted from genome analysis, another unknown metabolic pathway might be present in *H. pylori* for L-lactate degradation[18]. The concentration of lactate detected in the culture media supplemented with FBS is about 0.8 mM, which is consistent with the concentration found in the human gastric juice (0.3-1 mM)[18], although we were not able to identify which isoform is present in FBS.

Aspartate and proline were almost 100% consumed in all experiments, coherent with the results in experiments where these compounds were used as carbon sources (where some consumption was verified when the initial concentrations were much higher).

Glutamate, citrate and succinate were detected in the culture medium in all experiments at 0 h of culture, originating from FBS. These compounds were differently utilized by *H. pylori,* being consumed in some experiments and produced in others (supplementary material 3, Table 5.5) When it was not the main carbon source, glutamate was completely consumed in the experiments where glutamine and serine were the main carbon source. Since glutamine was completely consumed, it can be hypothesized that glutamate was used in this experiment as an “extra” carbon source. The same did not happen in the serine experiment, as serine was not completely consumed, suggesting a preference for glutamate. In experiments where asparagine, proline and pyruvate were the

main carbon source, glutamate was not consumed. As explained previously, the arrest in growth in those experiments was not associated with the carbon source, and can be associated with the production of some toxic compounds or other unknown factors and thus the presence of glutamate did not avoid growth arrest.

The percentage of citrate in the culture medium at 48 hours increased in experiments using glutamine and aspartate. In experiments using alanine, asparagine, proline and pyruvate as main carbon sources, citrate was consumed by *H. pylori* (supplementary material 3, Table 5.5) The influence of citrate in *H. pylori* growth and viability was studied by Albertson *et al*. (1998) concluding that citrate did not enhance *H. pylori*'s growth, but increase its viability[45].

Succinate, which can be used by *H. pylori* as a carbon source, was not consumed in experiments using asparagine, proline, serine and pyruvate, whilst it was consumed in experiments using alanine, aspartate, glutamine and glutamate. Studies on by products formed by the catabolism of amino acids detected succinate as a by-product of alanine, aspartate, glutamate, fumarate and pyruvate[7]. Besides an increase in viability, Albertson *et al*. (1998) did not detect any growth improvement in *H. pylori* when succinate was added to culture medium[45]. In the published *in silico* metabolic models, succinate is pointed out as a possible carbon source[25,46], although, in our previous experiments, succinate was not able to improve growth as discussed above in the case of citrate.

Tyrosine was only detected in two experiments (with glutamine or glutamate as carbon sources), with a 2-fold increase of its percentage at 48 hours of culture. However, the concentrations detected are very low, indicating that it could be present in all experiments at concentrations below the limit of detection of the method used.

The accumulation of L-tyrosine in the culture medium was also observed when the complete culture medium (with 20 amino acids) was used, as discussed in the previous chapter.

Regarding essential amino acids, which were also analysed by GC/MS, the obtained results are detailed in supplementary material 3 (Table 5.5). Overall, the consumption of essential amino acids was not clearly noticeable in some cases. This fact can be explained by the relatively high concentrations of some amino acids (leucine,

phenylalanine and valine) in the medium, making the measurements of their consumption inaccurate since the utilization by *H. pylori* cells is small compared to the total content.

Histidine was only detected in the experiments using glutamine and glutamate as the main carbon sources due to problems with the derivatization method for that specific compound, making its detection very difficult and unreliable.

The formation of the by-products acetate and formate were also inspected by an enzymatic kit at 48 hours of culture. Acetate was detected in samples of the experiments using pyruvate and serine as carbon sources, with an increment of 0.029 g/L and 0.018 g/L, respectively, comparatively to 0 hours of culture. Acetate formation when pyruvate is metabolized is in agreement with the results obtained by other authors. The same happens with L-serine[42] since, as discussed, L-serine is metabolized by direct conversion into pyruvate. However, although L-alanine is also directly transformed into pyruvate, and acetate production has been reported[7], that compound was not detected in the L-alanine experiment. Acetate was also reported to be a by-product of aspartate, asparagine, glutamate and glutamine metabolism in *H. pylori*[8], but this was not verified in the present work.

Formate was not detected in any sample. It was expected to be produced in experiments using pyruvate or using amino acids that are metabolized via pyruvate, since the mixed-acid fermentation was proved by Mendz *et al.*[7,42].

5.5. *Conclusions*

In the present work, a comparison of *H. pylori* growing using different carbon sources was carried out. Even though other studies also reported experiments using amino acids as carbon sources, to our knowledge, this is the first work where different amino acids were tested as the main carbon sources using the same concentration (in terms of moles of carbon) and where growth parameters were compared using a semi-defined medium. Moreover, the measurement of the exometabolome is another novelty, allowing the comparison of *H. pylori*'s behaviour under several nutritional conditions.

Under the conditions used, glutamine was identified as the carbon source that yielded a higher growth. However, glutamine easily suffers degradation in aqueous medium. Moreover, it is converted to glutamate and ammonium by an enzymatic reaction in *H. pylori*'s periplasm. In addition, the use of glutamate as the main carbon source had a higher yield in biomass regarding substrate consumption. As such, we suggest glutamate as the carbon source of choice for *H. pylori*'s growth.

In line with other authors, the obtained results also proved that *H. pylori* is not constrained to a unique carbon source and can switch to different substrates when the preferential carbon source is not available, although with lower growth rates. Nevertheless, the utilization of amino acids that are reported to be present in the gastric environment might be not only related with acquiring nutrients, and it can be speculated that by depleting the compounds that are important for gastric health, *H. pylori* has another advantage, contributing to injury and virulence, as occurs with glutamine.

Notwithstanding, it should be emphasized that in our experiments FBS was used to supplement the defined medium used, having some impact in the results. Nevertheless, the FBS characterization performed in this work is also of interest and allowed the identification of some important components (amino and organic acids) and to estimate their impact in growth. Our attempts to grow *H. pylori* without FBS and without strain adaptation failed, indicating that some components are missing in the culture medium used or that FBS has another unknown function. Thus, further investigation is needed in this direction.

5.6. *References*

1. Rohmer, L., Hocquet, D. & Miller, S. I. Are pathogenic bacteria just looking for food? Metabolism and microbial pathogenesis. *Trends Microbiol.* **19,** 341–348 (2011).

2. Brown, S. A., Palmer, K. L. & Whiteley, M. Revisiting the host as a growth medium. *Nat. Rev. Microbiol.* **6,** 657–666 (2008).

3. Eisenreich, W., Dandekar, T., Heesemann, J. & Goebel, W. Carbon metabolism of intracellular bacterial pathogens and possible links to virulence. *Nat. Rev. Microbiol.* **8,** 401–12 (2010).

4. Nagata, K. *et al.* L-serine, D- and L -proline and alanine as respiratory substrates of *Helicobacter pylori*: correlation between *in vitro* and *in vivo* amino acid levels. *Microbiology* **149,** 2023–2030 (2003).

5. Noach, L. A., Rolf, T. M. & Tytgat, G. N. J. Electron microscopic study of association between *Helicobacter pylori* and gastric and duodenal mucosa. *J. Clin. Pathol.* **47,** 699–704 (1994).

6. Van Amsterdam, K. & van der Ende, A. Nutrients released by gastric epithelial cells enhance *Helicobacter pylori* growth. *Helicobacter* **9,** 614–621 (2004).

7. Mendz, G. L. & Hazell, S. L. Aminoacid Utilization by *Helicobacter pylori*. *Int. J. Biochem. Cell Biol.* **27,** 1085–1093 (1995).

8. Stark, R. M., Suleiman, M. S., Hassan, I. J., Greenman, J. & Millar, M. R. Amino acid utilisation and deamination of glutamine and asparagine by *Helicobacter pylori*. *J. Med. Microbiol.* **46,** 793–800 (1997).

9. Cerda, O., Rivas, A. & Toledo, H. *Helicobacter pylori* strain ATCC700392 encodes a methyl-accepting chemotaxis receptor protein (MCP) for arginine and sodium bicarbonate. *FEMS Microbiol. Lett.* **224,** 175–181 (2003).

10. Abdollahi, H. & Tadjrobehkar, O. The role of different sugars, amino acids and few other substances in chemotaxis directed motility of *helicobacter pylori*. *Iran. J. Basic Med. Sci.* **15,** 787–794 (2012).

11. Lertsethtakarn, P., Ottemann, K. M. & Hendrixson, D. R. Motility and chemotaxis in *Campylobacter* and *Helicobacter*. *Annu. Rev. Microbiol.* **65,** 389–410 (2011).

12. Nagata, Y. *et al.* High concentrations of D-amino acids in human gastric juice. *Amino Acids* **32,** 137–40 (2007).

13. Segawa, K. *et al.* Amino acid patterns in human gastric juice in health and gastric disease. *Japanose J. Med.* **24,** 244–249 (1985).

14. Deng, K. *et al.* Three amino acids in gastric juice as potential biomarkers for gastric malignancies. *Anal. Chim. Acta* **694,** 100–107 (2011).

15. Deng, K. *et al.* High levels of aromatic amino acids in gastric juice during the early stages of gastric cancer progression. *PLoS One* **7,** 1–10 (2012).

16. Shibayama, K. *et al.* Metabolism of glutamine and glutathione via g-glutamyltranspeptidase and glutamate transport in *Helicobacter pylori*: possible significance in the pathophysiology of the organism. *Mol. Microbiol.* **64,** 396–406 (2007).

17. Komorowska, M., Szafran, H., Popiela, T. & Szafran, Z. Free amino acids of human gastric juice . *Acta Physiol. Polish* **32,** 7336988 (1981).

18. Takahashi, T. *et al.* L-lactic acid secreted from gastric mucosal cells enhances growth of *Helicobacter pylori*. *Helicobacter* **12,** 532–540 (2007).

19. Piper, D., Fenton, B. & Goodman, L. Lactic, pyruvic, citric, and uric acid content of gastric juice. *Gastroenterology* **53,** 42–48 (1967).

20. Sainsus, N., Cattori, V., Lepadatu, C. & Hofmann-Lehmann, R. Liquid culture medium for the rapid cultivation of *Helicobacter pylori* from biopsy specimens. *Eur. J. Clin. Microbiol. Infect. Dis.* **27,** 1209–1217 (2008).

21. Nedenskov, P. Nutritional requirements for growth of *Helicobacter pylori*. *Appl. Environ. Microbiol.* **60,** 3450–3453 (1994).

22. Reynolds, D. J. & Penn, C. W. Characteristics of *Helicobacter pylori* growth in a defined medium and determination of its amino acid requirements. *Microbiology* **140,** 2649–2956 (1994).

23. Testerman, T. L., Gee, D. J. M. C. & Mobley, H. L. T. *Helicobacter pylori* growth and urease detection in the chemically defined medium Ham ' s F-12 nutrient mixture. *J. Clin. Microbiol.* **39,** 3842–3850 (2001).

24. Testerman, T. L., Conn, P. B., Mobley, H. L. T. & McGee, D. J. Nutritional requirements and antibiotic resistance patterns of *Helicobacter* species in chemically defined media. *J. Clin. Microbiol.* **44,** 1650–1658 (2006).

25. Schilling, C. H. *et al.* Genome-scale metabolic model of *Helicobacter pylori 26695*. *J. Bacteriol.* **184,** 4582–4593 (2002).

26. Tomb, J.-F. *et al.* The complete genome sequence of the gastric pathogen *Helicobacter pylori*. *Nature* **388,** 539–547 (1997).

27. Resende, T., Correia, D. M., Rocha, M. & Rocha, I. Re-annotation of the genome sequence of *Helicobacter pylori* 26695. *J. Integr. Bioinform.* **10(3),** 1–13 (2013).

28. Newsholme, P., Procopio, J., Lima, M. M. R., Pithon-Curi, T. C. & Curi, R. Glutamine and glutamate–their central role in cell metabolism and function. *Cell Biochem. Funct.* **21,** 1–9 (2003).

29. Roth, E. Nonnutritive effects of glutamine. *J. Nutr.* **138,** 2025S–2031S (2008).

30. Leduc, D., Gallaud, J., Stingl, K. & Reuse, H. De. Coupled amino acid deamidase-transport systems essential for *Helicobacter pylori* colonization. *Infect. Imunity* **78,** 2782–2792 (2010).

31. Bumann, D. *et al.* Proteome analysis of secreted proteins of the gastric pathogen *Helicobacter pylori*. *Infect. Immun.* **70,** 3396–3403 (2002).

32. Nakamura, E. & Hagen, S. J. Role of glutamine and arginase in protection against ammonia-induced cell death in gastric epithelial cells. *Am. J. Physiol. Gastrointest. Liver Physiol.* **283,** G1264–75 (2002).

33. Ki, M. R., Yun, N. R. & Hwang, S. Y. Glutamine-induced production and secretion of *Helicobacter pylori* gamma-glutamyltranspeptidase at low pH and its putative role in glutathione transport. *J. Microbiol. Biotechnol.* **23,** 467–472 (2013).

34. Ricci, V., Giannouli, M., Romano, M. & Zarrilli, R. *Helicobacter pylori* gamma-glutamyl transpeptidase and its pathogenic role. *World J. Gastroenterol.* **20,** 630–638 (2014).

35. Marais, A., Mendz, G. L., Hazell, S. L. & Mégraud, F. Metabolism and genetics of *Helicobacter pylori*: the genome era. *Microbiol. Mol. Biol. Rev.* **63,** 642–674 (1999).

36. Bray, H. G., James, S. P., Raffan, I. M. & Thorpe, W. V. The enzymic hydrolysis of glutamine and its spontaneous decomposition in buffer solutions. *Biochem. J.* **44,** 625–7 (1949).

37. Doig, P. *et al. Helicobacter pylori* physiology predicted from genomic comparison of two strains. *Microbiol. Mol. Biol. Rev.* **63,** 675–707 (1999).

38. Rivera-Ordaz, A. *et al.* The sodium/proline transporter putP of *Helicobacter pylori*. *PLoS One* **8,** e83576 (2013).

39. Caspi, R. *et al.* The MetaCyc database of metabolic pathways and enzymes and the BioCyc collection of pathway/genome databases. *Nucleic Acids Res.* **40,** D742–D753 (2012).

40. Reuse, H. De & Skouloubris, S. in *Helicobacter pylori Physiol. Genet.* (HLT, M., GL, M. & SL, H.) (ASM Press, 2001).

41. Tomii, K. & Kanehisa, M. A Comparative Analysis of ABC Transporters in Complete Microbial Genomes. *Genome Res.* 1048–1059 (1998). doi:10.1101/gr.8.10.1048

42. Mendz, G. L., Hazell, S. L. & van Gorkom, L. Pyruvate metabolism in *Helicobacter pylori*. *Arch. Microbiol.* **162,** 187–192 (1994).

43. Chalk, P. A., Roberts, A. D. & Blows, W. M. Metabolism of pyruvate and glucose by intact cells of *Helicobacter pylori* studied by 13C NMR spectroscopy. *Microbiology* **140,** 2085–2092 (1994).

44. Poncet, S. *et al.* in *Bact. Sens. Signal.* (Collin, M. & Schuch, R.) **16,** 1–15 (Karger, 2009).

45. Albertson, N., Wenngren, I. & Sjöström, J. E. Growth and Survival of *Helicobacter pylori* in Defined Medium and Susceptibility to Brij 78. *J. Clin. Microbiol.* **36,** 1232–1235 (1998).

46. Thiele, I., Vo, T. D., Price, N. D. & Palsson, B. Ø. Expanded Metabolic Reconstruction of *Helicobacter pylori* (iIT341 GSM / GPR): an *In Silico* Genome-Scale Characterization of Single- and Double-Deletion Mutants. *J. Bacteriol.* **187,** 5818–5830 (2005).

5.7. *Supplementary material*

5.7.1. Supplementary material 1

Table 5.2 describes the composition of the Ham's F-12 Nutrient Mixture, with the concentration and chemicals used to prepare the medium.

Table 5.2. Composition of the Ham's F-12 medium and characteristics of the compounds used to prepare the mixture.

Compounds	Purity (%)	Chemicals	Molecular weight (g/mol)	Concentration (mM)
Amino acids				
Glycine	>99.0	Fluka	75.07	0.10
L-alanine	>99.5	Fluka	89.09	0.10
L-arginine hydrochloride	>99.5	Fluka	211.00	1.0
L-asparagine	>99.5	Sigma	132.12	0.098
L-aspartate	>99.0	Sigma Ultra	133.10	0.10
L-cysteine hydrochloride	>99.0	Sigma	157.62	0.23
L-glutamate	>99.0	Sigma	147.13	0.10
L-glutamine	>99.0	Sigma	146.15	1.0
L-histidine hydrochloride	>99.5	Sigma	209.63	0.10
L-isoleucine	>99.5	Fluka	131.18	0.030
L-leucine	>99.0	Aldrich	131.18	0.10
L-lysine hydrochloride	-	Sigma	182.65	0.20
L-methionine	>99.5	Sigma	149.21	0.030
L-phenylalanine	>99.0	Fluka	165.19	0.030
L-proline	>99.0	Aldrich	115.13	0.30
L-serine	>99.5	Fluka	105.09	0.10
L-threonine	>99.5	Fluka	119.12	0.10
L-tryptophan	>98.0	Fluka	204.23	0.010
L-tyrosine	>99.0	Sigma	181.19	0.030
L-valine	>99.5	Fluka	117.15	0.10

Table 5.2.. Composition of the Ham's F-12 medium and characteristics of the compounds used to prepare the mixture. (Continue)

Compounds	Purity (%)	Chemicals	Molecular weight (g/mol)	Concentration (mM)
Vitamins				
Biotin	>98.5	Merck	244.31	0.000030
Choline chloride	99.0	Acros	139.62	0.10
D- Calcium panthotenate	>99.0	Fluka	476.54	0.0010
Niacinamide	>98.0	Acros	122.13	0.00030
Pyridoxine hydrochloride	>99.5	Merck	205.64	0.00030
Riboflavin	>98.0	Riedel-de-Haen	376.37	0.000098
Thiamine hydrochloride	>99.0	Sigma	337.27	0.00089
Vitamin B12	>98.5	Sigma	1355.00	0.0010
*i*nositol	>99.0	Sigma	180.16	0.10
Folic acid	>95.0	Merck	441.41	0.0030
Inorganic Salts				
Calcium chloride ($CaCl_2.2H_2O$)	>99.0	Riedel-de-Haen	147.02	0.30
Cupric sulphate ($CuSO_4.5H_2O$)	>99.0	Riedel-de-Haen	249.69	0.000010
Iron sulphate ($FeSO_4.7H_2O$)	>99.0	Panreac	278.02	0.0030
Zinc sulphate ($ZnSO_4.7H_2O$)	>99.5	Panreac	287.54	0.0030
Potassium chloride (KCl)	>99.5	Fluka	74.56	2.98
Magnesium chloride ($MgCl_2.6H_2O$)	>99.0	Panreac	203.30	0.601
Sodium bicarbonate ($NaHCO_3$)	-	Fisher Scientific	84.01	14
Sodium chloride (NaCl)	>98.0	Riedel-de-Haen	58.44	131
Sodium phosphate dibasic (Na_2HPO_4)	>99.0	Fluka	177.99	1.0
Other components				
Thymidine	-	Sigma	194.00	0.0030
Putrescine	99.0	Acros	88.15	0.0010
Linoleic acid	>99.0	Sigma	280.00	0.00030
Lipoic acid	-	Fisher	206.33	0.0010
Phenol red	-	Acros	354.38	0.0030
Hypoxanthine	>99.5	Acros	136.11	0.029
Sodium pyruvate	>99.0	Sigma Ultra	110.04	1.0
D-glucose	>99.5	Sigma	180.00	10

5.7.2. Supplementary material 2

Table 5.3 shows the compounds identified in fetal bovine serum (catalog no 10500-064, origin: South America, Invitrogen-Gibco, Spain) by GC-MS.

Table 5.3. Compounds identified in the fetal bovine serum by GC-MS, mean of two technical replicates and the corresponding concentration in the final broth. The original concentration of the same compounds added to the Ham's F12 medium for carbon source experiments is also given for comparison purposes.

Compound	Concentration in FBS (Mean) (mM)	Final concentration (Mean) (mM) in the culture caused by 5% FBS	Concentration (mM) used in carbon source experiments
Amino acids			
Alanine	1.39	0.079	3.34
Aspartate	0.12	0.006	2.5
Cysteine	0.04	0.002	-
Glutamate	0.47	0.002	2.0
Isoleucine	0.35	0.018	-
Leucine	0.39	0.020	-
Methionine	0.08	0.004	-
Phenylalanine	0.13	0.007	-
Proline	0.25	0.012	2.0
Threonine	0.12	0.006	-
Tyrosine	0.01	0.001	-
Valine	0.31	0.016	-
Organic acids			
Citrate	0.93	0.046	-
Lactate	17.70	0.885	-
Succinate	0.13	0.006	-

5.7.3. Supplementary material 3

Table 5.4 and Table 5.5 show the compounds detected in the culture media and the respective percentage at 48 hours of culture (with reference to the initial concentration). Samples were analysed by GC-MS after derivatization with methylchloroformate (method described in Chapter 4).

Table 5.4. Essential amino acids identified in the culture medium by GC/MS at 48 h of *H. pylori* culture in percentage (percentage ± standard deviation) compared to the concentration at 0 h of culture. Abbreviations: his – histidine; ile – isoleucine; leu - leucine; met – methionine; phe – phenylalanine; val – valine.

Amino acids	**Experiments**							
	1	2	3	4	5	6	7	8
his	*	*	*	102% (± 18)	105% (±10)	*	*	*
ile	86% (± 11)	110% (± 5)	26% (± 3)	100% (± 15)	110% (± 10)	124% (± 4)	105% (± 12)	103% (± 9)
leu	92% (± 11)	118% (± 6)	34% (± 3)	103% (± 21)	106% (± 9)	128% (± 5)	116% (± 13)	105% (± 10)
met	93% (± 24)	120% (± 23)	54% (± 21)	94% (± 17)	38% (± 1)	107% (± 4)	106% (± 6)	103% (± 6)
phe	88% (± 4)	108% (± 5)	98% (± 75)	100% (± 17)	107% (± 12)	111% (± 5)	115% (± 7)	102% (± 2)
val	12% (± 1)	121% (± 4)	43% (± 9)	94% (± 18)	103% (± 10)	118% (± 4)	112% (± 6)	110% (± 4)

* Not detected in those experiments.

Carbon source	**Experiment number**
L-alanine	1
L-asparagine	2
L-aspartate	3
L-glutamine	4
L-glutamate	5
L-proline	6
L-serine	7
Pyruvate	8

Table 5.5. Compounds identified in the culture medium by GC/MS at 48 h of culture in percentage compared to the concentration at 0 h of culture. Abbreviations: ala – alanine; asp – aspartate; glu - glutamate; pro – proline; thr – threonine; tyr – tyrosine; cit – citrate; lac – lactate; succ – succinate.

Compounds identified	**Experiments**							
	1	2	3	4	5	6	7	8
ala	__	↓ (0%)	↓ (0%)	↓ (0%)	↓ (0%)	↓ (0%)	↓ (0%)	↓ (0%)
asp	↓ (0%)	↓ (0%)	__	↓ (0%)	↓ (0%)	↓ (0%)	↓ (0%)	↓ (0%)
glu	↓(83%)	↑(106%)	↓ (0%)	↓ (0%)	__	↑(108%)	↓ (0%)	↓ (99%)
pro	↓ (0%)	↓ (0%)	↓ (0%)	↓ (0%)	↓ (0%)	__	↓ (0%)	↓ (18%)
thr	↑ *	↑ *	↑ *	↑ *	↑*	n.d.	n.d.	n.d.
tyr	n.d.	n.d.	n.d.	↑(274%)	↑(265%)	n.d.	n.d.	n.d.
cit	↓(36%)	↓ (42%)	↑(265%)	↑(146%)	↑(117%)	↓ (57%)	↓ (91%)	↓ (42%)
lac	↓ (0%)	↓ (0%)	↓ (0%)	↓ (0%)	↓ (0%)	↓ (0%)	↓ (0%)	↓ (0%)
succ	↓(81%)	↑(105%)	↓ (24%)	↓ (64%)	↓ (50%)	↑(106%)	↑(118%)	↑(108%)

↓ - represents a decrease of that compound in the culture medium from 0 to 48 h; ↑- represents an increase of that compound in the culture medium; "n.d." – means that the compound was not detected in neither at 0 nor at 48 hours; __ – means that the compound was not accounted here since it is the chosen carbon source for that experiment. * means that this compound was not present at 0 hours of culture, only was detected at 48 hours of culture.

Chapter 6

Characterization of the growth of *H. pylori* using glutamate as the main carbon source

Daniela Matilde Correia, Rafael Carreira, Maria João Vieira, Nuno Filipe Azevedo and Isabel Rocha.

Characterization of the growth of *H. pylori* using glutamate as the main carbon source.

(To be submitted)

6.1. *Abstract*

The determination of nutritional requirements of pathogenic organisms is of great significance for understanding host-pathogen interactions. For *H. pylori*, some nutritional requirements have been disclosed; however, relevant information is still missing. Although amino acids have been identified as possible carbon sources for *H. pylori*, in the few described defined or semi-defined media several potential carbon sources are made available and the consumed ones are not clearly identified. Thus, the present work was conducted with the goal of uncovering the metabolic capacities of *H. pylori*, its nutritional requirements and the most commonly used metabolic pathways.

As such, the growth of *H. pylori* 26695 in liquid medium using L-glutamate as the main carbon source was studied. Additionally, ^{13}C L-glutamate was used to clarify some metabolic features. The obtained results confirmed L-glutamate as a potential sole and effective carbon source for *H. pylori*, also corroborating the essentiality of the amino acids isoleucine, histidine, leucine, methionine, phenylalanine and valine. We were also able to demonstrate that, under the conditions used, *H. pylori* makes full usage of the complete TCA cycle. Additionally, we hypothesized that L-proline is produced from L-arginine, while L-alanine is probably produced from pyruvate by alanine dehydrogenase.

Keywords: *Helicobacter pylori*, metabolomics, ^{13}C labeling.

6.2. *Introduction*

Despite the knowledge obtained so far concerning amino acid requirements in *H. pylori*, it is still unclear which are the metabolic pathways used for biosynthesis and catabolism. Thus, information on the carbon flow in this organism is required. Glutamate is a very important metabolite in bacterial metabolism that can be used as a carbon and nitrogen source. As described by other authors[1,2] and shown in our previous studies, glutamate and glutamine can be used by *H. pylori* as sole carbon sources, with succinate, acetate and formate having been identified as metabolic by-products of glutamate consumption in *H. pylori*[6]. Glutamate plays yet another relevant role, as D-glutamate is an essential metabolite for the biosynthesis of peptidoglycan for the cell wall. Strategies of glutamate racemase inhibition have been investigated in the last years[3], since this enzyme converts L-glutamate to D-glutamate.

^{13}C flux analysis has been largely applied to characterize phenotypes[4] by quantifying *in vivo* the carbon fluxes. One of the most important applications of this approach is the identification of active pathways in less-studied organisms[5]. In ^{13}C labeling experiments, an isotopic labeled substrate is used, and after an isotopic steady-state is achieved, free metabolites can be analyzed or proteinogenic amino acids can be measured after biomass hydrolysis. The analysis of the amino acids present in protein biomass is often preferred, since it provides broad labeling information and is less affected by errors, allowing to infer about active metabolic pathways and the carbon flow[6].

In order to characterize the growth of *H. pylori* using glutamate as substrate, this bacterium was grown under semi-defined conditions using a medium with L-glutamate as the main carbon source. A metabolic footprinting, together with a metabolite profiling approach was applied to identify the consumption and secretion of metabolites into the culture medium. This experiment was performed with different objectives: first, the results from the screening described in the previous chapter for the use of glutamate as the main carbon source needed to be validated with more replicates and it was also important to characterize in more detail the consumption of this compound. Furthermore, this characterization was important for the design of ^{13}C labeling experiments with ^{13}C-glutamate

that aimed at clarifying the metabolic pathways used by *H. pylori* under defined conditions by analyzing the labeled amino acids in biomass hydrolysates.

6.3. *Methods*

6.3.1. Culture conditions

Helicobacter pylori 26695 (strain NCTC 12455) was cultivated in Columbia Base Agar (CBA) (Liofilchem, Italy) supplemented with 5% (v/v) defibrinated horse blood (Probiologica, Portugal) at 37 °C under microaerophilic conditions (5% O_2, 10% CO_2, 85% N_2) in a Cell Culture Incubator (Incubator HERAcell 150, Kendro Laboratory, Germany) for 3 days.

An inoculum was prepared in Ham's F-12 nutrient mixture with glutamine (Medium composition detailed in Chapter 5) previously supplemented with 5% of fetal bovine serum (FBS) (vol/vol) (catalog no 10500-064, origin: South America, Invitrogen-Gibco, Spain), incubated at 37 °C under 130 rpm of shaking speed (Heidolph Unimax 1010 orbital shaker, Germany) in microaerophilic conditions (5% O_2, 10% CO_2, 85% N_2) for approximately 16 h, in order to reach the exponential phase. Afterwards, cells were harvested by centrifugation (5000 x *g*, 10 min.), washed twice in phosphate buffer saline (PBS) and ressuspended in culture medium. The initial Optical Density at 600 nm was adjusted to 0.06 - 0.07. Each experiment was performed in 1000-mL Erlenmeyer flasks with 150 mL of the medium described in Table 6.1. Independent inocula were used to inoculate three Erlenmeyer flasks (biological replicates). The pH was adjusted to 7.0. The culture was incubated at 37 °C under 130 rpm of shaking speed under microaerophilic conditions (5% O_2, 10% CO_2, 85% N_2). The experiment was carried out during 48 hours.

6.3.2. Culture medium

The culture medium used was chosen based on the results described in Chapter 5, with glutamate. The medium composition is described in Table 6.1, based on Ham's F-12 nutrient mixture. The medium was supplemented with 5% fetal bovine serum (FBS) (vol/vol) and was prepared in distilled water and filter-sterilized using a filtration unit Sartolab P20, 0.2 µm (Sartorius, Germany).

Table 6.1. Culture medium composition.

	Compounds (concentration)
Amino acids	L-arginine (10 mM), L-histidine (1 mM), L-isoleucine (0.3 mM), L-leucine (1 mM), L-methionine (0.3 mM), L-phenylalanine (0.3 mM), L-valine (1 mM), L-glutamate (1 mM)
Inorganic salts	Calcium chloride (0.2993 mM), Cupric sulphate (0.00001 mM), Ferric sulphate (0.003 mM), Magnesium chloride (0.6010 mM), Potassium chloride (2.981 mM), Sodium bicarbonate (14 mM), Sodium chloride (131 mM), Sodium phosphate dibasic anhydrous (1 mM), Zinc sulphate (0.0030 mM)
Vitamins	Biotin (0.00003mM), Choline chloride (0.1mM), D-calcium panthothenate (0.0010mM), Folic acid (0.0029mM), Niacinamide (0.0003mM), Pyridoxine hydrochloride (0.0003mM), Riboflavin (0.0001mM), Thiamine hydrochloride (0.0009mM), Vitamin B12 (0.0010mM), *i*-inositol (0.1mM)
Other components	Hypoxanthine (0.0294mM), Linoleic acid (0.0003mM), Lipoic acid (0.0010mM), Phenol red (0.0032mM) Putrescine (0.0010mM), Thymidine (0.0029mM)

6.3.3. Growth assessment

During the cultures, biomass was determined by measuring the optical density (OD) to infer the cell dry weight (CDW). Samples were collected until 48 hours of culture to evaluate OD at 600 nm by using an ELISA microplate reader (TECAN Sunrise, Switzerland).

For cell dry weight determination, a calibration curve was made by filtering 10 mL of culture in pre-weighted 0.2 µm mixed cellulose esthers filters (Advantec, Japan). The filtrate was then dried in a microwave to a constant weight. The calibration curve is shown in supplementary material 1.

To verify culture purity, at each time point the bacterial culture was plated in Columbia base agar (CBA) (Liofilchem, Italy) supplemented with 5% (v/v) defibrinated horse blood and Tryptic Soy Agar (Liofilchem, Italy) media and then incubated at 37°C in microaerophilic and aerobic conditions, respectively, during 5-7 days.

6.3.4. Metabolites analysis

At each time point (0-48 hours) samples of the culture supernatant (1 mL, in triplicate) were collected to analyze amino and non-amino organic acids by GC-MS in order to measure the consumption of amino acids and detect possible by-products secreted by *H. pylori* (method performed according to Smart *et al.* (2010)[7] and detailed in Chapter 4).

Acetate production was assayed enzymatically by a UV kit (Acetic acid UV-method - Cat. No. 10 148 261 035, Boehringer Mannheim/R-Biopharm, Roche, Germany). (Experimental procedure according to kit's instructions).

6.3.5. ^{13}C labeling experiments

Using the same culture protocols as described above (medium in Table 6.1), experiments (3 biological replicates) using 100% uniformly labeled ^{13}C-glutamic acid ([U-^{13}C]-glutamic acid) (99%, Cambridge Isotope, USA) were performed. Biomass hydrolysates were analyzed to evaluate the incorporation of ^{13}Carbon. Briefly, at the late-exponential phase (9 hours of culture), cultures were harvested (total volume of the culture) and pelleted by centrifugation (7000 x *g*, 10 min.). Cell pellets were hydrolyzed in 6 M HCl (495 µL) with thioglycolic acid (5 µL) (to preserve some amino acids), at 105 °C for 24 hours in sealed vials. After hydrolysis, samples were neutralized with 10 M NaOH (100 µL). Then, samples were lyophilized during 24 hours and derivatized prior to GC-MS analysis, as described in Chapter 4 and summarized in Figure 6.1.

Samples (1 mL, in triplicate) were collected at 0 h and 9 h of culture for analysis of extracellular metabolites and treated as described in Chapter 4 for extracellular metabolite analysis.

A control experiment (with three biological replicates) with ^{12}C-glutamic acid was also performed.

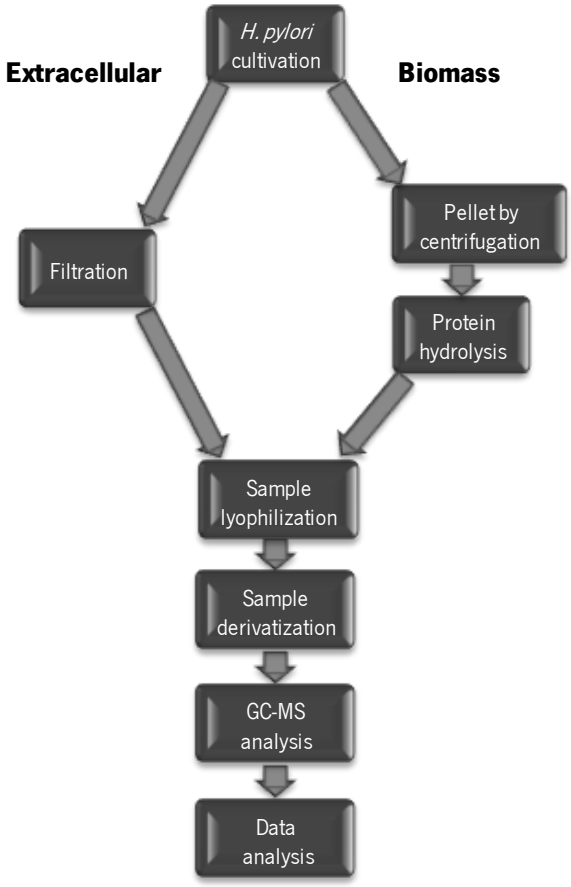

Figure 6.1. Flowchart applied for extracellular metabolites and biomass hydrolysates analysis by GC-MS.

6.3.6. Data analysis

Amino and organic acids present in the extracellular medium were identified using an in-house library, by matching retention time and mass spectrum, using the AMDIS software[8]. Data normalization was achieved by the normalization of the peak intensities by the intensity of the internal standard (d4 –alanine) in each sample. Data processing and analysis were performed with Excel and Multi Experiment Viewer (MeV)[9].

Amino acids present in the protein of biomass hydrolysates were identified using the same library as for extracellular metabolites. In order to analyze the ^{13}C labeling patterns, from each major fragment (or molecular ion) generated by MS fragmentation of

the amino acids obtained from biomass hydrolysates, mass fractions were calculated for each mass isotopomers (*m+0, m+1*, *m+2*, *m+3...m+n*) with *n* being number of carbons isotopicaly labeled.

Those ratios were compared with those found in natural metabolites (from cells grown in ^{12}C-glutamic acid). A correction of natural abundance of each atom was applied for the atomic composition of each mass fragment analyzed. A correction for unlabeled biomass was also performed by subtraction of the inoculum contribution (about 60% in the performed experiments). The mass fragments used for the final analysis were chosen based on abundance and on the amount of information that could be obtained from each one. Fractional labeling for those fragments were calculated based on Equation 6.1[10] using the mass fractions calculated.

$$\mathrm{FL} = \frac{\sum_{i=0}^{n} i.m_i}{n \sum_{i=0}^{n} m_i}$$ Equation 6.1.

Where *n* is the number of amino C atoms in the fragment, and *mi* is the mass isotopomers fractions, *i*s the number of labeled carbons in each fraction

The labeling patterns of the amino acids were used to infer about active metabolic pathways.

6.4. *Results and Discussion*

6.4.1. Growth of *H. pylori* with glutamate

Based on previous experiments, glutamate was selected as the most suitable carbon source for the growth of *H. pylori*. The growth curve of *H. pylori* 26695 growing using glutamate as carbon source is depicted in Figure 6.2. The growth parameters calculated for the experiments performed are showed in Table 6.2. The exponential phase occurred between 2 and 10 hours of growth, with a specific growth rate of 0.126 h^{-1}

(doubling time of 5.6 hours), which is consistent with the value obtained in the previous chapter in the carbon source screening experiments. It is not possible to compare this value with other media using a sole carbon source because, to the best of our knowledge, experiments with only one carbon source with *H. pylori* have not been reported in the literature. Nevertheless, previous reports indicate that *H. pylori* 26695 is one of the *H. pylori* strains with the lowest growth rates [11].

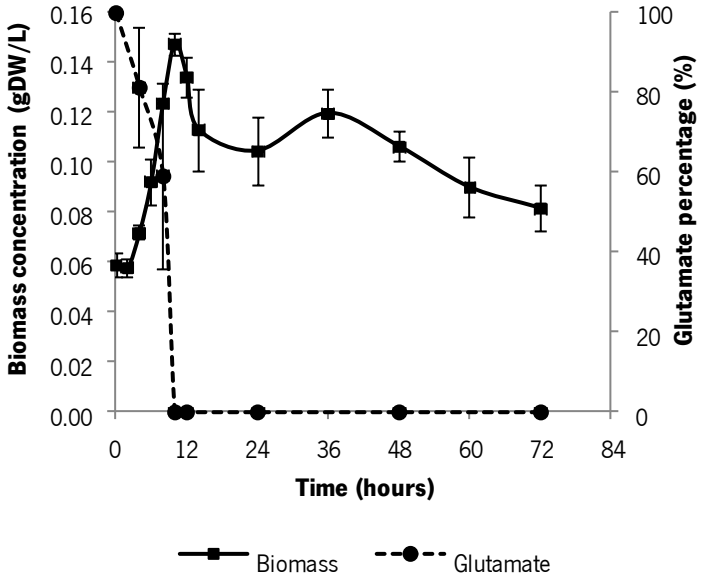

Figure 6.2. Biomass concentration represented by Cell Dry Weight (CDW) and L-glutamate in the culture medium along time as a percentage of the initial concentration. Mean of three biological replicates. Error bars represent standard deviation at each time point.

Table 6.2. Growth parameters for *H. pylori* 26695 growing in liquid medium with L-glutamate.

Exponential phase (h)	**Specific growth rate (h^{-1}) mean ± std dev**	**Doubling time (h) mean ± std dev**	**Biomass yield (Yx/s) (g g^{-1})* mean ± std dev**
2 – 10	0.126 ± 0.004	5.6 ± 0.2	0.60 ± 0.05

*Calculated for glutamate.

6.4.2. Extracellular metabolites analysis

Metabolites present in the supernatant represent metabolites that were present or were secreted into the culture medium. Extracellular metabolites analysis was performed in order to evaluate if carbon sources and essential amino acids were effectively being consumed and identify by-products excreted by *H. pylori* at the conditions used. Figure 6.3. shows a heat map representing the percentages of amino and organic acids identified in the supernatant along the fermentation time (numeric values for those percentages and standard deviations for the biological replicates can be found in supplementary material 2 - Table 6.3). Some compounds that were completely consumed (L-alanine, L-proline, L-aspartate and lactate) were not added to the culture medium and were present in low concentrations due to the 5% of FBS added, as described in detail in the previous chapter. The consumption occurs by the following order: L-proline, lactate, L-aspartate and L-alanine. L-glutamate was completely consumed within the first 10 hours of growth, corresponding to the exponential phase (Figure 6.2). Lactate was present in the culture medium but was not accumulated and was completely consumed, suggesting that it is being used as an extra carbon source. Takahashi *et al*. (2007), also detected an improvement in the growth of *H. pylori* in the presence of L-lactate secreted by gastric mucosal cells[12].

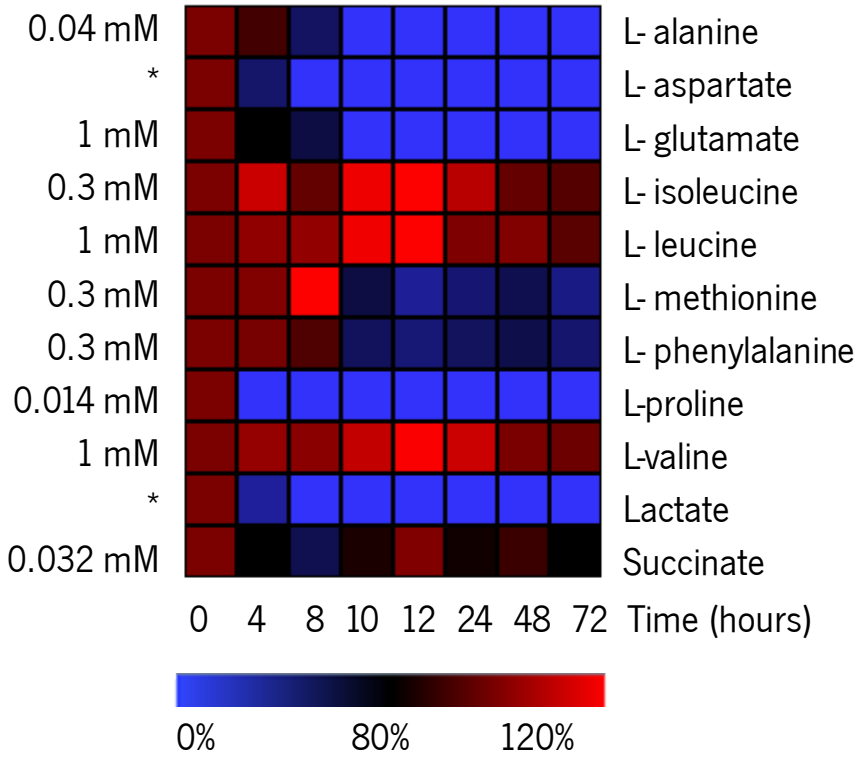

Figure 6.3. Heat map obtained with MeV[9] representing the compounds identified in the supernatant of the *H. pylori* culture along the fermentation time as a percentage of the initial concentration (of three biological replicates). * Detected.

Regarding the by-products that could be secreted by *H. pylori*, acetate was analyzed by an enzymatic kit, and was not detected in the supernatant of the culture, which is in agreement with the results obtained in the previous chapter but in contrast with the results reported by Mendz *et al.* (1995), that detected acetate as a metabolic product of glutamate consumption by *H. pylori*[2]. The observed differences may be due to differences in the *H. pylori* strain or the experimental conditions used. Succinate, another by-product detected by Mendz *et al.* (1995)[2], was present in the culture medium due to FBS, was consumed during the exponential phase and secreted after this phase, with a consumption after 12 hours of culture (Figure 6.3).

6.4.3. ^{13}C labeling analysis

Labeling experiments using ^{13}C L-glutamate were performed and the biomass hydrolisate was analyzed by GC-MS. In those ^{13}C labeling experiments, extracellular metabolites were also analyzed at 0 hours and at 9 hours of culture. The metabolite profiles obtained were similar to the ones obtained for the non-labeled experiments described in the previous section. Glutamate was not completely consumed, remaining about 38% of its initial concentration in the culture medium when the biomass was collected for hydrolysis (9 hours), which confirms that the cells were in the exponential phase as required for the experiment. As described in the methods section, a control experiment (with ^{12}C glutamate) was used to confirm that no isotopes fragments were observed in the mass spectra of the amino acids resulting from biomass hydrolisates, besides the natural isotopic abundance.

The mass fraction calculation allows determining the contribution of the labeling in each carbon of the analyzed fragments. The mass fractions obtained for each fragment of the amino acids analyzed are shown in supplementary material 3 (Table 6.4). The fractional labeling calculated for the major fragments observed for each amino acid is depicted in Figure 6.4 and the selected fragments are shown in the supplementary material 4. A correction for the unlabeled biomass, which is derived from the inoculum, was applied. The inoculum contribution in this case is very high (about 60%), due to the low growth observed. The fractional labeling without unlabeled biomass correction is also depicted in Figure 6.4. The information obtained with the calculation of the fractional labeling allows to conclude about the percentage of each molecule that is labeled and to infer about the active metabolic pathways.

Several amino acids did not show any labeling (isoleucine, histidine, leucine, methionine, phenylalanine and valine), while others are not measurable due to technical limitations already reported in the previous chapters (arginine). The fact that isoleucine, histidine, leucine, methionine phenylalanine and valine are not labeled confirms their status as essential amino acids, as hypothesized in Chapter .4

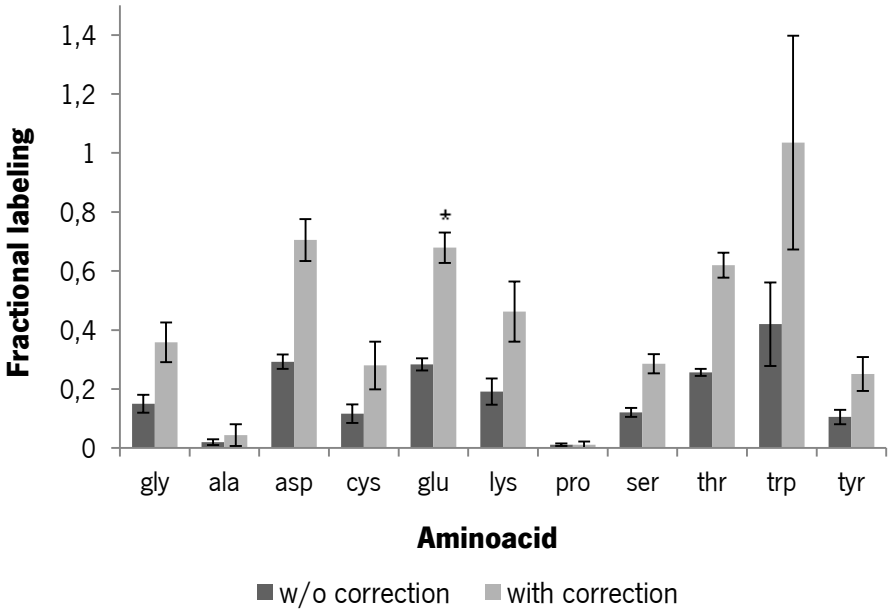

Figure 6.4. Fractional labeling (with and without unlabeled biomass correction) calculated for each amino acid present in the protein of biomass hydrolysates. Mean of three biological replicates. Error bars represent standard deviation. *asparagine and glutamine included in aspartate and glutamate, respectively.

During biomass hydrolysis, asparagine and glutamine are deaminated to aspartate and glutamate, respectively. Tryptophan and cysteine are also partially degraded during protein hydrolysis. Thus, thioglycolic acid, a reduced agent, was added in order to avoid tryptophan degradation[13]. Also, in the biomass of *H. pylori*, tryptophan and cysteine are present in very low percentages, only accounting for 1% (each) of the total proteinogenic amino acids (estimated from the genome). Thus, the analysis of these amino acids in biomass hydrolysates is not accurate, explaining the high standard deviation observed for the fractional labeling of tryptophan. Nevertheless, both amino acids appeared labeled, showing that they are being produced with a contribution of carbon from L-glutamate.

The fractional labeling of L-glutamate in biomass is around 0.7 (with unlabeled biomass correction), suggesting that L-glutamate is also being produced from other compounds. One possible source of L-glutamate is for instance L-proline, which can be converted into L-glutamate in two steps[14]. Another possibility is that lactate, that is being

consumed, is also contributing with carbon by conversion to pyruvate (by lactate dehydrogenase), and subsequent incorporation in the tricarboxylic acid (TCA) cycle, thus contributing probably not only for unlabeled glutamate but also for other unlabeled amino acids. L-glutamine, determined together with L-glutamate, is directly produced from L-glutamate by glutamine synthetase (glnA, HP0512), with ATP consumption[15], as described in the previous chapter.

L-proline is the only amino acid that is not labeled, besides the known required amino acids. L-proline, which is present in FBS, appeared in the extracellular culture medium at a very low concentration (Figure 6.3). Testerman *et al*. (2006) determined that L-proline is essential for *H. pylori* growth[16], although *in silico* it is not an essential nutrient[17], as mentioned in Chapter 4. It seems that the need of L-proline could be strain specific[18,19]. As mentioned in Chapter 4, there are two possible biosynthetic routes of L-proline in *H. pylori*, the first one from L-glutamate (via L-glutamate 5-semialdehyde and L-1-pyrroline 5-carboxylate), with the enzymes involved in that pathway identified by sequence homology[20]. The second one is from L-arginine, an absolute requirement for *H. pylori* growth. In that case, L-arginine is converted to ornithine, and subsequently to L-glutamate 5-semialdehyde, which will be converted to L-proline via L-1-proline-carboxylase. However, the conversion from ornithine to L-glutamate 5-semialdehyde is not proved in *H. pylori*[21]. In our previous studies (Chapter 5), proline was tested as a carbon source and the observed growth was quite low, although *H. pylori* seems to have the necessary enzymatic capabilities to degrade it. Although some uncertainty remains, proline auxotrophy is not proved in our results, since as shown in Figure 6.2 and Figure 6.3, L-proline is exhausted from the culture medium at 4 hours of culture while the exponential phase lasts until 10 hours of culture. Given the lack of labeling, it is likely that L-proline is synthesized in *H. pylori* from L-arginine rather than from L-glutamate, although further studies need to be performed to confirm this hypothesis.

Another doubtful topic about the nutritional requirements of *H. pylori* is the need of L-alanine. Similarly to L-proline, it has been described that L-alanine is an absolute nutritional requirement for some strains[18,19]. In *in silico* experiments described by Thiele *et al*. (2005), L-alanine can be used as a carbon source[17], although being essential.

Testerman *et al*. (2006) also described L-alanine as an essential amino acid[16]. In the present results, the fractional labeling of L-alanine is around 0.04, with a high standard deviation (0.04), explained by the low percentage of labeling. It is also important to highlight that alanine is present in FBS, and the low percentage of labeling is also due to that contribution. It seems that, despite the fact that there is a very high contribution of unlabeled carbon, L-glutamate also can contribute to L-alanine synthesis. The most plausible source of L-alanine is pyruvate, which could be obtained from L-lactate, as discussed above. In fact, *H. pylori* possess alanine dehydrogenase (ald; HP1398), which converts L-alanine into pyruvate and we have observed (results described in the previous chapter) that alanine can indeed be used effectively as a carbon source. However, despite the fact that the mentioned reaction is found to be reversible in several organisms, for instance in *Mycobacterium tuberculosis*[22], there is no certainty that it is reversible in *H. pylori*. Additionally, using eQuilibrator[23], a web interface created to estimate thermodynamic parameters, it is possible to confirm that the most favorable reaction direction in terms of energy is indeed the production of alanine from pyruvate. Another possible pathway for L-alanine production from pyruvate, which is used by *E. coli*, is through a transaminase such as valine-pyruvate transaminase or pyruvate-glutamate transaminase[21,24], which are not proved as present in *H. pylori*. Other authors also identified alanine production from pyruvate and suggested that this conversion is due to the action of a transaminase[25–27].

The fractional labeling of aspartate (with asparagine included) is around 0.7, showing that the carbon flow is passing through the TCA cycle with conversion of L-glutamate into alpha-ketoglutarate and further incorporation into the TCA cycle, being L-aspartate produced from oxaloacetate by a transaminase (aspartate transaminase). The presence of this transaminase was inferred from homology[15,20]. Since L-asparagine is not an absolute requirement for *H. pylori* growth, it is thought that L-asparagine is synthesized from L-aspartate, via a tRNA dependent process in three steps[21,28]. L-lysine and L-threonine, which have a fractional labeling of 0.5 and 0.61, respectively, can also be derived from L-aspartate[15,29]. The biosynthesis of L-lysine is achieved from L-aspartate using the

diaminopimelate pathway, involving succinylated intermediates[21,30]. Threonine, in turn, is synthesized from L-aspartate via homoserine[21].

The biosynthesis of L-tyrosine is known to be achieve with chorismate as precursor, sharing several steps with L-tryptophan biosynthesis[21,31] The fractional labeling of tyrosine is around 0.25, showing again a high contribution of unlabeled carbon sources, that could be explained by the low level of pyruvate labeling, as discussed previously.

It is described that L-serine biosynthesis occurs through 3-phospho-D-glycerate, an intermediary of glycolysis/gluconeogenesis, and that it can be a precursor for the production of L-cysteine and glycine. However, the fractional labeling of glycine is higher (0.36) than the one observed for serine (0.28). Given the standard deviations observed, this difference might not be meaningful. Nevertheless, if validated, this could mean that L-serine is probably being produced from another pathway. The conversion of L-serine to glycine is achieved by a single reaction catalyzed by serine hydroxymethyltransferase (glyA, HP0183)[21]. There is no certainty about the reversibility of this reaction in *H. pylori*, although for *E. coli* it is described that the conversion of glycine to L-serine can also occur, meaning that glycine would have another biosynthetic route, such as from threonine by threonine aldolase with the production of acetaldehyde. In fact, this biosynthetic route has not been reported for *H. pylori* but is reported for other organisms such as *E. coli*[21]. Serine can also be converted to pyruvate, as it was reported by Mendz *et al.* (1994) that serine is one of the major sources of pyruvate[26] in *H. pylori*. The fractional labeling of cysteine (0.28) is similar to the one observed for serine (0.28), consistent with the described biosynthesis of cysteine from serine in two steps through *O*-acetyl-L-serine, with production of acetate[21].

The metabolic pathways proposed to be active under the conditions used are represented in Figure 6.5 .

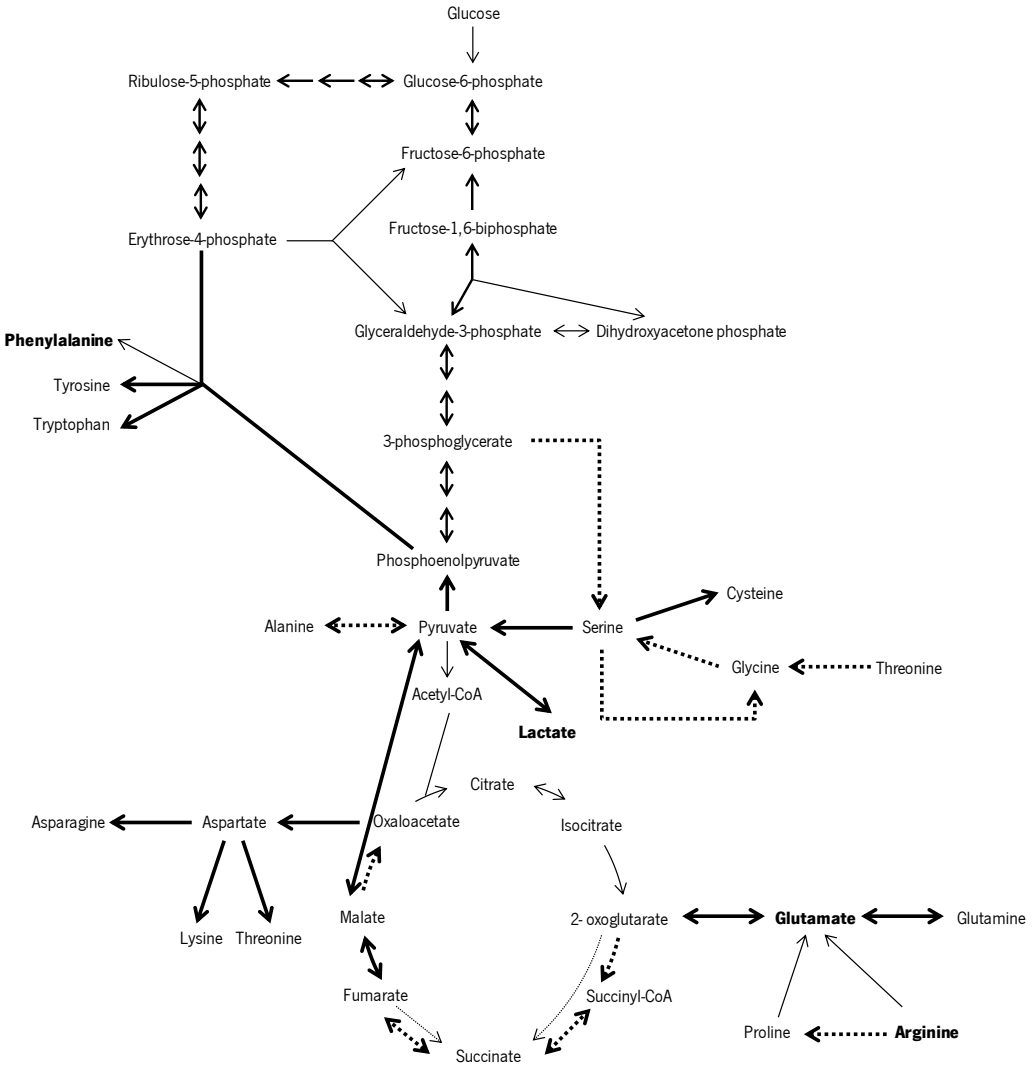

Figure 6.5. Schematic representation of *H. pylori*'s metabolic pathways active under the conditions of the described experiments. Compounds added to the culture medium are shown in bold. Arrows in bold represent the hypothetical carbon flow through known pathways in *H. pylori*. Dashed arrows represent possible steps for which there is no certainty.

6.5. *Conclusions*

The present study attempted to analyze the growth of *H. pylori* using L-glutamate as the main carbon source. An exometabolome analysis allowed determining the consumption pattern of the compounds present in culture medium. Under the conditions used, no acetate production was detected, showing that no fermentation is occurring. Additionally, the carbon flow was determined using ^{13}C L-glutamate as the carbon source and measuring the labeling in proteinogenic amino acids, making this, to the best of our knowledge, the first study conducted with the goal of determining the carbon flow in *H. pylori*. Despite the use of fetal bovine serum, which contributed with lactate and consequently with unlabeled carbon, it was proved that glutamate is indeed the main carbon source under the conditions used and that it can be used as the sole carbon source, as suggested by other authors[2].

Overall, all amino acids suggested as non-essential in Chapter 4, except proline, presented a ^{13}C labeling pattern. Although a definite proof is still needed, our results indicate that L-proline is not an essential amino acid and indicate that it is probably produced from L-arginine, which is present in the culture medium as an essential amino acid. Despite the controversy around the need of L-alanine as an absolute requirement, in the present study a low percentage of ^{13}C labeling was detected in L-alanine, suggesting it can be produced by *H. pylori*, potentially from pyruvate. However, in order to confirm this result, experiments without FBS are needed. Finally, contributing to clarify the controversy around the existence of a complete TCA cycle in *H. pylori*, evidences were obtained with the presence of labeled aspartate.

Finally, the fact that the amino acids isoleucine, histidine, leucine, methionine, phenylalanine and valine did not exhibit any labeling corroborates their essentiality.

6.6. *References*

1. Stark, R. M., Suleiman, M. S., Hassan, I. J., Greenman, J. & Millar, M. R. Amino acid utilisation and deamination of glutamine and asparagine by *Helicobacter pylori*. *J. Med. Microbiol.* **46,** 793–800 (1997).
2. Mendz, G. L. & Hazell, S. L. Aminoacid utilization by *Helicobacter pylori*. *Int. J. Biochem. Cell Biol.* **27,** 1085–1093 (1995).
3. Basarab, G. S. *et al.* Design of inhibitors of *Helicobacter pylori* glutamate racemase as selective antibacterial agents: incorporation of imidazoles onto a core pyrazolopyrimidinedione scaffold to improve bioavailabilty. *Bioorg. Med. Chem. Lett.* **22,** 5600–5607 (2012).
4. Tang, Y. J. *et al.* Advances in analysis of microbial metabolic fluxes via 13C isotopic labeling. *Mass Spectrom. Rev.* **28,** 362–375 (2009).
5. Zamboni, N. & Sauer, U. Novel biological insights through metabolomics and 13C-flux analysis. *Curr. Opin. Microbiol.* **12,** 553–558 (2009).
6. Wittmann, C. Fluxome analysis using GC-MS. *Microb. Cell Fact.* **6,** 1–17 (2007).
7. Smart, K. F., Aggio, R. B. M., Van Houtte, J. R. & Villas-Bôas, S. G. Analytical platform for metabolome analysis of microbial cells using methyl chloroformate derivatization followed by gas chromatography-mass spectrometry. *Nat. Protoc.* **5,** 1709–1729 (2010).
8. Davies, A. N. The new automated mass spectrometry deconvolution and identification system (AMDIS). *Spectrosc. Eur.* **10,** 24–27 (1998).
9. Saeed, A. I. *et al.* TM4: a free, open-source system for microarray data management and analysis. *Biotechniques* **34,** 374–378 (2003).
10. Nanchen, A., Fuhrer, T. & Sauer, U. in *Methods Mol. Biol. vol. 358 Metabolomics Protoc.* (Weckwerth, W.) **358,** 177–197 (Humana Press Inc., 2007).
11. Douraghi, M. *et al.* Comparative evaluation of three supplements for *Helicobacter pylori* growth in liquid culture. *Curr. Microbiol.* **60,** 254–262 (2010).
12. Takahashi, T. *et al.* L-lactic acid secreted from gastric mucosal cells enhances growth of *Helicobacter pylori*. *Helicobacter* **12,** 532–540 (2007).
13. Davidson, I. in *Methods Mol. Biol. Vol. 211 Protein Seq. Protoc.* (Smith, B. J.) **211,** 111–122 (2003).

14. Krishnan, N. & Becker, D. F. Oxygen reactivity of PutA from *Helicobacter* species and proline-linked oxidative stress. *J. Bacteriol.* **188,** 1227–1235 (2006).

15. Tomb, J.-F. *et al.* The complete genome sequence of the gastric pathogen *Helicobacter pylori*. *Nature* **388,** 539–547 (1997).

16. Testerman, T. L., Conn, P. B., Mobley, H. L. T. & McGee, D. J. Nutritional requirements and antibiotic resistance patterns of *Helicobacter* species in chemically defined media. *J. Clin. Microbiol.* **44,** 1650–1658 (2006).

17. Thiele, I., Vo, T. D., Price, N. D. & Palsson, B. Ø. Expanded metabolic reconstruction of *Helicobacter pylori* (ΔT341 GSM/GPR): an *in silico* genome-scale characterization of single- and double-deletion mutants. *J. Bacteriol.* **187,** 5818–5830 (2005).

18. Nedenskov, P. Nutritional requirements for growth of *Helicobacter pylori*. *Appl. Environ. Microbiol.* **60,** 3450–3453 (1994).

19. Reynolds, D. J. & Penn, C. W. Characteristics of *Helicobacter pylori* growth in a defined medium and determination of its amino acid requirements. *Microbiology* **140,** 2649–2956 (1994).

20. Magrane, M. & Consortium, U. UniProt Knowledgebase: a hub of integrated protein data. *Database* **2011,** 1–13 (2011).

21. Caspi, R. *et al.* The MetaCyc database of metabolic pathways and enzymes and the BioCyc collection of pathway/genome databases. *Nucleic Acids Res.* **40,** D742–D753 (2012).

22. Hutter, B. & Singh, M. Properties of the 40 kDa antigen of *Mycobacterium tuberculosis*, a functional L-alanine dehydrogenase. *Biochem. J.* **672,** 669–672 (1999).

23. Flamholz, A., Noor, E., Bar-Even, A. & Milo, R. eQuilibrator - the biochemical thermodynamics calculator. *Nucleic Acids Res.* **40,** D770–D775 (2012).

24. Rudman, D. & Meister, A. Transamination in *Escherichia coli*. *J. Biol. Chem.* **200,** 591–604 (1953).

25. Chalk, P. A., Roberts, A. D. & Blows, W. M. Metabolism of pyruvate and glucose by intact cells of *Helicobacter pylori* studied by 13C NMR spectroscopy. *Microbiology* **140,** 2085–2092 (1994).

26. Mendz, G. L., Hazell, S. L. & van Gorkom, L. Pyruvate metabolism in *Helicobacter pylori*. *Arch. Microbiol.* **162,** 187–192 (1994).

27. Kaihovaara, P., Höök-Nikanne, J., Uusi-Oukari, M., Kosunen, T. U. & Salaspuro, M. Flavodoxin-dependent pyruvate oxidation, acetate production and metronidazole reduction by *Helicobacter pylori*. *J. Antimicrob. Chemother.* **41,** 171–177 (1998).

28. Fischer, F. *et al.* The asparagine-transamidosome from *Helicobacter pylori*: a dual-kinetic mode in non-discriminating aspartyl-tRNA synthetase safeguards the genetic code. *Nucleic Acids Res.* **40,** 4965–4976 (2012).

29. Doig, P. *et al. Helicobacter pylori* physiology predicted from genomic comparison of two strains. *Microbiol. Mol. Biol. Rev.* **63,** 675–707 (1999).

30. Velasco, a M., Leguina, J. I. & Lazcano, A. Molecular evolution of the lysine biosynthetic pathways. *J. Mol. Evol.* **55,** 445–459 (2002).

31. Marais, A., Mendz, G. L., Hazell, S. L. & Mégraud, F. Metabolism and genetics of *Helicobacter pylori*: the genome era. *Microbiol. Mol. Biol. Rev.* **63,** 642–674 (1999).

6.7. *Supplementary material*

6.7.1. Supplementary material 1

A biomass calibration curve was achieved by plotting the cell dry weight (CDW) versus the optical density at 600 nm. The calibration curve obtained is depicted in Figure 6.6.

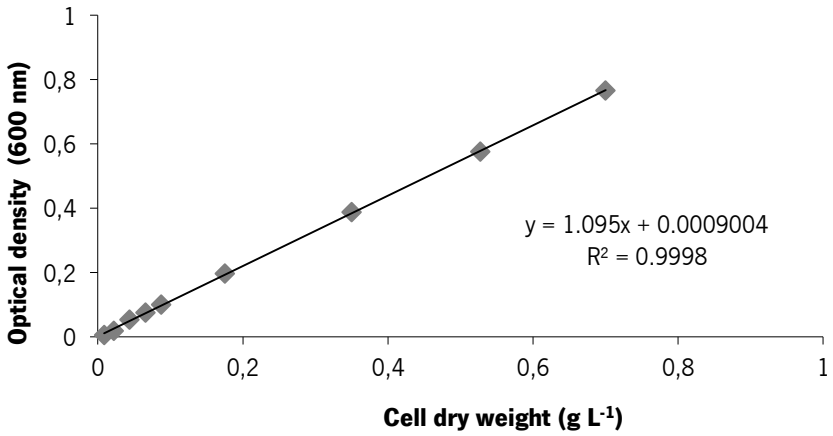

Figure 6.6. Biomass calibration curve.

6.7.2. Supplementary material 2

Table 6.3 shows the compounds identified in the medium and the respective percentage of the initial concentration along the fermentation time obtained by GC-MS after derivatization with methylchloroformate (method described in Chapter 3).

Table 6.3. Evolution of the compounds identified in the culture medium as a percentage of the initial concentrations obtained by GC/MS. Mean of three biological replicates with three technical replicates. Mean ± Standard deviation. Abbreviations: L-ala – L-alanine; L-asp – L-aspartate; L-glu – L-glutamate; L-ile – L-isoleucine; L-leu – L-leucine; L-met – L-methionine; L-phe – L-phenylalanine; L-pro – L-proline; lac – lactate; succ – succinate; L-val – L-valine.

Compounds identified	Time (hours)						
	4	8	10	12	24	48	72
L-ala	91% (± 22)	50% (±19)	0%	0%	0%	0%	0%
L-asp	detected	0%	0%	0%	0%	0%	0%
L-glu	81% (± 15)	59% (±23)	0%	0%	0%	0%	0%
L-ile	112% (± 26)	96% (±9)	118% (± 19)	125% (±31)	110% (± 29)	97% (±14)	94% (± 15)
L-leu	104% (± 12)	104% (±11)	118% (± 31)	120% (±37)	100% (± 3)	101% (±15)	95% (± 14)
L-met	101% (± 21)	126% (±18)	59% (± 32)	33% (±27)	45% (± 22)	56% (±23)	39% (± 23)
L-phe	99% (± 61)	93% (±40)	52% (± 29)	43% (±23)	51% (± 27)	57% (±25)	46% (± 16)
L-pro	0%	0%	0%	0%	0%	0%	0%
L-val	104% (± 10)	102% (±10)	111% (± 8)	120% (±18)	112% (± 20)	100% (±14)	98% (± 13)
lac	detected	0%	0%	0%	0%	0%	0%
succ	80% (± 28)	55% (±7)	85% (± 29)	101% (±41)	84% (± 21)	90% (±17)	81% (± 13)

6.7.3. Supplementary material 3

Table 6.4 shows the mass fractions calculated for each fragment analyzed for each derivatized amino acid in biomass hydrolysates.

Table 6.4. Mass fractions calculated for mass isotopomers of each derivatized amino acid in biomass hydrolysates. Mean of three biological replicates (± standard deviation). *m*, *m+1*, *m+2*, *m+3*...*m+n* – mass isotopomer, *n* – number of carbons isotopicaly labeled.

Amino acid (mass to charge ratio of the ion cluster)	Mass isotopomer	Mass fraction	
		Without unlabeled biomass correction	With unlabeled biomass correction
Glycine (148)	*m*	0.839 (± 0.035)	0.624 (± 0.081)
	m+1	0.039 (± 0.030)	0.064 (± 0.075)
	m+2	0.133 (± 0.032)	0.336 (± 0.075)
Alanine (162)	*m*	0.973 (± 0.024)	0.980 (± 0.061)
	m+1	0.001 (± 0.015)	-0.046 (± 0.038)
	m+2	0.012 (± 0.003)	0.030 (± 0.008)
	m+3	0.015 (± 0.009)	0.039 (± 0.023)
Aspartate/ Asparagine (220)	*m*	0.624 (± 0.028)	0.108 (± 0.090)
	m+1	0.052 (± 0.008)	0.068 (± 0.022)
	m+2	0.102 (± 0.002)	0.259 (± 0.013)
	m+3	0.035 (± 0.005)	0.089 (± 0.011)
	m+4	0.209 (± 0.026)	0.531 (± 0.079)
Cysteine (252)	*m*	0.863 (± 0.025)	0.702 (± 0.068)
	m+1	0.028 (± 0.024)	0.022 (± 0.060)
	m+2	0.004 (± 0.008)	0.010 (± 0.019)
	m+3	0.104 (± 0.033)	0.266 (± 0.085)

Table 6.4. Mass fractions calculated for mass isotopomers of each derivatized amino acid in biomass hydrolysates. Mean of three biological replicates (± standard deviation). *m*, *m+1*, *m+2*, *m+3*...*m+n* – mass isotopomer, *n* – number of carbons isotopicaly labeled. (Continue)

Amino acid (mass to charge ratio of the ion cluster)	**Mass isotopomer**	**Mass fraction**	
		Without unlabeled biomass correction	**With unlabeled biomass correction**
Glutamate/ Glutamine (234)	*m*	0.669 (± 0.027)	0.240 (± 0.071)
	m+1	0.018 (± 0.011)	-0.034 (± 0.027)
	m+2	0.034 (± 0.004)	0.085 (± 0.011)
	m+3	0.061 (± 0.007)	0.155 (± 0.015)
	m+4	0.029 (± 0.007)	0.073 (± 0.017)
	m+5	0.213 (± 0.018)	0.542 (± 0.053)
Lysine (277)	*m*	0.647 (± 0.093)	0.202 (± 0.222)
	m+1	0.055 (± 0.026)	0.045 (± 0.069)
	m+2	0.055 (± 0.028)	0.136 (± 0.070)
	m+3	0.107 (± 0.022)	0.270 (± 0.052)
	m+4	0.089 (± 0.029)	0.218 (± 0.072)
	m+5	0.017 (± 0.007)	0.042 (± 0.018)
	m+6	0.040 (± 0.017)	0.101 (± 0.042)
Proline (128)	*m*	0.958 (± 0.010)	0.958 (± 0.025)
	m+1	0.042 (± 0.005)	0.043 (± 0.013)
	m+2	-0.0006 (± 0.007)	-0.002 (± 0.010)
	m+3	-0.0003 (± 0.0001)	-0.0007 (± 0.0004)
	m+4	0.0008 (± 0.001)	0.002 (± 0.003)
Serine (178)	*m*	0.846 (± 0.016)	0.658 (± 0.034)
	m+1	0.040 (± 0.006)	0.053 (± 0.014)
	m+2	0.039 (± 0.002)	0.099 (± 0.003)
	m+3	0.082 (± 0.015)	0.207 (± 0.033)

Table 6.4. Mass fractions calculated for mass isotopomers of each derivatized amino acid in biomass hydrolysates. Mean of three biological replicates (± standard deviation). *m*, *m+1*, *m+2*, *m+3*...*m+n* – mass isotopomer, *n* – number of carbons isotopicaly labeled. (Continue).

Amino acid (mass to charge ratio of the ion cluster)	**Mass isotopomer**	**Mass fraction**	
		Without unlabeled biomass correction	**With unlabeled biomass correction**
Threonine (192)	*m*	0.676 (± 0.012)	0.241 (± 0.048)
	m+1	0.045 (± 0.003)	0.051 (± 0.008)
	m+2	0.080 (± 0.002)	0.203 (± 0.003)
	m+3	0.025 (± 0.002)	0.065 (± 0.005)
	m+4	0.190 (± 0.012)	0.484 (± 0.042)
Tryptophan (276)	*m*	0.186 (± 0.121)	-0.896 (± 0.300)
	m+1	0.102 (± 0.092)	0.099 (± 0.233)
	m+2	0.064 (± 0.093)	0.151 (± 0.233)
	m+3	0.045 (± 0.046)	0.114 (± 0.122)
	m+4	0.042 (± 0.033)	0.107 (± 0.084)
	m+5	0.103 (± 0.102)	0.260 (± 0.254)
	m+6	0.097 (± 0.093)	0.246 (± 0.233)
	m+7	0.235 (± 0.341)	0.593 (± 0.856)
	m+8	0.003 (± 0.046)	0.007 (± 0.115)
	m+9	0.054 (± 0.032)	0.136 (± 0.125)
	m+10	0.018 (± 0.032)	0.047 (± 0.083)
	m+11	0.063 (± 0.055)	0.162 (± 0.141)
Tyrosine (236)	*m*	0.644 (± 0.056)	0.239 (± 0.141)
	m+1	0.131 (± 0.029)	0.196 (± 0.074)
	m+2	0.062 (± 0.011)	0.152 (± 0.029)
	m+3	0.071 (± 0.015)	0.180 (± 0.039)
	m+4	0.035 (± 0.015)	0.089 (± 0.036)
	m+5	0.027 (± 0.005)	0.068 (± 0.015)
	m+6	0.017 (± 0.007)	0.043 (± 0.018)
	m+7	0.005 (± 0.002)	0.013 (± 0.006)
	m+8	0.003 (± 0.005)	0.007 (± 0.011)
	m+9	0.005 (± 0.009)	0.013 (± 0.022)

6.7.4. Supplementary material 4

Table 6.5 shows the mass of the ion fragments used to determine the fractional labeling for each amino acid and the respective fractional labeling with and without unlabeled biomass correction.

Table 6.5. Fractional labeling determined for the fragments used for each amino acid. Mean of three biological replicates (± standard deviation).

Amino acid	Mass ion fragments/ Number of amino acid carbons	Fractional labeling	
		Without unlabeled biomass correction	With unlabeled biomass correction
Glycine	148/3	0.150 (± 0.030)	0.359 (± 0.067)
Alanine	162/3	0.023 (± 0.015)	0.044 (± 0.037)
Aspartate/ Asparagine	220/4	0.293 (± 0.024)	0.705 (± 0.071)
Cysteine	252/3	0.117 (± 0.031)	0.280 (± 0.081)
Glutamate/ Glutamine	234/5	0.283 (± 0.020)	0.679 (± 0.051)
Lysine	277/6	0.191 (± 0.045)	0.463 (±0.102)
Proline	128/4	0.011 (± 0.004)	0.011 (± 0.011)
Serine	178/3	0.121 (± 0.015)	0.286 (± 0.032)
Threonine	192/4	0.256 (± 0.012)	0.620 (± 0.043)
Tryptophan	276/11	0.420 (± 0.142)	1.035 (± 0.362)
Tyrosine	236/9	0.105 (± 0.024)	0.251 (± 0.057)

Chapter 7

Reconstruction and validation of a genome–scale metabolic model for *Helicobacter pylori* 26695

Tiago Resende, Daniela Matilde Correia, Sophia Santos, and Isabel Rocha

Reconstruction and validation of a genome-scale metabolic model for *Helicobacter pylori* 26695

(To be submitted)

7.1 *Abstract*

Helicobacter pylori is a pathogenic bacterium that colonizes the human gastric epithelia, causing duodenal and gastric ulcers, and gastric cancer. The genome of *H. pylori* 26695 has been previously sequenced and annotated. In addition, two genome-scale metabolic models have been developed. In order to maintain accurate and relevant the information on this bacterium and to generate new information and new approaches for its analysis, the assignment of new functions to *H. pylori* 26695's genes was performed and a new genome-scale metabolic model was reconstructed.

Model reconstruction originated the *i*TR370 metabolic model, a compartmentalized model containing 370 genes and composed by 666 different reactions and 432 metabolites. Gene essentiality analysis was performed to assess the predictive capabilities of the model, and growth simulations were performed using experimental data to adjust the nutrients uptake rates. Finally, the flux distributions predicted by the model using L-glutamate as the sole carbon source were analyzed.

It is shown that the *i*TR370 metabolic model is useful for predicting *H. pylori*'s phenotypic responses to gene deletions, and allows a very good agreement with experimental results obtained for cultivation experiments using a minimal medium. This model provides relevant biological information for the scientific community dealing with this organism by allowing the elucidation of new features in *H. pylori*'s metabolism, assisting in the identification of new drug targets and the development of new approaches for enhanced treatments.

Keywords: *Helicobacter pylori*. Genome-scale metabolic model. Genome re-annotation.

7.2 Introduction

The introduction of whole-genome high-throughput sequencing techniques and the development of several bioinformatics tools have been generating a vast amount of new information, changing completely our understanding on hundreds of species[1]. However, in this post-genomic era, assigning functions to genes in a sequenced genome is still a complex and difficult task, involving several steps[2].

H. pylori 26695, which presents a small size genome of around 1.67 Mbp with an average C+G content of 39%, was the first *H. pylori* strain to have its genome sequenced in 1997[3]. The last re-annotation of this organism was published in 2003 and generated a specific on-line database for *H. pylori* (PyloriGene)[4]. It also reduced the percentage of hypothetical proteins from approximately 40% to 33%, allowing the reassignment of functions to 108 CDS (coding sequences)[4]

The reconstruction of metabolic networks allows the development of a genome-scale metabolic model based on the well-known stoichiometry of biochemical reactions catalyzed by the enzymes encoded in the annotated genes of an organism[5,6]. These models can then be used for simulating *in silico* the phenotypic behavior of a microorganism under different environmental and genetic conditions, thus representing an important tool in metabolic engineering and drug design[5]. Numerous drugs used for the treatment of pathogenic bacteria target metabolic enzymes, and therefore genome-scale modeling of bacterial metabolism provides a powerful tool to identify and analyze pathways required for infection[7].

Two genome-scale metabolic models have been published for *H. pylori* 26695[8,9]. The first model was published in 2002 (*i*CS291) with 291 genes and 388 reactions[8] and, in 2005, an updated version was published, which accounts for 341 genes and 476 reactions, also including 355 gene-protein-reaction (GPR) associations. These models were constructed with information mainly taken from the genome, as very scarce biochemical knowledge was available for *H. pylori*. However, in the last years, a vast amount of data have been published that can be used to upgrade and refine the published metabolic models. A new genome re-anotation was also recently published by the authors of this chapter[10]. As such, the aim of this work was to reconstruct a new genome-scale metabolic model using the updated re-annotation. Also, the physiological data collected in previous chapters was used to validate the model.

7.3 *Methods*

Before the development of a metabolic model, the metabolic network has to be reconstructed. This network is defined as the set of biological reactions catalyzed by enzymes encoded in the genome. After the reconstruction of the metabolic network, more information is added, in order to develop a metabolic model[5,11].

The applied methodology in reconstructing the genome-scale metabolic model of *H. pylori* 26695 is shown in Figure 7.1. Several steps were performed including the metabolic network assembly and subsequent conversion to the metabolic model after the implementation of a biomass equation.

The Model Reconstruction Tool, a module within the in-house *merlin* software (Metabolic Models Reconstruction using Genome-Scale Information)[12] (available for download at http://sysbio.uminho.pt/merlin/), was used throughout this work. Briefly, this tool allows the researcher to load generic and organism-specific reaction and metabolite information from KEGG[13], predict transport reactions, define pathways and integrate all the information with data from annotation. Afterwards, the draft metabolic model can be generated and stored in the Systems Biology Markup Language (SBML) format[12].

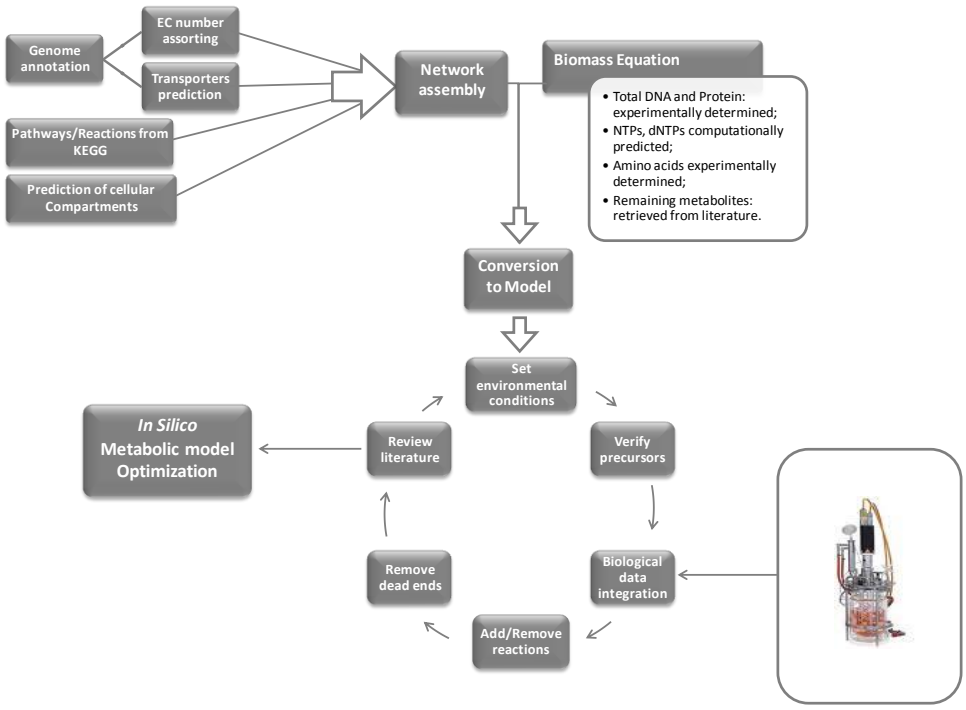

Figure 7.1. Genome-scale metabolic model reconstruction workflow.

7.3.1 Metabolic network assembly

Making use of the updated annotation[10] the reactions promoted by each complete EC number identified were retrieved from KEGG by *merlin*, and their metabolic information was used to assemble the draft network. In order to prevent an overload of futile reactions, gaps and dead ends in the network, due to the inclusion of every reaction associated to each EC number, *merlin* uses KEGG pathways. Thus, only reactions for which the corresponding EC number is present in the same pathways were included in the model. From KEGG, reactions classified as spontaneous were also included.

After the assembly of all enzymatic reactions encoded in the annotated genome and spontaneous reactions, transport reactions also need to be included, in order to allow the input and output of metabolites in the model. From the re-annotation[10], a list of all the transporter proteins identified from the genome was made available. From those, the elaboration of the transport reactions can be made automatically in *merlin*. However, as the number of metabolites that can be possibly transported by a transport protein is very large, only those which were already present in the reactions within the network were assigned with a transport reaction and included in the model, preventing the introduction of gaps.

7.3.2 Reactions compartmentation

Being *H. pylori* a prokaryote and despite its cell compartmentation being limited to the cytosol and the periplasmic space, information on protein location and reaction compartmentation is very important when reconstructing the metabolic model.

The prediction of the location and consequent assignment to compartments of enzymes and transport proteins was also performed using *merlin.* After the prediction of proteins localization, this information was integrated in the metabolic network.

7.3.3 Assignment of reversibility to reactions

The attribution of the correct reversibility to model reactions is very important. Models with an excess of reversible reactions are not sufficiently constrained, and futile cycles may occur, making the model unrealistic and causing problems during optimization[11]. In the KEGG database, all reactions are set to be reversible. To overcome this problem, in the reconstruction

of *H. pylori*'s model, a database developed by Stelzer *et al.* (2011)[14] was used to perform the initial assignment of reversibility to reactions. This database includes the assignment of reversibility to KEGG reactions, therefore facilitating its implementation in our work. Additionally, the estimation of the standard Gibbs free energy of formation ($\Delta_f G^\circ$) and of reaction ($\Delta_r G^\circ$) was also utilized to determine reaction reversibility. Those thermodynamic parameters can be used to determine how much energy is required for a particular biochemical reaction to occur and in which direction the reaction will flow under given cellular conditions. Standard Gibbs free energy values can be obtained for most KEGG reactions using eQuilibrator (http://equilibrator.weizmann.ac.il/), a web interface that enables thermodynamic analysis of biochemical reactions[15]. Because it cannot be automatically propagated to every reaction in the model, this approach was only used when information on reaction reversibility was scarce or when doubts occurred. Since the assignment of the wrong direction to a reaction has a significant impact in the model, if no information could be gathered, the reaction was left to be reversible.

7.3.4 Reactions stoichiometry

The stoichiometry of the metabolic reactions can be determined by balancing the elements on the substrate and product sides of the reaction. The KEGG database contains the charged formula for a large amount of metabolites within reactions; however, for some metabolites included in the model reconstruction, the charged formula lacked, resulting in unbalanced reactions. Another reason for the detected unbalanced reactions is the lack of protons and water molecules that many biochemical databases and textbooks omit in order to simplify the reactions[11]. Unbalanced reactions might spontaneously produce protons or ATP and therefore every metabolite must be in the correct amounts and correctly charged to balance both sides of the reaction. In most cases, unbalanced reactions were balanced by simply adding the missing proton or water molecule.

7.3.5 Gene-protein-reaction associations

In order to accurately determine gene essentiality and to improve the assignment of reactions to specific genes, gene-protein-reaction (GPR) associations are required features in a genome-scale metabolic model. In GPR associations, a single gene can be associated with a

single reaction, multiple reactions, or even be integrated among other genes in a reaction catalyzed by a protein complex. In these cases, the association of gene(s) to reaction(s) can be made by applying a Boolean rule, which can be "AND" or "OR, depending on if the presence of all genes is absolutely required or not for the reaction to occur, respectively.

The KEGG Brite database[13] was used within *merlin* to retrieve information from orthologues and a hierarchical classification and to create GPR associations in the metabolic network.

7.3.6 Biomass formation

The biomass equation is the most important reaction in the model. In this equation, all components considered essential to the overall cellular growth, with the corresponding fractional contributions are included. This reaction represents the biomass composition and is composed of several substrates that are originated in metabolic reactions of the model, and that can be divided in different categories: Protein, Nucleotides (DNA and RNA), Peptidoglycan, Lipopolysaccharide, Lipids, Cofactors and Energy. The same reaction has, as its products, besides biomass itself, orthophosphate, diphosphate and hydrogen.

As for the majority of bacteria, information on detailed biomass composition for *H. pylori* is not available. In the present work, the relative fractional contribution of biomass components was estimated either from the genome, experimentally, or retrieved from literature.

The first step was the estimation of the macromolecular composition of the biomass of *H. pylori*. Total protein and DNA content were experimentally determined from cultures of *H. pylori* in the exponential phase using Ham's F-12 (supplemented with 5% FBS) as growth medium (described in Chapter 4) using the Biuret[16] and fluorescence with DAPI[17] methods, respectively (detailed in Santos and Rocha (2013)[18]. Total content of RNA, lipids, peptidoglycan, lipopolysaccharide (LPS), and cofactors were retrieved from a genome-scale model of *E. coli* (*i*AF1260)[19] and their contribution was adjusted taking into account the content of the macromolecules experimentally determined (protein and DNA).

The RNA and DNA building-blocks, nucleoside triphosphates (NTPs) and deoxynucleoside triphosphates (dNTPs), respectively, were computationally predicted from the *H. pylori*'s genome sequence according to a published protocol[11] using a Java Tool (detailed in Santos and Rocha (2013)[18]. Monomers of proteins (amino acids) were also determined computationally using the genome sequence. In addition, amino acids were also confirmed experimentally by HPLC after

protein hydrolysis. The method used was the OPA and FMOC derivatives, with minor modifications[20].

The lipid building-blocks (fatty acids) composition was estimated according to the protocols described by Thiele and Palsson (2010)[11] and Bautista *et al.*, (2013)[21] . Data from specific *H. pylori* lipid composition were obtained from Hirai *et al.* (1995)[22] and Geis *et al.* (1991)[23].

The composition of cell wall components, peptidoglycan and lipopolysaccharide, was retrieved from the *E. coli* model (*i*AF1260) and from a previous *H. pylori* model (*i*T341), respectively.

The cofactors and their coefficients in the biomass equation were retrieved either from the list of universal biomass components developed by Henry, *et al.* (2010)[24] from an *E. coli* model (*i*JO1366)[25] and from the previous *H. pylori* model (*i*T341)[9].

The inclusion of the biomass equation allowed converting the genome-scale metabolic network into a draft genome-scale metabolic model. The units of the flux through the biomass reaction are h^{-1}, since its precursor fractions are given in mmol/gDW. Thus, the biomass equation accounts for the number of moles of each precursor necessary to produce 1 g of dry weight of cells.

7.3.7 Growth medium requirements

Information on growth-enabling media is of great importance in the development of an accurate metabolic model. The starting point in *H. pylori*'s metabolic model growth medium requirements was the Ham's F12 defined medium[26], which has been used to grow *H. pylori*. The minimal medium experimentally obtained in previous chapters for *H. pylori* growth was also used for simulations and the *in silico* results were compared with experimental data in order to assess model accuracy.

7.3.8 Model curation

After the complete assembly of the metabolic network, and posterior addition of GPR associations, the biomass reaction, and the establishment of growth medium requirements, the metabolic network was finally converted to a draft model, capable of being simulated and optimized. However, a manual curation of the model was still required, as, although very useful, these automatic methods are fallible. The manual curation was performed with a revision of the literature, and by consulting organism-specific databases, and tried to solve inconsistencies on

protein-reaction identifiers, ambiguous data, duplicated information, and propagated errors from annotation. After the first curation, a tool within *merlin* was applied in order to automatically eliminate reactions with dead-end metabolites from the model, being either biochemical or transport reactions. If a given metabolite is not consumed nor transported by another reaction, such reaction was deleted from the model. This was a recursive process because the removed reactions can sometimes originate dead-ends to other metabolites, and therefore, such process was performed with great care, in order to prevent the loss of valuable information from the model. Once curated, the genome-scale metabolic model of *H. pylori* was ready for simulation and optimization.

7.3.9 Simulation and model optimization

Metabolic model simulations were performed with parsimonious Flux Balance Analysis (pFBA)[5]. For the *H. pylori*'s genome-scale metabolic model, the linear programming problem of pFBA was solved using OptFlux, an in-house developed and user-friendly software tool, open-source and compatible with SBML. OptFlux accommodates several tools and algorithms developed for the manipulation and optimization of metabolic models[27].

7.3.10 Model validation

In this step, the genome-scale metabolic model was evaluated and its overall performance validated. For the validation of the model, the analysis of strategic fluxes was performed. The evaluation parameters were focused on specific growth rates, by-products formation and corresponding yields, for different growth conditions. These results were then compared with the experimental data collected in previous chapters.

Reactions with existing fluxes were analyzed and when inconsistencies between model and experimental data arose, the model was revised and corrected.

Another evaluation approach consisted in the assessment of essential genes and its comparison with experimental data, published in the OGEE database[28]. When the gene essentiality simulations did not match with experimental data, the genome annotation was reviewed.

7.4 *Results and Discussion*

7.4.1 Genome re-annotation and network assembly

As mentioned before, a re-annotation of the genome has been performed by the authors of this chapter and the detailed procedure and results can be found in Resende *et al.* (2013)[10]. Briefly, the developed annotation pipeline successfully reviewed all the 1573 coding sequences (CDS) from *H. pylori* 26695's genome, finding functions to 1212 of its genes and assigning EC numbers to 581 of them. Also, 155 CDS were classified as transporter-encoding genes. As depicted in Figure 7.2., the total number of coding sequences can be divided into 712 genes (45%) with a metabolic function and 500 (32%) with non-metabolic functions. The number of hypothetical CDS was 361, representing a total of 23% of the CDS in the genome, a lower number than the previous annotation which contained 510 hypothetical proteins (32%).

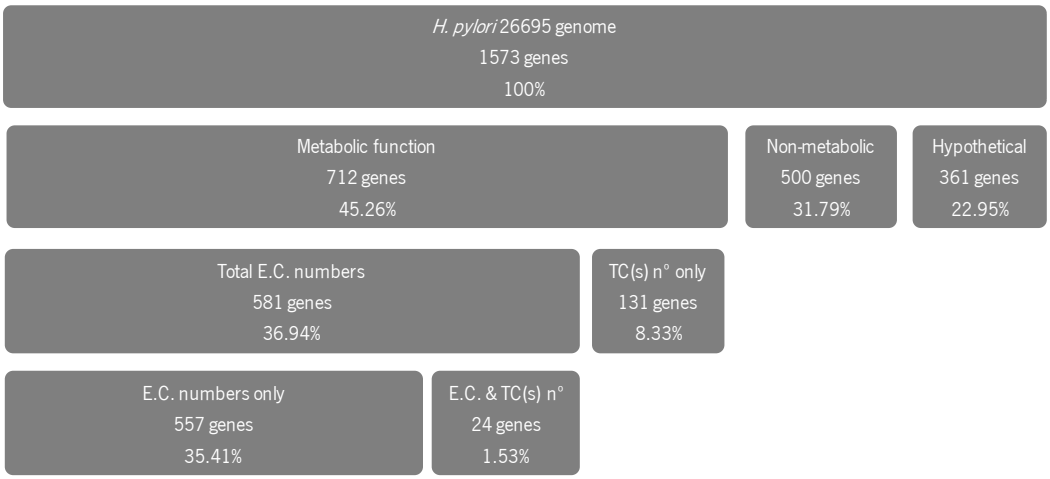

Figure 7.2. *H. pylori* 26695 re-annotation results and statistics (detailed results can be found in Resende *et al.* (2013)[10].

After the genome-wide re-annotation of this bacterium and subsequent attribution of metabolic and transport functions to its genes, the metabolic network was assembled by integrating KEGG reactions information, transport reactions and enzyme localization data. This automatic process originated a draft network containing approximately 1800 reactions, though a large number of which were unconnected or erroneously integrated and, therefore, were removed once the model was curated, lowering the final number of reactions in the model.

7.4.2 Biomass formation

In order to convert the metabolic network into a metabolic model, a biomass equation was formulated to represent the biomass composition of *H. pylori*. Each category and the corresponding metabolites are concisely described next. More information about biomass estimation can be found in supplementary material E1 (electronic version). The macromolecular composition and their coefficients are showed in Table 7.1.

Table 7.1. Macromolecular composition of the biomass of *H. pylori* and respective contribution to the overall biomass.

Biomass contribution (g/g)	
Protein	0.500
DNA	0.070
RNA	0.224
Lipids	0.099
Peptidoglycan	0.027
Lipopolisaccharides	0.037
Cofactors and other	0.043

7.4.2.1 Protein entity

Biomass protein composition was estimated from genome information (with the referred Java tool), by inspecting the composition of the protein-encoding genes, and determined experimentally. Results are displayed in Table 7.2. All amino acids were experimentally determined, exception made for cysteine and tryptophan, that were not detected with the method used. In this case, the assumed coefficient was the one obtained by estimation from genome information. Also, during hydrolysis glutamine and asparagine were deaminated to glutamate and aspartate, respectively, and thus the coefficient for each of those four amino acids was adjusted using the values obtained from genome information. In the cases of glycine and threonine, as well as isoleucine and phenylalanine, the same correction was applied since they are being analyzed together in HPLC. All the remaining coefficients are taken directly for experimental data. The amount of each amino acid in biomass is presented in mmol of amino acid per gram of cell dry weight (mmol.gDW^{-1}).

Table 7.2 Total amount of amino acids in biomass composition. All components are located in the cytoplasm

Amino Acid	KEGG id	Coefficient (mmol.gDW^{-1})
Glycine	C00037	0.111850
L-Alanine	C00041	0.274183
L-Arginine	C00062	0.151668
L-Asparagine	C00152	0.185275
L-Aspartate	C00049	0.185275
L-Cysteine	C00097	0.400096
L-Glutamine	C00064	0.153044
L-Glutamate	C00025	0.282238
L-Histidine	C00135	0.103177
L-Isoleucine	C00407	0.093398
L-Leucine	C00123	0.400877
L-Lysine	C00047	0.237732
L-Methionine	C00073	0.109041
L-Phenylalanine	C00079	0.070296
L-Proline	C00148	0.048062
L-Serine	C00065	0.152764
L-Threonine	C00188	0.085215
L-Tryptophan	C00078	0.257262
L-Tyrosine	C00082	0.149287
L-Valine	C00183	0.280943

7.4.2.2 Nucleotide content

The estimation of each dNTP (i.e., dATP, dCTP, dGTP and dTTP) is shown in Table 7.3. Their prediction was performed using the same *in-house* developed Java tool referred previously, but this time, by calculating the frequency of each nucleobase in the whole genome.

Table 7.3. Total amount of dNTPs in the biomass composition. All components are located in the cytoplasm

dNTP	KEEG id	Coefficient (mmol.gDW^{-1})
dATP	C00131	0.043574
dGTP	C00286	0.027699
dTTP	C00459	0.044322
dCTP	C00458	0.028200

The determination of the nucleotides (NTP) ATP, CTP, GTP and UTP, was performed with some changes in the referred protocol to account for the three main different types of RNA,

namely rRNA, tRNA and mRNA, existing in the cells. Biomass nucleotides composition is displayed in Table 7.4.

Table 7.4. Total amount of NTPs in the biomass composition. All components are located in the cytoplasm

NTP	KEEG id	Coefficient (mmol.gDW^{-1})
ATP	C00002	0.117241
CTP	C00063	0.095900
GTP	C00044	0.113151
UTP	C00075	0.125639

7.4.2.3 Peptidoglycans and Lipopolysaccharides

Peptidoglycan biosynthesis is a complex process involving several steps. Due to the lack of experimental data, the reaction originating peptidoglycan was adapted from the previous *H. pylori* model (*i*T341 GSM/GPR)[29]. This metabolite was then inserted in the biomass equation with the coefficient calculated as previously explained.

The lipopolysaccharide biosynthesis is also a very complex process, encompassing several reactions. The total amount of lipopolysaccharide in the biomass was adapted from the last *H. pylori* model (*i*T341 GSM/GPR)[9]. Both metabolites are shown in Table 7.5 with the respective biomass coefficient.

Table 7.5. Total amount of cell wall metabolites in the biomass composition.

Metabolite	KEEG id	Compartment	Coefficient (mmol.gDW^{-1})
Peptidoglycan	C00889	periplasmic	0.015001
Lipopolysaccharide	C00338	periplasmic	0.008404

In Table 7.5, all cell wall metabolites are located in the periplasm. Although this did not occur in the previous model due to the lack of compartments, once produced, peptidoglycans, lipopolysaccharides and other cell wall compounds are transported to the periplasm.

7.4.2.4 Lipids

In order to produce lipids, a fatty acid entity was inserted in the model to represent the average fatty acid composition of the cell. Then, the reaction R_fattyacid was also included to represent the aggregation of the fatty acids experimentally identified in *H. pylori* (Geis, *et al.*

(1990)[23] and Hirai *et al.* (1995))[22] The substrates of this reaction are six fatty acids: myristic acid (tetradecanoic acid), palmitic acid (hexadecanoic acid), stearic acid (octadecanoic acid), oleic acid ((9z)-octadecenoic acid), linoleic acid (linoleate), and phospholipid cyclopropane fatty acid. The substrate coefficients needed to produce 1 entity of fatty acid are: 0.4995 (myristic acid), 0.0511 (palmitic acid), 0.0594 (stearic acid) and 0.0998 (oleic acid), 0.0220 (linoleate) and 0.2680 (phospholipid cyclopropane). The fatty acid entity allows the drainage of lipids for biomass, because it requires the production of Acyl-coA (reaction R00389) which is a precursor of all lipids present in the biomass equation. Such lipids are displayed in Table 7.6.

The coefficients were determined as detailed in supplementary material E1 (electronic version).

Table 7.6. Total amount of different lipids in the biomass composition.

Lipid	KEEG id	Compartment	Coefficient (mmol.gDW^{-1})
Cardiolipin	C05980	periplasmic	0.026586
Phosphatidylethanolamine	C00350	cytoplasmic	0.071349
Phosphatidylglycerol	C00344	cytoplasmic	0.015580
Phosphatidylserine	C02737	cytoplasmic	0.002473

7.4.2.5 Cofactors

In our model, cofactor metabolites classified by Henry, *et al.* (2010)[24]as universal components of biomass were added to the biomass equation (Table 7.7.). Cofactors coefficients were retrieved from the *i*JO1366 model[25] and their contribution was adjusted considering the other biomass components.

Table 7.7. Different cofactors in the biomass composition with the respective coefficient. All components are located in the cytoplasm.

Cofactor	***KEEG id***	***Coefficient (mmol.gDW^{-1})***
10-Formyltetrahydrofolate	C00234	0.001042
2-Demethylmenaquinone 6	C05818	0.001042
5-Methyltetrahydrofolate	C00440	0.001042
5,10-Methylenetetrahydrofolate	C00143	0.001042
Acetyl-CoA	C00024	0.001303
Acyl-carrier protein	C00229	0.001042
Ammonia	C00014	0.057827
Biotin	C00120	0.000009
Chorismate	C00251	0.001042
Coenzyme A	C00010	0.000785
Flavin adenine dinucleotide oxidized (FAD)	C00016	0.001042
Heme	C00032	0.001042
Malonyl-CoA	C00083	0.000145
Menquinone 6	C00828	0.001042
Nicotinamide adenine dinucleotide (NAD)	C00003	0.008348
Nicotinamide adenine dinucleotide - reduced (NADH)	C00004	0.000210
Nicotinamide adenine dinucleotide phosphate (NADP)	C00006	0.000523
Nicotinamide adenine dinucleotide phosphate - reduced (NADPH)	C00005	0.001565
Putrescine	C00134	0.155416
Pyridoxal phosphate	C00018	0.001042
Riboflavin	C00255	0.001042
S-Adenosyl-L-methionine	C00019	0.001042
Spermidine	C00315	0.031504
Succinyl-CoA	C00091	0.000458
Tetrahydrofolate	C00101	0.001042
Thiamine	C00378	0.001042
UDP-glucose	C00029	0.014014
di-trans,poly-cis-Undecaprenyl diphosphate	C04574	0.000257

7.4.2.6 Energy requirements

Growth–associated energy requirements in terms of ATP molecules needed per gram of biomass synthesized are also needed to be included in the biomass equation.

The growth ATP requirements adopted in this model were retrieved from the *E. coli* (*i*JO1366) metabolic model[25].The coefficient representing ATP consumption requirements for cell growth was set to 53.95 mmol.gDW^{-1}.

The depletion of ATP by processes other than growth was represented in the model by an equation that forces ATP consumption throughout a specific flux. The boundaries of this flux were also retrieved and adapted from the *E. coli* model *i*JO1366[25].

7.4.3 Model curation

The first step in model curation was to look for reactions with wrong compartmentation information. After the first curation step, the size of the model was decreased by automatically removing reactions, either biochemical or transport, with dead end metabolites from the model. This process reduced the total number of reactions from about 1800 to approximately 700 reactions. As it is a recursive method, some reactions of the model were erroneously removed, disabling the model's simulating capability. After this process, the origin of each biomass precursor was verified to identify unconnected reactions. For that purpose the model was exported into the SBML format, and imported into OptFlux[27], so that simulations could be performed. Initially, the boundaries of all uptake drains of the model were unrestricted to determine whether the model was able to produce, or not, biomass.

Having, finally, a model capable of simulating the production of biomass (although with all entries unconstrained), the model was checked for unbalanced reactions.

Once the metabolic model was properly curated, it was ready for evaluation and characterization.

7.4.4 Model Evaluation

The outcome of the previous tasks allowed obtaining a genome-scale metabolic model of *H. pylori* 26695 based in its most recent genome re-annotation. The metabolic model is available, in the SBML format, in the supplementary material E2 (electronic version).

7.4.4.1 Model characterization

When reconstructing the metabolic model, 370 metabolic genes from the performed annotation were used. Though still available for the continuous improvement of the metabolic

model, the remaining annotated metabolic genes were not included in this version of the model. This happened either because the metabolites on their catalyzed reactions were unconnected from the metabolic network, or due to a decision taken during the manual curation of the model. Another reason lies on the fact that some of these excluded metabolic genes encode enzymes only identified with a partial EC number, thus disabling any reaction integration possibility.

Table 7.8 displays the characteristics of the generated metabolic model. The 370 metabolic genes included in the model encode 254 different enzymes and 61 transport proteins, promoting a total of 666 different reactions, when combined with the spontaneous and manually added reactions.

Table 7.8. Metabolic model characteristics.

Genes	Enzymes	Transporters	Enzymatic reactions	Transport reactions	Metabolites	Compartments
370	254	61	450	216	432	2

There are 176 manually inserted reactions in the model (reactions not inferred directly from the annotation), being 91 of which transport reactions located in the periplasmic membrane, allowing for the exchange of metabolites between the internal compartments and the environment. The remaining manually inserted reactions correspond to metabolic reactions used in the gap filling, during the curation process of the model and also to reactions added from literature evidence. All reactions included in the model are available in supplementary material E3 (electronic version).

The implementation of GPR associations allowed the aggregation of enzymatic subunits into protein complexes in the model, which is very important when simulating the impact of deleting a subunit on a protein complex. If a subunit on a protein complex with a GPR association is deleted, the entire complex is disabled, enhancing the accuracy of model simulation and allowing for a better understanding of the metabolic fluxes. It also enhances the performance of the prediction of essential genes. In our model there are 505 reactions with gene associations, being 117 of which associated with 2 or more genes. GPR associations and the respective reactions are available in supplementary material E3 (electronic version).

A comparison between our model (*i*TR370) and the last *H. pylori* model, the *i*T341 GSM/GPR from Thiele, *et al.* (2005)[30] is depicted in Table 7.9.

Table 7.9. Comparison between the *i*T341 GSM/GPR[9] model and the metabolic model developed in this work (*i*TR370).

Parameter	***i*T341 GSM/GPR**[9]	***i*TR370**
No. of genes included	339	370
No. of Gene-Protein-Reaction associations	355	505
N. of GPRs with 2 or more genes	44	117
Total no. of reactions	477	666
No. of metabolites (internal/external)	408/77	432/76
No. of exchange fluxes	77	76

In this table we can see that our model has more genes included (31 more genes) and significantly more GPR association (150) than the previous model, especially when considering GPRs with more than one gene, where our model has nearly 3 times more associations. Over all, this model has more information included which translates into a greater number of total reactions (666 against 477 from the previous model). The number of internal metabolites is also higher; however, the number of external metabolites is almost the same.

7.4.4.2 Gene essentiality

In this section, *in silico* gene essentiality was assessed. For that purpose, the method for determining critical genes embedded in OptFlux was used, using loose environmental conditions, as gene essentiality *in vivo* has been performed in complex media. Thus, all reactions where metabolite exchange between the cell and the environment occurred were left unconstrained.

From the total amount of 370 genes included in the model, 147 were classified as essential genes when the simulations were performed. The results on gene essentiality were afterwards compared with the data available in the OGEE database[28], an online gene essentiality database with results from large-scale essentiality experiments. Gene essentiality information on *H. pylori* 26695 is related to the entire genome; however, only information on the genes present in the metabolic model was retrieved. Table 7.10. presents the results from the comparison between the essential genes predicted using our metabolic model, and the data from the OGEE database.

Table 7.10. Comparison between essential genes verified experimentally and retrieved from the OGEE database and model predictions.

		Ogee database[28]	
		Essential	**Non-essential**
Our model	Essential	51	96
	Non-essential	53	170

By observing the information in the table we can see that the results obtained in the comparison between models predictions and the OGEE database have a percentage of agreement of 59.7%, being the genes considered non-essential in a larger number than the essential ones. A few reasons for the mismatch in some of the genes might be related with the fact that the metabolic model is not able to simulate and incorporate all the components of the complex medium used in the OGEE experiments, mainly because some of these components are not fully characterized in the literature, such as serum and protein extracts. Gene essentiality results and a detailed comparison are depicted in the supplementary material E3 (electronic version).

7.4.4.3 Prediction of physiological data

In this section the results of growth simulations performed with the metabolic model are shown and analyzed. The environmental conditions used in the simulations are based on the results achieved in the previous chapters in defining the essential amino acids for *H. pylori* and also on identifying a suitable carbon source. The final minimal medium used to perform the simulations had in its composition 20 metabolites: 7 essential amino acids (L-Arginine, L-Histidine, L-Isoleucine, L-Leucine, L-Methionine, L-Phenylalanine and L-Valine), L-Glutamate as carbon source, 4 measured FBS compounds (L-Alanine, L-Proline, Lactate and Succinate), 2 vitamins (Biotin and Thiamine), hypoxanthine, water, oxygen, iron and inorganic compounds, such as, phosphate and sulfate.

For the simulations, the Optflux wild type simulation method was used (pFBA). After selecting the model and the reaction to maximize (biomass reaction, in this case) the environmental conditions were chosen and the model simulated.

Results of the simulations are depicted in Table 7.11, where the set of environmental conditions used, the specific growth rate, the consumed metabolites and the products originated

can be observed. The coefficients defined in the environmental conditions represent, in the model, the maximum uptake rate allowed for each compound, and correspond to values obtained experimentally for the amino-acids and FBS components during the exponential phase. All the remaining metabolites were set at a maximum uptake rate of 10, except for oxygen, that was limited to 5 $mmol.gDW^{-1}h^{-1}$. Due to the lack of experimental data, the reaction representing the ATP depletion by processes other than growth (ATPMaint) was also varied and served as a degree of freedom for model fitting.

Table 7.11. Metabolic model simulations performed using experimental data on uptake rates as environmental conditions and varying the flux of the ATP Maintenance reaction in the model.

Simulation	Environmental conditions (mmol.gDW^{-1}h^{-1})				ATPMaint	Consumption		Production	Biomass (h^{-1})
1	L-alanine	0,1097	Hypoxanthine	10	1	Oxygen	H2O	H^+	**0,1085**
	L-arginine	6,9444	Thiamine	10		Hypoxanthine	L-Proline	Carbonic acid	
	L-glutamate	1,3917	Fe^{2+}	10		L-Methionine	L-Histidine	Xanthine	
2	L-histidine	0,6944	Sulfate	10	2	L-Glutamate	L-Isoleucine	NH3	**0,1021**
	L-isoleucine	0,0444	Phosphate	10		Phosphate	Succinate	Biomass	
	L-leucine	0,1389	H2O	10		L-Leucine	Thiamine	AI-2	
3	L-methionine	0,1681	Biotin	10	3	Sulfate	Fe^{2+}	5-Methylthio-D-ribose	**0,0957**
	L-phenylalanine	0,2000	Oxygen	5		L-Arginine	Biotin		
	L-proline	0,0167	Lactate	1,2292		L-Valine			
	L-valine	0,1417	Succinate	0,0013		L-Phenylalanine			
4	L-arginine	6,9444	Hypoxanthine	10	1	L-Phenylalanine	L-Valine	H^+	**0,1070**
	L-glutamate	1,3917	Thiamine	10		L-Methionine	Oxygen	Carbonic acid	
	L-histidine	0,6944	Fe^{2+}	10		Hypoxanthine	L-Histidine	Xanthine	
5	L-isoleucine	0,0444	Sulfate	10	2	L-Glutamate	L-Isoleucine	NH3	**0,1006**
	L-leucine	0,1389	Phosphate	10		Phosphate	H2O	Biomass	
	L-methionine	0,1681	H2O	10		L-Leucine	Thiamine	AI-2	
6	L-phenylalanine	0,2000	Biotin	10	3	Sulfate	Fe^{2+}	5-Methylthio-D-ribose	**0,0942**
	L-valine	0,1417	Oxygen	5		L-Arginine	Biotin		

Table 7.11 displays the results of 6 simulations of the metabolic model under different environmental conditions. The simulations were divided into 2 groups, where each group shared the same environmental conditions, varying only the flux of the ATP maintenance reaction between 1, 2 and 3 mmol.gDW^{-1}h^{-1} (chosen based on the described range of ATP-maintenance consumption for *E. coli* [31]. In the first group (simulations 1, 2 and 3), the set of environmental conditions correspond to the uptake rates measured for all the compounds consumed, whereas in the second group (simulations 4, 5 and 6) the compounds corresponding to the FBS were removed in order to analyze their possible role in biomass growth. A detailed description of the simulation results is displayed in the supplemental material 4 (electronic version).

In simulations 1, 2 and 3 it is possible to observe that all metabolites had some consumption, with the exception of L-Alanine and Lactate. Our results also show that the limiting factor for the *in silico* growth of *H. pylori* is the amino acid L-glutamate, once this metabolite is the only compound that achieved the maximum uptake rate when the model was simulated (shown in supplementary material 4). These occurred in all simulations.

The variation of the maintenance ATP flux changed the biomass growth rate, as expected, being the growth rate inversely proportional to the flux of the maintenance ATP reaction.

Simulation 1, with an ATPMaint of 1 and the consumption of the FBS compounds L-proline and succinate, originated the growth rate most similar to the experimental data, with an *in silico* specific growth rate of 0.1085 h^{-1}, compared with the *in vivo* specific growth rate of 0.126 h^{-1}.

In simulations 4, 5 and 6, where the FBS compounds where excluded, the simulated growth rate was slightly lower than in the previous simulations. These results show that succinate and L-proline contribute to biomass production, although they are not essential. Also, their overall influence is small, due to the fact that FBS concentration in the minimal medium in also low.

It should be emphasized that previous models of *H. pylori* have failed in making quantitative predictions due to, on one hand, the usage of a non-specific biomass equation and, on the other, to the lack of experimental data available. Thus, the fact that there is a

remarkable match between *in silico* and *in vivo* physiological data indicates that the model here presented can, in the future, be used to make quantitative predictions for *H. pylori*.

In the metabolite production column we can observe that there are 5 metabolites that are always produced independently of the environmental conditions, when simulating *in silico* the growth of *H. pylori*. The proton H^+ is the metabolite excreted from the model with the higher fluxes in all conditions. As expected, Ammonium is produced as a byproduct of the decomposition of urea. Carbonic acid, generated in a reaction involving water and carbon dioxide is excreted from the model instead of carbon dioxide. Among the remaining metabolites produced, 5-Methylthio-D-Ribose and Autoinducer-2 are possibly the most peculiar in Table 7.11. 5-Methylthio-D-Ribose is part of the cysteine and methionine metabolism, but it originates in another pathway, the arginine and proline metabolism. In order to produce spermidine from putrescine, the reaction R01920 encoded by SpeE (HP0832) also produces 5'-methylthioadenosine that by its turn is catalyzed in reaction R01401 by HP0089, resulting in the formation of 5-methylthio-D-ribose. At this point, the only destination for this metabolite would be to continue ahead through a cascade of un-annotated reactions until the formation of L-methionine. As this solution is not viable, once it is well established that *H. pylori* is auxotrophic for L-methionine, the only solution was to excrete *in silico* the metabolite for the environment. If this excretion has any association with *in vivo* reality remains to be checked.

The Autoinducer-2 is regarded as a quorum sensing signaling molecule. Studies from[32] show that this molecule is formed in the cysteine methionime pathway, through a cascade of reactions that starts on S-adenosyl-l-methionine, a product of L-methionine metabolism, and ends on S-Ribosyl-L-homocysteine[33].also showed this cascade as a way to producing L-homocysteine. As it is a known quorum sensing molecule, reactions were added to the model in order to excrete this signaling molecule.

Besides these metabolites, Xanthine is also excreted, probably due to an overflow in the purine metabolism. Overall, no fermentation by-products were observed *in silico*, again matching the *in vivo* data from the previous chapter.

7.4.5 Flux distribution analysis

In this section, the analysis of the flux distribution predicted by the model is performed. The main pathways of the central carbon metabolism, important precursors and their fluxes were analyzed. Flux distribution and metabolite conversions were retrieved from simulation 4, where consumption of FBS components is not considered, for simplification purposes. Figure 7.3. depicts the most important metabolite conversions, and the respective reaction fluxes on 3 important pathways: Glycolysis/Gluconeogenesis, Pentose phosphate pathway, and the Citrate cycle (TCA cycle). Reactions occurring in alanine, aspartate, glutamate and proline metabolism are also presented.

When analyzing flux distributions, it is possible to observe that *H. pylori* is capable of performing Gluconeogenesis when not supplemented with carbohydrates. Phosphoenolpyruvate is originated from Pyruvate and flows through a reaction cascade in order to produce Glycerone phosphate (Glycerone-P). Glycerone phosphate is routed to the lipids biosynthesis where some biomass precursors are formed.

Fructose-6-phosphate (β-D-fructose-6P), also originated from Glycerone phosphate through a cascade of reactions in other pathways, is converted into glucose-6-phosphate (α-D-glucose-6P) which, in its turn, flows exclusively to the production of Lipopolysaccharides.

In the Pentose Phosphate pathway, fructose 6-phosphate and D-Erythrose 4-phosphate (D-Erythrose-4P) are converted in Sedoheptulose 7-phosphate (D-Sedoheptulose-7P) and D-Glyceraldehyde 3-phosphate (D-Glyceraldehyde-3P), which are directed into reactions generating 5-Phospho-alpha-D-ribose 1-diphosphate (PRPP). This metabolite is then part of the metabolism of Purines and Pyrimidines.

The TCA cycle is only partially completed. It begins with the conversion of 2-Oxoglutarate into Succinyl-CoA, followed by Succinate. After being converted from Succinate, Fumarate originates (S)-malate, which in its turn is converted to Oxaloacetate. (S)-malate also originates Pyruvate, at a rate of 2.287 $mmol.gDW^{-1}h^{-1}$. All reactions in the TCA cycle have high flux rates, going from 1.310 to 1.360 $mmol.gDW^{-1}h^{-1}$. This is due to the use of L-glutamate as the sole carbon source.

Pyruvate produces Acetyl-coA, a precursor of many essential reactions. In fact, the biosynthesis of peptidoglycan, fatty acids, phospholipids and cofactors is derived from Acetyl-CoA[34] which enhances the importance of this metabolite.

When analyzing the amino acids metabolism we can see that L-Alanine is derived from Pyruvate. Despite some controversy around this amino acid, with some authors claiming that it is an essential nutrient for *H. pylori* [9] experimental data generated in our group suggest otherwise. Reaction directionality analysis performed in eQuilibrator[15] for reaction R00396 (L-Alanine + NAD^+ + H_2O = Pyruvate + NH_3 + NADH + H^+) also supports this theory.

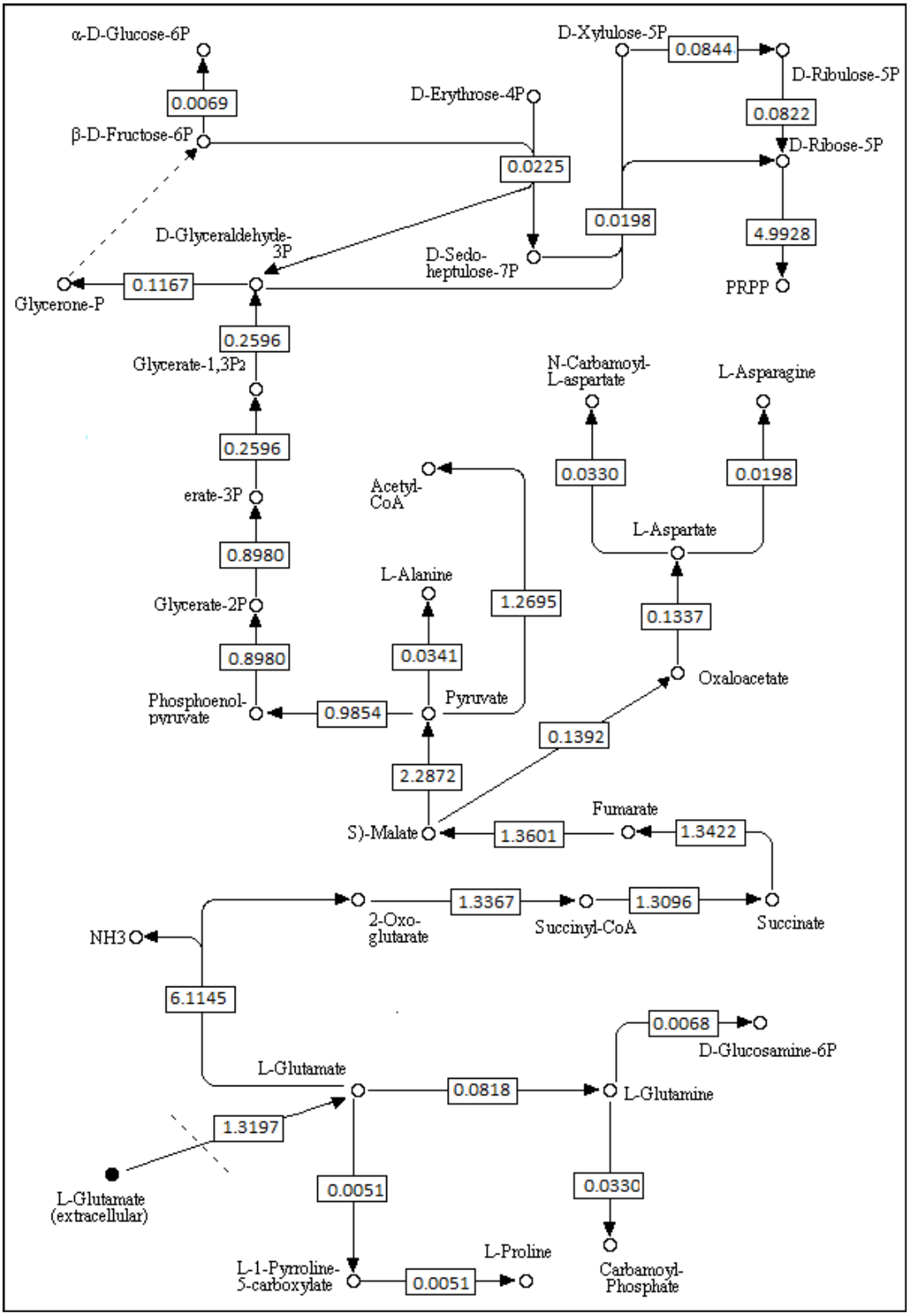

Figure 7.3. Metabolites and flux distribution in the central carbon pathways when simulating *i*TR370 in minimal medium.

The metabolism of L-glutamate, the limiting carbon source of the model when simulating with minimal medium, is also depicted. By following the fluxes in the model we can see that L-Glutamate is in the origin of several products, including several amino acids.

L-glutamate is directly converted to L-glutamine, which in its turn is converted in D-glucosamine 6-phosphate (D-glucosamine-6P) and directed to the aminosugars metabolism and to Carbamoyl phosphate which is routed to the pyrimidine metabolism.

From its conversion to (S)-1-Pyrroline-5-carboxylate (L-1-Pyrroline-5-carboxylate), L-glutamate also originates L-proline, although our results with ^{13}C labeled glutamic acid did not prove this conversion. With the set of environmental conditions of this simulation, L-proline is not being directed to any other metabolite, apart from the biomass, and the fact that *in silico* it is being excreted to the environment in not yet totally clear. L-Aspartate, originated from Oxaloacetate, can also be traced back to L-glutamate, passing through the TCA cycle. After its conversion, L-Aspartate originates L-Asparagine. L-glutamate can also be converted to L-tyrosine (data not shown) and enters the peptidoglycan biosynthesis.

These results allow a glimpse of the routes taken by L-glutamate in the model in order to produce other metabolites. They also allow us to verify how reactions flow in some of the major pathways, as in the case of the TCA cycle, which is only partially used. The results obtained with the model largely agreed with the obtained experimental ones.

7.5 *Conclusions*

In this work, the reconstruction of a genome-scale metabolic model of *H. pylori* 26695 is presented.

After genome annotation, the metabolic conversions and transport systems identified were retrieved and assembled in a metabolic network. The resulting network was complemented with protein subcellular localization and reaction reversibility information. A Biomass equation representing the cellular composition of *H. pylori* was formulated and the entities included were Protein, Nucleotides, Peptidoglycans, Lipopolysaccharides,

Lipids, Cofactors and Energy requirements. After the complete assembly of the metabolic network and the formulation of the biomass reaction, the metabolic network was converted into a draft metabolic model that was then manually curated.

The metabolic model contains 370 annotated genes, encoding 254 different enzymes and 61 transport proteins, promoting a total of 666 different reactions, being 450 enzymatic and 216 of transport. The model comprises 2 compartments, cytoplasm and periplasm, and contains 432 metabolites.

Simulations of biomass growth were performed using the model and the experimentally developed minimal medium, containing the essential amino-acids, L-glutamate as a carbon source, FBS components and other essential elements to the metabolic model, such as water, oxygen, phosphate, sulfate and hypoxanthine. Gene essentiality analysis was performed with this model, which was found to have 147 essential and 223 non-essential genes when simulated with all external metabolites unconstrained, which corresponds with an agreement of 60% comparing with experimental data available.

Growth simulations were performed using the uptake rates for the amino acids obtained experimentally. From the 6 simulations performed, the simulation with the most complete medium (including FBS components) and with the lower flux in the ATP maintenance reaction showed to be the best when predicting the *in vivo* specific growth rate of *H. pylori* (0.1085 h^{-1} *in silico* and 0.126 h^{-1} *in vivo*). These results show that, as opposed to previous models, the model here presented allows to perform quantitative predictions, besides having a significantly higher coverage of genes and GPR associations.

An analysis of the flux distributions obtained was performed for the central carbon metabolism, showing important metabolite conversions and the correspondent fluxes and allowing a better understanding of model predictions.

The presented results bring new and more comprehensive information on *H. pylori* 26695's genome and metabolism, increasing and improving the existing knowledge on this human pathogen. It is shown that the new metabolic model is able to predict the phenotypic behavior of *H. pylori*, therefore becoming a useful tool in assisting the research

work being perform on unveiling metabolic routes, identifying new drug targets and enhancing treatment efficiency.

7.6 References

1. Médigue, C. & Moszer, I. Annotation, comparison and databases for hundreds of bacterial genomes. *Res. Microbiol.* **158,** 724–736 (2007).
2. Simpson, J. T. & Durbin, R. Efficient de novo assembly of large genomes using compressed data structures. *Genome Res.* **22,** 549–556 (2012).
3. Tomb, J.-F. *et al.* The complete genome sequence of the gastric pathogen *Helicobacter pylori*. *Nature* **388,** 539–547 (1997).
4. Boneca, I. G. A revised annotation and comparative analysis of *Helicobacter pylori* genomes. *Nucleic Acids Res.* **31,** 1704–1714 (2003).
5. Rocha, I., Förster, J. & Nielsen, J. in *Methods Mol. Biol. vol. 416 Gene Essentiality* (Gerdes, S. Y. & Osterman, A. L.) **416,** 409–433 (Humana Press Inc., 2007).
6. Durot, M., Bourguignon, P.-Y. & Schachter, V. Genome-scale models of bacterial metabolism: reconstruction and applications. *FEMS Microbiol. Rev.* **33,** 164–190 (2009).
7. Raghunathan, A., Reed, J., Shin, S., Palsson, B. & Daefler, S. Constraint-based analysis of metabolic capacity of *Salmonella typhimurium* during host-pathogen interaction. *BMC Syst. Biol.* **3,** 38 (2009).
8. Schilling, C. H. *et al.* Genome-scale metabolic model of *Helicobacter pylori* 26695. *J. Bacteriol.* **184,** 4582–4593 (2002).
9. Thiele, I., Vo, T. D., Price, N. D. & Palsson, B. Ø. Expanded metabolic reconstruction of Helicobacter pylori (iIT341 GSM/GPR): an *in silico* genome-scale characterization of single- and double-deletion mutants. *J. Bacteriol.* **187,** 5818–5830 (2005).
10. Resende, T., Correia, D. M., Rocha, M. & Rocha, I. Re-annotation of the genome sequence of *Helicobacter pylori* 26695. *J. Integr. Bioinform.* **10(3),** 1–13 (2013).
11. Thiele, I. & Palsson, B. Ø. A Protocol for generating a high-quality genome-scale metabolic reconstruction. *Nat. Protoc.* **5,** 93–121 (2010).

12. Dias, O., Rocha, M., Ferreira, E. C. & Rocha, I. Merlin: metabolic models reconstruction using genome-scale information. in *Proc. 11th Int. Symp. Comput. Appl. Biotechnol. (CAB 2010)* (Banga, J. R., Bagaerts, P., Impe, J. Van, Dochain, D. & Smets, I.) 120–125 (2010).

13. Kanehisa, M. & Goto, S. KEGG: Kyoto Encyclopedia of Genes and Genomes. *Nucleic Acids Res.* **28,** 27–30 (2000).

14. Stelzer, M., Sun, J., Kamphans, T., Fekete, S. P. & Zeng, A.-P. An extended bioreaction database that significantly improves reconstruction and analysis of genome-scale metabolic networks. *Integr. Biol. (Camb).* **3,** 1071–1086 (2011).

15. Flamholz, A., Noor, E., Bar-Even, A. & Milo, R. eQuilibrator - the biochemical thermodynamics calculator. *Nucleic Acids Res.* **40,** D770–D775 (2012).

16. Verduyn, C., Postma, E., Scheffers, W. a & van Dijken, J. P. Physiology of *Saccharomyces cerevisiae* in anaerobic glucose-limited chemostat cultures. *J. Gen. Microbiol.* **136,** 395–403 (1990).

17. De Mey, M. *et al.* Comparison of DNA and RNA quantification methods suitable for parameter estimation in metabolic modeling of microorganisms. *Anal. Biochem.* **353,** 198–203 (2006).

18. Santos, S. & Rocha, I. Development of computational methods for determination of biomass composition and evaluation of its impact in genome-scale models prediction. (2013).

19. Feist, A. M. *et al.* A genome-scale metabolic reconstruction for *Escherichia coli* K-12 MG1655 that accounts for 1260 ORFs and thermodynamic information. *Mol. Syst. Biol.* **3,** 1–18 (2007).

20. Cliff, W. & John, W. H. J. *High-Speed Amino Acid Analysis (AAA) on 1.8 µm Reversed-Phase (RP) Columns Application*. 1–14 (2007).

21. Bautista, E. J. *et al.* Semi-automated curation of metabolic models via flux balance analysis: a case study with *Mycoplasma gallisepticum*. *PLoS Comput. Biol.* **9,** e1003208 (2013).

22. Hirai, Y. *et al.* Unique cholesteryl glucosides in *Helicobacter pylori*: composition and structural analysis . *J. Bacte* **177,** 5327–5333 (1995).

23. Geis, G., Leying, H., Suerbaum, S. & Opferkuch, W. Unusual fatty acid substitution in lipids and lipopolysaccharides of *Helicobacter pylori*. *J. Clin. Microbiol.* **28,** 930–932 (1990).

24. Henry, C. S. *et al.* High-throughput generation, optimization and analysis of genome-scale metabolic models. *Nat. Biotechnol.* **28,** 977–982 (2010).

25. Orth, J. D. *et al.* A comprehensive genome-scale reconstruction of Escherichia coli metabolism–2011. *Mol. Syst. Biol.* **7,** 1–9 (2011).

26. Ham, B. Y. R. G. & King, D. Clonal growth of mammalian cells in a chemically defined medium , synthetic medium. *Microbiology* 288–293 (1964).

27. Rocha, I. *et al.* OptFlux : an open-source software platform for *in silico* metabolic engineering. *BMC Syst. Biol.* **4,** 1–12 (2010).

28. Chen, W.-H., Minguez, P., Lercher, M. J. & Bork, P. OGEE: an online gene essentiality database. *Nucleic Acids Res.* **40,** D901–D906 (2012).

29. Thiele, I., Price, N. D., Vo, T. D. & Palsson, B. Ø. Metabolic capabilities *in silico* of the human pathogen Helicobacter pylori. 92093

30. Thiele, I., Vo, T. D., Price, N. D. & Palsson, B. Ø. Expanded metabolic reconstruction of *Helicobacter pylori* (*i*T341 GSM/GPR): an *in silico* genome-scale characterization of single- and double-deletion mutants. *J. Bacteriol.* **187,** 5818–5830 (2005).

31. Feist, A. M., Herrgård, M. J., Thiele, I., Reed, J. L. & Palsson, B. Ø. Reconstruction of biochemical networks in microorganisms. *Nat. Rev. Microbiol.* **7,** 129–143 (2009).

32. Schauder, S., Shokat, K., Surette, M. G. & Bassler, B. L. The LuxS family of bacterial autoinducers: biosynthesis of a novel quorum-sensing signal molecule. *Mol. Microbiol.* **41,** 463–476 (2001).

33. Doherty, N. C. *et al.* In *Helicobacter pylori*, LuxS is a key enzyme in cysteine provision through a reverse transsulfuration pathway. *J. Bacteriol.* **192,** 1184–1192 (2010).

34. Tomb, J. F. *et al.* The complete genome sequence of the gastric pathogen *Helicobacter pylori*. *Nature* **388,** 539–547 (1997).

7.7 Supplementary material (Electronic version list)

Supplementary material E1 - Biomass. xls.

Supplementary material E2 – Hpylori_metabolic_model.xml.

Supplementary material E3 – Model_features.xls.

Supplementary material E4 – Model_simulation_results.xls.

Chapter 8

Concluding Remarks

Helicobacter pylori is associated with gastric diseases, such as gastritis, peptic and duodenal ulcers, mucosa associated lymphoid tissue lymphoma and gastric adenocarcinomas. Despite more than half of the global population being infected with this bacterium, not all individuals will develop clinical symptoms. Nevertheless, its association with gastric cancer, the high infection rate, as well as the failures on eradication efforts and vaccine development lead to an important health concern. In order to better understand the mechanisms leading to disease and also to develop effective ways to fight *H. pylori* infection, it is important to understand its physiological and metabolic behavior.

H. pylori is a microaerophilic, gram negative, fastidious organism, for which no effective defined medium has been developed. Furthermore, current cultivation procedures use media that, even when semi-defined, have a variety of nutrients that can be used as carbon and energy sources. Under those conditions, the metabolic and physiological characterization of *H. pylori* is very difficult.

The aim of this work was thus to study the physiology and metabolism of *H. pylori* to allow a better understanding of the behavior and pathogenicity of this organism. For that aim, a systems biology approach was used where metabolomics data were used to characterize the nutritional requirements, and the potential and preferred carbon sources. These data, collected from experiments performed with semi-defined media, together with genomics and other information available, were used to build the first genome-scale metabolic model of *H. pylori* that is able to make quantitative predictions. This model can be used, in the future, to investigate novel drug targets and elucidate the metabolic basis of infection. Furthermore, a comparative study was performed that analyzed different methods for assessing growth, viability, culturability and morphology, as these are important physiological parameters.

During this work, important conclusions were taken that can be summarized as follows:

- For assessing *H. pylori* growth, different methods can be used that originate different results that often need to be interpreted with care. From the methods

evaluated, DAPI yielded the highest number of total cell counts when compared with the PNA FISH probe applied. Optical density measurements can also be used to assess growth with reliability. Nevertheless, before the application of any of those methods, it is important to perform disaggregation procedures, especially in samples taken after the exponential growth phase. In fact, cell-to-cell aggregation was visible and had a great impact in all measurements.

- Culturable cell counts were in general less than total cell counts performed with DAPI, especially after the exponential phase, showing the presence of nonculturable cells. The viable but non-culturable state was mostly observed at the end of the culture, after 60 hours.
- The evaluation of cell viability using Syto9/propidium iodide was not effective in analyzing cells during morphological changes, giving exaggerated numbers of nonviable cells, which is explained by the entrance of propidium iodide through the permeable cytoplasmatic membrane. Under the referred conditions, another method to estimate cell viability must be used, such as the measurement of membrane potential.
- The culturable cell counts in some samples were higher compared with the spiral cells observed at these time points, thus indicating the potential presence of culturable coccoid cells, previously reported by other authors, but still under controversy.
- At the end of the culture, mainly coccoid cells were observed. Taking into account that coccoid forms represent a cell adaptation to less favorable conditions, the present results suggest that some stressing factors are present that cause morphological changes, probably the unavailability of an essential nutrient. The presence of an increasing number and size of cell clusters also supports this hypothesis.
- The first report on the measurement of the exometabolome of *H. pylori* indicated that, as suggested by other authors, this organism has not a

preference for glucose as a carbon source in the presence of amino acids in the culture medium.

- In agreement with *in silico* and *in vitro* published data, some amino acids were confirmed to be essential under the conditions used: L-arginine, L-histidine, L-leucine, L-methionine and L-valine. Additionally, L-isoleucine and L-phenylalanine, for which there was no consensus, were identified to be essential for the growth of *H. pylori* 26695, under the conditions used in this study.
- Nevertheless, some doubts persisted for the essentiality of L-proline and L-alanine, as they have been detected in the fetal bovine serum added to the culture. Our attempts to grow *H. pylori* without FBS and without strain adaptation failed, indicating that some components are missing in the culture medium used or that FBS has another unknown function. Thus, further investigation is needed in this direction.
- Some essential amino acids were found to be completely consumed from the culture medium, such as L-methionine, emphasizing the need of adjusting the amino acids concentration.
- Regarding preferences and possible carbon sources, our exometabolome experiments have indicated that aspartate, glutamate, proline and alanine could be potentially preferred by *H. pylori*, since they were completely consumed in the mentioned order. Compared with amino acids, organic acids were not the preferred carbon sources, and, among the identified compounds, pyruvate seems to be the preferred one.
- When the potential carbon sources identified were used individually for growing *H. pylori*, glutamine was identified as the carbon source that yielded a higher growth. However, glutamine easily suffers degradation in aqueous medium and is converted to glutamate and ammonium by an enzymatic reaction in *H. pylori*'s periplasm. In addition, the use of glutamate as the main carbon source had a higher yield in biomass regarding substrate consumption

and also allowed to achieve a high specific growth rate. As such, we suggest glutamate as the carbon source of choice for *H. pylori*'s growth.

- When controlled experiments were performed with glutamate as the main carbon source, the specific growth rate was determined to be 0.126 h^{-1} and a biomass yield of 0.6 g/g was obtained.
- A strategy of ^{13}C labeling was applied to determine the carbon flow, using [U-^{13}C]-glutamic acid as the main carbon source. The determination of ^{13}C labeling patterns of proteinogenic amino acids in biomass hydrolysates provided important clues about carbon flow, allowing to confirm the set of essential amino acids.
- Proline is probably not essential and could be synthesized from L-arginine, rather than the described possible biosynthesis from L-glutamate, as it was not labeled during labeling experiments, although its exhaustion from the medium did not arrest growth.
- L-alanine is probably also not essential and could be obtained from pyruvate by alanine dehydrogenase, which would be reversible in *H. pylori*. This conclusion is based on the fact that a low percentage of ^{13}C labeling was detected in L-alanine, although with a high error associated.
- Another controversial point about the metabolism of *H. pylori* is the presence of a complete TCA cycle. In the present work, evidences of an almost complete TCA cycle were provided by the presence of labeled aspartate in ^{13}C-glutamate labeling experiments.
- A metabolic model was developed that represents 370 annotated genes, encoding 254 different enzymes and 61 transport proteins, that promote a total of 666 different reactions, being 450 enzymatic and 216 of transport. The model comprises 2 compartments, cytoplasm and periplasm, and contains 432 metabolites.
- Gene essentiality analysis was performed with this model, which was found to have 147 essential and 223 non-essential genes when simulated with all

external metabolites unconstrained, which corresponds with an agreement of 60% comparing with the experimental data available.

- A very good agreement of predictions with experimental data was obtained when the uptake rates for the amino acids obtained experimentally were used in the simulations (0.109 h^{-1} *in silico* and 0.126 h^{-1} *in vivo*). The estimated ATP maintenance consumption was set to 1 mmol.gDW.h^{-1}. Moreover, the flux distributions obtained are consistent with the know carbon flow.